N,N-Dialkylamides as Alternative Extractants in Nuclear Fuel Reprocessing

By

NEELAM KUMARI
CHEM01200804027
Bhabha Atomic Research Centre, Mumbai

A thesis submitted to the

Board of Studies in Chemical Sciences

In partial fulfillment of requirements

For the Degree of

DOCTOR OF PHILOSOPHY

of

HOMI BHABHA NATIONAL INSTITUTE

AUGUST, 2014

HOMI BHABHA NATIONAL INSTITUTE

Recommendations of the Viva Voce Board

As members of the Viva Voce Board, we certify that we have read the dissertation prepared by **Neelam Kumari** entitled **"*N,N*-Dialkylamides as Alternative Extractants in Nuclear Fuel Reprocessing"** and recommend that it may be accepted as fulfilling the dissertation requirement for the Degree of Doctor of Philosophy.

Date:

Chairman: Prof. A. Goswami

Date:

Guide: Dr. P. N. Pathak

Date:

Co-guide: Shri Shekhar Kumar

Date:

Member 1: Prof. B. S. Tomar

Date:

Member 2: Prof. P. K. Mohapatra

Final approval and acceptance of this dissertation is contingent upon the candidate's submission of the final copies of the dissertation to HBNI. I hereby certify that I have read this dissertation prepared under my direction and recommend that it may be accepted as fulfilling the dissertation requirement.

Date:

Place:

STATEMENT BY AUTHOR

This dissertation has been submitted in partial fulfillment of requirements for an advanced degree at Homi Bhabha National Institute (HBNI) and is deposited in the Library to be made available to borrowers under rules of the HBNI.

Brief quotations from this dissertation are allowable without special permission, provided that accurate acknowledgement of source is made. Requests for permission for extended quotation from or reproduction of this manuscript in whole or in part may be granted by the Competent Authority of HBNI when in his or her judgment the proposed use of the material is in the interests of scholarship. In all other instances, however, permission must be obtained from the author.

Neelam Kumari

DECLARATION

I, hereby declare that the investigation presented in the thesis has been carried out by me. The work is original and has not been submitted earlier as a whole or in part for a degree / diploma at this or any other Institution / University.

Neelam Kumari

Dedicated to …..

My Parents
&
Family

ACKNOWLEDGEMENTS

This thesis would not have been possible without the support and encouragement of many people who contributed and extended their valuable assistance in the completion of the research work. I feel short of words in expressing my appreciation for their help at various stages of this work.

First and foremost, I would like to express my sincere gratitude to my research guide Dr. P.N. Pathak for his continuous support to my work, his patience, encouragement, enthusiasm and immense knowledge. His intellectual ideas and guidance helped me in my research work and writing this thesis. He has always been a source of motivation for me in difficult times in research or otherwise. I express my deep sense of appreciation for his support and for energizing me to overcome all the hurdles.

I also wish to express my sincere gratitude to my co-guide Shri Shekhar Kumar for his valuable guidance in this work. It is my great privilege to thank Prof. V.K. Manchanda for his keen interest in my work and giving me valuable suggestions and encouraging me to learn the subject more deeply.

Besides my advisor, I would like to thank members of my doctoral committee; Prof. A. Goswami, Prof. B. S. Tomar, Prof. P. K. Mohapatra for their encouragement, insightful comments and fruitful ideas during the course of the thesis work which have been useful for the progress of the work.

I could not find words to express my gratitude to Shri D.R. Prabhu and Shri A.S. Kanekar for helping me in learning the instrumentation and experimental techniques. They have been there all the times to encourage and motivate me to work cheerfully. Their constant support and presence have been an emotional support for me to overcome all the obstacles on my path.

I am greatly thankful to Dr. M.S. Murali, Dr. S.A. Ansari, Dr. A. Bhattacharya, Dr. D.R. Raut, Dr. Pankaj Kandwal for their help and encouraging discussions during the course of my doctoral research.

It is my great pleasure to thank Pranay Kumar Sinha, Scientific Officer, IGCAR, Kalpakkam who helped in conducting various experiments there. I would also like to thank him for devoting his time in discussing and giving his invaluable feedback. I would also like to thank my friends Jayendra Gelatar, Bijendra Saini, Jammu Ravi, Pravati Swain and Nidhi Garg who made my stay enjoyable at Kalpakkam.

I would like to acknowledge my sincere gratitude to my lab mates and friends Ajay Patil, Praveen Verma, Rakesh Shinde, Dr. Rupali Lagad, Dr. Rajesh Gujar, Dr. Sadananda Das, Vivek Chavan, Aishwarya Kar, Dr. Sumit Kumar, Dr. Neetika Rawat, Dr. Deepavinta Das for their support and help throughout my doctoral research.

I take this opportunity to thank the technical and administrative staff of Radiochemistry Division for their immense help during the entire course of this work.

Apart from the intellectual support, an emotional support is always needed to conquer the hardships. For this, I would like to thank, from the bottom of my heart, my friends Sunil Sharma, Sharayu Kasar, Ajay Bhardwaj, Saurabh Singh, Dr. Bhuvnesh soni for their warm friendship. I feel extremely fortunate to have Manju Taxak, Jyoti Jain, Shikha Sharma, Neelam Shivran, Niharika Singh, Charu Diwedi, Ruma Gupta, Komal Chandra, Mohini Bhadwal, Suvarna Patil, Rajesh Saini, Deepak Tyagi, Amit Kumar, Aashish Panday, Rakesh Sharma, Deepak Rawat, Apurav Guleria, Vikas Gulia, Santosh Gupta, Dr. Saurabh Mukherjee, Paridhi, Deepa, Aruna as my friends who, be it a scientific or personal matter, were always be with me in any situation.

Last but not the least, my deepest gratitude is to my family for their warm support which brings belief and hope into my life; to my beloved parents, who have been so

caring and supportive to me all the time, who have always been a source of inspiration towards achieving the goals in life. Immense love and affection of my sisters Nisha, Anjali, Khushboo, Surbhi and brothers Mohit, Abhishek have been invaluable in the journey towards my goal. I am also thankful to my all relatives for their moral support during my study and to achieve this stage of my life.

Apart from all the people mentioned in this acknowledgment, there are many others who have helped me in various ways during the course of this thesis work. My sincere thanks and apologies to all those I may have forgotten to mention.

May, 2014 Neelam Kumari

CONTENTS

List of Publications

JOURNALS

1. Role of acetohydroxamic acid in selective extraction of Technetium and Uranium employing *N,N*-dihexyl octanamide as extractant. **Neelam Kumari**, P.N. Pathak, D.R. Prabhu, V.K. Manchanda. ***Sep. Sci. Technol.***, 46 (2011) 79-86.

2. Extraction studies of Uranium into a third-phase of thorium nitrate employing tributyl phosphate and *N,N*-dihexyl octanamide as extractants in different diluents. **Neelam Kumari**, D.R. Prabhu, P.N. Pathak, A.S. Kanekar, and V.K. Manchanda. ***J. Radioanal. Nucl. Chem.***, 289 (2011) 835-843.

3. Validation of solvent extraction scheme for the reprocessing of Advanced Heavy Water Reactor spent fuel using *N,N*-dihexyl octanamide as extractant. **Neelam Kumari**, D.R. Prabhu, A.S. Kanekar, P.N. Pathak. ***Ind. Eng. Chem. Res.***, 51 (2012) 14535-14542.

4. Recovery of Uranium, Plutonium, and Neptunium from High-Level Waste (HLW) solutions prior to actinide partitioning. **Neelam Kumari**, P.N. Pathak, D.R. Prabhu, V.K. Manchanda. ***Journal of Hazardous, Toxic, and Radioactive Waste Management***, 16 (2012) 327-333.

5. Comparison of extraction behavior of Neptunium from nitric acid medium employing tri-*n*-butylphosphate and *N,N*-dihexyl octanamide as extractants. **Neelam Kumari**, P.N. Pathak, D.R. Prabhu, V.K. Manchanda. ***Sep. Sci. Technol.***, 47 (2012) 1492-1497.

6. Redox behaviour of Neptunium(V) in tributylphosphate and *N,N*-dihexyl octanamide extractants dissolved in *n*-dodecane. P.N. Pathak, **Neelam Kumari**, D.R. Prabhu, V.K. Manchanda. ***J. Solution Chem.***, 41 (2012) 410-421.

7. Protactinium recovery from short-cooled spent fuel and high-level waste solutions in Thorium fuel cycle. **Neelam Kumari**, P.N. Pathak, D.R. Prabhu, V.K. Manchanda, ***Desalination & Water Treatment***, 38 (2012) 46-51.

8. Development of solvent extraction scheme for reprocessing of Advanced Heavy Water Reactor spent fuel using *N*,*N*-dihexyl octanamide as extractant. **Neelam Kumari**, P.N. Pathak, D.R. Prabhu, V.K. Manchanda. ***Desalination & Water Treatment***, 38 (2012) 159-165.

9. Evaluation of *N*,*N*-dihexyl octanamide as an alternative extractant for spent fuel reprocessing: batch and mixer settler studies. P.N. Pathak, D.R. Prabhu, **Neelam Kumari**, A.S. Kanekar, V.K. Manchanda. ***Desalination & Water Treatment***, 38 (2012) 40–45.

10. Optimization studies for the recovery of Thorium from Advanced Heavy Water Reactor - high-level waste using green solvents. P.K. Verma, **Neelam Kumari**, D.R. Prabhu, P.N. Pathak. ***Sep. Sci. Technol.***, 48 (2013) 626-633.

11. Biphasic kinetic investigations on the evaluation of non-salt forming reductants for Pu(IV) stripping from tributyl phosphate and *N*,*N*-dihexyl octanamide solutions in *n*-dodecane. D.R. Prabhu, A.S. Kanekar, **Neelam Kumari**, P.N. Pathak. ***J. Radioanal. Nucl. Chem.***, 298 (2013) 691-698.

12. Uranium extraction studies employing tributyl phosphate and *N*,*N*-dihexyl octanamide as extractants: counter-current centrifugal contactors runs. **Neelam Kumari**, D.R. Prabhu, P.N. Pathak. ***Sep. Sci. Technol.***, 48 (2013) 2479-2485.

13. Dynamic light scattering studies on the aggregation behavior of tri-*n*-butylphosphate and straight chain dialkyl amides as extractants during thorium extraction from nitric

acid medium. **Neelam Kumari**, P.N. Pathak, ***J. Ind. Eng. Chem.***, 20 (2014) 1382-1387.

SYMPOSIUM PAPERS

1. Extraction Behavior of Technetium under Process Conditions Using N,N-Dihexyloctanamide as Extractant. **Neelam Kumari**, P.N. Pathak, D.R. Prabhu, V.K. Manchanda, in the Proceedings of conference ***SESTEC-2010*** held in IGCAR, Kalpakkam during March 1-4, 2010.
2. Distribution Studies on Th(IV), Pa(V), U(VI) and Pu(IV) using N,N-dihexyl octanamide under AHWR Feed Conditions. **Neelam Kumari**, P.N. Pathak, D.R. Prabhu, V.K. Manchanda, in the Proceedings of conference ***SESTEC-2010*** held in IGCAR, Kalpakkam during March 1-4, 2010.
3. Protactinium Recovery from Short-Cooled Spent Fuel and High-Level Waste Solutions in Thorium Fuel Cycle, **Neelam Kumari**, P.N. Pathak, D.R. Prabhu, V.K. Manchanda, in the Proceedings of conference ***SESTEC-2010*** held in IGCAR, Kalpakkam during March 1-4, 2010.
4. Extraction Studies on Neptunium Employing Tributyl Phosphate and N,N-Dihexyloctanamide as Extractants. **Neelam Kumari**, P.N. Pathak, D.R. Prabhu, V.K. Manchanda, in the Proceedings of conference ***SESTEC-2010*** held in IGCAR, Kalpakkam during March 1-4, 2010.

5. Disproportionation of Neptunium(V) in Tributyl phosphate and N,N-dihexyloctanamide/n-dodecane Media. P.N. Pathak, **Neelam Kumari**, D.R. Prabhu,

and V.K. Manchanda. in proceeding of conference ***Plutonium Futures 2010 – The Science 2010*** held in Keystone, Colorado during September 19-23, 2010.

6. N, N-Dihexyloctanamide: A Promising Extractant of Neptunium. **Neelam Kumari**, P.N. Pathak, D.R. Prabhu, V.K. Manchanda, in proceeding of conference ***ANUP 2010***, held in Chennai during October 10-13, 2010.
7. Recovery of Uranium, Plutonium, and Neptunium from Pressurized Heavy Water Reactor (PHWR) High-Level Waste (HLW) Solutions. **Neelam Kumari**, P.N. Pathak, D.R. Prabhu, V.K. Manchanda, in the proceedings of conference ***NUCAR-2011*** held in GITAM University, Visakhapatnam during February 22-26, 2011.
8. Development of Process Flow-Sheet for AHWR Spent Fuel Reprocessing Using N,N-Dihexyl Octanamide as Extractant. P.N. Pathak, D.R. Prabhu, **Neelam Kumari**, A.S. Kanekar, V.K. Manchanda. In the proceedings of conference ***NUCAR-2011*** held in GITAM University, Visakhapatnam during February 22-26, 2011, B-106, p.384.
9. Spectrophotometric and Solvent Extraction Studies on Neptunium in the Presence of Hydrogen Peroxide. **Neelam Kumari**, P.N. Pathak, D.R. Prabhu, V.K. Manchanda. In the proceedings of conference ***NUCAR-2011*** held in GITAM University, Visakhapatnam during February 22-26, 2011.
10. Evaluation of N,N-Dihexyl Octanamide as An Alternative Extractant for the Reprocessing of Advanced Heavy Water Reactor Spent Fuel. P. N. Pathak, **Neelam Kumari**, D. R. Prabhu, A. S. Kanekar, V. K. Manchanda, in the proceedings of conference ***SESTEC-2012*** held in SVKM's Mithibai College during February 27 – March 1, 2012.
11. Evaluation of different extractants for the recovery of thorium from AHWR-High Level Waste (HLW) solutions. P.K. Verma, **Neelam Kumari**, D.R. Prabhu, P.N.

Pathak, in the proceedings of conference ***SESTEC-2012*** held in SVKM's Mithibai College during February 27 – March 1, 2012.

12. Redox Behavior of Pu(IV) in Tributyl Phosphate and N,N-Dihexyl Octanamide Extractants Dissolved in n-Dodecane. **Neelam Kumari**, D.R. Prabhu and P.N. Pathak, in the proceedings of conference ***SESTEC-2012*** held in SVKM's Mithibai College during February 27 – March 1, 2012.
13. Comparison of extraction and stripping behavior of uranium in centrifugal contactors using tributyl phosphate (TBP) and N,N-dihexyl octanamide (DHOA) as extractants. **Neelam Kumari**, D.R. Prabhu and P.N. Pathak, in the proceedings of conference ***SESTEC-2012*** held in SVKM's Mithibai College during February 27 – March 1, 2012
14. Uranium Recovery from Assorted Laboratory Organic Waste Solutions Using Centrifugal Contactors, D.R. Prabhu, **Neelam Kumari**, and P.N. Pathak, in the proceedings of conference ***SESTEC-2012*** held in SVKM's Mithibai College during February 27 – March 1, 2012.
15. Comparison of Third-phase Formation Tendency of Tri-n-butyl Phosphate and Dialkyl Amides During Thorium Extraction from Nitric Acid Medium: Dynamic Light Scattering Studies. **Neelam Kumari** and P.N. Pathak, in the proceedings of conference ***NUCAR-2013*** held in Govt. Science College, R. D. University, Jabalpur during February 19-23, 2013.

SYNOPSIS

In view of the increasing demand of electricity in developing countries like India, there is a need for identifying potential sources of energy. However, there is also a growing concern to save our planet from Carbon emissions and green house gases which are inevitable till a viable alternative to fossil fuels is available. Green house gas emissions are significantly lower for electricity produced by nuclear fuels *vis-à-vis* fossil fuels. Due to limited resources of natural fissile isotope ^{235}U, future nuclear power plants are expected to depend on the manmade fissile materials like ^{233}U and ^{239}Pu. The spent nuclear fuel emanating from reactor is either directly disposed off in the deep geological repositories (once through fuel cycle) or is reprocessed for the recovery of valuables like ^{239}Pu and ^{233}U (closed fuel cycle). High Level Waste (HLW) is proposed to be vitrified and disposed in the repositories without/with actinide partitioning.

Closed fuel cycle is one of the viable strategies for enhancing the nuclear fuel utilization. India has opted for the closed nuclear fuel cycle option to sustain its nuclear power program. The challenging task of recovery and purification of ^{239}Pu from irradiated U and of ^{233}U from irradiated Th are accomplished presently by the well known *PUREX* (Plutonium Uranium Reduction EXtraction) and *THOREX* (THORium uranium EXtraction) processes, respectively [**1**]. These processes employ tri-*n*-butylphosphate (TBP) dissolved in long chain aliphatic hydrocarbon viz. *n*-dodecane, as the solvent. Though TBP has been the workhorse of nuclear fuel reprocessing industry for the last five-six decades, yet a few drawbacks associated with the use of TBP have caused concern to the separation scientists and technologists. The main problems of TBP are: (i) its vulnerability to high radiation field and deleterious nature of its degradation products (mainly monobutyl phosphoric acid, H_2MBP and dibutyl phosphoric acid, HDBP)

adversely affecting the product recovery, (ii) poor fission product decontamination particularly with respect to fission products like Zr and Ru, (iii) relatively lower distribution coefficient of Pu(IV) as compared to that of U(VI), (iv) third-phase formation tendency under loading condition of tetravalent actinides such as Th(IV) and Pu(IV), (v) its solubility towards aqueous phase, and (vi) non-incinerable nature of the spent solvent yielding large volumes of secondary radioactive waste. These shortcomings are of serious concern particularly during the reprocessing of (i) short cooled mixed oxide (MOX) thermal reactor spent fuels, (ii) fast reactor spent fuels containing larger Pu content and significantly higher burn up, and (iii) thorium based reactor spent fuels. Sustained efforts are desirable to overcome at least some of these problems.

Based on pioneering work of Siddall, *N*,*N*-dialkyl amides have been identified as alternative extractants of TBP [**2-9**]. The amide family of compounds complies with the CHON principle, and is therefore completely incinerable resulting in a restricted volume of secondary waste generated. The physico-chemical properties of amides can be suitably modified by the judicious choice of the alkyl groups. This class of extractants offers better fission product decontamination as compared to that of TBP.

N,*N*-dihexyloctanamide (DHOA) has been identified as a promising alternate to TBP in spent nuclear fuel reprocessing of Pressurized Heavy Water Reactor (PHWR). However to our knowledge, DHOA has not been evaluated for the reprocessing of fast reactor and Advanced Heavy Water Reactor (AHWR) spent fuels. Present work compares the performance of DHOA *vis-à-vis* TBP as extractants for reprocessing of fast reactor and AHWR spent fuel dissolver solutions under simulated conditions. Extraction data have been generated by batch experiments as well as by mixer settler/centrifugal contactors under the relevant conditions of fast reactors and AHWR fuels, respectively.

The effects of high radiation field of short cooled fast reactor and thorium based AHWR fuels on the process performance of this extractant are also investigated.

The thesis has been divided in seven chapters. A brief description of each chapter is given below:

Chapter 1: General Introduction

This chapter provides a general introduction to nuclear fuel cycle, Indian nuclear power program, comparison of PUREX and THOREX processes, chemistry of actinides, different methods for actinides separations, basic principles of solvent extraction, classification of extractants, criteria for selecting extractants, and different extractants used in nuclear hydrometallurgy. A brief discussion on the factors influencing the distribution ratio of metal ions is also included. Salient features of *N*,*N*-dialkyl amides as extractants along with several studies on their evaluation for spent fuel reprocessing are summarized. Third-phase formation phenomenon during metal/acid extraction is discussed. The basic principles underlying co-current, counter-current (mixer settler and centrifugal contactor) runs for metal extractions are described. The importance of radiolytic and thermal degradation studies of different extractants in nuclear fuel reprocessing is highlighted. Finally, the scope of the thesis regarding the evaluation of *N*,*N*-dialkyl amides for spent fuel reprocessing is presented.

Chapter 2: Experimental

Different experimental methods and instrumental techniques used in present study have been discussed in this chapter. The preparation and purification methods of the radiotracers such as Pu (^{239}Pu as principal isotope), ^{237}Np, ^{233}Pa and ^{233}U in present studies have been described. Batch distribution studies of different radionuclides have

been carried out by equilibrating known volumes of organic and aqueous phases in stopper glass tubes at constant temperature in a water bath. The assay of gamma-emitting radiotracers was carried out by gamma spectrometry employing NaI(Tl) and HPGe detectors. The estimation of alpha and beta-emitting isotopes was performed by liquid scintillation counter. The basic principles and working of these detectors have been mentioned in this Chapter. UV-visible absorption spectrophotometry has been used for analysis of lower concentrations of Th and U. The complexometric titrations and Davies-Gray carried out for the analysis of thorium and uranium, respectively, are also mention in this chapter. A brief discussion about mixer-settler, centrifugal contactor and Zetasizer-3000 DLS spectrometer (aggregate size measurements during third-phase formation studies) also included.

Chapter 3: Evaluation of *N,N*-dihexyloctanamide for reprocessing of Pu rich fuels

This chapter presents the batch as well as mixer settler studies for uranium and plutonium extraction and stripping to evaluate DHOA *vis-à-vis* TBP for the reprocessing of Pu rich fuels. These studies show that uranium extraction using DHOA as extractant is comparable to that of TBP; however, it displays better stripping behavior than TBP. Plutonium extraction behavior is better in the case of DHOA as compared to that of TBP. Even though Pu stripping is better in the case of DHOA, mixer settler runs indicate towards the need of reducing agent in the stripping cycle for both the extractants. Quantitative Pu stripping can be achieved employing 0.5 M NH_2OH in 0.5 M HNO_3 in the case DHOA in single contact. By contrast, 3-4 contacts are required for complete removal of plutonium from loaded TBP phase.

Counter-current centrifugal contactors runs have been performed for uranium extraction studies from feed solutions of varying compositions employing TBP and

DHOA as extractants. These runs have demonstrated that DHOA is a promising alternative of TBP for various hydrometallurgical operations dealing with recovery of uranium from solutions of various origins including spent fuel dissolver solutions.

In addition, Tc extraction behavior has been studied using DHOA and TBP solutions in *n*-dodecane, under varying experimental conditions such as acidity, extractant concentration and uranium loading (50 g/L, Pu rich spent fuel feed solutions). The effect of acetohydroxamic acid concentration on U, Pu, Np, and Tc extraction behavior has also been investigated. Pu(IV)- Acetohydroxamic acid (AHA) interaction and its influence on extraction using TBP and DHOA extractants has been studied spectrophotometrically. The experimental results suggest that 1.1 M DHOA is better than 1.1 M TBP with respect to co-extraction of Tc and U, and U decontamination with respect to Np/Pu.

Chapter 4: Extraction studies of ^{237}Np using *N,N*-dihexyloctanamide

Neptunium-237 is an important nuclide formed during the irradiation of uranium in PHWR as well as in fast reactors from nuclear waste management point of view because of its long half-life and high radiotoxicity. This chapter deals with Np extraction studies as a function of nitric acid concentration (0.5-6 M), uranium loading (50 and 300 g/L relevant to Pu rich and PHWR spent fuels) in the presence of either oxidizing ($K_2Cr_2O_7$) or reducing agents (Fe(II)) using DHOA and TBP as extractants. DHOA shows comparable extraction behavior for Np to TBP at higher acidities ($\geq$ 3 M HNO_3) and better stripping behavior at lower acidity. The stoichiometry of the extracted species of Np(IV) and Np(VI) in the organic phases have been found as $Np(NO_3)_4 \cdot 3A$ and $NpO_2(NO_3)_2 \cdot 2A$, where A = DHOA.

The conditions for co-recovery of U, Pu, and Np have been optimized using 1.1M TBP and 1.1M DHOA dissolved in *n*-dodecane as solvents under PHWR-HLW conditions for simplifying the subsequent actinide partitioning steps.

Chapter 5: Evaluation of *N,N*-dihexyloctanamide for Advanced Heavy Water Reactor spent fuel reprocessing

AHWR is being designed for the utilization of vast resources of Th in India. The spent fuel of AHWR will also contain Th, in addition to U ,Pu , minor actinides and fission products [**10**]. This chapter describes distribution studies of Th(IV), Pa(V), U(VI) and Pu(IV) under simulated AHWR spent fuel feed conditions employing TBP and DHOA. Batch experiments as well as counter-current mixer settler runs have been carried out on a simulated AHWR feed [~2 g/L U + Pu tracer + 100 g/L Th + 0.03 M HF + 0.1 M $Al(NO_3)_3$ at ~3.5 M HNO_3] using 0.18 M TBP and 0.36 M DHOA/*n*-dodecane as extractants. A reprocessing scheme has been proposed for the reprocessing of three component (U, Pu and Th) AHWR spent fuels. Radiolytic degradation and hydrodynamic parameters of 0.36 M DHOA are also evaluated *vis-à-vis* 0.18 M TBP in *n*-dodecane.

Dynamic Light Scattering (DLS) studies have been carried out to investigate the aggregation behavior of 1.1 M solutions of TBP, DHOA and of *N,N*-dihexyl decanamide (DHDA) in *n*-dodecane equilibrated with varying concentrations of nitric acid (0.1-6 M) and of Th (10-200 g/L). There is a gradual increase in thorium extraction with increased aqueous phase acidities. A significant enhancement in the aggregate sizes is observed with increasing concentration of thorium in the organic phase. The effect of 1-octanol as phase modifier has also been investigated on the aggregation behavior of extracted species for TBP system.

The effect of uranium extraction on third-phase formation behavior from aqueous phases containing $1x10^{-2}$-0.1 M U(VI) + 0.86 M Th(IV) at 4 M HNO_3 has been studied using 1.1 M TBP and 1.1 M DHOA solutions in different diluents viz. *n*-dodecane, 10% 1-octanol + *n*-dodecane, and decahydronaphthalene (decalin). Third-phase formation has been observed in both the extractants using *n*-dodecane as diluent. There is a gradual decrease in Th(IV) concentration in the third-phase (Heavy Organic Phase, HOP) with increased aqueous U(VI) concentration. An empirical correlation has been developed for predicting the concentrations of uranium and thorium in HOP for both the extractants. No third-phase has been observed during the extraction of uranium and thorium from the aqueous phases employing 10% 1-octanol + *n*-dodecane, or decalin as diluents.

Chapter 6: Thermal degradation studies of *N,N*-dihexyloctanamide/*n*-dodecane solvent

Thermal decomposition studies of DHOA/*n*-dodecane system are described in this chapter. These studies have been carried out to understand the possible run-away reaction and red-oil formation in nitric acid medium [**11**]. Single phase experiments have been performed in an adiabatic calorimeter, ARSST (Advanced Reaction System Screening Tool) using pure DHOA, 0.36 M and 1.1M DHOA/*n*-dodecane solutions (sample size: 30-50 mg) under different conditions. Pressurization of DHOA/*n*-dodecane-HNO_3 mixtures has been found ~10-15 bars/g. Decomposition reaction initiation temperature is ~410-420 K. ARRST run have also been performed on aqueous acidic samples to find total pressurization. Typically, total pressurization in case of aqueous sample containing 0.36M DHOA/*n*-dodecane is approximately 10 bars/g whereas in case of aqueous sample containing 1.1 M DHOA/*n*-dodecane is ~12 bars/g.

Chapter 7: Summary and conclusions

The present research work deals with evaluation of *N,N*-dialkylamides as alternative extractants to TBP for spent nuclear fuel reprocessing and waste management. DHOA shows better extraction ability for Pu and extraction of U is comparable to TBP. DHOA shows better stripping behavior for U, Pu and Np as compared to TBP. DHOA was found to be good extractant for the reprocessing of fast reactor spent fuels, thorium based fuels reactor (AHWR), short cooled reactor as compared to TBP. A process flow sheet has been developed for the reprocessing of AHWR spent fuels under simulated conditions. DLS studies show a gradual increase in the aggregate sizes with increasing concentration of thorium in the organic phase. Radiolytic and thermal degradation studies have shown that DHOA is a promising alternative of TBP for spent fuel reprocessing.

References

1. W.W. Schulz, L.L. Burger, J.D. Navratil and K.P. Bender (Eds.), "Science and Technology of Tributyl Phosphate", Vol. 3, CRC Press, Inc., Boca Raton, (1990).
2. T.H. Siddall III, Applications of Amides as Extractants, Savannah River Laboratory, USAEC Report, DP – 541, (1961).
3. G.M. Gasparini and G. Grossi, Solv. Ext. and Ion Exch., 15(4), 825, (1980).
4. C. Musikas, Sep. Sci. Technol., 23, (12-13), 1211, (1988).
5. G. Thiollet, C. Musikas, Solv. Extr. Ion Exch., 7 (5), 813, (1989).
6. C. Musikas, Inorg. Chim. Acta, 14, 197, (1987).
7. N. Condamines, C. Musikas, Solv. Ext. and Ion Exch., 10(1), 69, (1992).
8. C. Musikas, Min. Process. Extr. Metal. Review, 17(4), 109, (1997).
9. V.K. Manchanda, P.N. Pathak, Sep. and Purif. Technol., 35, 85, (2004).
10. R.K. Sinha, A. Kakodkar, Nucl. Engg. Design, 236, 683, (2006).
11. T.S. Rudisill, W.J. Crooks, III Sep. Sci. Technol., 38(12,13), 2725, (2003).

LIST OF FIGURES

Page No.

CHAPTER-III

CHAPTER-VI

LIST OF TABLES

CHAPTER III

CHAPTER IV

CHAPTER V

CHAPTER 1: GENERAL INTRODUCTION

The growing energy demand with world population and depleting fossil fuels like coal, petroleum etc. has necessitated the exploration of alternative sources. Wind, solar, hydro and nuclear energies have been identified as alternative sources and being harnessed for power generation. Among these sources, nuclear energy appears quite attractive, as very large amount of energy is released from a given amount of nuclear fuel and small amount of waste is generated per unit production of the electrical energy. Enormous amount of energy is released by neutron induced fission of fissile materials like ^{235}U, ^{239}Pu. The nuclear reaction is utilized to obtain the controlled release of energy in the nuclear power reactors. The future nuclear energy program is largely dependent on the availability of the man-made fissile materials like ^{233}U and ^{239}Pu due to limited natural resources of the fissile materials like ^{235}U. India has opted for closed fuel cycle to sustain nuclear power program beyond the availability of naturally occurring ^{235}U. The closed fuel cycle emphasizes on the recycling of the spent fuel. During reprocessing of the spent fuel, in the closed fuel cycle, the valuables like plutonium and uranium are recovered by a hydrometallurgical process, leaving behind highly radioactive liquid waste solution, referred to as High-Level Waste (HLW).

1.1. Nuclear fuel cycle

Closed nuclear fuel cycle comprises of front-end and back-operations. The front-end includes various stages like mineral exploration, processing, purification of uranium/thorium fuel fabrication and reactor operation; while spent fuel reprocessing, radioactive waste management etc. are the back-end operations (Figure 1.1).

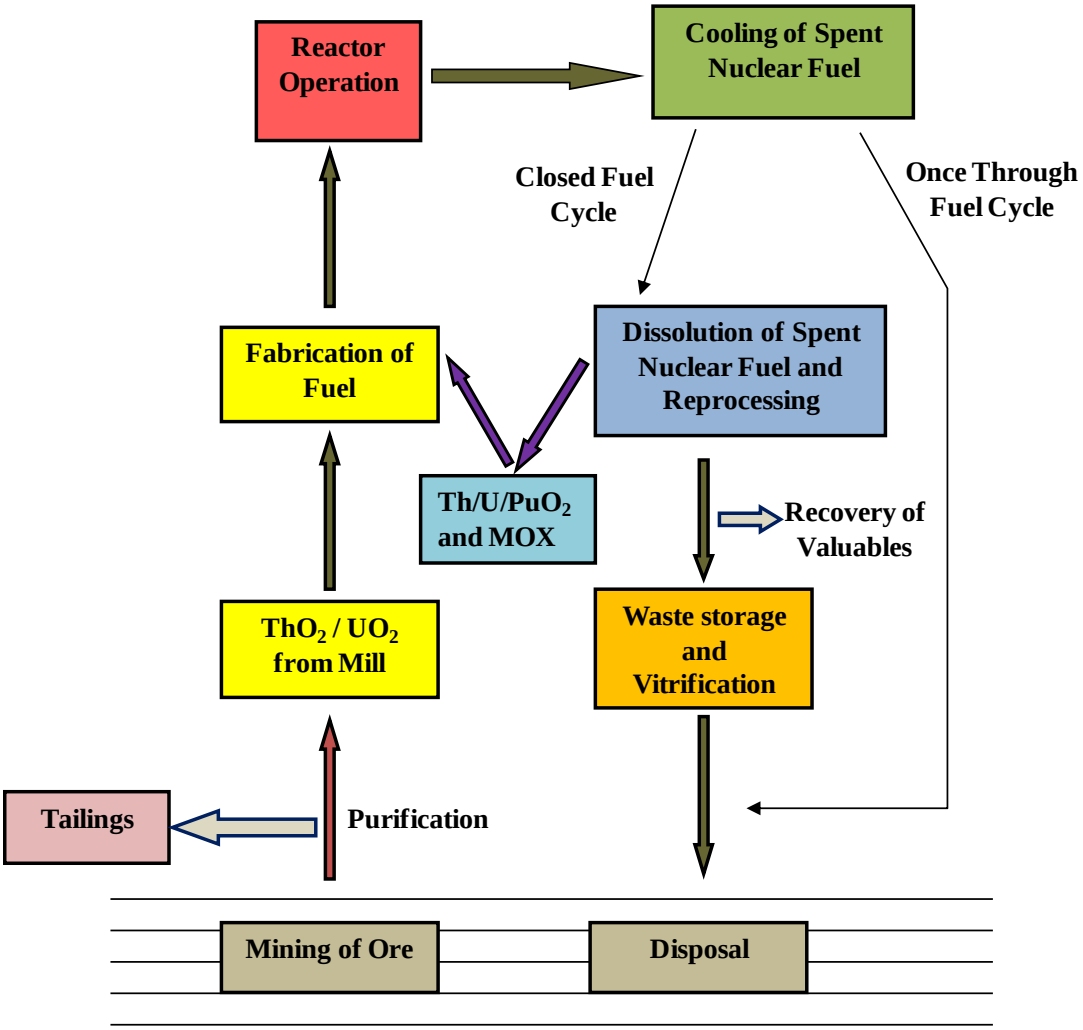

Fig. 1.1. Nuclear fuel cycle

Fission and transmutation reactions take place during the irradiation of nuclear fuel in the reactor. ^{235}U is the only naturally occurring fissile isotope. ^{238}U and ^{232}Th, the fertile isotopes, are converted to ^{239}Pu and ^{233}U, the fissile isotopes by the absorption of a slow neutron, respectively, as follows:

$$^{238}U + n \longrightarrow {}^{239}U \xrightarrow[23.5\ min]{\beta^-} {}^{239}Np \xrightarrow[2.3\ days]{\beta^-} {}^{239}Pu \qquad (1.1)$$

$$^{232}Th + n \longrightarrow {}^{233}Th \xrightarrow[22\ min]{\beta^-} {}^{233}Pa \xrightarrow[27\ days]{\beta^-} {}^{233}U \qquad (1.2)$$

^{239}Pu absorbs a neutron to form ^{240}Pu, which also undergoes fission. In nuclear fission, mass loss occurs with the liberation of corresponding amount of energy (~200 MeV/fission/^{235}U atom) [**1**]. 2-3 neutrons are emitted during fission of fissile element in which one is utilized in bringing about the fission of another heavy atom. This can be controlled to generate a self-sustaining controlled chain reaction in nuclear reactor for the generation of energy or neutrons for research and isotope production. These nuclear reactors can be categorized on the basis of their applications, energy of neutrons and coolant / moderator system. Reactor used for energy generation are called "*power reactor"*. Reactors which are used for the studies involving neutron beams for understanding the physical and chemical nature of materials as well as for the production of isotopes are commonly referred to as "*research reactors*". In "*thermal reactor***"** a moderator is used to slow down the neutrons; However, there is no requirement of moderator and sufficient quantity of fissile isotope concentration is required in the fuel to sustain the fission chain reaction in "*fast reactors*".

1.2. Indian nuclear power programme

Natural uranium reserves of India are (~172,000 tons of U_3O_8) while thorium are quite adequate (~650,000 tons) [**2, 3**]. In view of this, India's nuclear power programme is based on a unique mix of uranium and thorium resources available in the country. Keeping this in mind, future nuclear power programme of India is broadly divided in to three interlinked stages:

1. In the first stage, the ^{235}U component of natural uranium not only undergoes fission but also causes ^{239}Pu production from the fertile ^{238}U. Projected resources of natural uranium can be used to install about 10,000 MWe of *Pressurized Heavy*

Water Reactors (PHWRs). At present, 20 nuclear reactors are in operation and are generating 4,780 MW energy [**4**] The PHWR discharged fuel contains on an average about 0.35 % by weight of plutonium of which ~70 % is fissile. The discharged fuel contains unutilized uranium i.e. ~0.2 % ^{235}U and the rest ^{238}U called is "*depleted uranium*".

2. The second stage of the power programme envisages a series of *Fast Breeder Reactors* (FBRs). Plutonium and depleted uranium from the first stage would be used in these reactors. These reactors are capable of generating more fuel than being consumed, and thus technically capable of growing the nuclear capacity to as much as ~3,50,000 MWe. After establishing significant FBRs from bred Pu, thorium can be introduced at an appropriate time during the second stage of the programme in the "*blankets*" of FBRs to produce ^{233}U, which will be employed in the third stage of the power programme.
3. The third stage of nuclear power programme will utilize thorium and ^{233}U in reactors. For effective utilization of thorium and bred ^{233}U, the following technologies should be essential to develop: (a) processing of thorium ore to get nuclear grade material, (b) design of suitable reactor, (c) design and fabrication of thorium based fuels, (d) reactor physics analysis of thorium based fuel, (e) post irradiation examination to prove the related reactor physics and to gain irradiation experience, (f) reprocessing of irradiated thorium, and (g) fabrication of reprocessed fuel involving ^{233}U.

1.3. Characteristics of thorium fuel

The third stage reactor will be based on the thorium fuel. Therefore, it is important to know the characteristics of thorium fuel.

1.3.1. Physical Characteristics

The thermal conductivity of ThO_2 is higher than that of UO_2. As a result, fuel temperatures for thorium fuel will be lower than that of uranium resulting in reduced fission gas release. The thermal expansion coefficient of ThO_2 is less as compared to UO_2 inducing less strain in the fuel clad. Thus ThO_2 retains dimensional stability at high burn ups. It is very stable oxide and does not oxidize, resulting in less release of fission products in the coolant, in the event of clad breach. The fission product release rates for ThO_2 are one order of magnitude lower than that of UO_2. Fuel deterioration is slower allowing the fuel to reside in the reactor for higher periods of operation. To summarize, thorium as a fuel material has improved physical properties and has higher radiation resistance than uranium.

1.3.2. Nuclear Characteristics

The nuclear characteristics of thorium have an immense bearing on the selection and development of technologies associated with thorium fuel cycle. On irradiation in a reactor, neutron capture by ^{232}Th leads to the formation of fissile isotope ^{233}U (Equation 1.2). Long- lived minor actinides resulting from the burn-up chain are in much less quantity for thorium fuel cycle, if the reactor operates purely in the ^{233}U-Th cycle. Actinides having masses beyond 237 are produced in negligible quantities. This is an important advantage, as the burden of management of long-lived radioactive waste is significantly reduced. Absorption cross section (σ_a) for thorium is considerably higher than that for ^{238}U [$\sigma_a(Th) = 7.4b$; $\sigma_a(^{238}U) = 2.73b$ where b = barns (10^{-24} cm^2)]. It is clear that ^{232}Th offers greater competition to capture of the neutrons and as such a lower proportion of the neutrons will be lost to structural and parasitic materials. This improves

the conversion of ^{232}Th to ^{233}U as compared to that of ^{238}U to ^{239}Pu. This also means that, to ensure criticality for a given reactor the fissile content of Th based fuel should be at least 2 times as high as that needed for U based fuel [**5**].

Importance of a fissile isotope can be obtained from the parameter 'number of fission neutrons produced per neutron absorbed in a fissile isotope' commonly referred to as "*eta*" (η) value. As can be seen from Table 1.1, the highest eta value of 2.28 for ^{233}U in thermal neutron flux allows an equal amount of ^{233}U to be produced to that which is destroyed [**6**]. A "*conversion ratio*" (ratio of fissile isotopes produced to the fissile isotopes consumed) of unity can therefore be achieved in thermal reactors. Production of the fissile isotopes depends on the conversion ratio as well as the burn up of the fuel. Reactors in which the conversion ratio exceeds unity are called "***breeder reactors***".

Table 1.1: Nuclear data of fissile isotopes for thermal and fast reactors

Nuclear data	^{233}U		^{235}U		^{239}Pu	
	Thermal	Fast	Thermal	Fast	Thermal	Fast
σ_F	527	2.8	579	2.0	741	1.9
σ_C	54	0.3	100	0.5	267	0.7
n/fission (ν)	2.5	2.5	2.4	2.5	2.9	2.9
η	2.28	2.5	2.06	2.2	1.94	2.6

On irradiation of thorium, in situ ^{233}U concentration increases. The multiplication factor, K_∞, of a thorium fuel increases with irradiation but never rises beyond 0.95 [**7**]. Even though thorium begins to generate fissile ^{233}U, it is essential to invest some fissile materials like Pu, ^{235}U or ^{233}U along with it for sustained conversion of thorium to ^{233}U.

1.4. Thorium based nuclear reactors

In view of the high eta value of 2.28 for ^{233}U in thermal neutron flux, only thermal reactor system is being considered for the thorium fuel cycle. The different thermal reactors in which Th - ^{233}U fuels have been considered are the following [**8**]:

(a) Light Water Reactor (LWR): This reactor comprises the Seed and Blanket system (S&B), the Spectral Shift Controlled (SSC) and the normal LWR. The first depends on changing leakage for long-term reactivity control, the second depends on changing neutron spectrum, and the third on neutron poisons. As a result, the first two systems manage to save all the neutrons that are wasted in poisons in LWR, and make use of them in the conversion of fertile material to fissile [**9**].

(b) High Temperature Gas Cooled Reactor (HTGCR): Owing to the comparatively higher average energy of thermal neutrons in a HTGCR, the "*eta value*" of both ^{235}U and ^{239}Pu would be lower than in other types of thermal reactors. In view of its high eta value and insensitivity to neutron energy, ^{233}U based thermal reactors would be a suitable choice. High thermal efficiency, the ability to produce process heat at high temperatures (1500 ^{o}F) and relatively efficient use of natural uranium resources when fed with thorium as fertile material highlight HTGCR as a possible candidate for future commercial use. The reactor core consists of hexagonal blocks of graphite. Power generation in this type of reactor would be from ThC_2 + UC_2 where uranium enrichment should be ~ 93%. Graphite is used as cladding material and moderator. '***He***' gas works as the coolant [**10**].

(c) Molten Salt Breeder Reactor (MSBR): This is based on circulating fluid fuel. The fuel is molten fluoride of uranium and thorium which flows through tubes passing through graphite blocks. On-line reprocessing removes fission products, and thereby losses of neutrons are minimized [**11**]. Since the circulating fuel spends quite a long time

outside neutron flux, the probability of ^{233}Pa decaying to ^{233}U rather than getting converted to ^{234}Pa through neutron absorption is increased. On both counts, breeding ratio increases resulting in a thermal breeder, even though the breeding ratio may not be very high.

(d) Aqueous Suspension Reactor (ASR): The advantages of MSBR come from circulating fuel. Its disadvantages come from the highly chemically reactive molten fluoride used as fuel material. A successful attempt has been reported to replace the molten fluoride with slurry of thorium oxide in water [**12**].

(e) Pressurized Heavy Water Reactor (PHWR): The PHWR is the work horse of the Indian nuclear power programme. The cycles studied for this reactor include the self sustaining cycle, the high burn up cycle, and the once through thorium cycle. Besides this, thorium has been already used for initial power flattening [**13**]. Studies have also been carried out on combined loading of (U,Pu) mixed oxide (MOX) with natural thorium in PHWR [**14**].

(f) Advanced Heavy Water Reactor (AHWR): The Indian Advanced Heavy Water Reactor (AHWR) is designed and developed to achieve large-scale use of thorium for the generation of commercial nuclear power [**15, 16**]. This reactor will produce most of its power from thorium, with no external input of ^{233}U in the equilibrium cycle. The AHWR is a 300 MWe, vertical, pressure tube type, boiling light water cooled, and heavy water moderated reactor. The reactor incorporates a number of passive safety features and is associated with a closed fuel cycle having reduced environmental impact. AHWR contains 30 (Th,^{233}U) MOX pins and 24 (Th,Pu) MOX pins. The composite cluster consists of a circular array of 54 fuel pins. The fuel assembly has a central structural tube made of Zircaloy-2. The inner and middle ring of 12 and 18 pins contain (Th,^{233}U) MOX

and the outer ring of 24 pins contain (Th, Pu) MOX. The inner ring of 12 pins has a ^{233}U content of 3.0% by weight and the middle ring of 18 pins has 3.75% ^{233}U. The outer ring of (Th,Pu) MOX pins have average of 3.25% by weight of total plutonium. The lower half of the active fuel will have 4.0 % Pu and the upper part will have 2.5 % Pu. In closed nuclear fuel cycle, Th, inbread ^{233}U, and Pu will be recovered spent fuel.

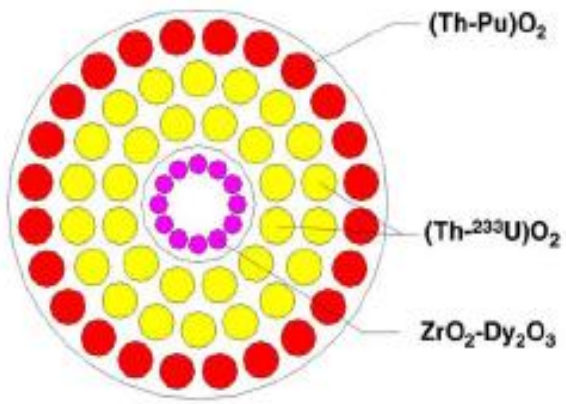

Fig. 1.2. AHWR fuel composition: 54 pins fuel cluster

The fuel will be reprocesses followed by pin-segregation as (Th-$^{233}U)O_2$ and (Th-Pu)O_2 pins, and chopping. ThO_2 and, the dissolution of the fuel will also be a major challenge. At present, due to inert nature of ThO_2, this fuel is dissolved in concentrated nitric acid in the presence of fluoride. $Al(NO_3)_3$ is added to suppress the corrosive nature of fluoride and to prevent precipitation of thorium tetrafluoride. (Th-$^{233}U)O_2$ fuel-pins will require two way Th-^{233}U separation, whereas, the (Th-Pu)O_2 fuel-pins will require the three-way separation of Th-^{233}U-Pu. **THOREX** (THORium uranium EXtraction) cycle separates uranium from thorium, whereas **PUREX** (Plutonium Uranium Reduction EXtraction) cycle separates plutonium and uranium from spent fuels [**3, 17**]. In AHWR spent fuel reprocessing, these two processes will be combined together and three-way separation of Th-^{233}U-Pu apparently will be assumed. The inbread ^{233}U recycled, and at

equilibrium the two inner rings of the assembly will be replaced by (Th-^{233}U)O_2 fuel-pins (30 pins) [**18**].

(g) A Thorium Breeder Reactor (ATBR): This is a new reactor concept which proposes the induction of thorium in an enriched uranium reactor [**19**]. Each fuel assembly consists of an enriched uranium seed zone and a thoria blanket zone. This is a heavy water moderated reactor, where boiling light water is used as the coolant. The ^{235}U enrichment is about 5%.

1.5. Thorium Fuel Reprocessing: THOREX Process

Recovery of ^{233}U from irradiated thorium and fission products is necessary for power generation in thorium fuel cycle. Investigations show that solvent extractions have feasibility for this purpose. In thorium fuel cycle, the probability of the formation of transuranium elements is much less during the irradiation of thorium. The reprocessing of spent thorium based fuels has been proposed to be done by THOREX process, using tributyl phosphate (TBP) as the extractant. THOREX process has not matured to the same extent as the PUREX largely due to lack of its immediate use in the technologically developed countries [**20**]. Due to highly stable nature of thorium oxide, the dissolution step is more complicated in thorium fuel reprocessing. Some of the aspects of the THOREX process which call for special attention are:

I. Difficulty in dissolution of irradiated thorium.
II. ^{233}Pa, formed by neutron capture of ^{232}Th, decays to ^{233}U with a half life of 27.4 days. This necessitates a longer cooling period for the complete recovery of ^{233}U in one step.

III. The radioactive contamination from ^{232}U in the separated ^{233}U product and from ^{228}Th in the separated thorium product will have to be taken into consideration, while handling these products.

The major steps in the reprocessing of thorium fuel by THOREX process are as follows:

1.5.1. Head end processes

(A) Decladding: NaOH and $NaNO_3$ are used for aluminum clad thorium fuel for chemical decladding. The soluble sodium aluminate formed can be disposed as medium active waste and the off gas is mainly ammonia. For the zircaloy-clad fuel, mechanical chop-leach process is employed.

(B) Dissolution of irradiated thorium fuel: For the dissolution of thorium in nitric acid small amount of fluoride has to be added [**21**]. Appropriate amounts of aluminum (in the form of $Al(NO_3)_3$) has to be added to complex the excess fluoride thus limiting the concentration of free fluoride ion, to overcome the corrosion of stainless steel [**22**]. Once the dissolution is initiated, thorium present in macro amounts can also form strong complex with fluoride and will help in the reduction of free fluoride ion concentration. Thorium metal dissolves without much difficulty in 10-15 M HNO_3 containing HF (~0.03 M). During the dissolution of zircaloy-clad thorium fuel, dissolution of the zirconium clad takes place to a small extent along with the thorium fuel and this has to be taken into account during subsequent solvent extraction steps [**23**].

1.5.2. Extraction process

5% TBP has been used as extractant for the selective extraction of ^{233}U in BARC (Bhabha Atomic Research Centre). 30-45 % TBP has been employed for co-extraction of Th and

^{233}U. However, co-extraction of thorium and ^{233}U leads to "*third-phase formation*" [**24**]. This refers to a phenomenon in solvent extraction, in which the organic (extractant) phase splits into two phases. One of the phases is diluent rich, whereas the other is rich in extractant and also contains the metal solvate. The latter is commonly referred to as the "*third phase*" [**25**]. It depends on a number of factors like the initial thorium content, salt content and acidity of the aqueous and organic phases, temperature during the extraction, and the concentration of the \extractant and the nature of the diluents used. The solvent loading of TBP phase with thorium is restricted in THOREX process to avoid third phase formation.

1.5.3. Tail end purification

After one cycle of extraction, scrubbing and stripping, the aqueous ^{233}U stream contains significant amount of thorium, minor quantities of other actinides and fission products. Further purification is achieved by additional extraction cycles employing low percentages of TBP or by ion exchange. At BARC, the tail end purification of the product ^{233}U from thorium, carried out by an anion exchange process during the reprocessing of CIRUS reactor's thoria fuel assemblies, has certain disadvantages such as (a) change from nitrate to chloride medium, (b) corrosion of the equipment, (c) gassing of the column due to the high concentration of hydrochloric acid, and (d) poor decontamination factor from the corrosion product, Fe. To alleviate these problems, three alternative methods have been tested for the purification of product ^{233}U.

I. Anion exchange in hydrochloric acid / acetic acid medium for selective sorption of uranium as its anionic acetate complex [**26, 27**].

II. Cation exchange in nitric acid for preferential sorption and removal of tetravalent thorium [28].

III. Precipitation and separation of thorium from ^{233}U as oxalate [**29, 30**].

The cation exchange method was found suitable for application as a continuous process in a plant scale operation.

1.6. PUREX process

PUREX is an aqueous reprocessing process which is used for the recovery of uranium and plutonium from spent nuclear fuels. This method is universally followed in nuclear reprocessing plant all over the world. This process was developed by Anderson and Asprey at the Metallurgical Laboratory at the University of Chicago, as part of the Manhattan Project [**31**]. In PUREX process, the irradiated fuel is dissolved in nitric acid solution (dissolver solution). This dissolver solution treated with organic solvent TBP dissolved in an inert diluent (*n*-dodecane or kerosene). The PUREX process can be divided into seven major steps [**32**]:

1. De-jacketing of fuel sub-assembly, dissolution of spent fuel in Nitric acid and feed preparation.
2. Recovery of uranium and plutonium from fission products.
3. Partitioning of uranium and plutonium.
4. Plutonium purification cycle.
5. Uranium purification cycle.
6. Solvent recovery.
7. Waste disposal and nitric acid recovery.

The PUREX process employs 30 % (v / v) TBP in an inert hydrocarbon diluents for extraction of uranium and plutonium over other actinides and fission products from the moderately concentrated (~3 M) nitric acid solutions [**17**]. During extraction, mass transfer takes place and, U(VI) and Pu(IV) are transferred to organic phase. These extracted metals are stripped back to aqueous phase by changing process parameters like acidity, and oxidation state. The fission products remain in the aqueous phase during the extraction step due to their poorer extraction.

The chemical reaction for U(VI) extraction from nitric acid medium is:

$$UO_2^{2+} + 2NO_3^- + 2TBP \leftrightarrow UO_2(NO_3)_2.2TBP \quad (1.3)$$

The Equation for the Pu in the +4 oxidation state is

$$Pu^{+4} + 4NO_3^- + 2TBP \leftrightarrow Pu(NO_3)_4.2TBP \quad (1.4)$$

By contrast, Pu(III) and other actinides and lanthanides in the +3 or lower oxidation states are not extracted in the PUREX Process. Partitioning of U and Pu is done by their oxidation state adjustment. Np(VI) present in the spent fuel can be co-extracted with the U and Pu. The highly selective extraction of the +4 and +6 oxidation states results in the effective utilization of the PUREX process for separation of uranium and plutonium from nearly all of the other metals present in the used nuclear fuel.

1.7. Comparison of PUREX and THOREX processes

The important factors in the THOREX process are (a) the extractability of Th(IV), Pa(V), U(VI) and the fission products from nitric acid medium, (b) poor Limiting Organic Concentration (LOC) of Th, and (c) the preparation of suitable feed solution from the irradiated thoria. Similar to the PUREX process, the fission products of significant extractability are Zr, Ru and Tc

Table 1.2: Salient features of PUREX and THOREX process

Feature	**PUREX Process**	**THOREX Process**
Feed composition	~300g/L U + ~1g/L Pu + M.A.+ F. Ps. in 3M HNO_3	~200g/L Th + ~200mg/L U + F. Ps. in 4M HNO_3
Extractant	30% TBP in *n*-dodecane	5% TBP in *n*-dodecane
Principal radionuclide	Pu (^{239}Pu)	U (^{233}U)
Precursor of principal radionuclides	^{239}Np ($T_{1/2}$ = 2.3d)	^{233}Pa ($T_{1/2}$ = 27d)
Separation schemes	• Co-extraction of Pu(IV) and U(VI) preferentially over M.A. and F.Ps. • Scrub cycle to improve D. F. from F.Ps. • Partition Pu(III) from U(VI) / U(IV)	• Preferential extraction of U(VI) over Th(IV) and F.Ps. • Scrub cycle to improve D.F. from Th as well as F.Ps.
LOC and stoichiometry of extracted species of the bulk elements	• > 120 g/L U • $UO_2(NO_3)_2$. 2TBP	• 30 g/L Th* • $Th(NO_3)_4$.3TBP
Radiologically important radionuclide	^{241}Pu - ^{241}Am (14.9y) (433y)	^{232}U - ^{228}Th (72y) (2y)

*M.A.: Minor Actinides, F.Ps.: Fission Products, D. F.: Decontamination Factor, *: 1.1 M TBP in n-dodecane*

Table 1.2 compares some of the salient features of PUREX and THOREX processes. Pu(III) is poorly extracted by 30% TBP so separation of U and Pu in PUREX process is based on the conversion of Pu(IV) to Pu(III). Selective extraction of U over Th is carried out using 5% TBP solution in *n*-dodecane in THOREX process. Decay products of ^{232}U – ^{228}Th (especially ^{212}Bi and ^{208}Tl) are hard gamma emitters which necessitates additional shielding arrangements during reprocessing as compared to that needed in the PUREX process in view of the softer gammas (60 keV) emitted by ^{241}Am.

1.8. Challenges in the fast reactor fuel reprocessing

In India, successful implementation of three stages nuclear programme calls for development of fast reactor fuel reprocessing technology for the recovery of plutonium which will be utilized for mix oxide (MOX) fuel fabrication for second and third stage nuclear reactors. Fast reactor fuel reprocessing has posed several challenges in implementation to plant scale both from process as well as equipment point of view. This is essentially due to high Pu inventory and its high specific activity. On the other hand, spent fuel from thermal reactors has low burn up, Pu content less than 1 %, and low fission product activity [**33**]. Because of this, issues related to equipment size and criticalities are to a lesser extent, than in fast reactor spent fuels. Due to high Pu content (~15 %) in fast reactor fuels equipment with low hold-up are required. Further solvent degradation (TBP) is more because of high specific activity of dissolver solution. In this context, centrifugal contactors (CE's) are being proposed due to their low contact time and low hold-up volume. Fabrication and remote maintenance of CE's and other equipment of fast reactor fuel reprocessing is another challenge as all process activities are carried in hot cells [**34**].

Short cooling in case of fast reactor fuels affects chemical stability of process solvents. TBP/*n*-dodecane, which is used as solvent in PUREX process, degrades easily in the case of fast reactor fuel reprocessing, compared to thermal reactor. This also poses a great challenge as high waste volume is generated which has to be managed later. To achieve higher decontamination factor, several cycles of extraction and stripping has to be used, which in turn increases process complexity and man-rem expenditure. In Indian context, the irradiated fuels discharged from *Fast Breeder Test Reactor* (FBTR) and future *Prototype Fast Breeder Reactor* (PFBR) have to be reprocessed with least delay to keep reactors running. Carbide fuel of FBTR is pyrophoric in nature which is another challenge during dissolution and requires organic destruction as organic acids produced during dissolution step otherwise they can create problems in extraction and stripping steps [**35, 36**].

1.9. Chemist's role in nuclear fuel cycle

Actinide complexes play a pivotal role at different stages of nuclear fuel cycle, viz. (a) recovery and purification from ores, (b) chemical quality control of nuclear fuels, (c) reprocessing of the spent fuel, (d) waste management, and (e) speciation and migration of actinides in the environment. Understanding the basic chemical, thermodynamic and kinetic behavior of actinides in solution in help us solving the problems, which are being encountered at the various stages of nuclear fuel cycle.

The objective of the present thesis is to investigate the distribution behavior of Th, U, Pu, Np and fission products using *N*,*N*-dialkyl amides as alternative extractant for their possible process applications. In this context, a brief description of the chemistry of actinides is desirable and hence is being given in the next section.

1.10. Chemistry of actinides

The actinide series are also known as the *"5f transition series"* due to successive addition of electrons to the empty 5f orbitals of the precursor element, contain fourteen elements from actinium (Ac, Z = 89) to lawrencium (Lr, Z = 103) in the Periodic Table. In these elements uranium (^{238}U, ^{235}U) and thorium (^{232}Th) have half lives (~$4.5x10^9$, $7.0x10^8$ and $1.4x10^{10}$ years) exceeding the estimated half life of the earth and hence occur in nature in appreciable amounts. Formation and decay of ^{227}Ac and ^{231}Pa depends on decay of their parent atom ^{235}U, a long-lived isotope. Other elements beyond U are man-made elements, though some evidence exists for trace occurrence of Np and Pu by nuclear reactions involving ^{238}U in nature. Among actinides, Pu and to a lesser extent Np, Cm, Am are produced in nuclear reactors and elements beyond Cm are produced in particle accelerators by bombardment of heavy transplutonium elements.

1.10.1. Electronic configuration

In actinides, 5f and 6d shells are of similar energy and the 5f electrons are so not well shielded as the 4f electrons. Table 1.3 represents the actual or predicted electronic configurations of actinide elements. The 6d shell is still preferred before the 5f shell at the beginning of the actinide series. These configurations are determined from an analysis of spectroscopic data obtained from the emission lines of neutral and charged gaseous atoms [**37**].

Table 1.3: Electronic configuration of actinide atoms and ions

Symbol	Gaseous atom	$M^{+}(g)$	$M^{2+}(g)$	$M^{3+}(g)$	$M^{4+}(g)$
Ac	$6d^{1}7s^{2}$	$7s^{2}$	$7s^{1}$	[Rn]	
Th	$6d^{2}7s^{2}$	$6d^{1}7s^{2}$	$5f^{1}6d^{1}$	$5f^{1}$	
Pa	$5f^{2}6d^{1}7s^{2}$	$5f^{2}7s^{2}$	$5f^{2}6d^{1}$	$5f^{2}$	$5f^{1}$
U	$5f^{3}6d^{1}7s^{2}$	$5f^{3}7s^{2}$	$5f^{3}6d^{1}$	$5f^{3}$	$5f^{2}$
Np	$5f^{4}6d^{1}7s^{2}$	$5f^{5}7s^{1}$	$5f^{5}$ (?)	$5f^{4}$	$5f^{3}$
Pu	$5f^{6}7s^{2}$	$5f^{5}7s^{1}$	$5f^{6}$	$5f^{5}$	$5f^{4}$
Am	$5f^{7}7s^{2}$	$5f^{7}7s^{1}$	$5f^{7}$	$5f^{6}$	$5f^{5}$
Cm	$5f^{7}6d^{1}7s^{2}$	$5f^{7}7s^{2}$	$5f^{8}$	$5f^{7}$	$5f^{6}$
Bk	$5f^{9}7s^{2}$	$5f^{9}7s^{1}$	$5f^{9}$	$5f^{8}$	$5f^{7}$
Cf	$5f^{10}7s^{2}$	$5f^{10}7s^{1}$	$5f^{10}$	$5f^{9}$	$5f^{8}$
Es	$5f^{11}7s^{2}$	$5f^{11}7s^{1}$	$5f^{11}$	$5f^{10}$	$5f^{9}$
Fm	$5f^{12}7s^{2}$	$(5f^{12}7s^{1})$	$(5f^{12})$	$(5f^{11})$	$(5f^{10})$
Md	$5f^{13}7s^{2}$	$(5f^{13}7s^{1})$	$(5f^{13})$	$(5f^{12})$	$(5f^{11})$
No	$5f^{14}7s^{2}$	$(5f^{14}7s^{1})$	$(5f^{14})$	$(5f^{13})$	$(5f^{12})$
Lr	$5f^{14}6d^{1}7s^{2}$	$(5f^{14}7s^{2})$	$(5f^{14}7s^{1})$	$(5f^{14})$	$(5f^{13})$

1.10.2. Actinide contraction

This is a consequence of the poor shielding of the 5f electrons, as there is a steady increase in effective nuclear charge and contraction in size of the electron cloud with increasing atomic number. Actinides have less ionization potential due to poor screening

as compared to lanthanide homologs, because of less electrostatic force. This behavior has played an important role in the complexation properties of actinides and their similarity with 4f and 5d elements. Table 1.4 exhibits the metallic and ionic radii of different actinides [**38**].

Table 1.4: Metallic and ionic radii (Å) of the actinides (M) and the interatomic distances in the actinyl (V) and actinyl (VI) ions; Co-ordination Number : 12 (metallic radii) and 6 (ionic radii)

Element	**M**	**M^{3+}**	**M^{4+}**	**M^{5+}**	**M^{6+}**	**M(V) - O**	**M(VI) - O**
Ac	1.88	1.076					
Th	1.80		0.984				
Pa	1.63		0.944	0.90			
U	1.56	1.005	0.929	0.88	0.83		1.71
Np	1.55	0.986	0.913	0.87	0.82	1.98	
Pu	1.60	0.974	0.896	0.87	0.81	1.94	
Am	1.74	0.962	0.888	0.86	0.80	1.92	
Cm	1.75	0.946	0.886				
Bk		0.935	0.870				

1.10.3. Solution chemistry of actinides

As the processes of separation and purification of actinides on large scale are essentially based on hydrometallurgical techniques, the study of solution chemistry of actinides has received considerable attention. The actinide elements exist in multiple

oxidation states and most of their separation processes are based on the effective exploitation of these properties. It is, therefore, desirable to understand the various oxidation states of actinides in solution.

1.10.3.1. Oxidation states

Actinides show multiple oxidation states due to lesser attraction from the nuclear charge than the corresponding 4f electrons of lanthanides, which exhibit mainly trivalent oxidation state. In the earlier members of actinide series, tetravalent state is more stable due to the smaller values of fourth ionization potential for 5f electrons as compared to 4f electrons of lanthanides, an effect which has been observed experimentally in the case of Th and Ce [**39**]. +3 oxidation states become dominant only for transplutonium elements. Different oxidation states of actinides are shown in Table 1.5 [**40**]. All the oxidation states are well known except +7 states for Np and Pu, which exist in alkaline solution [**41**]. Penta and hexavalent actinide ions exist in acid solution as oxygenated cations, viz. MO_2^+ and MO_2^{2+}.

Figure 1.3 shows the standard potentials of various couples in $HClO_4$ medium. In early actinides the standard potentials are so close that appreciable concentration of several oxidation states can coexist in the same solution. It has been found that the M^{3+}/M^{4+} and MO_2^+/MO_2^{2+} couples are reversible and fast as they involve the transfer of only single electron. On the other hand, the other couples are irreversible and achieve equilibrium slowly as they involve the formation or rupture of metal oxygen bonds.

Table 1.5: Oxidation states of actinides in aqueous solutions

89	90	91	92	93	94	95	96	97	98	99	100	101	102	103
Ac	Th	Pa	U	Np	Pu	Am	Cm	Bk	Cf	Es	Fm	Md	No	Lr
						(2)		(2)				(2)	(2)	
3	3	3	3	3	3	3	3	3	3	3	3	3	3	3
	4	4	4	4	4	4	4	4						
		5	5	5	5	5								
			6	6	6	6								
				7	7									

(Numbers with underline refer to the most stable oxidation states; Numbers in parantheses refer to the oxidation states which are not known in solution).

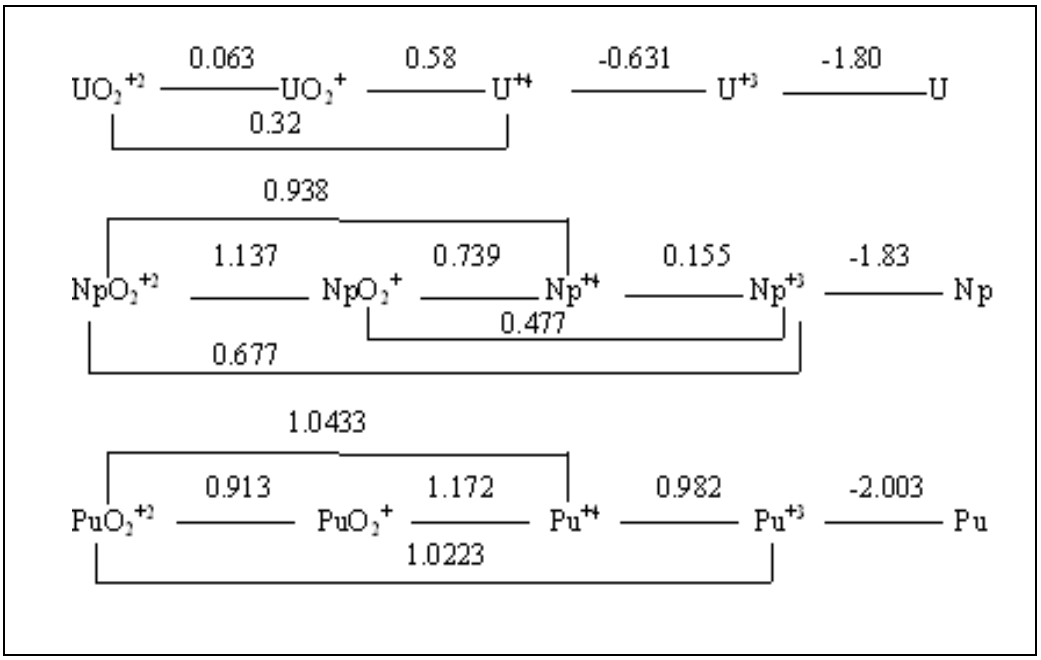

Fig. 1.3. Redox potential of actinide ions (volts); Medium: $HClO_4$

1.10.3.2. Disproportionation

This reaction is referred to as self oxidation reduction reactions which depend on the closeness of the electrode potentials of redox couples involved. In case of Pu, four oxidation states, viz. III, IV, V and VI are in equilibrium with each other. In general, disproportionation reactions of MO_2^+ (M = U, Pu or Np) ions can be represented as follows:

$$2MO_2^+ + 4H^+ \leftrightarrow M^{4+} + MO_2^{2+} + H_2O \quad (1.5)$$

It is clearly demonstrated from the equilibrium reaction (1.5) that the presence of hydrogen ion and complexing ions like F^- and SO_4^{2-}, which complex strongly with M^{4+} and MO_2^{2+} ions, have pronounced effect on disproportionation reactions. Table 1.6 shows equilibrium constants for the disproportionation reactions of U, Np, Pu and Am [**40**].

Table 1.6: Disproportionation reactions of actinides in aqueous solutions

Element	**Oxidation state**	**Reaction**	**log$K^{\#}$ (25^{o}C)**
U	V = IV + VI	$2UO_2^+ + 4H^+ \Longleftrightarrow U^{4+} + UO_2^{2+} + 2H_2O$	9.30
Np	V = IV + VI	$2NpO_2^+ + 4H^+ \Longleftrightarrow Np^{4+} + NpO_2^{2+} + 2H_2O$	-6.72
Pu	V = IV + VI	$2PuO_2^+ + 4H^+ \Longleftrightarrow Pu^{4+} + PuO_2^{2+} + 2H_2O$	4.29
	V = III + VI	$3PuO_2^+ + 4H^+ \Longleftrightarrow Pu^{3+} + 2PuO_2^{2+} + 2H_2O$	5.40
	IV + V = III + VI	$Pu^{+4} + PuO_2^+ \Longleftrightarrow Pu^{3+} + PuO_2^{2+}$	1.11
	IV = III + VI	$3Pu^{4+} + 2H_2O \Longleftrightarrow 2Pu^{3+} + PuO_2^{2+} + 4H^+$	-2.08
Am	IV + V = III + VI	$Am^{4+} + AmO_2^+ \Longleftrightarrow Am^{3+} + AmO_2^{2+}$	12.5
	IV = III + VI	$Am^{4+} + AmO_2^+ \Longleftrightarrow Am^{3+} + AmO_2^{2+}$	32.5
	IV = III + V	$2Am^{4+} + 2H_2O \Longleftrightarrow Am^{3+} + AmO_2^+ + 4H^+$	19.5

#: Equilibrium constant.

1.10.3.3. Hydrolysis and polymerization

In view of their large ionic potential, the actinide ions in various oxidation states exist strongly as hydrated ions in the absence of complexing ions. The actinide ions in divalent to tetravalent oxidation states are present as M^{2+}, M^{3+} and M^{4+}, respectively. The penta- hexavalent oxidation states are prone to more hydrolysis as compared to lower oxidation states. These oxidation states exist as partially hydrolyzed actinyl ions, viz. MO_2^{+} and MO_2^{2+} and can get further hydrolyzed under high pH conditions. The oxygen atoms of these ions are not basic in nature and thus do not coordinate with protons. The degree of hydrolysis for actinide ions decreases in the order: $M^{4+} > MO_2^{2+} > M^{3+} > MO_2^{+}$ which is similar to their complex formation properties [**42**]. In general, the hydrolysis of the actinide ions can be represented as follows:

$$M^{n+} + xH_2O \leftrightarrow M(H_2O)_x^{n} \leftrightarrow M(OH)_x^{(n-x)+} + xH^{+} \quad (1.6)$$

Although all of the polynuclear species of the actinide ions are of scientific interest, the polymers of Pu(IV) have attracted attention in particular because of practical considerations. As the Pu(IV) polymers are very stable with high molecular weight from few thousand to (10^{10}) and depolymerisation is quite difficult, and the erratic behavior of Pu(IV) solutions can pose major problem in nuclear fuel processing [**43**]. The rate of polymerization differ with temperature, acidity, Pu(IV) concentration, the nature of anion present etc. Depolymerisation is best accomplished by heating the Pu solution in 6-10 M HNO_3. The addition of fluoride, sulphate or other strong complexing ions markedly increases the rate of depolymerisation [**44**].

1.10.3.4. Complexation

The actinide ions show complex formation tendency in aqueous solutions. This property of actinides is helpful for their separation and purification. Strength of the complex is

dependent on the ionic potential (or charge density) of the metal ions, which is the ratio of ionic charge to ionic radius. Higher the ionic potential, stronger is the complex formation due to greater the electrostatic attraction between cations and anions. The complexing strength of actinide ions in different oxidation states follows the order: M^{4+} > MO_2^{2+} > M^{3+} > MO_2^{+}. Similarly, for the given metal ions of same oxidation state, the complexing ability increases with the atomic number due to increase in the ionic potential as a result of actinide contraction [**40**]. However, the above generalized statement may be valid when complexation is primarily ionic in nature. There are large number factor affecting complex formation tendency viz. where hybridization involving 5f orbitals, steric effects, and hydration of metal ions.

Stability of complexes between metal ions and ligands is based on the concept of hard and soft acids and bases (HSAB) [**45**]. Those metal ions are called 'hard' which have a small radius and high charge and do not possess valence shell electrons that are easily distorted. The soft metal ions have the opposite characteristics. When similar classification is applied to the ligands, it is observed that the hard metal ions form stronger complexes with hard ligands and soft metal ions have a preference for the soft ligands. Actinide ions are categorized as 'hard acids' and these ions interact with hard bases such as 'O' or 'F' rather than soft ligands like 'N', 'S' or 'P' donors. However, actinides show the preference soft donor ligand as compared to lanthanides because of f-orbital participation exhibit covalent character in the ions. The complex formation reactions are endothermic because of breaking of strong bonds between metal ions and water molecules in the primary hydration sphere which require large energy while reverse is true for the soft ions. Removal of water molecules is driven by large increase in entropy [**40**]. "Inner-sphere complex" is formed when the primary hydration shell is

broken while "outer sphere complexes" do not require breaking of the primary hydration shell. The actinide ions interact with soft bases in organic solvents of low solvating power but not in aqueous solutions where the soft bases would have to replace inner sphere water molecule which is a hard base. Thus, depending upon the nature of ligand and medium actinide cations form inner or outer sphere complexes.

For monovalent ligands the complexing tendency decreases in the order: F^- > CH_3COO^- > SCN^- > NO_3^- > Cl^- > Br^- > I^- > ClO_4^-. For divalent ligands, the complexing ability decrease in the order: CO_3^{2-} > SO_3^{2-} > $C_2O_4^{2-}$ > SO_4^{2-}, however these ligands form stronger complexes than the monovalent anions. The complexing ability of some of the organic ligands with Th(IV) varies as: EDTA > Citrate > Oxalate > HIBA > Lactate > Acetate. The stabilities of the complexes are also governed by the coordinating groups [**46**].

Nitrate complexes of the early actinides (Th, Pa, U, Np and Pu) have great relevance with respect to the separation methods employed in the nuclear industry. Uranyl nitrate compounds are widely used in the extraction and purification of uranium. Uranyl nitrate exists in the form of several hydrates viz. $UO_2(NO_3)_2.2H_2O$, $UO_2(NO_3)_2.3H_2O$ and $UO_2(NO_3)_2.6H_2O$. Extraction processes employing a neutral donor 'S' (TBP, hexone or diethyl ether) are based on formation of solvated species of the type $UO_2(NO_3)_2.2S$. Series of the nitrato complexes of the type $Pu(NO_3)_x^{(4-x)}$ (where x = 1 to 6) have been reported [**47**]. Dominating species are $Pu(NO_3)_4$ (2-4 M HNO_3), $HPu(NO_3)_5$ (4-11 M HNO_3), $H_2Pu(NO_3)_6$ (>11 M HNO_3) and the tetranitrato species form a ternary adduct with TBP which finds wide application in the PUREX process (employed widely for nuclear fuel reprocessing). Macrocyclic ligands possess excellent size selective complexing ability for alkali as well as alkaline earth metal ions due to their pre-

organized conformation, size selective nature and hydrophilic interior /hydrophobic exterior [**48-50**]. Crown ethers have been employed as polydentate neutral donors in synergistic extraction of actinides from weak acidic solutions and as ion-pair extractants from strong acid solutions [**51**].

1.10.4. Co-ordination numbers of actinides

Actinides show higher coordination numbers as compared to other elements like the d-block element due to; (a) large cation size for accommodating more ligands, and (b) lower electron density on metal ion due to higher oxidation state. Actinides displayed coordination number from 6 to 12 (Table 1.7). Trivalent ions show mostly 8 or 9 coordination number. Oxygenated hexavalent species like UO_2^{2+} show coordination numbers between 6-8 more common [**38, 52**].

Table 1.7: Coordination number of various oxidation states of actinides

Oxidation state	Co-ordination number
III	6,8,9,12
IV	6 to 12
V	6 to 9
VI	6 to 8
VII	6

1.10.5. Absorption spectra

Actinides displayed different colors in their aqueous solution which arise mainly from three types of transitions viz.

(a) f-f transitions: These transitions may occur 5*f*-5*f* levels of different angular momentum between the orbitals of the same sub-shell. These transitions are *Laporte forbidden* transitions and therefore their absorption band intensity is low. These transitions occur in inner shells and are not affected by environment, and their bands are sharp. The energy differences between the various energy levels are of such an order of magnitude that the bands due to 5f-5f transitions appear in UV, visible and near IR regions. The molar absorption coefficient is in the range of 10-50 $M^{-1}cm^{-1}$.

(b) f-d transitions: These transitions take place between *f* and *d* orbitals (different azimuthal quantum number). These transitions are *Laporte allowed* therefore, relatively more intense. They are influenced from the surroundings so their absorption bands are broad. The energy differences are generally larger so that the bands appear mostly in ultraviolet region and their molar absorption coefficient is of the order ~ 1000 $cm^{-1}M$.

(c) Ligand to metal (L→M) charge transfer: These transitions occur between the 5f shells of actinide ions and the ligand's orbital. Therefore, nature of ligand plays an important role. These transitions are significantly affected by the environment; therefore, the charge transfer bands are broad. The deep and vivid color characteristics of many actinide complexes are due to charge transfer bands. These bands are less intense than *5f-6d* transitions and appear in the UV region.

The absorption spectra of actinide ions in different oxidation states differ widely, which have been successfully exploited for the quantitative analysis of their mixtures present in different oxidation states. The absorption bands of actinide ions have

also been used for studying the redox reactions. The structure and bonding of actinide complexes can be inferred from the number, appearance, energy and intensity of the absorption bands. This also helps in seeking information about the electronic configuration of the actinide atoms, coordination number, the stereochemistry of the complexes formed, and the nature of the bonds involved. Therefore, change in absorption spectra due to the presence of ligands have often been used to establish complex formation, and in some cases, even for the calculation of their stability constants. The complexes of some of the actinides formed with many organic and inorganic ligands have very high absorption in visible region. This property has been fruitfully exploited to develop sensitive analytical methods for the detection and estimation of actinide ions.

1.11. Separation methods for actinides

Separation of any metal ion is governed by scientific principles viz. chemical reaction equilibrium kinetics, fluid mechanics, and mass transfer from one phase to another. The theory of separation utilizes these principles in different processes including solvent extraction, extraction chromatography as well as in membrane processes. During the development of any separation technique, the differences in the oxidation states and the complexing ability of the metal ions is exploited. In these techniques "*Solvent Extraction*" also called the liquid-liquid extraction, is extensively used for separation, preparation, purification, enrichment and analysis on micro scale to large industrial processes.

The present work is an attempt to understand the separation chemistry of actinides mainly thorium, uranium, plutonium and fission products employing solvent extraction technique. Therefore, it is relevant to understand the salient features of this technique.

1.11.1. Solvent extraction

Solvent extraction is based on the principle that a solute can distribute itself in a certain ratio between the two immiscible solvents, one of which is usually water and the other is an organic solvent. In certain cases, the solute can be more or less completely transferred into the organic phase. This method has got several applications in extraction of oils, natural products and in nuclear industry during the recovery of actinides from ores and in post irradiation reprocessing operations. The liquid-liquid distribution systems can be thermodynamically explained with the help of phase rule [53]. Gibb's phase rule is usually stated as:

$$P + F = C + 2 \quad (1.7)$$

Where P = number of phases, C = number of components, and F = degrees of freedom.

In a binary system, liquid-liquid distribution has two phases P = 2, assuming number of components i.e. C = 1 (solute) and F = 1 (at constant temperature and pressure). According to Nernst distribution law, the concentration of a particular species (M) in the organic phase and in the aqueous phase at equilibrium can be expressed as follows [**53**]:

$$K_d = [M]_{(org.)} / [M]_{(aq.)} \quad (1.8)$$

Where K_d is the "*distribution coefficient*" and is independent of the total solute concentration. The term in subscripts 'org.' and 'aq.' denote the organic and aqueous phases respectively. At the equilibrium, the chemical potentials of the species (M) in the two phases are equal and therefore

$$\mu_{(aq.)} = \mu_{(org.)} \quad (1.9)$$

$$\text{or, } \mu^{o}_{(aq.)} + RT \ln[M]_{(aq.)} + RT \ln\gamma_{(aq.)} = \mu^{o}_{(org.)} + RT \ln[M]_{(org.)} + RT \ln\gamma_{(org.)} \quad (1.10)$$

where μ^o = standard chemical potential of solute, M in a hypothetical ideal 1 molar solution,

[M] = Molar concentration and γ = Molar activity coefficient.

The distribution coefficient, K_d can be written as

$$K_d = \gamma_{(aq.)}/\gamma_{(org.)} \cdot \exp [-(\mu^o_{(org.)} - \mu^o_{(aq.)})]/RT \quad (1.11)$$

At a given temperature, $[-(\mu^o_{(org.)} - \mu^o_{(aq.)})]/RT$ is a constant and therefore K_d will be constant provided $\gamma_{(aq.)}/\gamma_{(org.)}$ is constant. "*Thermodynamic distribution constant*" (K_d^T) can be expressed using activity instead of concentration of the solute.

$$K_d^T = \{M\}_{(org.)} / \{M\}_{(aq.)} \quad (1.12)$$

K_d^T is a constant at a given temperature

$$K_d^T = \gamma_{(org.)} [M]_{(org.)} / \gamma_{(aq.)} [M]_{(aq.)} \quad (1.13)$$

$$\text{or, } K_d^T = \gamma_{(org.)} / \gamma_{(aq.)} \cdot K_d \quad (1.14)$$

After ignoring the activity coefficient of the species of the solute in the organic and in the aqueous phases, both K_d and K_d^T become identical for a particular extractable species. Extraction process for metal ion "*Distribution ratio*" (D) which is defined as "*the ratio of the analytical concentration of the metal ion in the organic phase* $[M(org.)]_{total}$ *to that in the aqueous phase* $[M(aq.)]_{total}$ " is more commonly use.

For practical purpose instead of using D, percentage extraction (%E) is preferred which is defined as follows:

$$\%E = [V_o [M]_{(org.)} / \{V_o [M]_{(org.)} + V_a [M]_{(aq.)} \}] \times 100 \quad (1.15)$$

$$\%E = [D / (D + V_a / V_o)] \times 100 \quad (1.16)$$

where V_a = volume of the aqueous phase, and V_o = volume of organic phase.

1.11.2. Extraction isotherm

To establish any solvent extraction process, the determination of extraction isotherm is an important step. In this, varying amounts of metal salts in aqueous solutions are contacted with varying volumes of the solvent and thoroughly mixed for a predetermined time. Metal contents are determined in the two phases after separation. The extraction of metal ion depends on the distribution coefficient, solvent volume and initial metal concentration. The extraction isotherm is obtained by plotting the metal concentration in the aqueous phase along the x-axis and that in the organic phase along the y-axis.

1.11.3. Multiple extractions

For quantitative extraction of metal, the aqueous solution of metal ions is repeatedly brought in contact with the organic phase. There are two different ways for multiple extraction of metal

1.11.3.1. Co-current extraction

In this process, after each extraction step, fresh solvent is added for treatment of raffinate (Figure 1.4). This process is repeated as many times as required. Distribution ratio (D) can be expressed as follows:

$$D = [(W-W_1)/V_o] / (W_1/V_a) \quad (1.17)$$

Where V_o = volume of the organic phase, V_a = Volume of the aqueous phase, W = Initial weight of the metal in the aqueous solution, and W_1 = Weight of the metal in the aqueous solution after first extraction. It can be shown that after first extraction:

$$W_1 = [1/ (1+D. V_o/V_a)] \times W \quad (1.18)$$

and after the n^{th} contact of the raffinate with V_o volume of fresh solvent, W_n = weight of the metal left in the aqueous solution

$$W_n = [1/ (1+D. V_o/V_a)]^n \times W \quad (1.19)$$

W_n should be as low as possible to extract metal ion quantitatively, using higher values 'V_o/V_a' and 'n'. Practically V_o is to keep small and increase of the number of contacts.

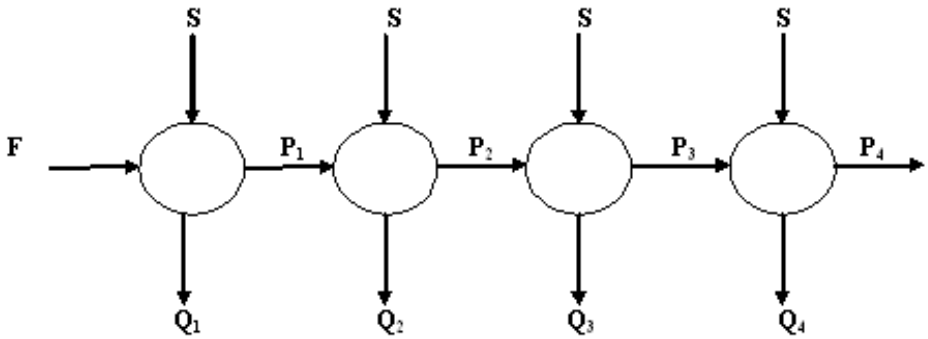

Fig. 1.4. Co-current extraction in four stages

where S = solvent, F = feed, P = raffinate and Q = loaded organic phase.

Co-current extraction having some limitations such as:

(a) Large solvent inventory.

(b) Dilute organic extract.

(c) Inefficient use of the solvent.

1.11.3.2. Counter-current extraction

In this system, the fresh solvent is brought in contact with aqueous solution containing the least amount of the metal (1st stage) and the aqueous solution having the highest

concentration (nth stage) is contacted with the solvent which is reaching its maximum loading capacity (Figure 1.5).

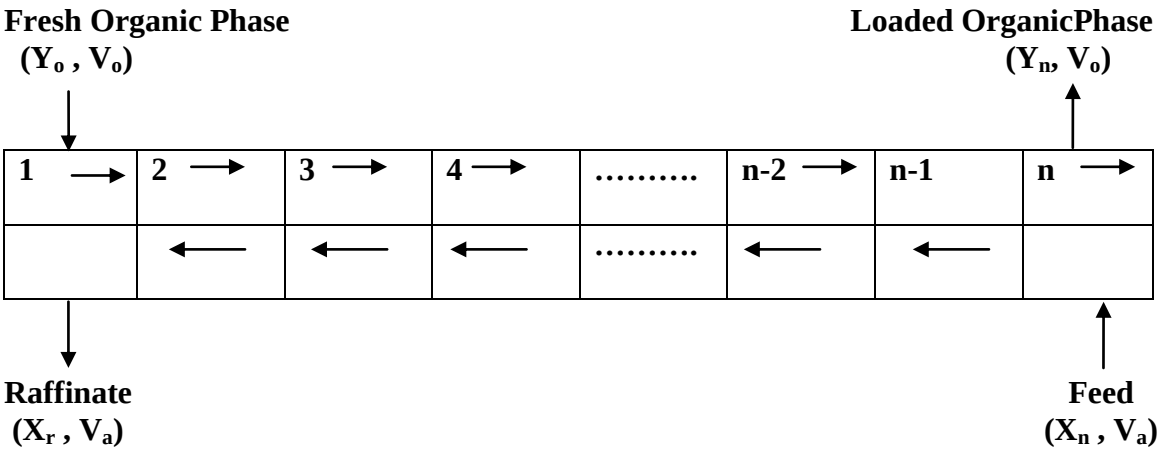

Fig. 1.5. Counter-current extraction scheme

Where n = no. of stages i.e. 1, 2, 3,....., X = metal content in the aqueous phase, Y = metal content in the organic phase, V_o = volume of the organic phase and V_a = volume of the aqueous phase. Metal ions are distributed between the solvent and the aqueous phases due mass balance.

[Metal content in the fresh solvent + metal content in the fresh aqueous solution] =

[Metal content in the loaded solvent + metal content in the aqueous raffinate]

Therefore,

$$Y_n V_o + X_r V_a = Y_o V_o + X_n V_a \quad (1.20)$$

$$\text{or, } Y_n = (V_a / V_o) X_n + (Y_o - X_r V_a / V_o) \quad (1.21)$$

Here X_n = concentration in the feed organic phase, and Y_o = concentration in the fresh organic phase. Metal concentration in the raffinate to be negligible, i.e. $X_r \sim 0$ and $Y_o \sim 0$ for fresh solvent, so we can write as:

$$Y_n = (V_a / V_o) X_n \quad (1.22)$$

If metal concentrations in the solvent and aqueous phases are plotted along y- and x-axis respectively, this is an equation of straight line. The slope of this line is V_a / V_o. This line is known as "*operating line*" and expresses the material balance of the extraction system. This plot gives the information about concentration of metal ion in the organic phase at any stage. "*McCabe-Thiele*" diagram gives the information about number of stages required any counter current extraction operation which contain extraction isotherm and the operating line on the same graph. Number of stages required for extraction or scrubbing stages during counter current continuous operations are determined by "*Kremser equation*" [**54**] given as:

(a) For extraction

$$[X_r - (Y_o / D)] / [X_n - (Y_o / D)] = [\varepsilon - 1] / [\varepsilon^{n+1} - 1] \text{ for } \varepsilon \neq 1.0$$

$$= [1 / n+1] \text{ for } \varepsilon = 1.0 \quad (1.23)$$

Where X_r = Metal concentration in raffinate, X_n = Metal concentration in feed, Y_o = Metal concentration in the lean organic phase ≈ 0, D = Metal distribution ratio, ε = Metal extraction factor = $D (V_o / V_a)$, and n = Number of stages. Further simplification of the equation leads to

$$[X_r] / [X_n] = [\varepsilon - 1] / [\varepsilon_{n+1} - 1] \quad (1.24)$$

Where $[X_r] / [X_n]$ = unextracted fraction of the metal ion and ε is assumed to be constant during the process.

(b) For scrubbing

$$[Y_r - X_s \,.\, D] / [Y_o - X_s \,.\, D] = [(1/\varepsilon) - 1] / [(1/\varepsilon^{n+1}) - 1] \quad (1.25)$$

Where Y_o = Metal concentration in the organic phase before scrubbing, Y_r = Metal concentration in the organic phase after scrubbing, and X_s = Metal concentration in the aqueous phase before scrubbing ≈ 0. On simplification,

$$[Y_r / [Y_o\ ] = [(1/\varepsilon) - 1] / [(1/\varepsilon)^{n+1} - 1] \quad (1.26)$$

There are general assumptions which are used for these calculations are:

1. Two phases the organic and aqueous are completely immiscible.

2. During extraction and scrubbing the volume of the both phases does not changed.

3. No back mixing occurs.

1.11.4. Factors influencing the distribution of solutes

There are several factors which affect the distribution of metal ions. Some of the prominent are: nature and concentration of solute (metal ions), extractant, diluent, complexing agent present in the aqueous phase, acidity of the aqueous phase, salting agent presence in the aqueous phase, and temperature [**55**]. These factors are important to achieve the desired separation.

1.11.5. Classification of extractants

Extraction of metal ions follows certain mechanisms such as:

(i) Solvation: The extraction of metal ions by neutral ligands is followed by solvation mechanism. The extraction process proceeds via replacement of water molecules from the co-ordination sphere of metal ions by basic donor atoms such as ‘O’ or ‘N’

of the ligand molecules. The well known example is the extraction of U(VI) by TBP from nitric acid medium [**56**].

(ii) Chelation: The extraction of metal ions proceeds via the formation of metal chelates with chelating ligands. The example of this type is the extraction of Pu(IV) by thenoyltrifluoroacetone (HTTA) in benzene [**57**].

(iii) Ion pair extraction: In this extraction, formation of neutral ion-pair species between the metal ions and ionic organic ligands. Acidic ligands provide anions by liberating protons which then complexed with the metal cation to form ion-pair such as sulphonic acids, carboxylic acids and organophosphoric acids. Basic ligands provide cations which complex with aqueous anion metal complex to form ion-pair viz. quaternary ammonium salts.

(iv) Synergistic extraction: In this mechanism, extraction of metal ions take place in the presence of two or more extractants and give more distribution than that expected from the sum of extraction employing individual extractants. Extraction of Pu(IV) from nitric acid medium by a mixture of HTTA and tri-*n*-octyl phosphine oxide (TOPO) in benzene is well known example of synergistic extraction [**58**].

1.11.6. Criteria for the selection of extractants

A number of factors are taken into account while choosing a particular extractant for industrial applications [**59**]. These are as follows:

1. Ease of synthesis / availability at a reasonable cost.
2. High solubility in the non-polar solvent (diluents).
3. Low aqueous solubility.
4. Non-volatility, non-toxicity and non-inflammability.

5. Better complexation ability with metal ion of interest.
6. High solubility of the metal complex in the organic phase.
7. Easy stripping of the metal ion from the organic phase.
8. Ease of regeneration of the extractant for recycling.
9. High selectivity for the metal ion of interest over other metal ions present in the aqueous solution.
10. Low viscosity for ease of flow and high Inter Facial Tension (IFT) to enable a faster rate of phase disengagement.
11. High resistance to radiolytic and chemical degradation during operation (particularly relevant in back-end operation of nuclear industry).

There are large numbers of extractant employed in different laboratories in which only a few solvents have found for commercial uses. Table 1.8 shows different extractants used in nuclear industries.

Table 1.8: Extractants employed in nuclear hydrometallurgy

Class	**Extractant**	**Application**
Acidic	HDEHP (Di-2-(ethylhexyl) phosphoric acid)	Uranium extraction from ores, Actinides and rare earths separation
	PC88A (dialkyl phosphinic acid)	Rare earths separation
	Versatic acid	Rare earths separation
Basic	Alamine 336 (*N,N*-dioctyloctan-1-amine)	Uranium extraction from ores, Zr / Hf separation
	Aliquat 336	Rare earths separation
	Trilauryl amine	Pu purification
Neutral	TBP	U and Th purification Zr / Hf separation Nb / Ta separation Fuel reprocessing U recovery from phosphoricacid
	TOPO	Fuel reprocessing
	Mono amides CMP, CMPO and diglycomides (TODGA, TEHDGA)	Recovery of minor actinides from high level waste

CMP: Carbamoyl methyl phosphonate; CMPO: Carbamoyl methyl phosphine oxide; TODGA: N,N,N′,N′-tetraoctyl diglycolamide; TEHDGA: N,N,N′,N′-tetra-2-ethylhexyl diglycolamide; Aliquat 336: N-methyl-N,N-dioctyloctan-1-ammonium chloride; Trilauryl amine: N,N-didodecyldodecan-1-amine.

1.12. Limitations of TBP

TBP has been used in nuclear industry as extractant for last six decades. In PUREX and THOREX processes, it has been utilized for ^{233}U and ^{239}Pu separation from spent nuclear fuel from reactor. However, based on experiences gained over year, separation scientists have identified certain limitation of TBP; these are [**60-64**]:

a) High aqueous solubility.
b) Lower distribution ratio (*D*) of Pu(IV) compared to U(VI), which can lead to Pu losses to raffinate.
c) Poor decontamination factor (DF) values of Pu/U with respect to fission products,
d) Third-phase formation tendency during the extraction of tetravalent metal ions such as Th(IV) (relevant for Th fuel cycle) and Pu(IV) (relevant for fast reactor reprocessing).
e) Poor radiation stability.
f) Deleterious nature of degradation products (mono- and dibutyl phosphoric acids) leading to decreased decontamination of U and Pu from fission products, loss of U and Pu to organic phase during stripping.
g) Generation of a large volume of secondary radioactive waste.

These shortcomings are of serious concern particularly during the spent fuel reprocessing of (i) short cooled (MOX) thermal reactor, (ii) fast reactors containing larger Pu content and significantly higher burn up, and (iii) thorium based reactors. Therefore, efforts are being made to overcome at least. In this context *N*,*N*-dialkyl amides have been found potential alternative extractants to TBP.

1.13. *N,N*-dialkyl aliphatic amides: Extractants for nuclear fuel reprocessing

T.H. Siddall first identified the potential of amide group of extractants for actinide separations. He found that *N,N*-dialkyl amide can be promising alternative of TBP in spent fuel reprocessing. He suggested that their use can allow us in getting rid of some problems arising out of radiolytic degradation of organophosphorous extractants like TBP, in nuclear industry [**65-67**] . The results reported by Siddall have been confirmed almost during the same period by the researchers of Oak Ridge National Laboratory (ORNL) [**68,69**]. French and Japanese researchers have also performed extensive studies on the evaluation of amide extractants for actinide separations [**70,71**]. *N,N*-dialkyl aliphatic amides have some advantages as extractants of actinides over TBP, which can be summarized as follows:

a) Amides offer comparable extraction behavior of metal ions as TBP.
b) Their degradation products are mainly carboxylic acids and secondary amines which are innocuous in nature.
c) These show good decontamination factors over fission products.
d) The reduced volume of the secondary waste due to completely incinerability [**72,73**].
e) These extractants are easy to synthesis on a large scale.
f) Possibility of tailoring the ligands according to the intended applications

Metal extraction in the amides takes place by the co-ordination of carbonyl oxygen. Siddall has suggested that alkylation of the C_α atom adjacent to the carbonyl group suppresses the extraction of quadrivalent actinides and fission products as compared to the hexavalent metal ions. So these ligands offer better separation of hexavelant metal ions over tetravalent [**74**]. The branching in the alkyl group adjacent to the carbonyl

group of amides decreases Th(IV) extraction due to steric hindrance [**75**]. Due to lack of U in India the future of nuclear energy is depends on our large thorium resources. In this context Fast reactor, AHWR has been proposed for Th utilization. Reprocessing of AHWR spent fuel will be three ways separation of ^{233}U, Pu, Th where the fissile isotope ^{233}U, produced on the irradiation of ^{232}Th, needs to be separated efficiently from the bulk of thorium and large number of fission products.

As a part of this thesis, R&D work on this challenging area has been carried out using of *N,N*- dialkyl aliphatic amides synthesized in our laboratory as extractants [**76**]. The straight chain diamide DHOA (*N,N*-dihexyl octanamide) has been found to be a promising candidate for the separation of ^{233}U and Pu from irradiated thorium which was investigated extensively. In addition, DHOA studied under PUREX cycle (PHWR and fast reactor) appeared distinctly better than TBP with respect to Am(III), fission products and structural materials decontamination of U/Pu [**77**]. Distribution study of U, Pu, Th and fission products using different amides which are synthesized in our laboratory found that amides are better than TBP [**78-81**].

1.14. Third-phase formation

This refers to a situation where organic phase splits into two new phases (a) the diluents rich light phase, (b) heavy third phase containing the metal solvate (Figure 1.6)**.** This heavy organic phase (HOP) appears at the interface of the two phases light phase and aqueous phase. Third-phase formation occurs during the extraction of large concentrations of metal ions and acids using different solvents. Third-phase appears due to incompatibility of the polar metal solvate or acid in non polar diluents. Third-phase formation is expressed in terms of LOC of the metal ion under desired experimental

conditions. It is not desirable during plant scale operations for the recovery of metal ions [**25**]. Third-phase formation is generally attributed to the aggregation of the extracted species (reverse micelle) in the organic phase [**82**]. These reverse micelles are subjected to two contrasting physical forces. The thermal energy k_BT keeps the micelles dispersed in the solvent. On the other hand, the energy of intermicellar attraction makes the micelles stick together. As long as these two energies are comparable, the organic phase is stable. When the energy of attraction becomes substantially larger than the thermal energy, third-phase formation takes place.

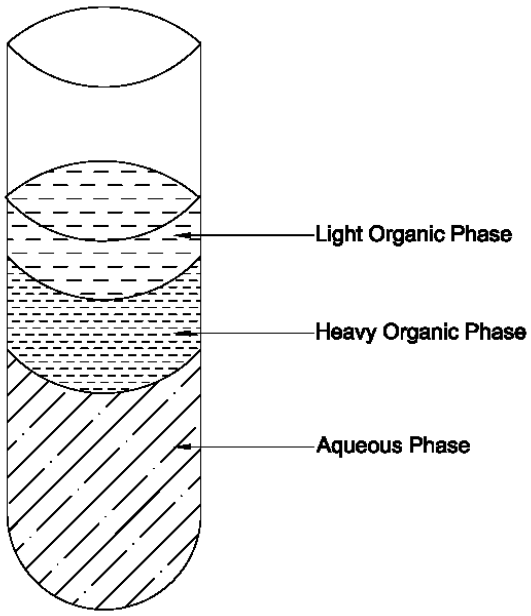

Fig. 1.6. Pictorial representation of third phase

Third-phase formation during the extraction of metal ions employing extractants like TBP dissolved in aliphatic diluents was mostly studied to find out the composition of the organic phase species before and after phase splitting. To understand the structure and morphology of the organic phase species, different techniques have used such as spectrophotometry, small-angle neutron scattering (SANS), small-angle X-ray scattering

(SAXS), vapor pressure osmometry (VPO), tensiometry and conductivity etc [**83-88**]. SANS data and the Baxter model is giving the explanation of third phase. Organic phase obtained during Th extraction studies from nitric acid medium have shown the existence of a trisolvate $Th(NO_3)_4 \cdot (TBP)_3$ species. The third-phase also contains HNO_3 (though small amount) through hydrogen-bonding to the trisolvated complex. These studies have shown that the formation of the heavy phase is a result of the attractive interactions of small reverse micelle-like aggregates of 3 to 4 TBP molecules per metal nitrate complex. This behavior has been particularly noted during TBP extraction from nitric acid solutions containing Zr(IV), Th(IV), U(VI), and Pu(IV). The formation of large ellipsoidal aggregates has been found to be responsible for the appearance of third-phase during extraction studies. Unlike the TBP system, third-phases appeared in *N*,*N*-dialkyl derivatives under high uranium loading conditions [**89**].

To avoid the third phase formation, the knowledge of LOC values is needed for a particular extractant. LOC is influenced by several parameters such as: organic phase composition, aqueous phase composition, temperature etc. Organic phase composition is alter by the diluents, polar and branched diluents increase LOC value. LOC values increase with carbon chain length and decreasing with branching at carbonyl group in case of *N*,*N*-dialkyl amide [**90**]. The presence of inextractable ions or salts, other metal ions, medium and acidity of aqueous phase affect third phase. Third phase formation also takes place by TBP during acid uptake in the following order: $HClO_4 > H_2SO_4 > HCl > H_3PO_4 > HNO_3$ [**91**]. LOC is with temperature and extractant concentration. There are hydrogen bond between extractant and acid in the organic phase. These bonds are weaker and easily broken with temperature therefore, decrease in the aquophilicity of the

extractant-acid complex. This will eventually lead to an increase in the transfer of this complex to the diluent-rich phase thus reducing third-phase formation [**92**].

1.15. Solvent degradation

This is an important issue and requires thorough understanding during the development of different solvents in the nuclear fuel reprocessing. The solvents used in reprocessing of spent nuclear fuels undergo degradation mainly by three routes:

1.15.1. Hydrolytic degradation

TBP in paraffin diluents is used in PUREX and other processes for separating uranium, thorium, and plutonium from spent fuel by contacting with aqueous nitric acid. Nitric acid has appreciable solubility in tributyl phosphate and gets transferred to organic phase during solvent extraction operation. Nitric acid, which is present to the tune of several moles per liter in aqueous phase leads to degradation of extractant and renders it unusable. Degradation products include dibutyl phosphoric acid, monobutyl phosphoric acid, orthophosphoric acid, polymeric substances, unsaturated hydrocarbons, and unidentified nitrogen-containing organic compounds [**93**]. These degradation products cause loss of uranium, plutonium and thorium. Decontamination of these valuable metals from fission products are severely affected. These degradation products has to be removed before further extraction experiments by contacting the solvent with aqueous sodium carbonate and/or sodium or potassium hydroxide solution to remove the acid degradation products [**94**]. The concentrations of these products must be reduced by a factor of 10 or more for recycling the solvent [**95**]. Excess concentration of DBP and MBP may also produce interfacial precipitates (crud) or emulsions (due to the sparingly

soluble compounds formed with zirconium) which will disturb phase separation and equipment operation.

1.15.2. Radiolytic degradation

In nuclear fuel reprocessing and partitioning, extractants are used influenced by radiation exposure, and contact with nitric acid solution at different stages. These extractants are degraded by hydrolysis and radiolysis. Different extractants such as TBP, amides, digyclomides, TODGA, TEHDGA used in different processes after degradation change extraction phenomena. 30% TBP in *n*-dodecane in nitric acid media after irradiation form degradation products like DBP, MBP, phosphoric acid, higher molecular-weight products are created by radical-addition reactions, acidic phosphates, hydroxylated, and ketones, carboxylic acids are produced from the diluent. The acidic phosphates from TBP and nitro paraffinic molecules created by diluent are complexes with different actinide and fission-product such Zr, Ru and reduce decontamination factor. Degradation products decreased performance of extractant with regard to phase separation and solvent viscosity [**96, 97**].

The degradation products of T2EHDGA were identified as: bis-(2-ethylhexyl) amine, *N*,*N*-bis-(2-ethylhexyl) formamide, *N*,*N*-bis- (2-ethylhexyl) acetamide, *N*,*N*-bis-(2-ethylhexyl) glycolamide, *N*,*N*-bis-(2-ethylhexyl)-*N*,*N*-dipropyl diglycolamide [**98**]. Mo retention has been found on prolonged use in case of degraded T2EHDGA and TODGA. Hydrodynamic parameters such as viscosity and interfacial tension are not affected significantly by the irradiation of these solvent [**99, 100**]. The radiolytic products of *N*,*N*-diakylamides such as DHOA are caprylic acid, dihexyl amine, dihexylketones while D2EHIBA irradiated products are bis(2-ethylhexyl)amine and isobutyric acids. These

products increase the density and viscosity of irradiate solvent. These product are completely incinerable and easily washed out so does not increase secondary radioactive waste. These have less retention U, Pu and fission products as compared to TBP [**101**].

1.15.3. Thermal degradation

HLW generated after reprocessing of spent nuclear fuel in PUREX and THOREX processes goes for evaporation in the evaporator tank. At elevated temperatures, TBP reacts with nitric acid and can undergo exothermic reactions to form complex mixtures known as "Red Oil" (called mainly because of color of the mixture) [**102**]. This reaction can be thermal "runaway" if reactants are heated to temperatures where heat of reaction exceeds heat loss from the system [**103, 104**]. TBP in *n*- dodecane has been used as extractant in PUREX and THOREX process. On thermal degradation of TBP gaseous products includes N_2, CO, CO_2, NO, N_2O, hydrocarbons etc are generated. Liquid products include Di-butyl phosphoric acid, Mono-butyl phosphoric acid, butyl nitrate, butanol, unreacted TBP and water. Studies of thermal degradation of tri iso-amyl phosphate in n-dodecane and reversed TALSPEAK solvent [0.3M HDEPHA in 0.2M TBP in *n*-dodecane] have been shows approximately similar results with pressure, acidity, and temperature [**105, 106**].

Thermal degradation of *N*,*N*-dialkylamides substitutes for the TBP such as *N*,*N*-di-(2-ethylhexyl)-3,3-dimethylbutyramide (DEHDMBA) is not sufficiently degraded by operating in a nitrogen atmosphere, even at 250°C. Effect of the oxygen level was much stronger for DEHDMBA degradation than temperature. Major degraded products are carbonyl compounds such as amides, substituted amides, ketones, acids and aldehydes, and some intermediate imides with high molecular weights. Many compounds were

secondary degradation products, such as imides, and oxidative products, like acids [**107**]. Gaseous products are the reason for the violent explosion. Runaway reactions of nitric acid -industrial solvent extraction solvents mixtures are potentially damaging in nature as evident from the explosion occurred in B-204 facility (now Sellafield) of BNFL (British Nuclear Fuels Ltd) in 1973. The exothermic reactions produced gases which escaped from the process cell and spread through the upper floors of building B-204. Subsequently, the plant was closed and the sealing the fate of BUTEX process (diBUTyl carbitol EXtraction) for nuclear fuel reprocessing [**108**].

1.16. Literature studies

The present thesis work deals with the evaluation of *N*,*N*-dialkyl amide as extractants for the reprocessing of spent nuclear fuel from AHWR and fast reactor. In this context, *N*,*N*-dihexyl octanamide (DHOA) has been identified as a promising alternate to TBP. DHOA has been studied well for PHWR spent nuclear fuel reprocessing. Table given below represent the previous studies on DHOA.

Table 1.9: Previous studies on DHOA:

Solvents	Studies	Results	References
DHOA	1. Extraction of nitric acid	Acid uptake constant K_H = 0.188	**[109]**
	2. U and Pu extraction studies:	Both D_U and D_{Pu} value increase with aqueous phase acidity upto 5-6 M HNO_3. D_U value decreases beyond 6 M HNO_3 due to less availability of ligand while D_{Pu} value are invariant due to ion pair formation	
	(a) Using different acidities		
	(b) Under U loading	D_U value decreases due less availability of free ligand	
	(c) Stoichiometry	Disolvated species are formed with U and Pu as $UO_2(NO_3)_2$.2TBP and $Pu(NO_3)_4$.2TBP respectively at 3.5 M HNO_3.	
	(d) Effect of temperature	D_U and D_{Pu} values decrease with temperature suggesting exothermic nature of extraction.	
	(e) Extraction of Fission product	Poor extraction of fission products leading to high S.F. values as compared to TBP	

DHOA	U(VI), Pu(IV), Am(III), and Zr(IV) distribution studies: (a) As a function of nitric acid (b) Mixer settler studies of extraction and stripping of U under PHWR feed conditions	Pu(IV) is more efficiently extracted than U(VI), extraction of Am(III) and Zr(IV) is insignificant in the acidity range 1-6 M HNO_3 suggesting reasonably high separation factors for U and Pu over these ions. Uranium extraction by DHOA is comparable to TBP, while stripping is better than TBP.	**[110]**
DHOA and TBP	Studies on Simulated PHWR feed conditions: (a) Extraction and Stripping (b) Stoichiometry of Pu (c) Separation Factor D_U/D_{Pu}	Co-processing of PHWR spent fuel can be achieved in lesser number of stages using DHOA (extraction: 2; stripping: 4) as compared to that of TBP (extraction: 3; stripping: 6). Disolvated species is formed at lower acidity while more than two DHOA molecules are involved in the extracted species of Pu(IV) at higher acidity ($\geq$ 4 M HNO_3). Pu/U ratio can be increased in the case of DHOA during the	**[77]**

	(d) Fission product	stripping step at 0.5M HNO_3 It offers better decontamination from Am (III), fission products, and structural materials as compared to TBP.	
DHOA and TBP	Separation factor of U/Pu over Th	Negligible variation in D_{Th} (0.033 ± 0.003) values in the entire range of acidity (1-6 M HNO_3). TBP is more favorable for preferential extraction of U over Th, while DHOA is better for preferential extraction of Pu over Th.	**[78]**
DHOA and TBP	Extraction behavior of U, Pu, and fission product under PHWR feed conditions using irradiated solvents	The degradation of DHOA (without pre-equilibration) was significantly low (absorbed dose of 100 M Rad), which suggested the stability of DHOA against radiation. D value decrease with irradiated DHOA as compared to unirradiated DHOA. By contrast, the reverse trend was observed with TBP due to the formation of its radiolytic degradation product. There was significant retention of Pu, U, and fission products in the	**[101]**

		irradiated TBP as compared to that of DHOA even after three contacts with the stripping solutions	

1.17. Scope of the thesis

Present work deals with evaluation of DHOA for the reprocessing of fast reactor and AHWR spent fuels. The content of the Thesis can be summarized as follows:

1. Evaluation of DHOA for reprocessing of Pu rich fuels.
2. Extraction studies of ^{237}Np using DHOA.
3. Evaluation of DHOA for Advanced Heavy Water Reactor spent fuel reprocessing.
4. Thermal degradation studies of DHOA/*n*-dodecane solvent.

CHAPTER 2: EXPERIMENTAL

In the present work, the extraction behavior of various metal ions such as U(VI), Pu(IV), Np(IV), Np(VI), Tc(VII), and Th(IV) have been investigated under different experimental conditions using *N*,*N*-diakyl amides and TBP as the extractants, both batch as well as counter current extraction studies (using mixer settlers and centrifugal contactors) have been performed using different feed solutions. The basic technique used for the separation studies of metal ions was solvent extraction. The details of various apparatus, materials, experimental equipment and analytical techniques used in the present work are discussed in this chapter.

2.1. Radiotracers

The separation studies on metal ions presented in the thesis were carried out with radiotracers. Procurement, preparation as well as purification of various radiotracers is given below:

2.1.1. Uranium-233 (^{233}U)

^{233}U tracer ($t_{1/2}$ = 1.59x10^5 years) was produced by irradiation of ^{232}Th in reactor followed by purification from the daughter / decay products of ^{232}U in 6M HCl medium using anion exchange procedure [**26, 111**]. Uranium in 6M HCl solution forms anionic complex which is held on the anion exchange column, whereas ^{228}Th and its daughter products are not retained on the column. The column was washed with excess of 6M HCl to remove any adsorbed impurity. Finally, the loaded uranium was eluted with 0.01 M $HNO_3$and used as stock solution (at 0.5M HNO_3). The purity of ^{233}U tracer was ensured by alpha spectrometry.

2.1.2. Neptunium-237 (^{237}Np)

^{237}Np ($t_{1/2}$ = 2.16x10^{6}*y*) is produced during the irradiation of uranium in thermal reactors (a) by successive neutron capture of ^{235}U followed by beta decay of ^{237}U, and (b) as an alpha decay product of ^{241}Am ($t_{1/2}$ = 432.7 *y*).^{237}Np decays to^{233}Pa by α-decay and therefore purification of ^{237}Np from the latter was carried out using di-*iso*-butyl carbinol (DIBC), as an extractant. Hardy *et al.* reported the presence of hydrolyzed cationic, neutral and anionic species $[Pa(OH)_2(NO_3)_4]^-$ of Pa in equilibrium in nitric acid media, and the interchange between them is a function of the aqueous phase acidity [**112**]. ^{237}Np solution at 6-7 M HNO_3 was equilibrated 2-3 times with pure DIBC after that the dissolved organic was removed by multiple xylene wash. The purity of ^{237}Np was ascertained by alpha and gamma ray spectrometry (for the presence / absence of ^{233}Pa).

2.1.3. Plutonium-239 (^{239}Pu)

^{239}Pu was purified by a reported procedure and its radiochemical purity was ascertained by gamma spectrometry for the absence of ^{241}Am [**113**]. The valency of Pu was adjusted to Pu(IV) with sodium nitrite and subsequently extracted by 0.5M HTTA (2-thenoyltrifluoro acetone) in xylene at 1M HNO_3 followed by stripping with 8MHNO_3. The resulting plutonium solution was used as stock for Pu(IV). Further, plutonium valency in the aqueous phase was adjusted and maintained in tetravalent state by the addition of 0.05M $NaNO_2$ + 0.005M NH_4VO_3 (holding oxidants). On the other hand, Pu(IV) was reduced to Pu(III) by addition of a mixture of 0.2M hydroxyl ammonium nitrate (HAN) and 0.2M hydrazinium nitrate (HN). A mixture of 0.2M HAN and 0.2M HN was optimized as an efficient reductant for Pu [**79**].

2.1.4. Other Tracers

Tracers of fission products viz. ^{99}Tc, ^{95}Zr, ^{141}Ce, $^{152\ -154}$Eu, ^{137}Cs and the structural material *i.e.*^{59}Fe, were procured from BRIT, Mumbai. These tracers were used after suitable dilution. Radiochemical purity of the radiotracers was ascertained by gamma spectrometry. Nuclear data for different radionuclides used in the present studies are included in Table 2.1.

Table 2.1: Nuclear data for different radionuclides used in the present study

Element	Decay mode	Decay %	Half life	Energy (KeV)	Counting mode
^{99}Tc	β-, γ	100	2.1x10^{5}y	300	β
^{95}Zr	β-, γ	100	64 d	724, 756	γ
^{59}Fe	β-, γ	100	44.5 d	1099	γ
^{237}Np	α	100	2.14X10^6 y	4.78,4.77	α
^{239}Pu	α	100	24360 y	5.15,5.14	α

2.2. Materials used in these studies

2.2.1. Thorium

Thorium (nitrate form) obtained from Indian Rare Earths Limited, Mumbai was used as received.

2.2.2. Uranium-238 (^{238}U)

^{238}U (as U_3O_8) procured from Uranium Extraction Division (UED) BARC, Mumbai.

2.2.3. *N,N*-dialkylamides

N,N- dialkylamides extractant were used in present studies was synthesized in our laboratory as per the following procedure:

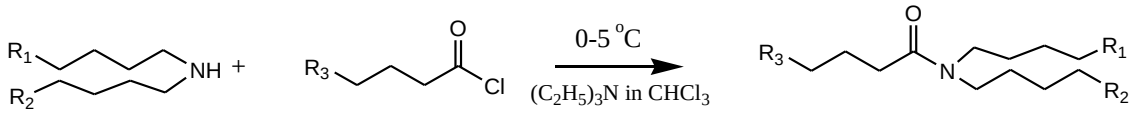

N,N-dialkyl amide

Amides were purified by vacuum distillation. Overall yield of the synthesised product was 80–90%. Characterisation of the ligands obtained after vacuum distillation was done by elemental analysis, IR and NMR [**114**]**.** Analytical data of *N,N*-dihexyl octanamide (DHOA) are given in Table 2.2.

Table 2.2: Analytical data of DHOA

Parameter(s)	**Details**
Molecular formula	$C_{20}H_{41}NO$
Carbon (%)	76.6 (77.1)*
Hydrogen (%)	12.9 (13.3)*
Nitrogen(%)	4.72 (4.49)*
Amides (%)[#]	99.3
Viscosity (cP)	13.30
Basicity (K_H)	0.188
Density (gm/c.c)	0.81
Refractive index	1.45
Boiling point (^oC)	183 - 185 (0.2 mm)
$\nu_{C=O}$ (cm^{-1})	1645

** Expected value; [#] Determined potentiometrically.*

2.2.4. Other chemicals

The list of the various chemicals used in the present work is given in Table 2.3. Analytical Grade (A.R) reagents were used throughout the present studies. Millipore deionized water (18 MΩ/cm) was used in all the experiments. Solutions were prepared by the required diluents or mixture of diluents using standard procedures.

Table 2.3: The list of various chemicals and reagents used in the studies

Chemical reagents	**Purity**	**Source**
Tri butyl phosphate	> 99.9	Heavy Water Board, India
Di- hexyl octanamide	> 99.9	Synthesized in house
Xylene	AR Grade	Merck Germany
n-Dodecane	AR Grade	Lancaster, U.K.
Nitric acid	AR Grade	S.D. Fine Chemical
1-Decanol	AR Grade	Merck Germany
1-Octanol	AR Grade	Sisco Research Ltd.
Diisobutylcarbinol (DIBC)	AR Grade	Aldrich
2-theonyltrifluoroacetone (HTTA)	AR Grade	Merck, Germany
Hydroxyl amine nitrate (HAN)	AR Grade	Lancaster, U.K.
Acetohydroxamic acid (AHA)	AR Grade	Aldrich
Hydroxy urea (HU)	AR Grade	Aldrich
Decalin	AR Grade	Fluka
Acetaldoxime (AOX)	AR Grade	Lancaster, U.K.
DIBC	AR Grade	Aldrich

2.2.5. Preparation of simulated AHWR feed solution

The proposed composition of AHWR feed solution is 2 g/L U + 2 g/L Pu + 100 g/L Th + 0.03 M HF + 0.1 M $Al(NO_3)_3$ at 3.5 M HNO_3, respectively [**115, 116**]. Tracer concentration of Pu (~10^{-5} M) was used in the simulated feed solution instead of proposed 2 g/L Pu due to marginal variation in the distribution behavior of Pu at trace or 2 g/L concentrations. Appropriate quantities of uranium, plutonium and thorium from their stock solutions were mixed to get the final concentrations. Calculated quantities of $Al(NO_3)_3$, and of HF were also added to get their final concentrations as 0.1M and 0.03M, respectively. The feed acidity was adjusted to 3.5 M HNO_3.

2.2.6. Preparation of simulated fast breeder reactor (FBR) feed solution

Currently, the proposed feed composition for the reprocessing of a typical Pu rich (relevant to fast reactor) spent fuel is 50 g/L U + 20 g/L Pu at ~ 4 M HNO_3 [**117**]. This feed is proposed to be prepared by external addition of uranium, which should be sufficient for electrolytic reduction of Pu to Pu(III) during partitioning cycle. During reprocessing, the proposed organic-to-aqueous phase ratio (O/A) in the extraction cycle is ~ 2.5, thereby diluting the uranium and plutonium concentrations in organic phase to 20 g/L and 7 g/L, respectively. In this context, the feasibility studies for reprocessing were carried out using a diluted feed solution having 20 g/L U + 7 g/L Pu at ~ 4 M HNO_3.In addition, U and Pu distribution (extraction/stripping) studies were carried out to evaluate TBP and DHOA in the presence of U (tracer, 20 & 50 g/L) by batch as well as mixer settler and centrifugal contactor studies.

2.2.7. Preparation of Simulated High Level Waste (SHLW)

The composition of PHWR-SHLW (burn up: 6500 MWD/THM (Megawatt day per ton of heavy metals) and Cooling period: ~ 5 years) is given in the Table 2.4 [**118**]. The SHLW solution was prepared by dissolving the metal ions salts in nitric acid. Care was taken to dissolve each of the salt separately in hot concentrated nitric acid before their addition to the mixture. The acidity of SHLW was adjusted as required with distilled water / HNO_3. The acidity of the SHLW was ascertained by acid-base titration in the presence of neutral saturated potassium oxalate ($K_2C_2O_4$which was used to complex with interfering metal ions). The acidity of PHWR-SHLW was usually in the range of 3-4M HNO_3solution. The concentration of various metal ions in SHLW is ascertained by Inductively Coupled Plasma -Auger Electron emission Spectroscopy (ICP-AES) or Energy Dispersive X-Ray Fluorescence (EDXRF) analysis.

Table 2.4: Composition of SHLW used in the present studies; Acidity: 3.5 M HNO_3

Element	Concentration (g/L)	Element	Concentration (g/L)
Na	5.50	Mo	0.14
K	0.22	Ba	0.06
Cr	0.12	Y	0.06
Mn	0.43	La	0.18
Fe	0.72	Ce	0.06
Sr	0.03	Pr	0.09
Cs	0.22	Nd	0.12
Zr	0.09	Sm	0.09

2.2.8. Coating of glass wares

5 % solution of dimethyl dichlorosilane (DMDCS) in toluene was used for coating inner surface of glass tubes used during ^{233}Pa extraction studies to minimize its loss due to sorption on the walls. The solution was then drained out after 3 hours and the tubes dried prior to their use for the solvent extraction studies [**119**].

2.3. Methods and equipments

Several techniques are known for the separation of metal ions, such as solvent extraction, extraction chromatography, and supported liquid membranes. The aqueous metal-ligand complexation, ligand-nitric acid complexation, thermodynamics of metal ion extraction etc were studies using solvent extraction technique in the present studies. The feasibility of the separation process on relatively large scale (3-4 L) was demonstrated in counter-current extraction employing a mixer-settler, and centrifugal contactors systems. The solvent degradation studies were carried out using ARSST (advanced reactive system screening tool) system.

2.3.1 Solvent extraction

For distribution studies of metal ions, suitable volumes (0.5-2 mL) of aqueous phase at the desired acidity containing the required metal ion tracer was equilibrated in glass stoppered equilibration tube with equal volume of organic phase containing desired concentrations of extractant(s) in the suitable diluents system. The organics phases were pre-equilibrated with the respective acid solutions to eliminate the effect of acid uptake in all studies. The agitation of the two phases was carried out by rotary motion in a thermo stated water bath (Figure 2.1) maintained at 25(±0.1)°C. After equilibration, the two

phases were centrifuged and assayed by suitable aliquots (25-500μL) from both the phases using different analysis instruments.

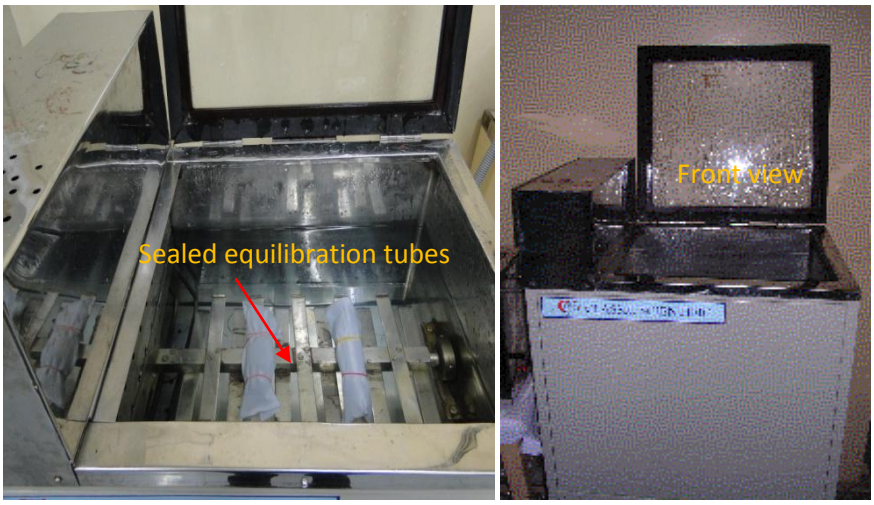

Fig. 2.1. Thermostated water bath for maintaining constant temperature

The distribution ratio (D) of the metal ions was calculated as the concentration of metal ions (in terms of counts per unit time per unit volume) in the organic phase to that in the aqueous phase. The concentrations of hydrogen ion in the two phases were obtained by titration with standard alkali (NaOH) solution using phenolphthalein as the indicator during acid distribution studies. Aqueous ethanol medium neutralized to phenolphthalein end point was used for organic phase titration. Distribution value was obtained in duplicate or triplicate and the agreement between these values was within ±2%. A good material balance (≥95%) was usually obtained in all the experiments.

2.3.2. Measurement of dispersion numbers

The dispersion number (N_{Di}) is used to characterize different solvents and for the design and scale-up of extraction equipments with discrete stages for centrifugal extractors or

mixer-settlers. Liquid-liquid dispersions created in mixing zone getting coalesced in a settling zone. It directly measures how long it will take for a liquid-liquid dispersion to coalesce completely and settling of different phases for a given system. Settling time (t_B) mainly depends upon the density difference, viscosity of the systems, interfacial tension, and surface elasticity etc. Dispersion number was measured by using 250 mL standard measuring cylinder. Volumes of aqueous and of organic phases taken for these measurements were 100 mL. Total height of the solution inside the measuring cylinder was 201mm [**120-122**]. Solutions inside the cylinder were shaken vigorously and allowed to settle under gravity. The time taken for complete coalesces to settled of the two phases was noted for the calculation of N_{Di} (dimensionless) by using the following formula [**123**]:

$$N_{Di} = \frac{1}{t_B}\sqrt{\frac{\Delta Z}{g}}$$

Where N_{Di} = Dispersion Number

t_B = Settling time (s)

ΔZ = Dispersion band height (m) (0.201m)

g = Acceleration due to gravity (m^2/s)

2.3.3. Mixer settler studies

Two different types of mixer settler units of made of acrylic and perspex, respectively were used for counter-current extraction/stripping studies. An eight-stage mixer and settler unit with bed volumes of 30 mL (mixer), and 130 mL (settler) and a total hold up volume of ~ 1300 mL was indigenously fabricated using acrylic material. On the other hand, twelve-stage mixer-settler unit (made up of perspex polymer) was procured from Sonal France (Batteries No. 36, Brevete S.G.D.G. (Figure 2.2). The unit had a total hold

up volume of ~500 mL with a mixer volume of ~10 mL and settler volume of ~30 mL. Mixer settler runs were carried out by employing turbine-type agitators made up of stainless steel. Peristaltic pumps (PP 20) procured from M/s Miclins, Chennai, India, were used for adjusting the flow rate of aqueous/organic solutions while flexible polypropylene tubing were used for the transportation of the solutions. Only uranium extraction run was carried out using eight-stage mixer settler unit while other runs were performed employing twelve-stage unit. The flow rates of feed solutions to the mixer settler units were maintained between (4-5 mL/min).

Org. IN →								**Org. OUT →**			
1	2	3	4	5	6	7	8	9	10	11	12
← Aq. OUT								**← Aq. IN**			

Fig. 2.2. 12 -Stages mixer settler unit for counter-current extraction run

The extraction, scrubbing and stripping runs were carried out independently at room temperature (T: 298 K). Since the mixer-settler unit was having 12 integrated stages, simultaneous extraction, scrubbing and stripping step were not possible in a single run. After extraction run, the loaded organic phase was collected and scrubbing was performed thereafter. Similarly, after the scrubbing operation, the scrubbed organic phase was used for stripping runs. No hydrodynamic problems were encountered in any of the

runs lasting for about four hours of each independent run. The attainment of the steady-state was checked by Liquid Scintillation Counting (LSC),by Davies-Gray method and ethylene diaminetetraacetic acid (EDTA) titrations of Pu, U and Th respectively, at the EXIT of the aqueous and organic phase streams. At the end of the experiment, the motors and pumps were switched off and subsequently, the samples from aqueous and the organic phases were collected from each of the settler units for the analysis of metal ions (U, Pu, Th) and concentration.

2.3.4. Centrifugal contactor studies

Centrifugal contactors are being proposed for counter-current extraction runs for metal ions from high burn up reactor spent fuels. The centrifugal contactors have salient features such as (a) high liquid through-put, (b) more compact design, (c) low liquid holdup volume, and (d) short residence time [**124, 125**]. Application of centrifugal contactors to fast reactor fuel reprocessing have a great advantage in criticality control, throughput and solvent degradation due to the short liquid residence time, while mixer-settlers and pulsed columns suffer from the limitations of relatively extended durations of phase separations. This process is essentially governed by gravity, and hence requires a higher liquid holdup volume. The compact size and high performance of centrifugal contactors are expected to be applicable to the solvent extraction process for advanced aqueous reprocessing in the fast reactor mixed oxide (MOX) fuel cycle with Pu and fission products (FPs) contents **[77]**.

High extraction and separation in centrifugal contactor is due to forcible mixing under rotor rotation and strong phase separation under centrifugal force. Here aqueous

and organic phases are mixed in the annular zone between the spinning rotor and the housing, and liquid-liquid dispersions are formed thereby coquette flow. This mixing disperses one phase as small droplets in the other to maximize the mass transfer area [**126**]. Centrifugal contactors have high single stage efficiency greater than 95% of theoretical for chemical processes with rapid kinetics. This requires a minimum of instrumentation for process operation [**127**].

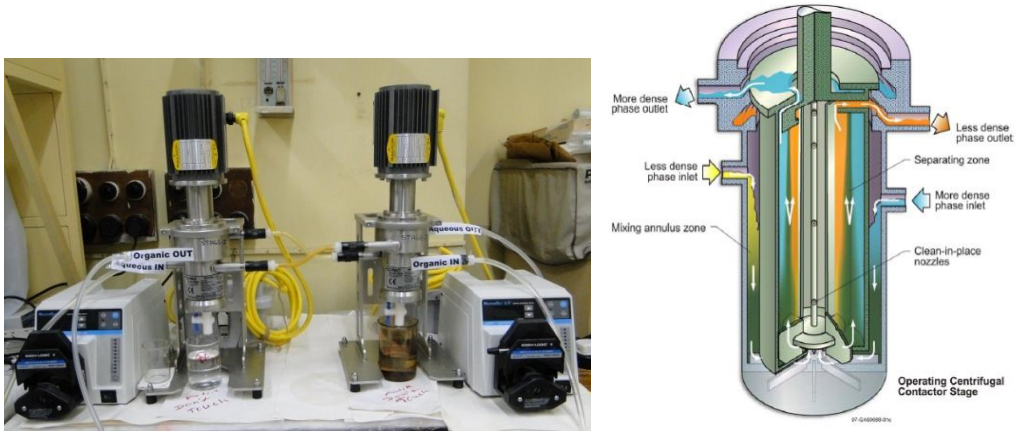

Fig. 2.3. Centrifugal contactor units and their cross sectional view

Two stages centrifugal contactors (Figure 2.3) were used for U extraction from feed solutions of varying compositions, simulated AHWR and fast reactor simulated feed solutions. These contactors had a bowl volume of 200 mL, with a provision of interchangeable weirs for accommodating liquids of varying specific gravity and viscosity. The aqueous and organic phases were passed in counter-current mode using metering pumps. Various parameters such as flow rate, motor rotation per minute (rpm) etc. were optimized for extraction and stripping of metal ions in centrifugal contactors. These runs were performed at room temperature (T: 298 K). The extraction and stripping runs were carried out independently. All of the phases collected and the samples from

aqueous and the organic phases were analyzed by Davies-Gray method, LSC and EDTA titrations for U, Pu and Th estimation respectively. Acidity of the sample was analyzed by acid-base titration method in saturated potassium oxalate medium.

2.3.5. Advanced reactive system screening tool (ARSST) studies

The thermal degradation studies due to runaway reaction between DHOA and HNO_3were conducted in ARSST unit. This is a calorimeter and is used to determine activation energies and to size vent relief valves for runaway exothermic reactions [**128**]. It consists of a spherical glass test cell (10 mL) surrounded by bottom heater jacket encapsulated in aluminum foil and with glass wool insulation for minimizing the heat loss with the surroundings (Figure 2.4). The bottom heater is belted to the test cell, provides a net resistance of approximately 24 Ω. Sample temperature is monitored by K-type Haste alloy thermocouple and pressure is sensed by 500psig pressure transducer. The insulated glass cell is kept in a 350 mL high pressure, high temperature stainless steel (SS-316) containment vessel which serves as both a pressure simulator and safety vessel. The containment vessel is hydrostatically tested to 3000 psig and it contains a Hastelloy rupture disk rated at about 900 psig to provide safety during the experiments. A magnetic stirrer bar is placed inside the test cell for stirring the liquid reaction mixture and is driven by an external magnetic stirrer. System is also provided with an external fill tube which can be used to add sample to the open test cell either before or during a test.

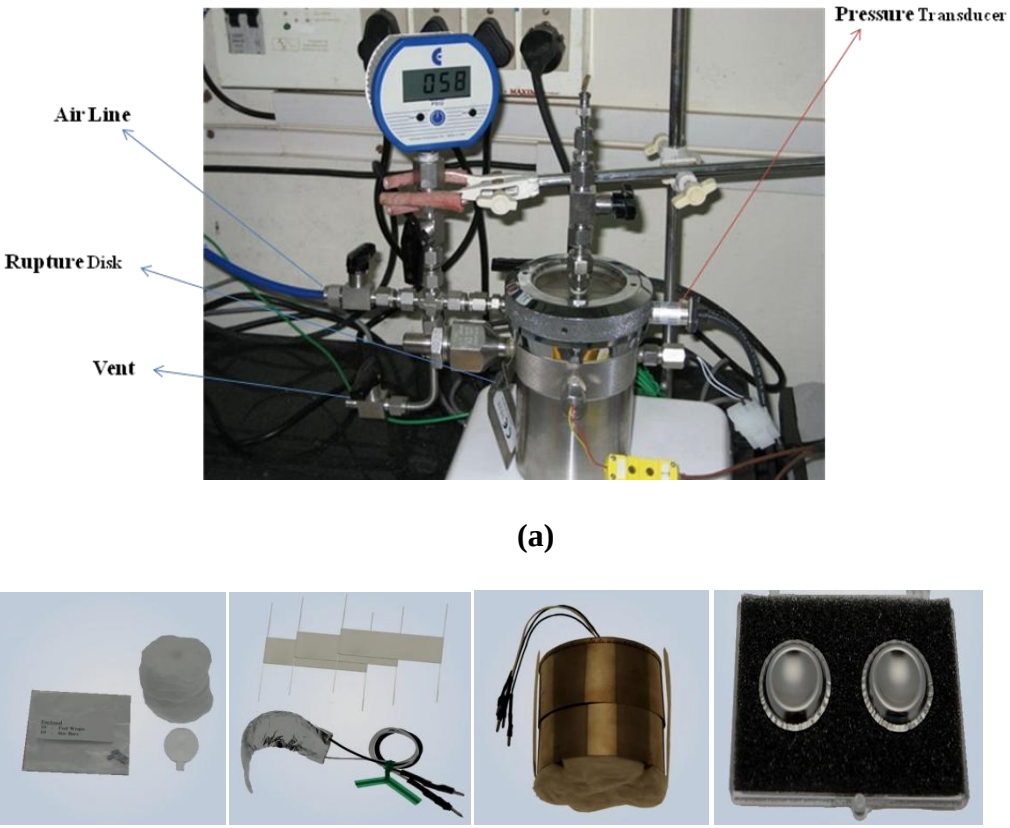

(a)

(b) (c) (d) (e)

Fig. 2.4. A view of containment vessel of ARSST and different parts: (a) ARSST containment vessel, (b) glass cell with glass wool, (c) 24 Ω electrical band heater, (d) glass cell along with heater and insulation, and (e) rupture disks

The ARSST control box contains the temperature and pressure amplifiers/circuits and the heater power supply which powers the bottom heater and provides power up to 17 W. Compressor line is connected to gas inlet line to provide compressed air for purging/pressurizing the system. The important features of this setup are its low effective heat capacity relative to that of the sample. This is expressed as φ-factor, which is approximately 1.05 (*i.e.* nearly adiabatic). So, the heat released by reaction taking inside the test cell goes to heat up the sample with negligible energy absorbed by the test cell

itself. This allows the measured data to be directly applied to industrial process scale. The maximum allowable working pressure (MWAP) is 3350 psi (227 bars) and maximum allowable working temperature (MAWT) is 454 ^{o}C.

The ARSST is computer controlled using operating software. The software records time, temperature, pressure and heater power during a test. The software automatically calibrates the heater/sample system for both constant ramp and adiabatic modes of operation which provides accuracy in maintaining a specified temperature ramp and adiabatic conditions.

A weighed amount of sample was taken in glass cell and a 3-4 mm long piece of SS-316 wire was also put inside the cell to simulate the metal surface of process vessels. The test cell was put in the high-pressure pressure vessel, sealed and was pressurized to approximately 5 bars (75 psi) to minimize evaporation during early heating. Electronic pressure sensing module was calibrated at two points using digital pressure gauge connected to the system. Temperature and pressure data were logged by ARSST system software at an interval of 1 psi as well as 1 K. After sealing and the pressurization cell was heated electrically at a rate of approximately 2 K/min in PID control mode with an auto-thermal shutdown at 573 K. After reaching temperature of 573K, input power to band heater was automatically cut-off and temperature started to fall and experiment was complete when temperature reached room temperature. After reaching ambient temperature, the vent was opened to release the gases formed by the reaction between solvents and HNO_3. The initiation temperature of the decomposition of nitrated solvents was estimated from the plots of temperature vs time.

2.3.6. Radiation stability studies

Radiolytic stability of the solvents was also investigated during the present studies. For this purpose, the solvents were irradiated for a given time to get exposed to a given amount of irradiation. A ^{60}Co gamma source of 1kGy/hour dose rate was used as the irradiator. Different solvents comprising of 0.18 M TBP and 0.36 M DHOA solutions in *n*-dodecane (proposed for AHWR spent fuel reprocessing) were kept in the gamma chamber equipped with ^{60}Co source and samples were periodically withdrawn for the estimation of extent of degradation by plutonium distribution studies.

2.3.6.1. Details of gamma source used for irradiation

The gamma chamber used for irradiation studies consists of ^{60}Co source pencils loaded in a cylindrical array in a source cage and stored at the centre of a lead flask (Figure 2.5). The central drawer is a long cylinder consisting of two stainless steel clad lead shields with a hollow sample chamber situated in between. The central drawer can be raised or lowered by a wire rope passing over a system of pulleys and wound on a drum by a geared motor. For irradiation, the drawer is lowered until the sample chamber is at the centre of the source cage. The movement of the sample chamber is controlled by an electrical control circuit panel. The dose rate was standardized by Fricke dosimetry.

2.3.6.2. Fricke dosimetry

Fricke dosimeter was originally developed as a dose measuring device and was used here for the calibration of Gamma chamber-900. It is most useful method to directly measure the numbers of reactive species in solution [**129-131**]. It relies on oxidation of ferrous ions in to ferric ions in an irradiated ferrous sulphate solution. The amount of ferric ions

produced in the solution is measured by absorption spectrometry with ultraviolet light at 304 nm, which is strongly absorbed by the ferric ions. Fricke dosimeter depends on an accurate knowledge of the radiation chemical yield of the ferric ions, measured in moles produced per 1J of energy absorbed in the solution. The chemical yield is related to a parameter 'G' which is defined as the number of ferric molecules produced in the ferrous sulphate solution by 100eV of absorbed energy. An accurate value of chemical yield is difficult to ascertain because the chemical yield is attached to the energy of the radiation, dose rate and temperature of the solution during irradiation and readout. The dose rate of the ^{60}Co irradiator was measured to be 1.0 kGy/hr.

Fig. 2.5. Gamma chamber at Radiochemistry Division BARC

2.4. Radiometric analysis

The different radio-analytical techniques were employed for the analysis of metal ions. For alpha emitting radionuclides (Pu(IV), U(VI), ^{237}Np) liquid scintillation counter was used, whereas NaI(Tl) scintillation counter and HPGe detector were used for the estimation of gamma emitting radionuclides such as ^{241}Am , ^{239}Np,^{147}Nd,^{137}Cs,^{99}Mo,^{95}Zr, ^{233}Pa etc.

2.4.1. Liquid scintillation counter

Liquid scintillation counter is the most widely used detector for quantitative analysis of alpha emitters. Detection efficiency of this detector is nearly 100 %, which is a great advantage as a few Becquerel (Bq) of alpha activity can be assayed with good precision. A scintillator is a material that luminescence in a suitable wavelength region when ionizing radiation interacts with it. Interaction of charged particles (alpha particles) with the scintillator results in emission of photons and the intensity of the emitted light is a quantitative measure of the incident radiation. The light emitted from scintillator is then collected at the photomultiplier tube (PMT) which produces signal representative of the primary radiation. In the case, when scintillator emits photons in the UV region, a wavelength shifter is added to the scintillator which has intermediate energy levels. In such cases, the de-excitation takes place via these intermediate energy levels and hence the wavelength of the emitted photons is shifted from UV to the visible region which is subsequently recorded in the PMT (as photocathode of most PMTs are compatible with visible light). The liquid scintillation counter is used to monitor gross alpha activity as it cannot distinguish between alpha energies and thus cannot be used for alpha spectrometry.

The liquid scintillation cocktail comprises of a solvent like dioxane or toluene, a scintillator like PPO (2,5-diphenyl oxazole) and a wavelength shifter such as POPOP [1,4-bis-2-(5-phenyl oxazolyl)-benzene]. The solvent is the main stopping medium for radiation and must be chosen to give efficient energy transfer to the scintillating solute. In case of toluene based scintillator, a suitable extractant such as di(2-ethylhexyl) phosphoric acid (HDEHP) is also added which facilitates estimation of alpha activity in the aqueous samples by transferring the radionuclides from the aqueous phase to the

organic phase. Dioxane based liquid scintillator consist of 0.1 % (v/v) PPO, 0.025 % (w/v) POPOP and 10 % (w/w) naphthalene. In addition to these, *tri*-octyl phosphine oxide (TOPO) is added which acts as an anti-quenching agent so as to suppress the effect of acid [**132, 133**]. Naphthalene is added to increase the shelf life of the cocktail mixture. On the other hand, the toluene based liquid scintillator consists of 10 % (v/v) HDEHP, 0.7 % (w/v) PPO and 0.03 % (w/v) POPOP. Suitable aliquots (25-100μL) of solutions containing alpha activity were taken in glass vials containing about 5 mL of the liquid scintillator solution. Each sample was counted for sufficient time so as to get more than 10,000 counts to restrict the statistical counting error to within ±1%.

2.4.2. NaI(Tl) Scintillation counter

Sodium iodide activated with 0.1 – 0.2 % of thallium, NaI(Tl), is widely used inorganic scintillator for the assay of gamma emitting radionuclides. Salient features of the detector are low cost, ease of operation, and ruggedness [**134**]. The band gap in NaI crystal is of the order of 5-6 eV. When a gamma ray falls on the detector its energy is used up either for excitation of the electrons from the valence band to conduction band or for the ionization of atom. De-excitation of the electrons from conduction band to the valance band leads to the emission of photons in the UV region as the band gap is large. To shift the energy of the emitted photons to the visible region, which is required for the detection by PMT, NaI crystal is doped with an activator impurity like thallium (Tl) which forms the intermediate level conduction band. The resolution of NaI(Tl) detector is about 7% at 662 keV. In the present work, a 3” x 3” well type NaI(Tl) detector coupled with a multi-channel analyzer (Figure 2.6) has been used for gamma counting. Nearly 100% detection efficiency for moderate energy photons in a well type NaI(Tl) detector offers great

advantages for counting of low activity samples. A suitable aliquot (usually 0.1 mL) of the desired analyte solution was taken in glass counting tubes which was then placed in the well of the detector. Each sample was counted for sufficient time so as to get more than 10,000 counts to restrict the counting statistics error to <1 %.

Fig. 2.6. NaI(Tl) detector used for gamma spectrometry

2.4.3. High purity germanium detector

High purity germanium (HPGe) detector coupled with multichannel analyzer (Figure 2.7) was employed for gamma ray spectroscopy to check the radiochemical purity and the estimation of radionuclides like ^{241}Am, ^{152,154}Eu, ^{239}Np, ^{147}Nd, ^{59}Fe, ^{99}Mo, ^{99}Tc, etc. The HPGe detector is made up of highly pure germanium in which the impurity level is around 10^{10} atoms/cc and thus it approaches the theoretical pure semiconductor. HPGe is the most widely used semiconductor detector for gamma spectrometry. The high energy resolution (typically, 1.9 keV at 1332 keV) is the key feature of this detector due to low energy band gap (0.7 eV). The major advantage of HPGe detector is that it can be stored at room temperature [**135**].

(a) (b) (c)

Fig. 2.7. HPGe detector used for gamma ray spectrometry

However under operating condition, it has to be cooled to liquid nitrogen temperature. The HPGe detectors are of two types, *p*-type and *n*-type. In case of *p*-type, the outer surface of the germanium crystal is heavily doped with *n*-type impurity. As a result, the detection efficiency falls drastically below 100 keV. On the other hand, *n*-type detectors are sensitive to wider range of photon energy. The *n*-type detector has added advantages in that it is more resistant to radiation damage in a neutron field as compared to a *p*-type detector because the damage sites preferentially trap holes rather than electrons. The *n*-type detector is therefore preferred as compared to the *p*-type detectors. In the present study, an *n*-type HPGe detector has been employed.

2.4.4. Spectrophotometer

JascoV-530 UV-Spectrometer (Figure 2.8) was employed for UV-Visible spectrophotometric analysis. The double beam spectrometer is used in which the light emerging from the monochromatic source is divided into two beams that take parallel but separate paths through the components. One of the two beams passes through the blank, which is called as the reference beam. The other passes through sample, which is called

as the sample beam. Over a short period of time, the spectrometer automatically scans all the components wavelengths in the manner described. The intensities of these lights beam are then measured by electronic detector.

Fig. 2.8. UV Visible Spectrophotometer (Jasco, Model V-530)

The software program can then manipulate the intensity of light passing through the sample (I) and compare it to the intensity of the reference beam (I_o) simultaneously to produce the spectrum of absorbance or transmittance, and is usually expressed as a percentage (%T). For measurement samples were put in the quartz cell (according to quantity it was 1-3 mL sample holding cell). Samples and respective blanks were put in the sample and blank chamber and run the software program.

2.4.5. Dynamic Light Scattering (DLS) spectrometer

The Zetasizer-3000 DLS spectrometer, procured from Malvern Instrument Company, UK (Figure 2.9) with a 4mW He-Ne laser beam at a wavelength of 632 nm, was used for aggregate size measurements in organic phases. All the measurements were performed at a scattering angle of 90° in a cell of 4mm path length with sample size 1.5-2mL at room

temperature of 25±1°C. The instrument was calibrated using standard colloidal suspension (polystyrene, Latex) before the size measurement of the actual samples. Each measurement was repeated at least five times to check the reproducibility of data.

Fig. 2.9. Zetasizer-3000 DLS spectrometer

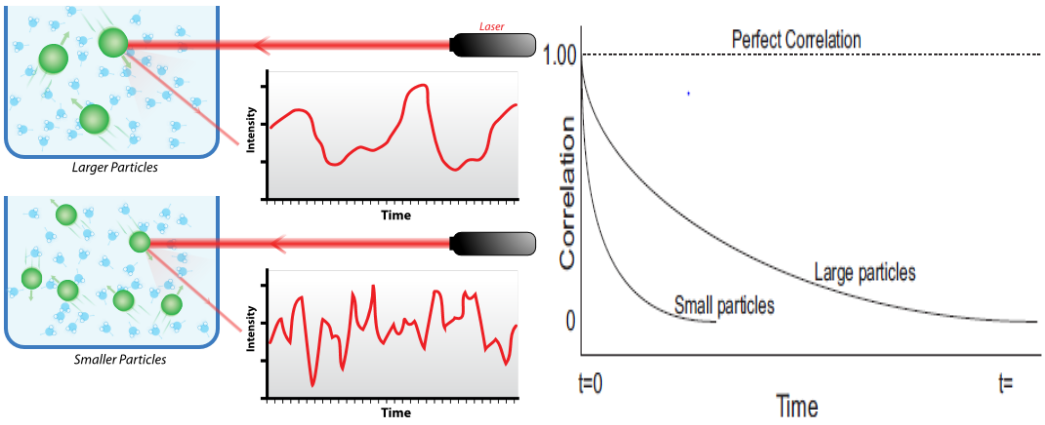

Fig. 2.10. Brownian motion of particle, interaction and correlation with incident light

The particles suspended in a liquid are under constant Brownian motion due to random collisions with the molecules of the liquid that surrounds the particles. When a monochromatic and coherent beam of light falls on such a suspension, the scattered light photons carry information about the size of the particles. DLS technique measures the fluctuations in the intensity of the scattered photons, which occur over short time intervals

due to scattering of the particles undergoing Brownian motion in the solution (Figure 2.10). These fluctuations are described quantitatively by the intensity of the autocorrelation function, C(τ) of scattered intensity as follows:

$$C(\tau) = A\left(1+\beta\int_{0}^{\infty} P(\Gamma)\exp(-\Gamma\tau)d\Gamma\right) \quad (1)$$

where, A is the baseline value, β is an instrumental constant and Γ is the characteristic line width of the distribution function P(Γ) and is related to the diffusion coefficient (*D*) of the species by the following expression:

$$\Gamma = Dq^2 \quad (2)$$

where, q is the scattering vector, which is constant for a given observation angle and wavelength of the incident light. Assuming the scattering species as hard sphere, the apparent hydrodynamic radius (r_h) of the species can be calculated through Stokes-Einstein equation:

$$r_h = k_B T /(6\pi\eta D) \quad (3)$$

Where, $k_B$is the Boltzmann constant, T is the absolute temperature and η is the viscosity of the dispersion medium.

2.4.6. Viscometer and interfacial tensiometer

The viscosity and the density of liquid samples were measured by a viscometer procured from Anton Paar, Austria (model number SVM 3000, (Figure 2.11). The interfacial tension (IFT) values of different samples were measured by Sigma 703D KSV interfacial tensiometer (Figure 2.12).

Fig. 2.11. The Anton Paar Viscometer used for the viscosity measurements

Fig. 2.12. The Sigma 703D KSV interfacial tensiometer

2.4.7. Estimation of uranium

2.4.7.1. Spectrophotometry

Uranium could be determined by spectrophotometry using 2-(5-bromo-2-pyridylazo)-5-(diethylamino) phenol (Br-PADAP) as a chromogenic reagent in the aqueous phase as well as in the organic phase [**136**]. Uranyl ion forms stable intense violet colored complex with Br-PADAP at pH 7-8 in the alcoholic medium buffered with triethanolamine

(TEA) which shows absorption maxima at 578nm with molar extinction coefficient of ~70,000.A known volume of uranium solution in standard flask (10mL), 1mL of complexing solution (1.25g CYDTA + 0.25g NaF + 3.25g sulphosalicylic acid dissolved in 100mL water adjusted to pH 7.8 with concentrated NaOH), 1mL buffer solution (14g TEA dissolved in 100mL water adjusted to pH 7.8 with perchloric acid) and 0.8mL Br-PADAP solution (50mg Br-PADAP dissolved in 100mL ethanol) were added, respectively. For organic samples the final volume (10mL) was made up with ethanol, while for aqueous samples the final volume (10mL) was adjusted with distilled water after addition of 4mL of ethanol. The final absorption measurements were performed after 30minute of color development at 578 nm. This method was found to be very sensitive and no interference of Pu, Th, Al and Fe was observed. The calibration curve was plotted in the concentration range of $1x10^{-6}$M to $1x10^{-4}$M with standard uranium solution. The concentrations of unknown samples were determined from the calibration plot.

2.4.7.2. Davies Gray titration

Uranium in the concentration above 50µg/mL was estimated volumetrically by Davies-Gray method employing potentiometric end point detection [**137, 138**]. The sample size was varied between 0.1-0.3 mL. This method involves the reduction of U(VI) to U(IV) by Fe(II) in the presence of concentrated phosphoric acid solution containing sulphamic acid. Then the excess Fe(II) is selectively oxidized by nitric acid in the presence of Mo(VI) which acts as a catalyst. The role of sulphamic acid is to destroy any trace of nitrous acid present in the solution which may oxidize Fe(II) and U(IV). The resulting U(IV) phosphate solution is then titrated with standard potassium dichromate solution to potentiometric end point. A small amount of V(IV) sulphate is added in the solution

which sharpens the end point. The concentration of uranium in the analyte solution is calculated from the volume of standard potassium dichromate solution consumed.

2.4.8. Estimation of thorium

2.4.8.1. Spectrophotometry (thoron method)

Th in microgram quantities in aqueous samples could be determined by spectrophotometric method [**139, 140**]. Thorium forms a red complex with thoron, 2-(2-hydroxy-3,6-disulpho-1-napthylazo)benzene arsenic acid, at pH 1-2. The colored complex has an absorption maximum at 545 nm (ε: ~15500 $M^{-1}cm^{-1}$). 0.2% solution of thoron reagent was prepared in distilled water. For sample preparation (10 mL), suitable Th aliquot, 0.2mL of concentrated HCl and 0.6mL of 0.2% thoron solution were taken in a standard flask and volume was made up using distilled water. After color development (~15 minutes after mixing), absorbance measurement of the sample was carried out at 545 nm against blank (0.2% thoron and HCl solution diluted to 10 mL without thorium). Calibration plot was obtained by measuring the absorbance of various samples at 545 nm.

2.4.8.2. Complexometric titration

When the concentration of thorium was in milligram and higher quantities, the conventional complexometric titration was followed. A suitable aliquot of Th solution was titrated against standard EDTA (ethylenediaminetetraacetic acid) solution at pH 3 using xylenol orange as an indicator [**140**]. The end point of the reaction was the change of color from deep purple to lemon yellow. The precision of these analyses was ±2% (~5mg Th). Similarly, the organic phase was also titrated with a precision of ±5% and each titration was done in duplicates.

CHAPTER 3: EVALUATION OF *N,N*-DIHEXYLOCTANAMIDE FOR REPROCESSING OF Pu RICH FUELS

3.1. Introduction

Reprocessing of spent nuclear fuel is vital for the long-term global nuclear power growth and is the major motivation to develop novel schemes for the separation of uranium, and plutonium from other elements with high decontamination factors (DFs). The *PUREX* process has undergone several modifications to address to the issues of high burn up, fewer solvent extraction cycles and reduced waste arising [**60**]. The evaluation of *N,N*-dialkyl amides as alternative extractants to tri-*n*-butyl phosphate (TBP) for reprocessing of spent fuel have suggested that straight chain *N,N*-dihexyloctanamide (DHOA) is a promising candidate for the reprocessing of irradiated uranium based PHWR fuels rather than TBP [**76, 77, 114**]. It was found that though uranium extraction using DHOA as extractant was comparable to that of TBP, DHOA displayed better stripping behavior. Plutonium extraction behavior was better in the case of DHOA as compared to that of TBP. During fuel reprocessing, solvent get exposed to high irradiation fields. As a consequence, severe solvent degradation is expected to occur. The radiolytic degradation of TBP is well studied with respect to the extraction and stripping behavior of U/Pu, and hydrodynamic properties such as viscosity, density, and phase disengagement time and found to be adversely affected as a consequence of the radiolytic degradation of TBP [**61-64**]. These limitations are of particular concern during the reprocessing of short-cooled thermal reactor fuels as well as fast reactor fuels. The radiolytic stability of DHOA was investigated to evaluate its performance under varying experimental conditions vis-à-vis TBP by gamma/alpha radiolysis [**101, 141**]. TBP showed significant retention of Pu, U, and fission products in the irradiated TBP as compared to that of DHOA even after

successive contacts with the stripping solutions. There was an increase in the density and viscosity for the irradiated solvents (TBP/DHOA). Detailed measurements of interfacial tension (IFT), viscosity, and phase separation time (PST) under uranium loading conditions suggested that DHOA can be used for spent-fuel reprocessing with a suitable adjustment of hydrodynamic parameters [**142**]. This chapter presents the evaluation of DHOA vis-à-vis TBP as extractants in batch, mixer settlers as well as in centrifugal contactor runs under the conditions relevant for reprocessing of Pu rich spent fuels.

^{99}Tc is an important beta emitting nuclide of concern ($t_{1/2}$ = 2.11×10^5 *y*, $E_{\beta\text{-max.}}$ = 295.5 keV) with high fission yield of about 6.13% for thermal neutron induced fission of ^{235}U for long-term nuclear waste management. Apart from the contamination of U and Pu products, technetium catalyzes the oxidation of hydrazine, which is used as a nitrite scavenger in the reductive separation of plutonium from uranium [**143**]. Therefore, systematic studies for Tc extraction have been carried out using these extractants under different experimental conditions. The effect of acetohydroxamic acid (AHA) concentration on U, Pu, Np, and Tc extraction behavior has been studies. Pu(IV)-AHA interaction under various process conditions has also been investigated.

3.2. Results and discussion

Prior to different extractions studies, various physical parameters like the dispersion numbers *(N_{Di}),* phase disengagement time (PDT) of DHOA were calculated and compared with different solvents proposed for back-end of fuel cycle operations.

3.2.1. Measurement of dispersion numbers

The dispersion numbers were measured for (a) 1.1 M DHOA/*n*-dodecane at 4 M HNO_3, (b) 1.1 M TBP/*n*-dodecane at 4 M HNO_3, and (c) 0.1 M TODGA /*n*-dodecane at 4 M HNO_3 systems [**112, 144**]. The calculated values were compared with those of different phosphonate extractants (which have been evaluated or proposed as alternatives for TBP) for the reprocessing of fast reactor spent fuels (Table 3.1) [**145**].

Table 3.1: Settling times (t_B) and dispersion numbers (N_{Di}) for different extraction systems; Diluent: *n*-dodecane; Aqueous phase: 4 M HNO_3; T: 298 K

System	t_B, s	ΔZ (m)	N_{Di}	Reference
1.1 M TBP	86	0.201	1.68×10^{-3}	p.w.
1.1 M DHOA	118	0.201	1.21×10^{-3}	p.w.
1.1 M TiAP[(a)]	63.7	0.200	1.66×10^{-3}	[**122**]
0.1 M TODGA	95	0.201	1.49×10^{-3}	p.w.
1.1 M DBBP[(b)]	84	0.200	1.70×10^{-3}	[**145**]
1.1 M DBHeP[(c)]	102	0.200	1.40×10^{-3}	[**145**]
1.1 M DBOP[(d)]	110	0.200	1.30×10^{-3}	[**145**]

(a) Triisoamyl phosphate; (b) Dibutyl butyl phosphonate; (c) Dibutyl hexyl phosphonate; (d) Dibutyl octyl phosphonate; p.w. present work

Based on the phase settling behavior and the dispersion number, the solvent acceptability criteria has been laid which says that solvents having N_{Di} values between 6×10^{-4} to 1.4×10^{-3} will have good phase disengagement rates and those with higher values will have excellent performance [**122**]. These measurements suggest that 1.1 M DHOA/ *n*-dodecane under the specified conditions will have good performance with respect to

phase disengagement behavior. However, these values may change with experimental conditions.

3.2.2. Batch distribution studies

Extraction studies were carried out to evaluate 1.1 M DHOA and 1.1 M TBP as extractants for the reprocessing of U and Pu under varying concentrations of nitric acid (0.5-6 M HNO_3) and of uranium (tracer, 20 & 50 g/L). Figures 3.1-3.4 suggest that DHOA appears to be a better choice for reprocessing of U and Pu. The plutonium fraction can be enriched with respect to uranium in the product stream using DHOA as the extractant **[77]**. The batch distribution data generated during these studies were used for the calculation of number of theoretical stages required for quantitative extraction of U and Pu from 4 M HNO_3 solutions in a continuous co-current/counter-current solvent extraction processes [**54**].

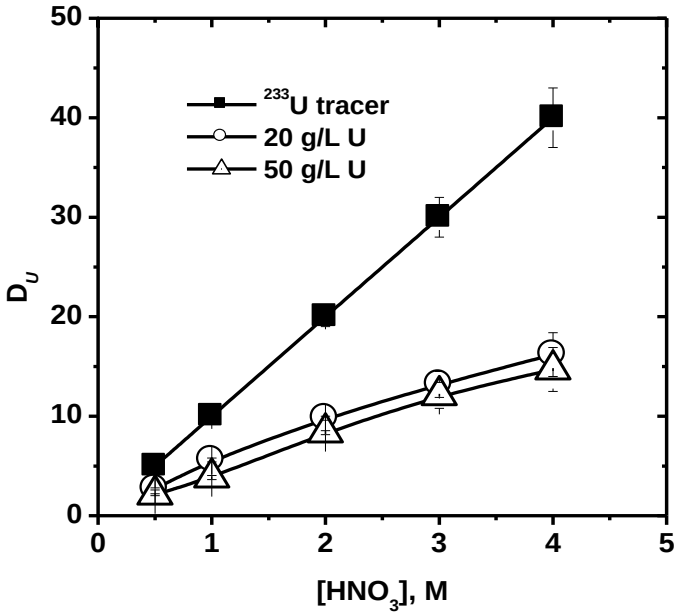

Fig. 3.1. Variation of D_U with aqueous phase U and HNO_3 concentrations; Solvent: 1.1 M TBP in *n*-dodecane; T: 298 K; O/A: 1

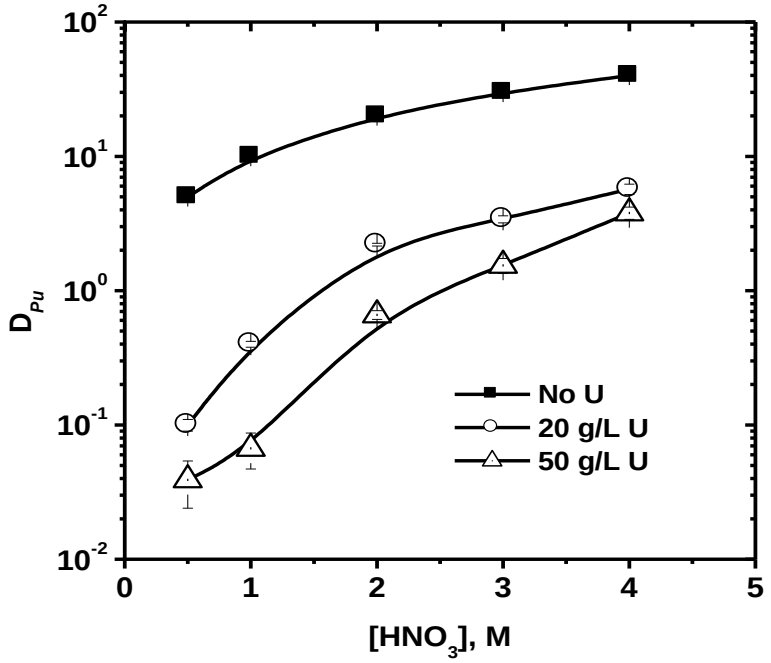

Fig. 3.2. Variation of D_{Pu} with aqueous phase U and HNO_3 concentrations; [Pu]: ~2 mg/L; Solvent: 1.1 M TBP in *n*-dodecane; T: 298 K; O/A: 1

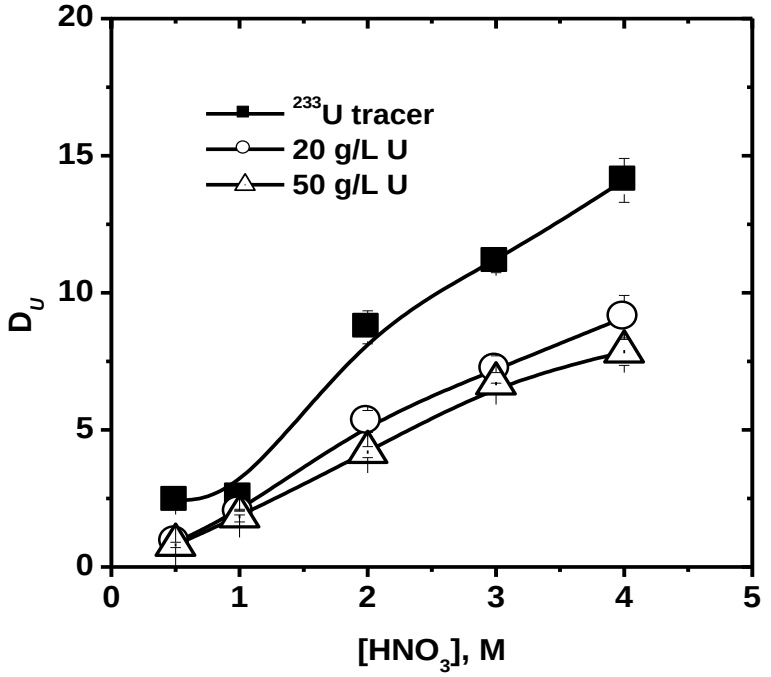

Fig. 3.3. Variation of D_U with aqueous phase U and HNO_3 concentrations; Solvent: 1.1 M DHOA in *n*-dodecane; T: 298 K; O/A: 1

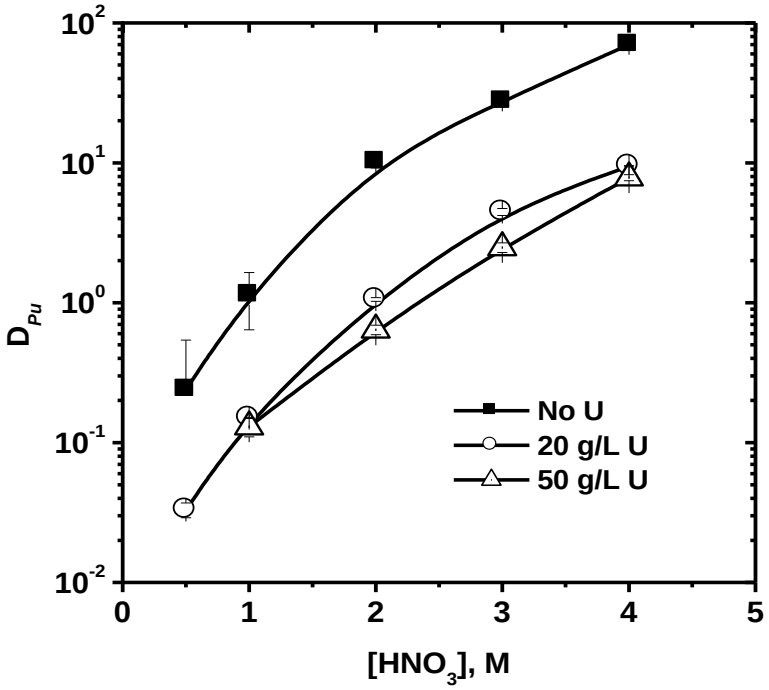

Fig. 3.4. Variation of D_{Pu} with aqueous phase U and HNO_3 concentrations; [Pu]: ~2 mg/L; Solvent: 1.1 M DHOA in *n*-dodecane; T: 298 K; O/A: 1

Table 3.2: Calculation of number of stages for quantitative extraction (99.9 %) of uranium and plutonium; [U]: 20 g/L; [Pu]: ~2 mg/L; [HNO_3]: 4 M; O/A: 1; T: 298 K

Extractant	***Metal ion***	***D_M***	**No. of stages for 99.9 % in different modes**	
			Co-current	**Counter-current**
1.1 M TBP	U(VI)	16	3	3
	Pu(IV)	5.7	4	4
1.1 M DHOA	U(VI)	9.7	3	3
	Pu(IV)	9.5	3	3

Table 3.2 compares the behavior of 1.1 M TBP and 1.1 M DHOA solutions with respect to quantitative U and Pu extraction from 4 M HNO_3 solutions maintaining

organic-to-aqueous phase ratio (O/A) as 1. It is evident that the two extractants do not show significant difference during the extraction of the metal ions except plutonium extraction which is better in case of DHOA.

3.2.3. Mixer settler studies

3.2.3.1. Extraction cycle for U

Uranium extraction studies were performed employing 1.1 M DHOA and 1.1 M TBP solutions in *n*-dodecane as solvents. The feed compositions were: 19.4 g/L U at 4.2 M HNO_3 (1.1 M TBP) and 25.4 g/L U (1.1 M DHOA) at 4.0 M HNO_3, respectively. The flow rates of the organic and aqueous phases were maintained as ~5 mL/minute. Overall organic to aqueous phase ratio (O/A) was maintained as 1.1. Analysis of the EXIT samples (organic and aqueous) suggested that equilibrium condition was reached after passing both the phases equivalent to one bed volume (~1300 mL). During the runs using 1.1 M TBP/*n*-dodecane as the extractant, the organic phase uranium concentration increased gradually from Stage 1 ($5x10^{-3}$g/L) to Stage 8 (17 g/L) (Figure 3.5). Similar increase was observed in nitric acid concentration in the organic phase [Stage 1 (0.6 M) to Stage 8 (0.8 M)]. The loaded organic phase composition was 17.0 g/L U + 0.9 M HNO_3 and that of raffinate was $8.5x10^{-4}$ g/L U + 3.11 M HNO_3. Similar run employing 1.1 M DHOA/*n*-dodecane as the extractant showed that organic phase uranium concentration increased from Stage 1($3x10^{-3}$g/L) to Stage 8 (24.5 g/L) (Figure 3.6).

Org. IN →						**Org. OUT →**	
1	2	3	4	5	6	7	8
← Aq. OUT						**← Aq. IN**	

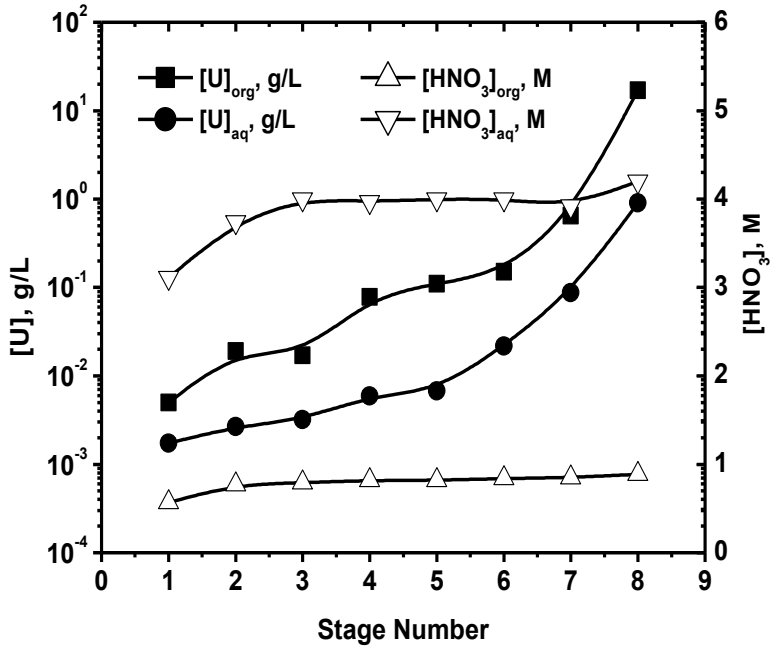

Fig. 3.5. Stage analysis data for U extraction; Feed: 19.4 g/L U at 4.2 M HNO_3; Solvent: 1.1 M TBP in *n*-dodecane; T: 298 K; O/A: 1.14

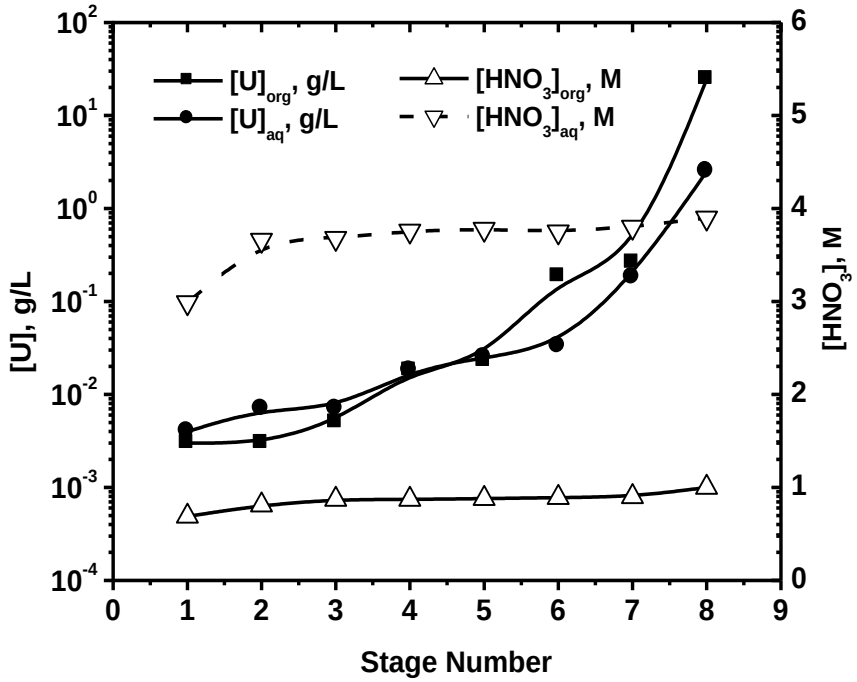

Fig. 3.6. Stage analysis data for U extraction; Feed: 25.4 g/L U at 4.0 M HNO_3; Solvent: 1.1 M DHOA in *n*-dodecane; T: 298 K; O/A: 1.08

Nitric acid concentrations in loaded 1.1 M TBP and DHOA phases were 0.8 M and 0.9 M, respectively. The loaded organic phase composition was 24.5 g/L U + ~1.0 M HNO_3 and that of raffinate was $2.0x10^{-4}$ g/L U + 2.8 M HNO_3. These studies suggested that uranium loss to raffinate and the acid uptake by the organic phase were comparable in both the extractants.

3.2.3.2. Extraction cycle for Pu

Figures 3.7 and 3.8 show the stage wise extraction profiles of Pu(IV) (2 mg/L, ~10^{-4} M) at 4 M HNO_3 using 1.1 M TBP and 1.1 M DHOA dissolved in *n*-dodecane as solvents. Flow rates of the organic and aqueous phases were maintained as 9 and 10 mL/min, respectively (O/A: 0.9). The equilibrium condition was achieved within 90 minutes in the case of DHOA; while ~120 minutes were required for TBP system. Stage analysis data showed that whereas 4 stages were sufficient for quantitative Pu extraction using 1.1 M DHOA as extractant; > 6 stages were required for 1.1 M TBP.

Org. IN →								**Org. OUT →**			
1	2	3	4	5	6	7	8	9	10	11	12
← Aq. OUT								**← Aq. IN**			

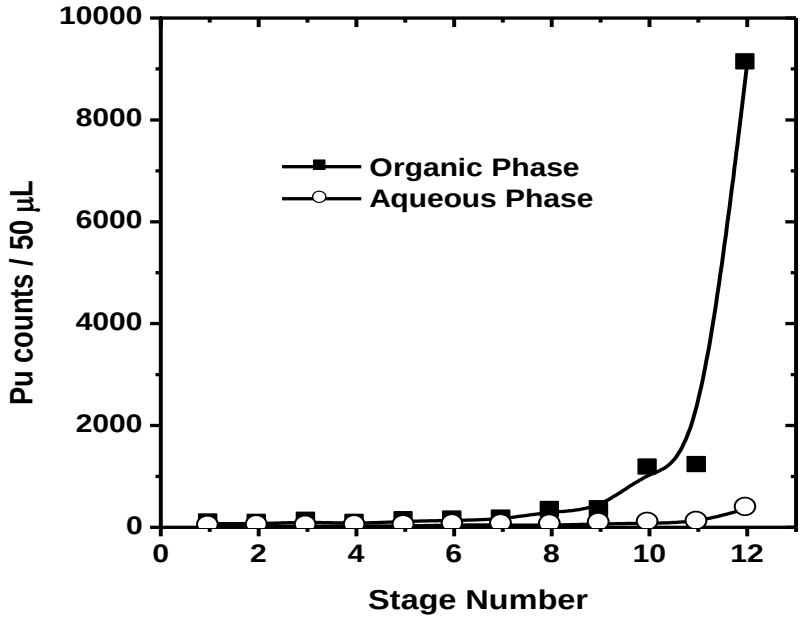

Fig. 3.7. Stage wise concentration profile of Pu(IV) during extraction cycle; Feed: 2 mg/L Pu at 4.0 M HNO_3; Solvent: 1.1 M TBP in *n*-dodecane; T: 298 K; O/A: 0.9

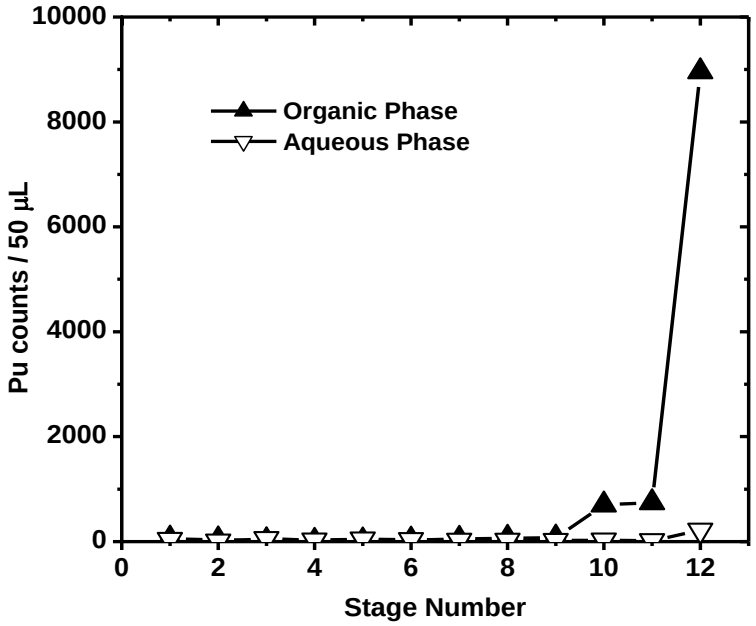

Fig. 3.8. Stage wise concentration profile of Pu(IV) during extraction cycle; Feed: 2 mg/L Pu at 4.0 M HNO_3; Solvent: 1.1 M DHOA in *n*-dodecane; T: 298 K; O/A: 0.9

3.2.3.3. Stripping Studies

The loaded organic phases from U and Pu extraction cycles were used as feed solutions for stripping studies employing 12 stage mixer settler unit. The experimental details are listed in Table 3.3. These studies clearly demonstrate DHOA is better with respect to U and Pu stripping behavior. Whereas quantitative stripping of uranium could be achieved employing DHOA as extractant while only 33 % Pu stripping was possible without reducing agent. By contrast, ~88 % (U) and 28 % (Pu) stripping can be was achieved employing TBP as extractant. This data indicated towards the need of reducing agent for Pu stripping.

Batch stripping studies (in co-current mode using fresh 0.5 M HNO_3 as strippant) reported earlier showed that only six stripping stages were sufficient for quantitative stripping of Pu from loaded DHOA phase. On the other hand, >10 stages were required for quantitative Pu stripping from loaded TBP phase and it became further difficult with the aging of the organic phase. By contrast, no such Pu retention was observed for aged DHOA solution [**76**]. The decreased stripping % in the current study was attributed to the acid build up in the aqueous phase during the counter-current mixer settler run. ~ 1M HNO_3 was present in the loaded organic phases during extraction cycles for both the extractants.

Stripping behavior of plutonium from loaded organic phases was compared under identical experimental conditions employing 0.5 M NH_2OH + 0.5 M HNO_3 as stripping solution maintaining organic-to-aqueous phase ratio (O/A) as 1. Whereas two contacts with the stripping solution was sufficient for quantitative removal of plutonium (>99.9%) from DHOA solutions; 3-4 contacts were required in the case of TBP. Interestingly, aged Pu loaded TBP phases showed very poor stripping of Pu essentially due to the formation

of the troublesome degradation products viz. dibutyl phosphate (DBP) along with the higher homologues of TBP, which are strong metal complexants [**141**].

Table 3.3: Comparison of performance of TBP and DHOA during 12 stage mixer settler runs for uranium and plutonium stripping from separately loaded (either with U or Pu) 1.1 M TBP and 1.1 M DHOA solutions in *n*-dodecane at flow rate ~10 mL/minute

Parameters	**1.1 M TBP**		**1.1 M DHOA**	
	U	**Pu**	**U**	**Pu**
Loaded organic phase	17.0 g/L, 0.9 M HNO_3	10500 cpm /50λ, 0.7 M HNO_3	24.5 g/L, 0.9 M HNO_3	8000 cpm /50λ, 0.7 M HNO_3
Strippants	0.01 M HNO_3	0.1 M HNO_3	0.01 M HNO_3	0.1 M HNO_3
O/A (stripping)	1	0.9	0.9	0.9
$[M]_{org,\ stripped}$	2.1 g/L U	7600 cpm /50λ	0.1 g/L U	5400 cpm /50λ
$[M]_{aq,\ stripped}$	15.2 g/L	2900 cpm /50λ	22.2 g/L	2600 cpm /50λ
$[H^+]_{aq,\ Stripped}$	0.6 M	0.7 M	0.3 M	0.6 M
Stripping %	87.6	~28	99.6	~33

3.2.4. Centrifugal contactor runs

3.2.4.1. Optimization of uranium extraction conditions

The operational parameters such as flow rate and rotor speed (rotations per minute, rpm) were optimized for U(VI) extraction from nitric acid solutions using two centrifugal contactors. Counter-current extraction studies were carried out using ~20 g/L U(VI) at 4 M HNO_3 as the aqueous phase and 1.1 M TBP/*n*-dodecane as the solvent at different flow rate & rotor speed (rpm) employing two stage centrifugal contactor (bowl volume: 200

mL) units. The extraction conditions used in this study were: (i) organic & aqueous phase flow rate(s): 20, 50, 100, 200 mL/min, and (ii) motor speed: 1500 to 4500 rpm (Figure 3.9). There was a gradual decrease with increased flow rate and motors rpm suggesting that time available for achieving equilibrium condition was not sufficient at higher flow rates and rpm. Based on these studies, the optimum flow rates and rpm were chosen as 20mL/min, 1500 rpm, respectively.

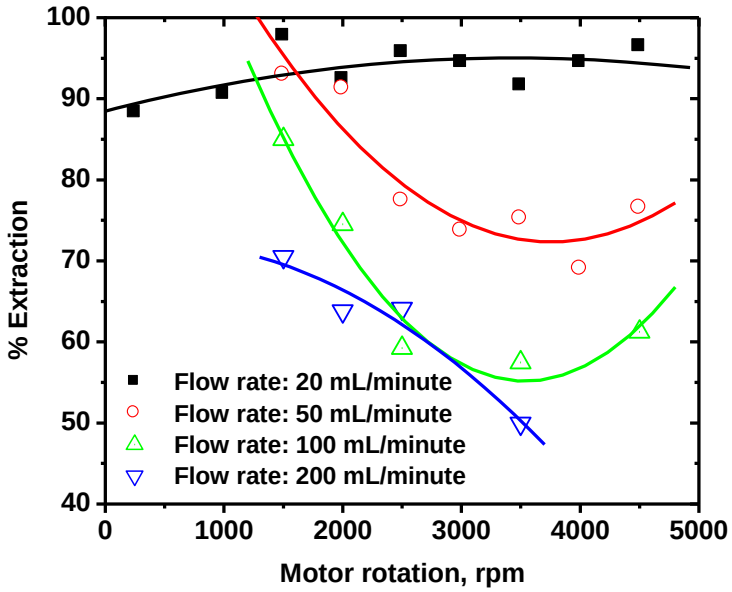

Fig. 3.9. Variation of U extraction (%) with flow rate and motor rotation using two stage centrifugal contactor; Feed: 20 g/L U at 4.0 M HNO_3; Solvent: 1.1 M TBP in *n*-dodecane; T: 298 K

3.2.4.2. Effect of feed acidity on uranium extraction/stripping

Uranium extraction studies were carried out using ~20 g/L U at 1-4 M HNO_3 as the aqueous phases and 1.1 M TBP and 1.1 M DHOA solutions in *n*-dodecane as the solvents. The extraction/stripping conditions used in this study were: (i) organic &

aqueous phase flow rate: 20 mL/min, and (ii) motor rotation: 1500 rpm. Table 3.4 compares the extraction and stripping behavior of the two solvents under the conditions of this study.

Table 3.4: Uranium extraction and stripping behavior as a function of feed acidity in two stage counter-current runs using centrifugal contactors; [U(VI)] feed: 20 g/L; Strippant: distilled water (D.W.); T: 298 K

$[HNO_3]_{feed}$, M	**Extraction cycle**				**Stripping Cycle**			
	% U Extraction		**$[HNO_3]_{org}$, M**		**% U Stripping**		**$[HNO_3]_{org}$, M**	
	1.1 M TBP	1.1 M DHOA	1.1 M TBP	1.1 M DHOA	1.1 M TBP	1.1 M DHOA	1.1 M TBP	1.1 M DHOA
1	80.4	66.1	0.2	0.1	77.4	94.1	0.05	0.03
2	86.8	79.9	0.4	0.37	50.6	86.6	0.06	0.07
3	88.9	88.8	0.6	0.47	47.8	84.5	0.12	0.10
4	97.6	96.0	0.7	0.62	41.2	83.3	0.22	0.11

As expected, uranium extraction increased with increased feed acidity for both the extractants. Stripping studies of uranium from loaded organic phase were carried out using distilled water. The stripping of uranium decreased with increased feed acidity (employed during extraction cycle). This behavior was explained in terms of acid reflux during the stripping cycle. These studies suggested that uranium extraction ability of DHOA at 3-4 M HNO_3 as feed acidity, is comparable to that of TBP. However, stripping behavior is better than that of TBP.

In next step uranium extraction and stripping studies carried out employing two stage centrifugal contactors using feed solutions containing ~ 20 and ~50 g/L U at 4 M HNO_3 (according to Pu rich spent fuel) and distilled water as feed and strip solutions, respectively. Table 3.5 summarizes the performance of the two extractants in extraction and stripping cycles.

Table 3.5: Comparison of uranium extraction and stripping behavior in two stage counter-current runs using centrifugal contactors; Feed acidity: 4 M HNO_3; Strippant: Distilled water (D.W.); T: 298 K

$[U]_{feed}$, g/L	O/A	Extraction cycle				Stripping Cycle			
		% U Extraction		$[HNO_3]_{org}$, M		% U Stripping		$[HNO_3]_{org}$, M	
		1.1 M TBP	1.1 M DHOA	1.1 M TBP	1.1 M DHOA	1.1 M TBP	1.1 M DHOA	1.1 M TBP	1.1 M DHOA
20	1	97.6	96.0	0.70	0.62	41.2	83.3	0.22	0.11
54.5	1	95.4	91.1	0.76	0.79	45.3	70.0	0.24	0.12
54.5	2	99.0	92.5	0.88	0.70	48.3	72.0	0.20	0.11

It is evident that TBP appears marginally better than DHOA in the extraction cycle. However, DHOA is distinctly better than TBP in the stripping cycle. Similar mixer settler runs employing 1.1 M TiAP (tris(isoamyl)phosphate)/*n*-dodecane on a typical feed solution (66.94 g/L U(VI) + 31.75 g/L Pu(IV) at 3.66 M HNO_3) showed that 3-4 stages were required for the extraction of U(VI) and Pu(IV) without any loss of heavy metals into the raffinate stream. However, the stripping run (using 4 M and 0.01 M HNO_3

solutions) indicated that ~16 stages were required for quantitative stripping of U(VI) and Pu(IV) from the loaded organic phase [**117**].

3.2.4.3. Studies on simulated fast reactor spent fuels feed solution

Centrifugal contactors runs were carried out for the reprocessing of fast reactor spent fuels under simulated conditions (Feed: 50.5 g/L U + 1.5 mg/L Pu at ~ 4 M HNO_3) using 1.1 M TBP and 1.1 M DHOA solutions in *n*-dodecane. Pu was taken in trace concentrations under the conditions of this study due to experimental limitations. Flow rate and rpm were maintained as 20 mL/minutes, 1500 rpm, respectively (Table 3.6).

Table 3.6: Simulated fast reactor spent fuels reprocessing by centrifugal contactor runs; Feed: 50.5 g/L U + 1.5 mg/L Pu at ~ 4 M HNO_3; Solvents: 1.1 M TBP and 1.1 M DHOA solutions in *n*-dodecane; Flow rate ~10 mL/minute; RPM: 1500

Cycle	**U**		**Pu**	
	1.1 M TBP	**1.1 M DHOA**	**1.1 M TBP**	**1.1 M DHOA**
Extraction (%)	95.3	95.6	94.5	>99.9
Partitioning (%)	4.95	19.8	78.5	80.5
U stripping (%)	74.8	> 95.4	--	--

Based on these runs, the following observations were made: (a) U extraction ability of DHOA was comparable to TBP (~95 %), (b) Pu extraction ability of DHOA (>99.9 %) was better than TBP (94.5 %), (c) Pu stripping comparable was comparable

(78-80 %) in both the solvents due to acid build up in the aqueous phase, (d) U loss during partitioning cycle was more for DHOA (19.8 %) than for TBP (5.0 %), and (e) U stripping was better for DHOA (95.4 %) than for TBP (74.8 %).

3.3. Tc extraction studies

As a part of the Advanced Fuel Cycle Initiative (AFCI), *UREX*$^{+}$ (URanium Extraction) process have been developed at Argonne National Laboratory, U.S.A., which consists of five solvent extraction steps that separate dissolved spent fuel into seven fractions [**146, 147**]. The five solvent-extraction steps were: (i) *UREX*: quantitative extraction of uranium and technetium; (ii) *CCD-PEG* (chlorinated cobalt dicarbollide - polyethylene glycol): recovery of Cs and Sr; (iii) *NPEX*: recovery of plutonium and neptunium; (iv) *TRUEX*: recovery of Am, Cm, REE (Rare Earth Elements) and fission products; and (v) *Cyanex 301*(bis(2,4,4-trimethylpentyl) dithiophosphinic acid): separation of Am and Cm from REE.

The *UREX* process focuses on the co-extraction of uranium and technetium at 1 M HNO_3. Upon dissolution of spent nuclear fuel in nitric acid, technetium passes into solution as pertechnetate ions. The solvent for the *UREX* process is the typical *PUREX* solvent, viz.; TBP dissolved in *n*-dodecane (30% v/v). In this process, a reductant / complexant is added to the scrub cycle to limit the extractability of plutonium and neptunium. The feed and the scrub are adjusted to 1 M HNO_3 to enhance the complexation of Pu and Np and increase the extractability of pertechnetate ion. The solvent, now loaded with uranium and technetium, is stripped of technetium in the Tc-Strip section using a high concentration of nitric acid. The Tc product stream is scrubbed of uranium in the Uranium Re-extraction Section. The combined solvent is then scrubbed

of excess nitric acid before entering the U-Strip section, where dilute nitric acid removes uranium from the solvent.

Hydroxamic acids (RCONHOH) are organic ligands which can act as strong chelating agents of metal ions by the formation of five-membered chelate rings (Figure 3.10). As O,O donor ligands, they have a strong affinity for '*hard*' metal ions such as Pu^{4+} [**148**]. Simple hydroxamates such as formohydroxamic acid (FHA, R = H) and acetohydroxamic acid (AHA, R = CH_3) are hydrophilic ligands which are not extracted in to organic phase to any appreciable degree. Aqueous soluble FHA and AHA were found to be very effective for the separation of U from Np and Pu as they reduce neptunium and plutonium rapidly. Both FHA and AHA have been reported to form a red complex with Pu(IV) ions, which transform into the blue Pu(III) complex after standing for several hours. Hydroxamic acids undergo hydrolysis and form hydroxylamine and the pertinent carboxylic acid [**149**].

$$RCONHOH + H_2O + H^+ \leftrightarrow RCOOH + NH_3OH^+ \quad (3.1)$$

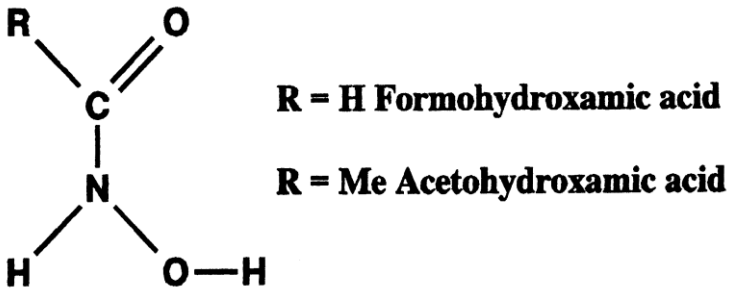

Fig. 3.10. Structure of hydroxamic acid

The hydroxamic acids are used at <3 M HNO_3, where the acid hydrolysis is suppressed [**150**]. The hydroxamic acid instability in nitric acid did not affected operations of centrifugal contactors, where the processing time is expected to be short

compared to the measured destruction half-life in nitric acid [**151**]. The strength of interaction of hydroxamic acids with actinides is quantified by stability constant data [**152, 153**].

3.3.1. Effect of acidity

Extraction studies of Tc(VII) were carried out at varying acidities (0.5 – 6 M HNO_3) as pure tracer (^{99}Tc) as well as in the presence of 50 g/L U in the aqueous phase using 1.1 M TBP and 1.1 M/1.5 M DHOA solutions in *n*-dodecane (Figure 3.11). Higher concentration of DHOA was chosen in view of the relatively lower extraction of U by 1.1 M DHOA as compared to that of 1.1 M TBP **[77]**. When DHOA was used as extractant, the distribution ratio of Tc (D_{Tc}) initially increased with acidity from 0.5 M HNO_3, passed through a maximum at ~ 2-3 M HNO_3, and decreased thereafter.

The initial increase in D_{Tc} was explained in terms of the formation and extraction of pertechnetic acid, $HTcO_4$, as the extractable species with increased nitric acid concentration. On the other hand, the decrease in D_{Tc} values at higher acidity was attributed to the competition from the extracted nitric acid. $HTcO_4$ formation will be favored at higher acidities, the extraction of nitric acid in the organic phase effectively reduces the free extractant concentration thereby suppressing the extraction of technetium. El-Kot and Pruett reported similar observation in the case of 1.1 M TBP as the extractant, however, the extraction maximum was observed at 0.5-0.6 M HNO_3 [**154, 155**].

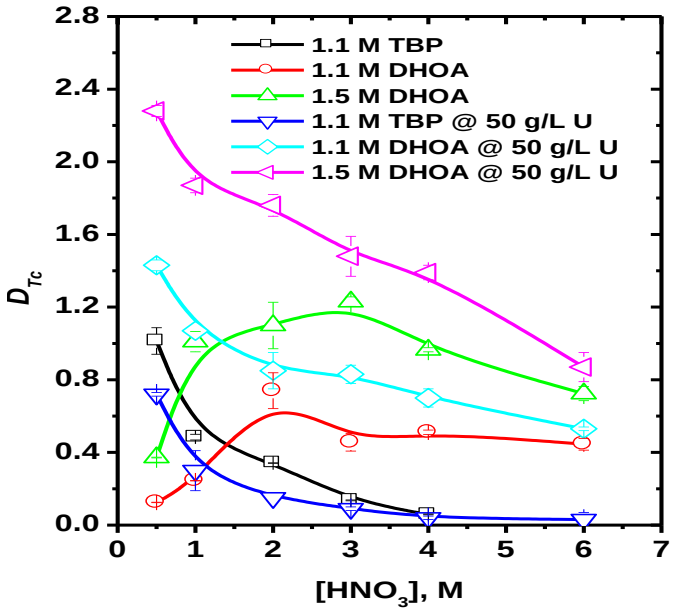

Fig. 3.11. Variation of D_{Tc} with aqueous phase acidity; T: 298 K

It was of interest to investigate the effect of uranium loading (50 g/L U) on Tc extraction. Remarkable enhancement in the extraction of technetium in the presence of uranium was noted at lower nitric acid concentrations (< 0.1 M). There was a minor decrease in D_{Tc} value from 0.48 (no U) to 0.3 (50 g/L U at 1 M HNO_3) in case of 1.1 M TBP [**156**]. While DHOA data indicate towards the salting out effect of uranium which facilitates the formation of $HTcO_4$ leading to its enhanced extraction. U extraction was higher in the case of TBP as extractant as compared to that of DHOA **[77]**. This suggests that presence of higher concentration of uranium in the case of latter, which reduces the water activity and favors the formation of $HTcO_4$ and followed by its extraction in the organic phase. It appears that mixed uranium-technetium complexes are responsible for higher extraction at > 2 M HNO_3 as shown by the following equilibrium:

$$UO_2(NO_3)_2(L)_2 + TcO_4^- \leftrightarrow UO_2(NO_3)(TcO_4)(L)_2 + NO_3^- \quad (3.2)$$

Where L = TBP or DHOA

These studies suggest that DHOA appears better for Tc recovery as compared to TBP under *UREX* process conditions. Similar observations were made during the co-extraction behavior of Tc(VII) and U(VI) by *n*-octyl(phenyl)-*N*,*N*-diisobutylcarbamoyl-methylphosphine oxide (CMPO) from nitric acid solution [**157**].

3.3.2. Stoichiometry of the extracted species

To find out the nature of extracted species, Tc extraction studies were carried out as a function of DHOA concentration at different acidities (0.5, 1 and 4 M HNO_3). Figure 3.12 shows a gradual decrease in slope values with increased aqueous phase acidity (3.93±0.04 (0.5 M HNO_3) to 2.48±0.01 (4.0 M HNO_3)).

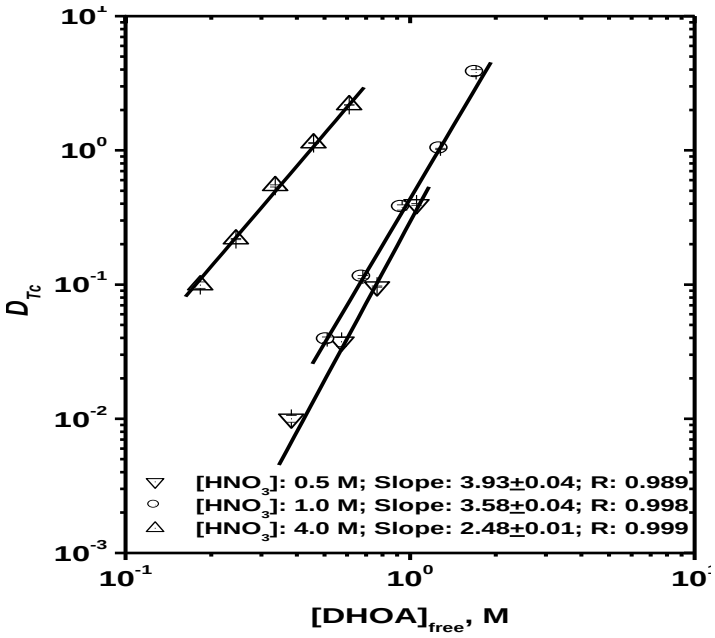

Fig. 3.12. Variation of D_{Tc} with DHOA concentration at different acidities; T: 25^{o}C

This suggests increasing competition of nitric acid with pertechnetic acid ($HTcO_4$) for extractant molecules. Similar observations have been reported during technetium

extraction using TBP as the extractant [**109**]. In TBP system where only three extractant molecules were present in the extracted species at 1 M HNO_3, more than three DHOA molecules (slope: 3.58±0.04) were found to be associated with the extracted species. This makes the extracted species involving DHOA more organophilic as compared to that of TBP resulting in higher extraction of Tc. A step-wise reduction in the coordination of $HTcO_4$ with DHOA for increasing HNO_3 concentration of the aqueous phase can be expressed by the following equilibrium reactions:

$$H^+_{aq} + TcO_4^-{}_{aq} + 4\ DHOA = HTcO_4 \bullet 4\ DHOA_{org} \quad (3.3)$$

$$HTcO_4 \bullet 4\ DHOA_{ong} + H^+_{aq} + NO_3^-{}_{aq} = HTcO_4 \bullet 3\ DHOA_{org} + HNO_3 \bullet DHOA_{org} \quad (3.4)$$

$$HTcO_4 \bullet 3\ DHOA_{ong} + H^+_{aq} + NO_3^-{}_{aq} = HTcO_4 \bullet 2\ DHOA_{ong} + HNO_3 \bullet DHOA_{org} \quad (3.5)$$

It appears that at 0.5 M HNO_3 equation (3.3) dominates while at 4 M HNO_3 equations (3.4) and (3.5) are dominating. Generally amides extract nitric acid by forming 1:1 amide-HNO_3 adducts as the predominant species [**109**]. The free extractant concentration was calculated by subtracting the organic phase nitric acid concentration. The later was measured by titration of the organic phase.

3.3.3. Effect of acetohydroxamic acid

Extraction of Pu and Np need to be suppressed to ensure selective extraction of U and Tc from spent fuel dissolver solution. In this context, an attempt was made to compare the extraction data of Tc, U, Pu, and Np for 1.1 M DHOA and 1.1 M TBP for the aqueous phases containing 50 g/L U and 0.5/1.0 M AHA solutions at 1 M HNO_3. Table 3.7 lists the distribution data of U, Pu, Np and Tc in the presence of 50 g/L U at 1 M HNO_3 containing 0.5 M and 1.0 M AHA.

Table 3.7: Extraction data of different metal ions in the presence of 50 g/L U at 1 M HNO_3; extractants: 1.1 M TBP & 1.1 M DHOA in *n*-dodecane; T: 298 K

Metal ions	**D_M at 50 g/L U in 1 M HNO_3**					
	0.5 M AHA			**1.0 M AHA**		
	1.1 M TBP	1.1 M DHOA	1.5 M DHOA	1.1 M TBP	1.1 M DHOA	1.5 M DHOA
Tc(VII)	0.3	1.1	1.9	0.3	1.1	1.9
U(VI)	3.9	2.0	3.7	3.8	2.0	3.7
Pu(V)	$2.2x10^{-2}$	$\sim10^{-4}$	$7.4x10^{-3}$	$8.8x10^{-3}$	$\sim10^{-4}$	$4.7x10^{-3}$
Np(IV)	$1.9x10^{-2}$	$4x10^{-3}$	$6.0x10^{-3}$	$1.2x10^{-3}$	$1.0x10^{-3}$	$6.0x10^{-3}$

Distribution ratio values of uranium and technetium were invariant in the absence/presence of AHA in the aqueous phase. It is also evident that DHOA offers better Tc recovery as compared to that of TBP. Typically, >50 % extraction of Tc can be achieved using 1.1 M DHOA maintaining organic-to-aqueous phase ratio as 1; while only ~23 % Tc can be extracted under identical conditions using 1.1 M TBP as the extractant. This data indicates that number of stages required for quantitative extraction of Tc will be lower in the case of 1.1 M DHOA and 1.5 M DHOA as compared to that of 1.1 M TBP. In addition, DHOA offers better decontamination for Tc over Pu and Np than that of TBP.

Figure 3.13 compares the separation factor (SF) values of U over Pu/Np for 1.1 M TBP, 1.1 M DHOA and 1.5 M DHOA solutions as extractants in the presence of 50 g/L U at 1 M HNO_3. The data suggest that 1.1 M DHOA is better than 1.1 M TBP as extractant for selective extraction of U over Pu/Np under the conditions of the experiment. The SF

values for U over Pu (D_U/D_{Pu}) are significantly higher for 1.1 M DHOA (~20,000) than those for 1.1 M TBP (180) and 1.5 M DHOA (500) using 0.5 M AHA in the aqueous phase. Use of 1.0 M AHA marginally improved the SF values U over Pu/Np for all the extractants.

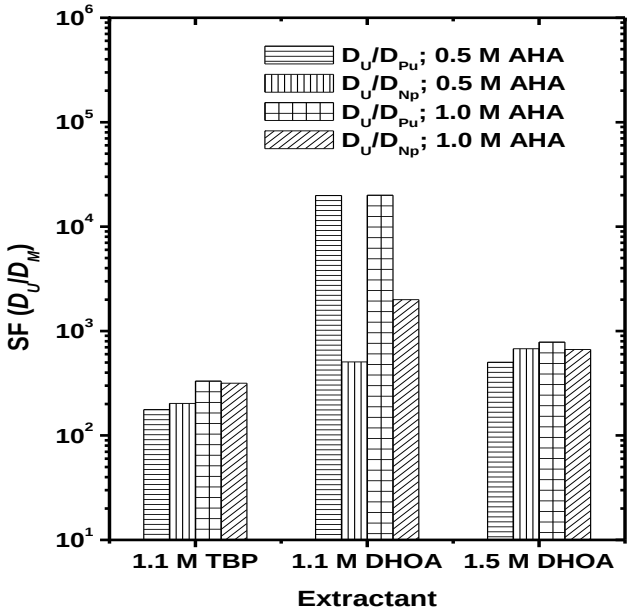

Fig. 3.13. Separation factors with DHOA and TBP in *n*-dodecane; aqueous phase: 50 g/L U at 1 M HNO_3 containing AHA; T: 298 K; M: Pu or Np

3.3.4. Stability of acetohydroxamic acid

AHA proposed in *UREX*$^+$ process to reduce Np and Pu and the resultant hydrophilic complexes were need to be separated from U by extraction with TBP. Few reports suggest that pertechnetate ion can be reduced to Tc by AHA over long periods, which can alter its fate in the fuel cycle [**158**]. Therefore, the effect of time of equilibration on D_{Tc} and D_{Pu} values from 1.0 M HNO_3 containing 0.5 M AHA (proposed scrub composition for *UREX* process) using 1.1 M TBP and 1.5 M DHOA as the solvents (Figure 3.14) has

also investigated. There was marginal variation in the extraction data of Tc and Pu under the conditions of present work. On the other side, minor decrease in D_{Tc} values for both TBP and DHOA were observed. The kinetics was too slow to affect its extraction profile under the process conditions as it takes 1-3 hours to complete the process.

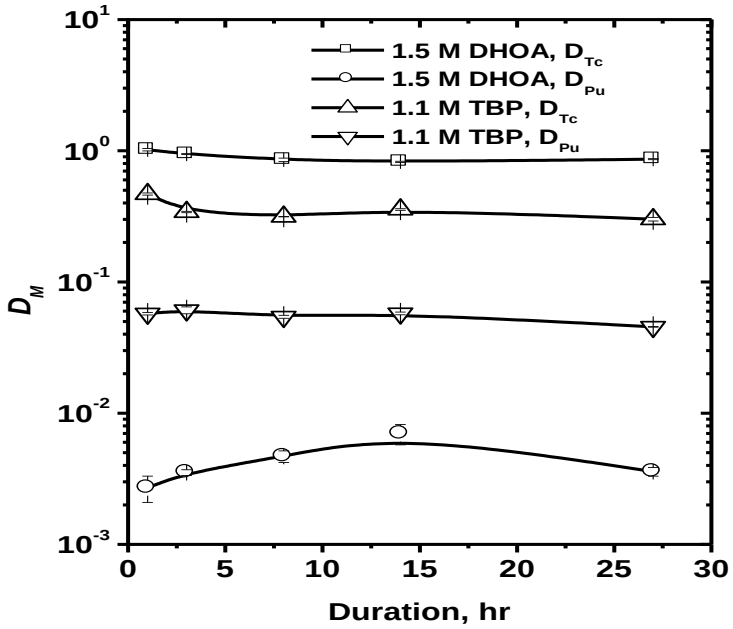

Fig. 3.14. Variation of D_M (M=Tc, Pu) with time of equilibration; Organic phase: 1.5 M DHOA & 1.1M TBP in *n*-dodecane; aqueous phase: 0.5 M AHA at 1 M HNO_3; T: 298 K

3.3.5. Spectrophotometric investigation on Pu-AHA interaction

The speciation of Pu(IV) in the presence of varying concentrations AHA ($2x10^{-4}$ – 0.5 M) in 1 M HNO_3 undergoes significant changes. Earlier studies have demonstrated that three Pu-acetohydroxamate species are formed [**159**]. Under conditions of low AHA concentrations (0.1M AHA), mainly the mono-acetohydroxamate species of Pu are formed. However, under *UREX* process conditions (≥ 0.1M AHA), the di-acetohydroxamate species of plutonium becomes predominant and also concentration of

Pu-tri-acetohydroxamate species grows up. Figure 3.15 shows Pu(IV) absorption spectra is unaffected upto $2x10^{-3}$ M AHA concentration beyond which a significant enhancement in the absorbance values was observed due to Pu-AHA complexation. The color of the solution changed to dark brown/red Pu(IV)-hydroxamate complexes depending on AHA concentration.

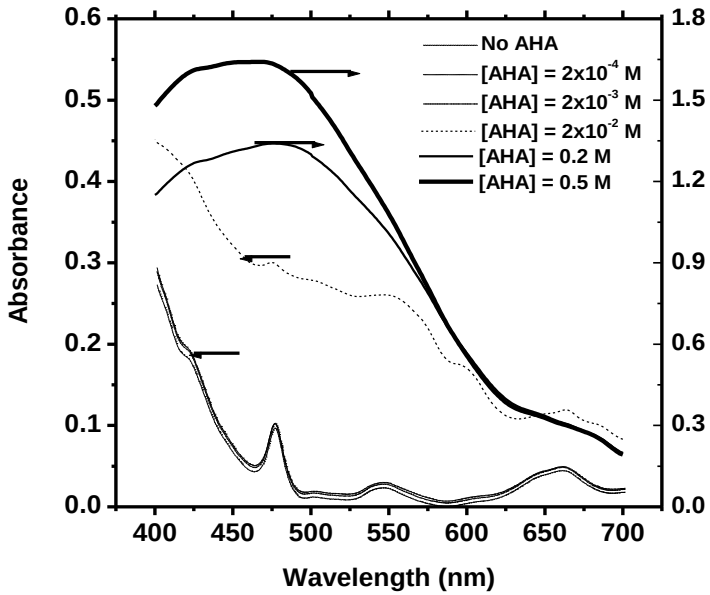

Fig. 3.15. Effect of AHA concentration on Pu(IV) absorption spectra; [Pu(IV)]: 2×10^{-3} M at 1 M HNO_3

The hydrolytic instability of hydroxamic acids should be taken in to consideration during the development of a process flow sheet. The effect of aqueous phase acidity and time on the absorption spectra of Pu-AHA complexes were presented in Figures 3.16 and 3.17. AHA complexation decreases with increased acidity from 1 to 4 M HNO_3. Similarly, decrease in absorbance of Pu(IV)-AHA complex with time were noted. Only marginal decrease in the absorbance takes place within 60 minutes duration which

indicates towards an induction period for the hydrolysis and reduction of Pu(IV) to Pu(III).

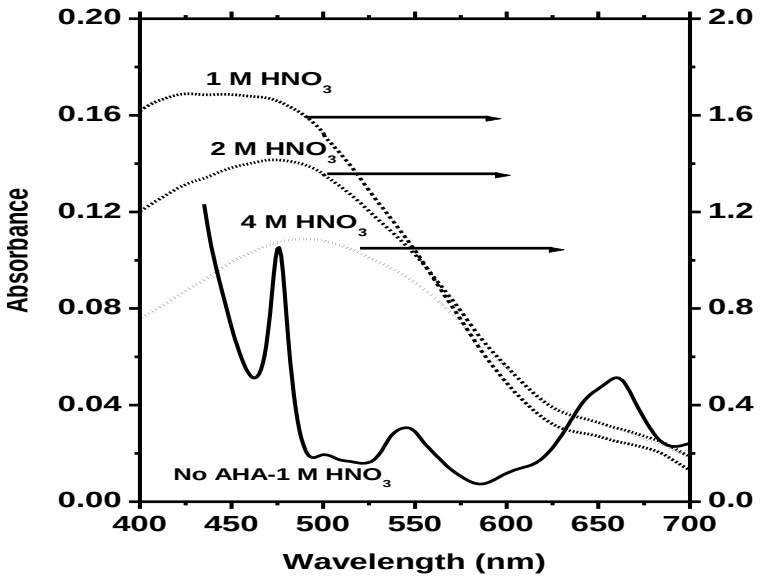

Fig. 3.16. Absorption spectra of Pu(IV)-AHA complex at different acidities; [Pu]: 2×10^{-3} M; [AHA]: 0.5 M

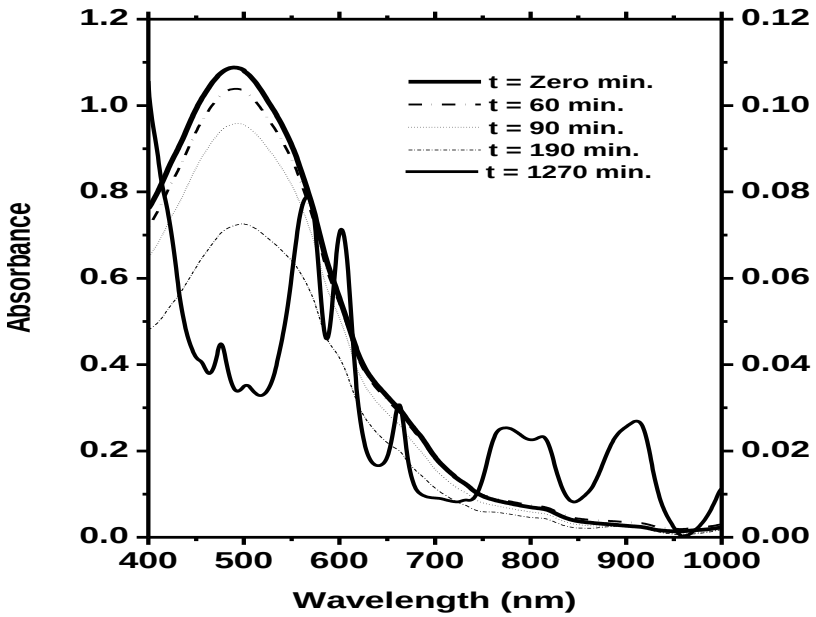

Fig. 3.17. Absorption spectra of Pu(IV)-AHA complex; Sample: 2×10^{-3} M Pu(IV) + 0.5 M AHA at 4 M HNO_3

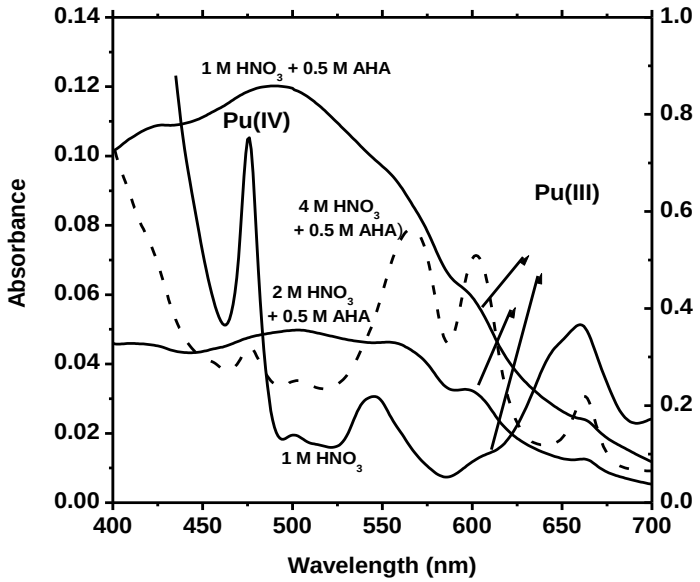

Fig. 3.18. Absorption spectra of Pu(IV)-AHA complex; [Pu]: 2×10^{-3} M; [AHA]: 0.5 M AHA at 1-4 M HNO_3; Duration: 1270 minutes; Pu(IV) spectrum is given for comparison purpose

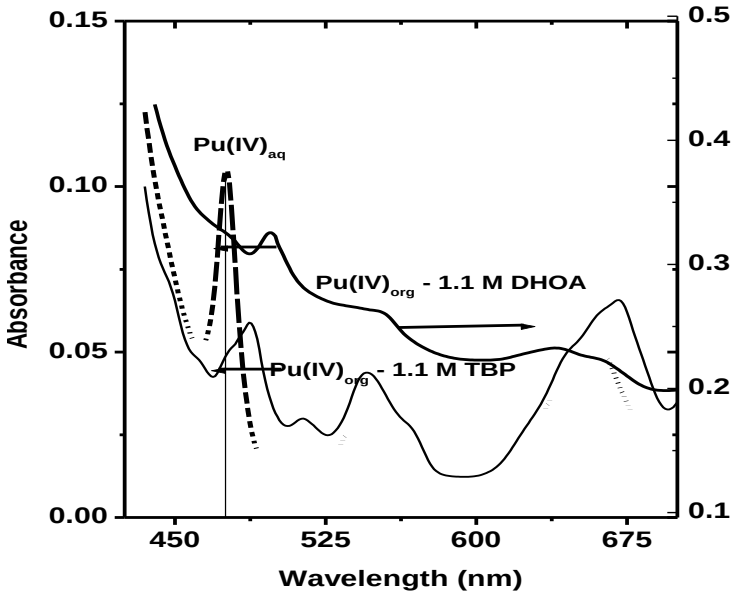

Fig. 3.19. Absorption spectra of Pu(IV) in organic extracts at 1 M HNO_3; diluent: *n*-dodecane

Figure 3.18 shows signatures of the formation of Pu(III) in the presence of 0.5 M AHA at 1, 2 and 4 M HNO_3 after 1270 minutes. Hydroxyl amine formed as a result of

hydrolysis of AHA is responsible for reduction of Pu(IV). Figure 3.19 shows a red shift in the characteristic wavelength of aqueous Pu(IV) absorption (476 nm) in the organic extracts, viz. 1.1 M TBP (489 nm) and 1.1 M DHOA (499 nm). This is in conformity with the relatively high affinity of DHOA for Pu over TBP **[77]**.

The absorption spectra of the organic phase/extract of Pu(IV)-AHA at 1 M HNO_3 were also recorded for 1.1 M TBP and 1.1 M DHOA solutions in *n*-dodecane. Results are presented in Figure 3.20. It clearly demonstrates that Pu extraction observed in the case of TBP indicate the ternary complex extraction. This was also evident from visual observation of the TBP extract which became light brown color after extraction. By contrast, no extraction was observed in the case of DHOA as extractant. This explains why DHOA offers better separation factor for U and Tc over Pu as compared to that of TBP under *UREX* process conditions.

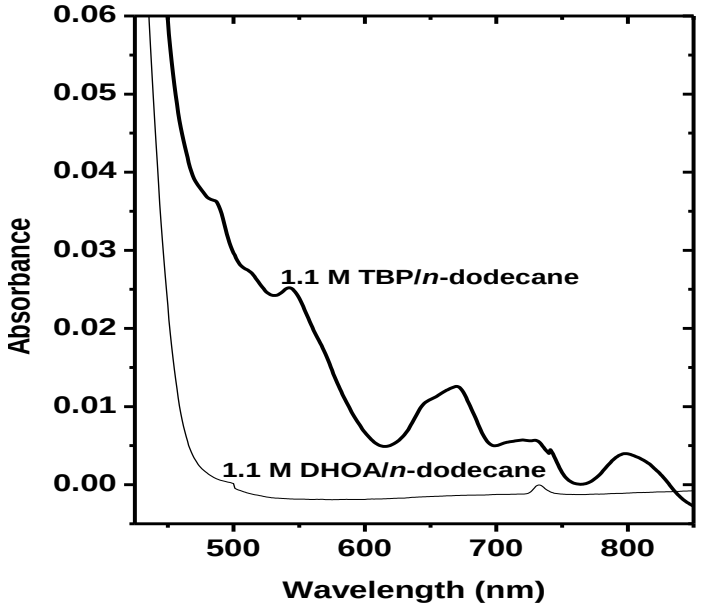

Fig. 3.20. Absorption spectra of extracted Pu(IV)-AHA complex; aqueous phase: 2×10^{-3} M Pu(IV) + 0.5 M AHA at 1M HNO_3

CHAPTER 4: EXTRACTION STUDIES OF ^{237}Np USING *N,N*-DIHEXYLOCTANAMIDE

4.1. Introduction

^{237}Np is one of the important nuclides for nuclear waste management, because of its long half-life and high radio toxicity. It is generated in significant quantities in Pressurized Water Reactors (PWRs) as well as in fast reactors. The spent fuel dissolver solution mainly contains uranium, plutonium, minor actinides (mainly Np, Am & Cm), fission/activation products, structure elements and process chemicals. Therefore, it is important to understand its process chemistry particularly while developing new extractants for spent fuel reprocessing. Neptunium in nitric acid solution can exist simultaneously in three oxidation states, viz. Np(IV) (Np^{4+}), Np(V) (NpO_2^+) and Np(VI) (NpO_2^{2+}) which are produced by the following disproportionation reaction depending on the nitric acid concentration [**160**]:

$$2NpO_2^+ + 4H^+ \leftrightarrow NpO_2^{2+} + Np^{4+} + 2H_2O \quad (4.1)$$

These oxidation states of Np exhibit different extraction behavior towards *tri*-butyl phosphate (TBP) in nitric acid medium. Whereas, Np(VI) is easily extracted, Np(IV) is relatively poorly extractable, and Np(V) is nearly inextractable [**161**]. The presence of nitrous acid affects the oxidation state of neptunium in nitric acid medium. Thermodynamically, HNO_2 is capable of reducing Np(VI) to Np(V), since the formal potential values for NO_3^-/HNO_2 and Np(VI)/Np(V) redox pairs are close to each other, 0.94 and 1.138 V/NHE (normal hydrogen electrode), respectively. At the same time, HNO_2 is also known to catalyze Np(V) oxidation with HNO_3. When nitrous acid is more than *ca.* 10^{-4} M, it acts as a reductant and reduces Np(VI) to Np(V). Thus, the extent of

Np(V) oxidation in HNO_3 medium is extremely sensitive to HNO_2 concentration [**162, 163**]:

$$2NpO_2^+ + 3H^+ + NO_3^- \leftrightarrow 2NpO_2^{2+} + HNO_2 + H_2O \quad (4.2)$$

These oxidation states are easily interconvertible, depending on the nitric acid and nitrous acid concentrations. The interconversion of NpO_2^+ to Np^{4+} requires an extensive rearrangement of the primary coordination sphere of NpO_2^+ (i.e., a change in the linear dioxo-structure) before electron transfer. This results in a relatively high activation barrier and therefore the rate of the disproportionation is slow.

In commercial PUREX reprocessing plants, Np is separated from uranium during the Uranium Purification (UP) cycle. Np(VI) is converted to Np(V) and is rejected to the aqueous raffinate [**164**]. The strategy of Partitioning of long-lived radionuclides followed by Transmutation (P&T) envisages the complete removal of minor actinides from radioactive waste solutions and their subsequent burning in the reactors/accelerators [**165**]. There is no universal process known so far for minor actinide partitioning from HLW.

Various diglycolamide derivatives, *N*,*N*,*N*′,*N*′-tetraoctyl diglycolamide (TODGA), and *N*,*N*,*N*′,*N*′-tetra(2-ethylhexyl) diglycolamide (TEHDGA) have been identified for partitioning of HLW due to their favorable physicochemical properties [**166, 167**]. These extractants suffer from a serious limitation of third-phase formation during the metal ions extraction under HLW conditions. It becomes essential to use phase modifiers along with these extractants during actinide partitioning studies. In this context, the presence of uranium in HLW solution adds to the loading for the proposed extractants and may aggravate the third-phase formation problem. The PHWR-HLW is expected to contain ~30mg/L ^{237}Np, ~100 mg/L of Am (^{241}Am + ^{243}Am), ~1mg/L of Cm, ~0.5-1 g/L

lanthanides in addition to unrecovered U/Pu and large number of fission products, activation products, and process chemicals [**33**]. It was thought of interest to optimize conditions for co-recovery of U, Pu and Np from the HLW. This step may simplify the subsequent actinide partitioning step. Several important studies have been reported on the process chemistry of Np which deals with its redox behavior, extraction and process control using TBP as extractant [**167-176**].

This chapter presents the extraction studies of Np using DHOA and TBP as extractants relevant to Pu rich fast reactor and Pressurized Heavy Water Reactor (PHWR) spent fuels. Also, conditions for co-recovery of U, Pu, and Np have been optimized using 1.1M TBP and 1.1M DHOA dissolved in *n*-dodecane as solvents under PHWR-HLW conditions for simplifying the subsequent actinide partitioning steps.

4.2. Results and discussion

4.2.1. Tracer studies

Figures 4.1 & 4.2 compare U(VI), Pu(IV), Np(IV) and Np(VI) extraction data of 1.1 M TBP and 1.1 M DHOA solutions in *n*-dodecane as solvents, as a function of nitric acid concentration in the aqueous phase. It is evident that TBP is a better extractant for U(VI) and Np(VI) ions than DHOA and $D_{U(VI)} > D_{Np(VI)}$ for both the extractants. However, Np(IV) extraction is comparable to TBP at higher acidities ($\geq$ 3 M HNO_3). DHOA displays distinctly better stripping behavior for Np(IV) at lower acidities even without the use of any reducing agent. Table 4.1 shows the distribution behavior of Np(IV) and Np(VI) with 1.1 M TBP and 1.1 M DHOA in *n*-dodecane.

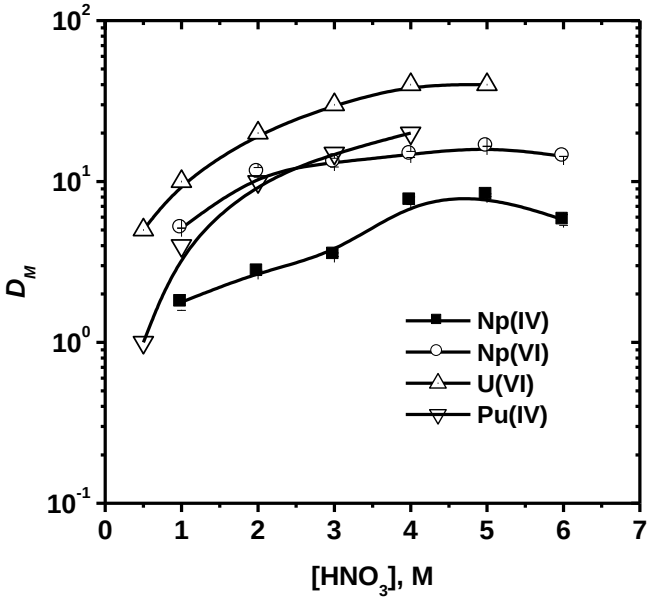

Fig. 4.1. Extraction of metal ions as a function of acidity; Solvent: 1.1 M TBP/*n*-dodecane; T: 298 K

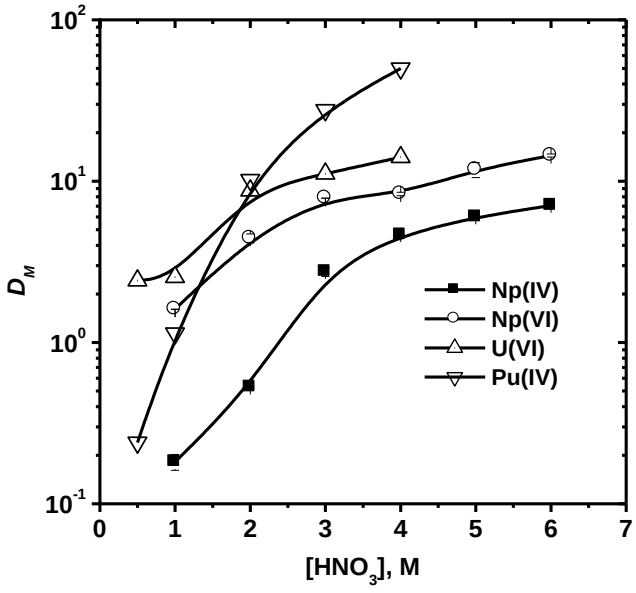

Fig. 4.2. Extraction of metal ions as a function of acidity; Solvent: 1.1 M DHOA/*n*-dodecane; T: 298 K

Table 4.1: Comparison of Np distribution behavior using TBP & DHOA as extractants; Diluent: *n*-dodecane; T: 298 K

$[HNO_3]$, M	1.1 M TBP		1.1 M DHOA	
	$D_{Np(IV)}$	$D_{Np(VI)}$	$D_{Np(IV)}$	$D_{Np(VI)}$
1	1.8(±0.2)	5.1(±0.1)	0.18(±0.02)	1.61(±0.01)
2	2.8(±0.1)	11.4(±0.8)	0.53(±0.01)	4.4(±0.3)
3	3.5(±0.1)	13.1(±0.8)	2.7(±0.2)	7.8(±0.8)
4	7.6(±0.4)	14.7(±0.6)	4.6(±0.1)	8.3(±0.2)
5	8.2(±0.2)	16.5(±0.1)	6.0(±0.1)	11.8(±1.2)
6	5.8(±0.4)	14.3(±0.7)	7.7(±0.1)	14.4(±0.30)

4.2.2. Evaluation of extraction constants of Np(IV) and Np(VI) using DHOA as extractant

The extraction of Np(IV) and Np(VI) by DHOA (A) can be given by the equations (4.3) and (4.4):

$$Np^{4+}_{aq} + 4NO_3^-{}_{aq} + mA_{org} \overset{K_{ex,\,Np(IV)}}{\leftrightarrow} Np(NO_3)_4 \cdot mA_{org} \quad (4.3)$$

$$NpO_2^{2+}{}_{aq} + 2NO_3^-{}_{aq} + nA_{org} \overset{K_{ex,\,Np(VI)}}{\leftrightarrow} NpO_2(NO_3)_2 \cdot nA_{org} \quad (4.4)$$

Where, $K_{ex,Np(IV)}$ and $K_{ex,Np(VI)}$ are the equilibrium constants for the biphasic extraction reactions (4.3 and 4.4), and their values can be expressed as:

$$K_{ex,Np(IV)} = a_{Np(NO3)4 \cdot nAorg} / (a_{Np^{4+}{}_{aq}} \cdot a^4_{NO3^-{}_{aq}} \cdot a^m_{Aorg}) \quad (4.5)$$

$K_{ex,Np(VI)} = a_{NpO2(NO3)2}.nA_{org} /(a_{NpO2}{}^{2+}{}_{aq}.a^{2}{}_{NO3-aq} \cdot a^{n}{}_{Aorg})$ (4.6)

The terms involved in equilibrium expressions (4.5) and (4.6) refer to the activities of species. The subscripts aq. and org. represent the aqueous and the organic phases, respectively. In view of the tracer concentrations of Np(IV) and Np(VI), the equilibrium constants (K_{ex}) for the extraction of Np(IV) and of Np(VI) were calculated using the following approximations: (a) the activity coefficients of the metal ion in the aqueous phase as well as of the metal solvate in the organic phase are assumed to be unity. Since, the concentration of the metal ions is in the trace level, and (b) $[A]_{free}$ is assumed to be equal to the activity of free amide (a_A). The activity of nitrate ion (a_{NO_3}) was used for the calculation of equilibrium constants [**177**]. Therefore, the activity terms involving metal ions species can be expressed in terms of their respective concentrations.

$K_{ex,Np(IV)} = [Np(NO_3)_4 \cdot mA]_{org} /([Np^{4+}]_{aq} \cdot a_{NO3-}{}^{4}{}_{aq} \cdot [A]^{m}{}_{org})$ (4.7)

$K_{ex,Np(VI)} = [NpO_2(NO_3)_2 \cdot nA]_{org} /([NpO_2{}^{2+}]_{aq} \cdot a_{NO3-}{}^{2}{}_{aq} \cdot [A]^{n}{}_{org})$ (4.8)

Various species of Np(IV) in the aqueous phase may be present such as Np^{4+}, $Np(NO_3)^{3+}$, $Np(NO_3)_2{}^{2+}$, $Np(NO_3)_3{}^{+}$, and $Np(NO_3)_4$……etc. Similarly, various species of Np(VI) in nitric acid medium can be represented as $NpO_2{}^{2+}$, $NpO_2(NO_3)^{+}$, $NpO_2(NO_3)_2$ ……etc. During these experiments, it was ensured that Np was present as Np(IV) and Np(VI) oxidation states, respectively by using Fe(II) and $K_2Cr_2O_7$ as reductant and oxidant, respectively. Taking into account the nitrate complexation of Np(IV) and Np(VI), equations (4.7) and (4.8) can be rearranged as follows:

$K_{ex,Np(IV)} = [Np(NO_3)_4 \cdot mA]_{org} \cdot (1 + \Sigma \beta_{x,Np(IV)}\, a^{x}{}_{NO3-}) / (C_{Np(IV)aq} \cdot a^{4}{}_{NO3-aq} \cdot [A]_{org}{}^{m})$ (4.9)

$K_{ex,Np(VI)} = [NpO_2(NO_3)_2 \cdot nA]_{org} \cdot (1 + \Sigma \beta_{y,Np(VI)}\, a^{y}{}_{NO3-}) / (C_{Np(VI)aq} \cdot a^{2}{}_{NO3-aq} \cdot [A]_{org}{}^{n})$ (4.10)

Where, $C_{Np(IV)aq}$ and $C_{Np(VI)aq}$ refer to total concentrations of Np(IV) and Np(VI) in the aqueous phases and β_x or β_y are their respective stability constants for nitrate

complexation. One can substitute $D_{Np(IV)}$ as $[Np(NO_3)_4 \cdot mA]_{org}/C_{Np(IV)aq}$ and $D_{Np(VI)}$ as $[NpO_2(NO_3)_2 \cdot nA]_{org}/C_{Np(VI)aq}$ in equations (4.9) and (4.10), respectively:

$$K_{ex,Np(IV)} = D_{Np(IV)} \cdot (1 + \Sigma\beta_{x,Np(IV)}\, a^{x}{}_{NO3^-}) / (a^{4}{}_{NO3^-aq} \cdot [A]_{org}{}^{m}) \quad (4.11)$$

$$K_{ex,Np(VI)} = D_{Np(VI)} \cdot (1 + \Sigma\beta_{y,Np(VI)}\, a^{y}{}_{NO3^-}) / (a^{2}{}_{NO3^-aq} \cdot [A]_{org}{}^{n}) \quad (4.12)$$

Both $K_{ex,Np(IV)}$ and $K_{ex,Np(VI)}$ represent 'conditional extraction constants' in view of the above mentioned approximations. However, these values may provide a guideline for the relative preferences of the metal ions for the extractant molecules **[178, 179]**.

4.2.3 Nitrate complexation for Np(IV) and Np(VI)

The values of nitrate complexation constants $(1 + \Sigma\beta_{x,Np(IV)}\, a^{x}{}_{NO3^-})$ for Np(IV) and $(1 + \Sigma\beta_{y,Np(VI)}\, a^{y}{}_{NO3^-})$ for Np(VI) cations at 4 M HNO_3 , respectively, were determined by cation exchange method [**178, 179**]. If D_o and D are the distribution ratios of metal ions (i.e. Np(IV) or Np(VI)) employing cation exchange resin (Dowex 50 x 8, 200 - 400 mesh size, H form, 50 mg) at 4 M $HClO_4$ and 4 M HNO_3, respectively. For a particular metal cation, it can be shown that

$$D_{o,Np(IV)}/D_{Np(IV)} = 1 + \Sigma\beta_{x,Np(IV)}\, a^{x}{}_{NO3^-} \quad (4.13)$$

and

$$D_{o,Np(VI)}/D_{Np(VI)} = 1 + \Sigma\beta_{y,Np(VI)}\, a^{y}{}_{NO3^-} \quad (4.14)$$

The aqueous nitrate ion complexation factors for Np(IV) and Np(VI) were independently determined at room temperature. Np oxidation states were adjusted to Np(IV) and Np(VI) using 0.1 M Fe(II) and 0.01 M $K_2Cr_2O_7$ solutions, respectively. The nitrate complexation constants for Np(IV) and Np(VI) cations were 33.5(±0.5) and 5.1(±0.1), respectively [**178, 179**]. The chloride ion complexation (Fe(II) used as

reductant) with Np(IV) was ignored in view of its lower concentration as compared to that of nitrate ion (~ 4 M).

4.2.4. Stoichiometry of extracted species

The number of DHOA molecules attached to each of Np(IV) or Np(VI) ion extracted in the organic phase were determined at 4 M HNO_3 as the aqueous medium and varying concentrations of DHOA (0.2-1.5 M, pre-equilibrated) as the organic phases. Figure 4.3 demonstrates the formation of trisolvated species for Np(IV) (Slope: 2.71(±0.08); R: 0.997) and of disolvated species for Np(VI) (Slope: 1.74(±0.05); R: 0.991) metal ions. Generally, one gets the non-integral slope values in such studies, and the solvation number assigned refers to the predominant extracted species of the metal ion under the conditions of experiment. Therefore, the stoichiometry of the extracted species of Np(IV) and Np(VI) in the organic phase were $Np(NO_3)_4 \cdot 3A$ and $NpO_2(NO_3)_2 \cdot 2A$, where A = DHOA. The conditional extraction constant ($log\ K_{ex}$) for Np(IV) and Np(VI) values were calculated as 1.83(±0.48) and 1.64(±0.32), respectively. Similar observations on stoichiometries and $log\ K_{ex}$ values for Np(IV) and Np(VI) have been reported elsewhere during the extraction of Np(IV) and Np(VI) using dibutyl decanamide (DBDA) and dihexyl decanamide (DHDA) from 3 M HNO_3 [**180**].

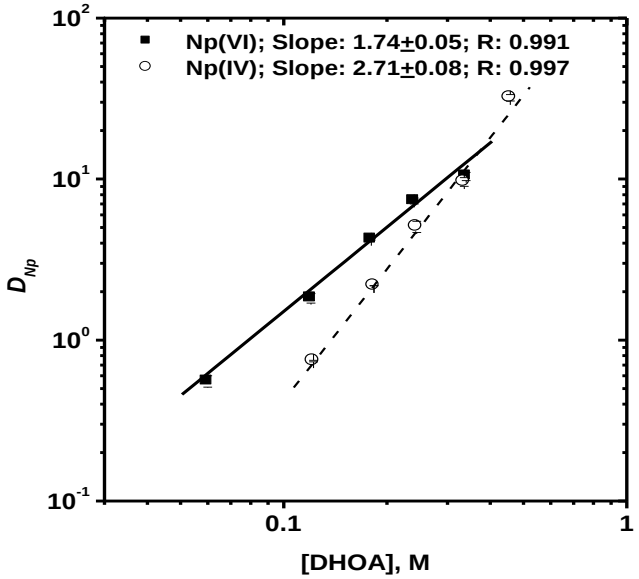

Fig. 4.3. Variation of $D_{Np(VI)}$ and $D_{Np(IV)}$ with DHOA concentration at 4 M HNO_3; Diluent: *n*-dodecane; Oxidant: 0.01 M $K_2Cr_2O_7$; Reductant: 0.1 M Fe(II); T: 298 K

4.2.5. Effect of uranium loading

Figures 4.4 & 4.5 clearly showed a decrease in neptunium extraction in the presence of 50 and 300 g/L U, [which are relevant to Pu rich (fast reactor) and Pressurized Heavy Water Reactor (PHWR) spent fuels, respectively] in the aqueous phase in the entire range of acidity **[114]**.

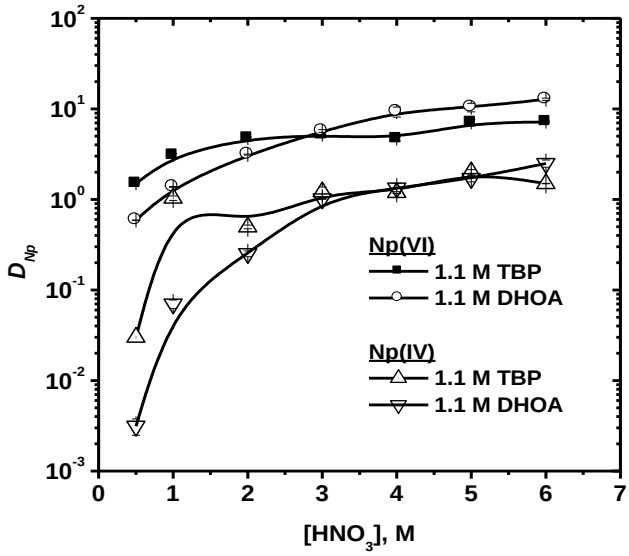

Fig. 4.4. Effect of uranium loading on Np extraction; Solvents: 1.1 M TBP/1.1 M DHOA solution in *n*-dodecane; Oxidant: 0. 1 M $K_2Cr_2O_7$; Reductant: 0.1 M Fe(II); $[U]_{aq}$: 50g/L; T: 298 K

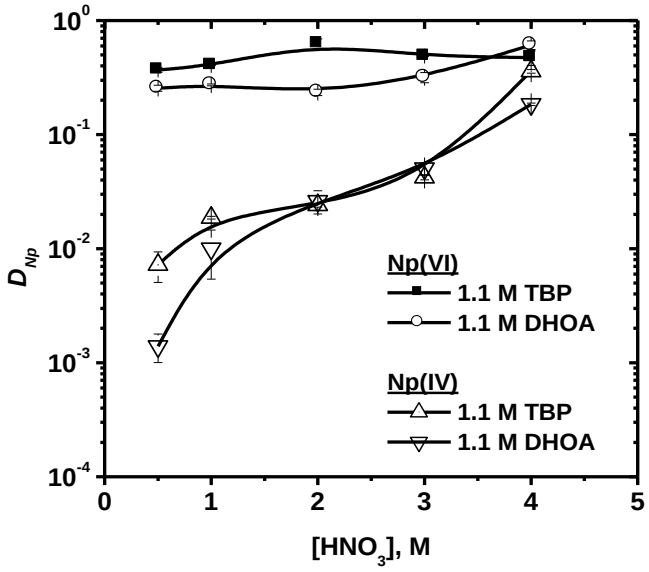

Fig. 4.5. Effect of uranium loading on Np extraction; Solvents: 1.1 M TBP/1.1 M DHOA solution in *n*-dodecane; Oxidant: 0. 1 M $K_2Cr_2O_7$; Reductant: 0.1 M Fe(II); $[U]_{aq}$: 300g/L; T: 298 K

It is interesting to note that $D_{Np(IV)}$ values are significantly lower (~ one order of magnitude) for 1.1 M DHOA at lower acidity than those for 1.1 M TBP both for tracer (Figures 4.1 & 4.2) as well as in the presence of macro concentrations of uranium (50, 300 g/L) in the aqueous phase. This observation suggests that DHOA could be useful for coprocessing (extraction and stripping) of U(VI), Pu(IV) and Np(IV) from Pu rich spent fuel dissolver solutions **[77]**.

4.3. Co-recovery of U, Pu, and Np from HLW

4.3.1. Extraction studies

Extraction behavior of U, Np and Pu, experiments were carried out in the presence of 6 g/L U (expected to be present in PHWR-HLW) at 4 M HNO_3 employing 1.1 M solutions of TBP and DHOA in *n*-dodecane. As expected, the distribution ratio values follow the order: U(VI) > Pu(IV) > Np(IV) under different experimental conditions (Table 4.2). H_2O_2 and $NaNO_2$ were used for valency adjustment of Np, Pu, and significant enhancement in Np extraction was found in the presence of 0.2 M H_2O_2 due to the formation of more extractable Np(IV) species (Equation 4.15) [**181-183**].

$$NpO_2^{+} + ½\ H_2O_2 + 3H^{+} \leftrightarrow Np^{4+} + ½\ O_2 + 2H_2O \qquad (4.15)$$

The addition of $NaNO_2$ in the aqueous phase, suppressed Np extraction for both the extractants which may be due to the generation of HNO_2 [**163**]. Nitrous acid is also formed during the dissolution of spent fuel and by the radiolysis of nitric acid. It is relatively well extracted by neutral extractants like TBP, and therefore gets distributed into different stages of the separation system. No significant improvement in the extraction of Pu was observed for both the extractants after the addition of $NaNO_2$ in the

aqueous phases. Therefore, 0.2 M H_2O_2 was used alone for the valency adjustment of Np to Np(IV) and Pu to Pu(IV).

HLW is generally maintained at an acidity of 3-4 M HNO_3, and therefore it was desirable to generate extraction data of U, Np and Pu at this acidities using 0.2 M H_2O_2. 1.1 M TBP/*n*-dodecane appeared better solvent as compared to 1.1 M DHOA/*n*-dodecane at 3 M HNO_3. On the other hand DHOA was more effective extractant, particularly with respect to Np and Pu extraction at 4 M HNO_3 acidity of HLW solution. This observation is consistent with better extraction ability of DHOA for Pu(IV) and Np(IV) at higher acidities [**77, 114**].

Table 4.2: Extraction behavior of U, Np and Pu in the presence of 6 g/L U; T: 298K

Extractant	**Aqueous phase**	$\mathbf{D_U}$	$\mathbf{D_{Np}}$	$\mathbf{D_{Pu}}$
1.1 M TBP	4 M HNO_3	13.7(±0.2)	0.9(±0.01)	6.5(±0.4)
	4 M HNO_3 + 0.2 M H_2O_2	14.6(±0.2)	2.5(±0.1)	7.0(±0.2)
	4 M HNO_3 + 0.2 M H_2O_2 + 0.05 M $NaNO_2$	14.3(±0.7)	1.7(±0.1)	8.2(±0.1)
1.1 M DHOA	4 M HNO_3	9.6(±0.5)	1.0(±0.03)	12.2(±0.5)
	4 M HNO_3 + 0.2 M H_2O_2	8.6(±0.5)	3.2(±0.2)	11.0(±0.2)
	4 M HNO_3 + 0.2 M H_2O_2 + 0.05 M $NaNO_2$	9.0(±0.4)	2.0(±0.1)	11.3(±0.6)
1.1 M TBP	3 M HNO_3 + 0.2 M H_2O_2	13.0(±1.0)	2.1(±0.4)	6.0(±0.9)
1.1 M DHOA	3 M HNO_3 + 0.2 M H_2O_2	7.2(±0.2)	1.3(±0.03)	6.6(±0.3)

4.3.2. Stripping studies

Various reductants viz. ferrous-sulphamate, ferrous-hydrazine and uranous-hydrazine have been employed earlier for the partitioning of Pu, their use leads to generation of large amounts of salts in radioactive effluents. Hydrazine may also form an explosive mixture with acid. Thus, there is a need to identify such reductants, the use of which (i) do not lead to generation of salt in secondary waste, (ii) safe in handling, and (iii) display fast kinetics of reduction of Pu(IV) under optimized process conditions. In the present work, two non-salt forming reductants acetohydroxamic acid (AHA) and hydroxy urea (HU) (Figures 4.6(a) & (b)) were evaluated for selective stripping of co-extracted Np (~10^{-6} M) and Pu (~10^{-6} M) along with U (~6 g/L) from the loaded organic phases of 1.1 M TBP and 1.1 M DHOA solutions in *n*-dodecane.

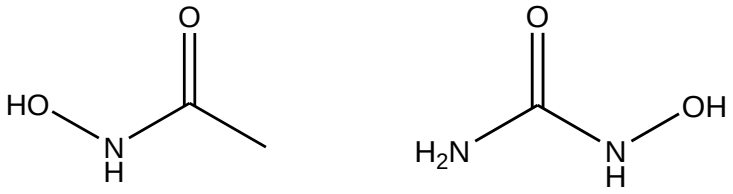

Acetohydroxamic acid (AHA) (a)

Hydroxyurea (HU) (b)

Fig. 4.6 (a) & (b). Structure of acetohydroxamic acid and hydroxyurea

4.3.2.1. Evaluation of AHA

A systematic study was carried out to evaluate the effect of aqueous phase acidity (1-4 M HNO_3) on the stripping behavior of Pu and Np from the loaded organic phases (viz. 1.1 M TBP/1.1 M DHOA solutions) employing 0.1-1.0 M AHA as the complexant/reductant. As shown in Figures 4.7-4.10, the stripping efficiency of AHA decreased with increased

aqueous phase acidity. This behavior was explained in terms of the instability of AHA at higher acidities. AHA undergoes hydrolytic degradation at higher acidities as follows [**159, 170**]:

$$RCONHOH + H_2O + H^+ \leftrightarrow RCOOH + H_3NOH^+ \quad (4.16)$$

From Figures 4.7 to 4.10, it was found that, at higher concentrations, AHA yielded better stripping of Pu and Np from the loaded organic phases (viz. 1.1 M TBP/1.1 M DHOA solutions). DHOA displayed distinctly better stripping of Pu and Np as compared to that of TBP under identical experimental conditions.

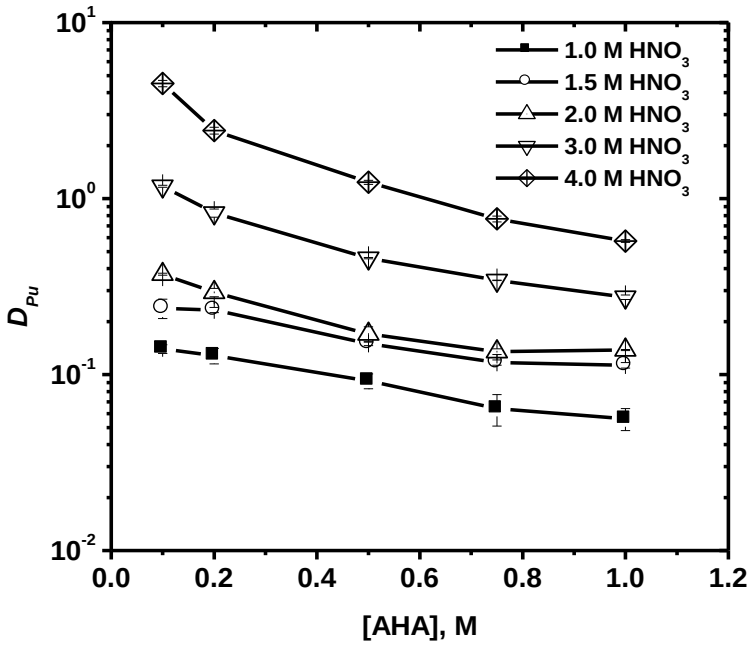

Fig. 4.7. Variation of D_{Pu} with AHA concentration at different phase acidities; Organic phase: 1.1 M TBP/*n*-dodecane loaded with Pu (~10^{-6}) and U (~6g/L); T: 298 K

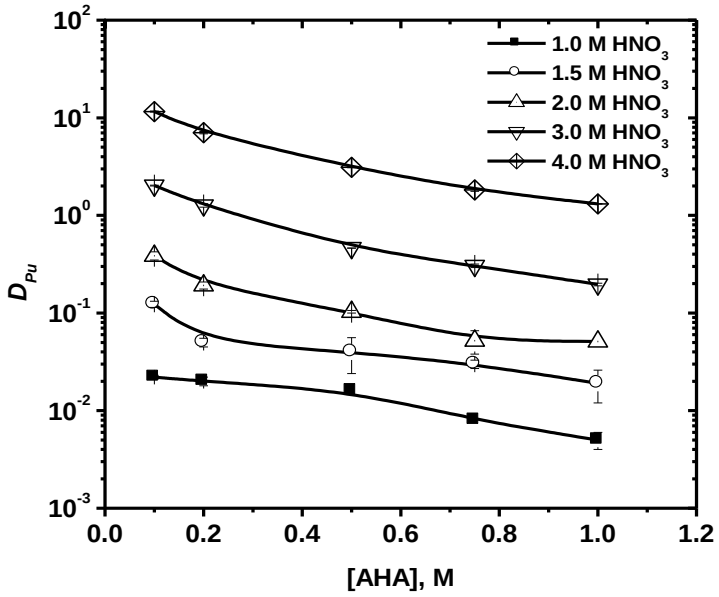

Fig. 4.8. Variation of D_{Pu} with AHA concentration at different phase acidities; Organic phase: 1.1 M DHOA/*n*-dodecane loaded with Pu (~10^{-6}) and U (~6g/L); T: 298 K

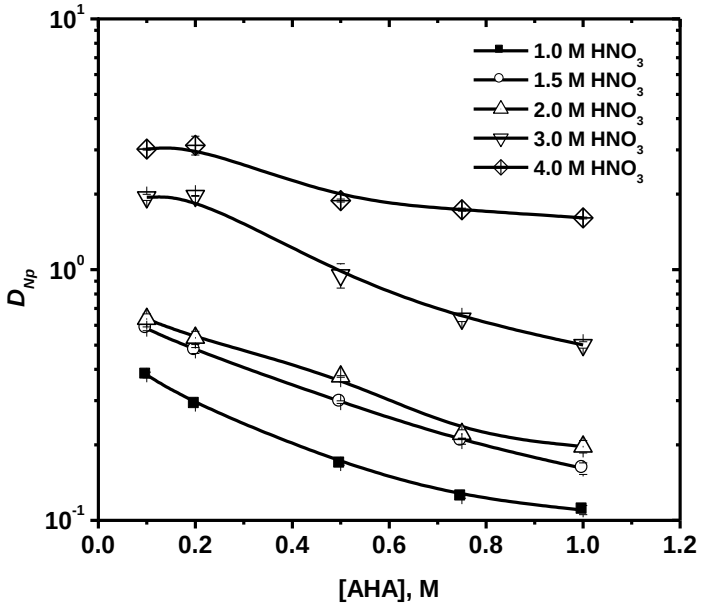

Fig. 4.9. Variation of D_{Np} with AHA concentration at different phase acidities; Organic phase: 1.1 M TBP/*n*-dodecane loaded with Np (~10^{-6}) and U (~6g/L); T: 298 K

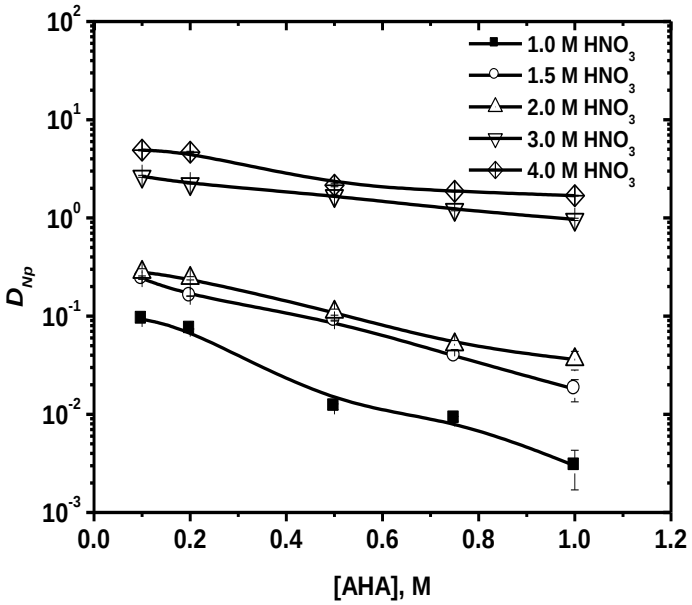

Fig. 4.10. Variation of D_{Np} with AHA concentration at different phase acidities; Organic phase: 1.1 M DHOA/*n*-dodecane loaded with Np (~10^{-6}) and U (~6g/L); T: 298 K

4.3.2.2. Evaluation of HU

HU has been identified as a very promising reductant for U/Pu and U/Np separation under the PUREX process conditions. It does not need holding reductants such as hydrazine, and can scavenge HNO_2 rapidly [**184**]. The presence of HU in the aqueous medium has negligible influence on the distribution behavior of U(VI). Solvent extraction studies using TBP as extractant showed that, HU can strip Np(VI) efficiently from the organic phase into the aqueous phase by reduction to inextractable Np(V).

The effectiveness of Np stripping decreased with aqueous phase acidity which inhibited the reduction of Np(VI) to Np(V) by HU. It was also observed that HU can further reduce Np(V) to Np(IV) even though the reduction kinetics was very slow [**185**]. Therefore, stripping studies were also performed on loaded 1.1 M TBP/1.1 M DHOA phases employing 0.1-1 M HU solutions at 1-4 M HNO_3. Figures 4.11-4.14 shows the

stripping of Pu and Np from the loaded organic phases: (a) decreased with increased aqueous phase acidity at a fixed HU concentration, (b) increased with HU concentration at a fixed acidity, and (c) Pu stripping was better than Np for both the extractants. Spectrophotometric investigations on the redox behavior of Np(IV) present in the organic phase (TBP/DHOA) showed the signatures of Np(V) in the aqueous phase when contacted with nitric acid solution. The observations of stripping studies are in conformity with the spectrophotometric and with the kinetic studies [**185**]. It was worth noting that HU was particularly ineffective for the stripping of Np from the loaded organic phases (TBP or DHOA) at ≥ 2 M HNO_3. These studies suggested that DHOA displayed better stripping of Pu and Np as compared to that of TBP under identical experimental conditions.

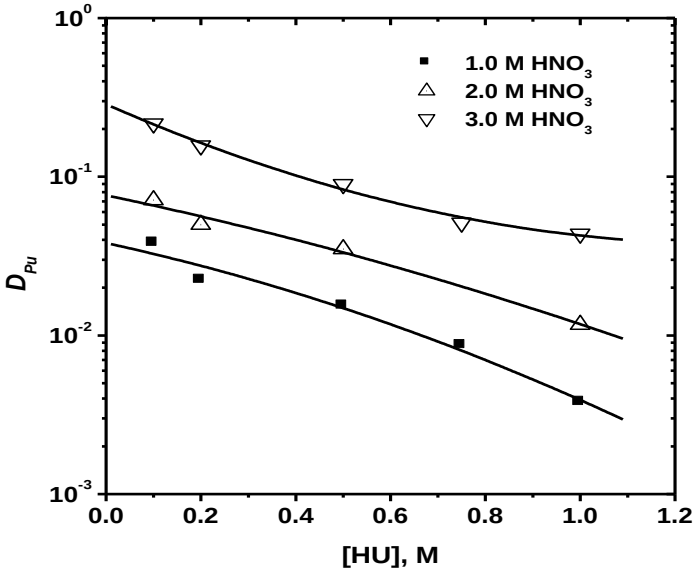

Fig. 4.11. Variation of D_{Pu} with HU concentration at different phase acidities; Organic phase: 1.1 M TBP/*n*-dodecane loaded with Pu (~10^{-6}) and U (~6g/L); T: 298 K

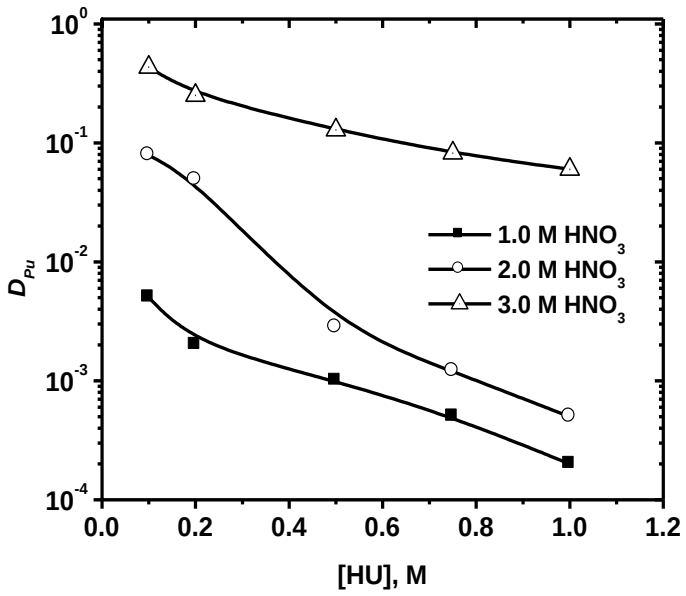

Fig. 4.12. Variation of D_{Pu} with HU concentration at different phase acidities; Organic phase: 1.1 M DHOA/*n*-dodecane loaded with Pu (~10^{-6}) and U (~6g/L); T: 298 K

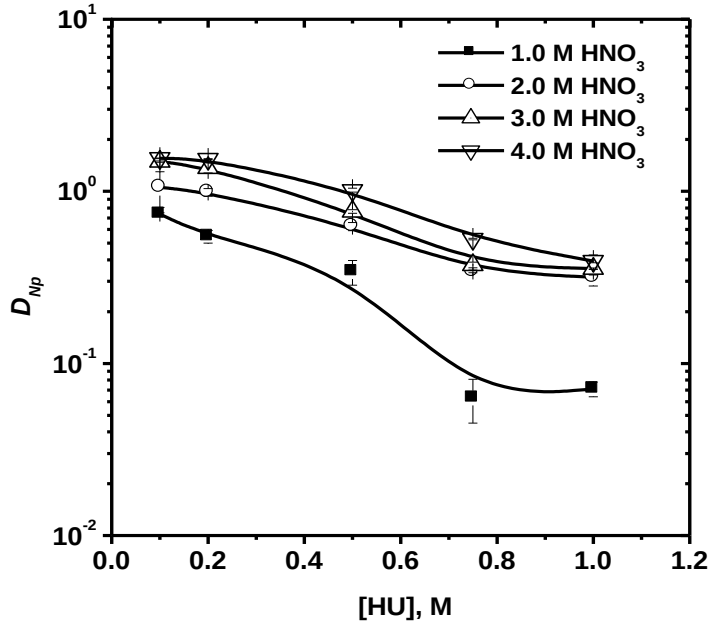

Fig. 4.13. Variation of D_{Np} with HU concentration at different phase acidities; Organic phase: 1.1 M TBP/*n*-dodecane loaded with Np (~10^{-6}) and U (~6g/L); T: 298 K

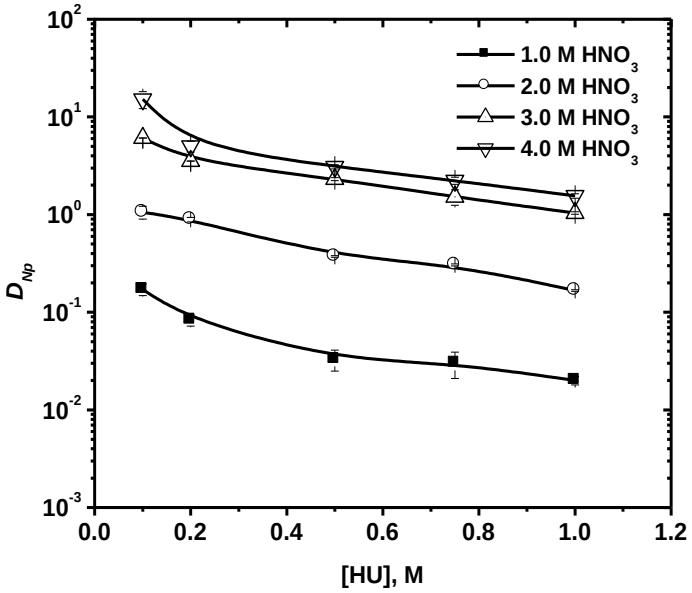

Fig. 4.14. Variation of D_{Np} with HU concentration at different phase acidities; Organic phase: 1.1 M DHOA/*n*-dodecane loaded with Np (~10^{-6}) and U (~6g/L); T: 298 K

4.3.2.3. Optimization of stripping conditions

It was essential to optimize conditions such as acidity, reductant/strippant concentration which could offer selective and efficient stripping of Np and Pu and provide maximum retention of uranium in the loaded organic phases. One can easily strip uranium from the loaded organic phases by contacting with dilute acid solutions (0.01 M HNO_3) after selective removal of Np and Pu. These studies pointed that higher acidity makes strippants like AHA and HU relatively ineffective for Pu and Np stripping from the loaded organic phases. Uranium can be better retained at higher acidities and is insensitive to the presence of either AHA or HU in the aqueous phases. These observations led us to evaluate 0.5 M solutions of AHA and HU at 1.5 M and 2 M HNO_3 as stripping solutions under the conditions of present work for both TBP/DHOA based loaded organic phases. Tables 4.3 & 4.4 summarize the stripping data of U, Np, and Pu

employing 0.5 M solutions of AHA and HU at 1.5 M and 2 M HNO_3 as stripping solutions.

Table 4.3: Stripping behavior of U (~5g/L), Np (~10^{-6} M) and Pu (~10^{-6} M) from the loaded organic phases at 3 M HNO_3; $[HNO_3]_{org}$: 0.6 M; O/A: 1; T: 298 K

Extractant	**Strippant**	**Stage #**	**% Stripping**		
			U	**Np**	**Pu**
1.1 M TBP	0.5 M AHA at 1.5 M HNO_3	I	5.8	86.1	89.6
		II	11.5	96.5	99.1
		III	17.5	98.5	99.8
1.1 M DHOA	0.5 M AHA at 1.5 M HNO_3	I	14.7	98.2	98.1
		II	27.2	99.9	99.9
		III	39.8	--	--
1.1 M TBP	0.5 M HU at 1.5 M HNO_3	I	5.4	61.0	97.5
		II	15.3	85.8	99.1
		III	24.1	94.8	99.9
1.1 M DHOA	0.5 M HU at 1.5 M HNO_3	I	24.5	85.5	99.5
		II	43.4	97.7	99.9
		III	57.1	99.9	--

Table 4.4: Stripping behavior of U (~5g/L), Np (~10^{-6} M) and Pu (~10^{-6} M) from the loaded organic phases at 4 M HNO_3; $[HNO_3]_{org}$: 0.7 M; O/A: 1; T: 298 K

Extractant	**Strippant**	**Stage #**	**% Stripping**		
			U	**Np**	**Pu**
1.1 M TBP	0.5 M AHA at 2 M HNO_3	I	3.5	84.1	87.4
		II	9.0	97.6	98.4
		III	15.0	99.4	99.8
1.1 M DHOA	0.5 M AHA at 2 M HNO_3	I	9.0	95.7	96.5
		II	19.9	99.9	99.9
		III	33.7	--	--
1.1 M TBP	0.5 M HU at 2 M HNO_3	I	4.3	43.9	96.1
		II	13.0	68.9	99.6
		III	20.5	81.6	99.9
1.1 M DHOA	0.5 M HU at 2 M HNO_3	I	20.7	68.9	97.6
		II	31.2	92.5	99.9
		III	48.0	97.8	--

The following observations can be made from Tables 4.3 and 4.4:

(a) Two stages were sufficient for quantitative stripping of Np and Pu from loaded DHOA employing 0.5 M AHA at 1.5 - 2.0 M HNO_3 as the strippant; while more than three stages were required in the case of TBP as extractant. However, 0.5 M AHA at 2.0 M HNO_3 would be preferable in view of lower U loss to the aqueous phase.

(b) 0.5 M HU at 1.5 - 2 M HNO_3 appears less effective for selective Np and Pu stripping for both the extractants.

(c) Uranium loss to the aqueous phase is more in the case of DHOA as compared to that of TBP.

CHAPTER 5: EVALUATION OF *N,N*-DIHEXYLOCTANAMIDE FOR ADVANCED HEAVY WATER REACTOR SPENT FUEL REPROCESSING

5.1. Introduction

Advanced Heavy Water Reactor (AHWR) will serve as a predecessor to the third-stage reactors of Indian nuclear power programme. This reactor will be based on Th-^{233}U fuel cycle and will provide the much needed vital information to initiate this fuel cycle. At equilibrium, the core of AHWR will consist of composite fuel assemblies each having 24 nos. of (Th, ^{239}Pu) MOX pins and 30 nos. of (Th, ^{233}U) MOX pins [**16**]. AHWR spent fuel adds new dimensions to reprocessing by the presence of Pu in the spent fuel. This requires additional provisions in the reprocessing plants and invokes the integration of PUREX and THOREX processes. However, due to limitation of TBP identified over the years, there is a need to look for alternative extractants for spent fuel reprocessing [**60-64**]. In this context, DHOA was evaluated as an alternative extractant to TBP for the reprocessing of three component AHWR spent fuels [**78**]. In this work, efforts have been made to optimize the conditions for the selective extraction of ^{233}U and Pu over Pa, Th using DHOA as extractant from simulated dissolved AHWR spent fuel solution in batch, mixer settlers as well as centrifugal contactor studies.

A series of non-salt forming reductants have been evaluated for the partitioning of plutonium. The fission products extraction behavior has also been examined under the simulated AHWR spent fuel feed conditions. Based on these observations, a solvent extraction scheme has been proposed for the reprocessing of three component U, Pu and Th system arising out of the irradiated AHWR (Th,Pu)O_2 pins. Hydrodynamic parameters such as density (ρ, gcm^{-3}), viscosity (η, mPa·s) and IFT ($mN \cdot m^{-1}$) values have been

measured and extraction studies were performed to compare the radiolytic degradation behavior of the proposed solvents under AHWR simulated feed conditions.

TBP dissolved in *n*-dodecane has a tendency to form third-phase during the extraction of tetravalent metal ions such as Th((IV) (relevant for Th fuel cycle) and Pu(IV) (relevant for fast reactor reprocessing) [**64**]. Several studies have been performed on the third-phase formation behavior of different extractants towards the extraction of metal ions and different acid solutions [**83, 86, 186-188**]. However, there is a need to get an insight in to the mechanism and conditions for third-phase formation. The extractants such as TBP would encounter an aqueous feed containing U(VI) and Th(IV) in different proportions in the back-end of nuclear fuel cycle. Therefore, it is essential to understand the third-phase formation behavior of different proposed process solvents using aqueous solutions containing at least two metal ions viz. U(VI) and Th(IV) in nitric acid derived species.

In this chapter, Dynamic Light Scattering (DLS) studies have been carried out to understand the third-phase formation/aggregation behavior of two straight chain amides DHOA, DHDA (*N,N*-dihexyl decanamide) (Figure 5.1) vis-à-vis TBP dissolved in *n*-dodecane during the extraction of Th(IV) from nitric acid medium.

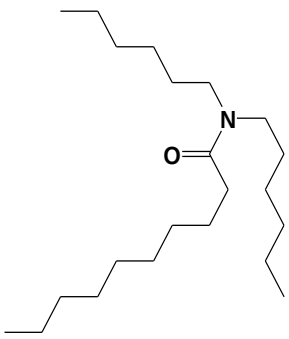

Fig. 5.1. *N,N*-dihexyl decanamide (DHDA).

5.2. Results and discussion

5.2.1. Batch extraction studies

Distribution studies of U, Pu, Th, minor actinides (Np, Pa, Am, Cm etc.) and fission products were done employing 0.36 M DHOA and 0.18 M TBP in *n*-dodecane. Scrubbing and partitioning studies of Th and Pu were also done from loaded organic phases.

5.2.1.1 Extraction behavior of Th, U and Pu

Table 5.1 compares the distribution ratio values of U, Pu and Th under earlier proposed THOREX feed conditions (200 g/L Th + 0.03 M F^-+ 0.1 M Al^{3+} at 4 M HNO_3) for 0.18 M (5 %) and 0.36 M concentrations of TBP and DHOA.

Table 5.1: D_M as a function of DHOA concentration under THOREX/AHWR feed condition; Diluent: *n*-dodecane; THOREX feed: 200 g/L Th + ~0.2 g/L U + 0.03 M F^-+ 0.1 M Al^{+3} at 4 M HNO_3; AHWR feed: 100 g/L Th + 2 g/L U + 2 g/L Pu + 0.03 M F^-+ 0.1 M Al^{+3} at 4 M HNO_3; T: 298 K

[Ligand], M	**TBP**			**DHOA**		
	D_{Th}	D_U	D_{Pu}	D_{Th}	D_U	D_{Pu}
0.18	0.04	2.3	1.6	0.01	1.1	1.3
0.18#	***0.05***	***2.1***	***1.1***	***0.01***	***1.8***	***0.8***
0.36##	0.043	2.4	2.0	0.05	4.0	5.7
0.36#	***--***	***--***	***--***	***0.06***	***3.1***	***3.3***

#Values in italics and bold refer to simulated AHWR feed solution; ##O/A=2.

Interestingly, DHOA has D_{Pu} similar to that of 0.18 M TBP. However, the lower D_{Th} values result in improved separation factor (SF) values with DHOA. Therefore, 0.18

M DHOA offers better SF values for both U and Pu over Th, yet the low D values for U and Pu (D_U: 1.1 and D_{Pu}: 1.3) are a limitation. On the other hand, 0.36 M DHOA appears to be a good compromise between SF and distribution ratio values.

In view of the average enrichment of 3.5 % Pu in proposed AHWR fuels, the concentration of thorium in the spent fuel feed solution was proposed to be kept ~100 g/L to limit the fissile content to < 7 g/L to maintain a safe concentration from the criticality viewpoint. Further studies were, therefore, carried out on a new composition of simulated AHWR feed solution. However, it should be noted that organic-to-aqueous phase ratio (O/A) was increased in the case of DHOA beyond ligand concentration 0.18 M to avoid third-phase formation under THOREX feed conditions [**60**]. While such problem was not encountered in the presence of 100 g/L Th in the proposed AHWR feed solution using DHOA as the extractant (Table 5.2).

Table 5.2: No. of stages required for 99.9 % U & Pu extraction from simulated AHWR feed solution; Extractants: TBP and DHOA; Diluent: *n*-dodecane; T: 298 K

[Ligand], M	**U**	**Pu**	**% Th extraction**
0.18 M TBP	6(7)	10(9)	38.6
0.18 M DHOA	9	12	13.3
0.36 M DHOA	5	5	25

*Values in bracket are taken from ref. no. [**115**].*

The data suggested that 6 and 10 contacts were required for quantitative extraction of U and Pu under co-current mode, employing 0.18 M TBP/*n*-dodecane as extractant. While 5 contacts of 0.36 M DHOA/*n*-dodecane were sufficient for achieving quantitative extraction. Studies carried out at FRD, BARC have shown that 7 and 9

contacts were required for quantitative extraction of U and Pu, respectively, employing 0.18 M TBP/*n*-dodecane as extractant [**115**]. Th extraction was expected to be 38.6 % (10 contacts) and 25.3 % (5 contacts), for 0.18 M TBP and 0.36 M DHOA solutions, respectively.

5.2.1.2. Scrubbing studies

During the extraction step, co-extracted thorium is required to be scrubbed using appropriate concentration of nitric acid. Table 5.3 lists the distribution data of U and Pu at 1-4 M HNO_3 for both the loaded organic phases.

Table 5.3: Scrubbing of U and Pu from loaded 0.18 M TBP and 0.36 M DHOA phases; Diluent: *n*-dodecane; O/A: 1; T: 298 K

Extractant	$[HNO_3]$, M	D_U	D_{Pu}
0.18 M TBP	1.0	0.6	0.2
	2.0	1.8	0.5
	3.0	2.7	0.8
	4.0	2.8	1.2
0.36 M DHOA	1.0	0.3	0.1
	2.0	1.0	0.5
	3.0	1.7	1.2
	4.0	2.3	2.4

The aim was to minimize the loss of U and Pu to the scrub solution. Th could not be detected in the loaded organic phase under all scrubbing conditions (D_{Th}: $<10^{-2}$). Based

on observations, 4 M HNO_3 solution was found to be suitable for scrubbing of Th with minimum loss of U and Pu in the scrub solution. Whereas 0.18 M TBP appears better with respect to U loss, 0.36 M DHOA is promising with respect to Pu loss in the scrubbing cycle.

5.2.1.3. Partitioning studies

Large quantities of natural uranous salt (~10 times the stoichiometric amount of Pu^{4+}) are required for partitioning of Pu. As a result, there will be isotopic dilution of ^{233}U during AHWR fuel reprocessing. Therefore, there is a need of the (a) evaluation of new non-salt forming reductants, and (b) development of equipment for in-situ reduction of Pu^{4+} to Pu^{3+}, for partitioning of Pu from U present in the loaded organic phases [**189**]. Pu partitioning studies were, therefore, carried out using 0.5 M solutions of different non salt forming strippant/reductant (such as hydroxyl amine nitrate (HAN), diethyl hydroxyl amine nitrate (DEHAN), hydroxy urea (HU), acetohydroxamic acid (AHA), acetoxamic acid (AOX)) solutions prepared in 2 M HNO_3 to minimize the loss of uranium in the strip solution.

Table 5.4 lists the distribution data of U and Pu along with their retention % in the organic phases. Most of the strippants appear very effective for the partitioning of Pu from loaded organic phases. U retention was observed to be ~65 % for 0.18 M TBP and ~41 % for 0.36 M DHOA as the extractant during the partitioning cycle. U lost in the partitioning cycle needs to be re-extracted after adjusting the feed acidity (~7 M HNO_3). The data suggested that at least three stages were required for quantitative stripping of Pu from the loaded TBP phase. By contrast, only two stages were sufficient for Pu stripping

from loaded DHOA phase. Loaded uranium can be stripped by dilute acid (0.01 M HNO_3) solution.

Table 5.4: Partitioning of U and Pu from scrubbed 0.18 M TBP and 0.36 M DHOA phases; Aqueous phase: 0.5 M solution of different reductants at 2 M HNO_3; O/A: 1; T: 298 K

Extractant	**Reductant**	**D_M**		**Retention, %**	
		U	**Pu**	**U**	**Pu**
0.18 M TBP	HAN	2.0	0.02	66.7	1.6
	DEHAN	2.2	0.01	70.0	1.1
	HU	1.3	0.002	57.3	0.2
	AHA	1.9	0.01	66.0	1.0
	AOX	2.3	0.004	69.5	0.4
0.36 M DHOA	HAN	0.7	0.009	41.2	0.9
	DEHAN	0.7	0.002	41.2	0.2
	HU	0.6	0.001	36.3	0.06
	AHA	0.8	0.004	43.8	0.4
	AOX	0.8	0.002	43.5	0.2

These studies suggested that 0.5 M HAN/AHA/HU/AOX solutions at 2 M HNO_3 solutions can be used as strippants for the partitioning of Pu during the reprocessing of AHWR spent fuels.

5.2.1.4. Protactinium extraction studies

Initially, the AHWR spent fuels are expected to reach a burn-up of 15000 MWd/Te which will be further raised to 24,000 MWd/Te under equilibrium conditions. Pu in AHWR burns faster due to large absorption cross-section that leads to loss in reactivity. It provides an option to reconstitute the fuel cluster after an average discharge burn-up of 24,000 MWd/Te. During this process, only (Th,Pu)O_2 pins will be replaced by fresh fuel pins. Thus, it is possible to obtain an additional burn-up of ~20,000 MWd/Te from the reconstituted cluster. The cluster reconstitution improves ^{233}U production and reduces the reprocessing load due to increased average cluster burn-up. Therefore, the reprocessing some of the fuel bundles after short-cooling to achieve a burn-up of ~ 40,000 MWd/Te and to get a pure ^{233}U product from the short cooled spent fuel appears attractive [**16, 189**]. In this context, Pa extraction profile becomes important.

Figure 5.2 shows the variation of D_{Pa} values with aqueous phase acidity for 0.18 M TBP, 0.36 M DHOA in *n*-dodecane as extractants. D_{Pa} value gradually increases with aqueous phase acidity and 0.36 M DHOA shows better extraction than 0.18 M TBP. This behavior can be explained by following equilibrium between the hydrolyzed cationic, neutral and anionic species of Pa in nitric acid medium. The interchange between these species is fast [**112**]:

$$[Pa(OH)_2(NO_3)]^{2+} \leftrightarrow [Pa(OH)_2(NO_3)_2]^{+} \leftrightarrow [Pa(OH)_2(NO_3)_3] \leftrightarrow [Pa(OH)_2(NO_3)_4]^{-} \leftrightarrow .....$$

(*extractable species*) (5.1)

However, D_{Pa} decreased under simulated AHWR/THOREX feed conditions for both the extractants. For 0.18 M TBP, the D_{Pa} values decreased from 0.1 (no Th) to 0.07 (AHWR feed) and 0.05 (THOREX feed). The corresponding values for 0.36 M DHOA were 0.6, 0.35, and 0.03, respectively. This behavior was attributed to (a) thorium loading

in the organic phase, and (b) the formation of inextractable anionic nitrate species due to the presence of ~ 6-7 M NO_3^- ions. Similar observations were made using D2EHIBA as extractant during the studies on extraction of protactinium in the presence of macro concentrations of thorium [**190**].

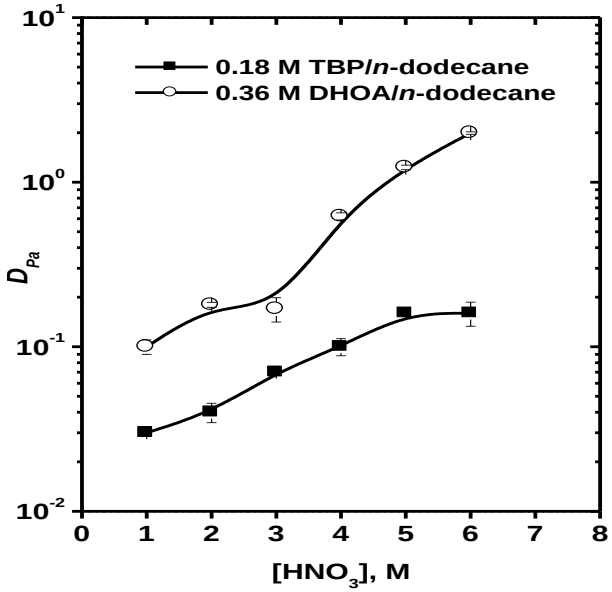

Fig. 5.2. Variation of D_{Pa} with aqueous phase acidity; T: 298 K

Figure 5.3 suggests that DHOA appears promising extractant for the preferential extraction of U and Pu from dissolver solution of AHWR spent fuel arising out of $(Th,Pu)O_2$ pins in view of improved separation factor (SF) of U and Pu over Th. However, SF values for U and Pu over Pa are relatively lower compared to those of 0.18 M TBP. Figure 5.4 shows that trisolvated species are formed with DHOA for both Pu and Th while disolvated and trisolvated species are reported to be formed in the case of TBP [**191**]. Therefore, D_{Pu} value is significantly enhanced with increased DHOA concentration as compared to that of TBP.

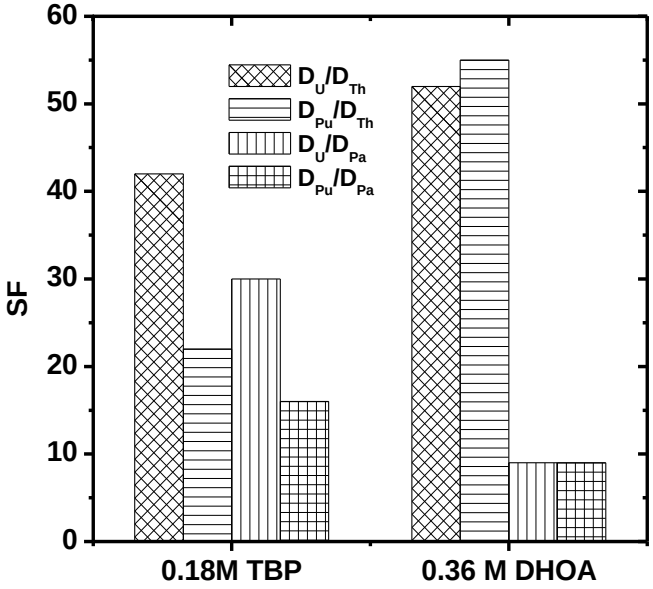

Fig. 5.3. Comparison of TBP, DHOA for U/Pu separation from Th and Pa under AHWR feed condition; T: 298 K

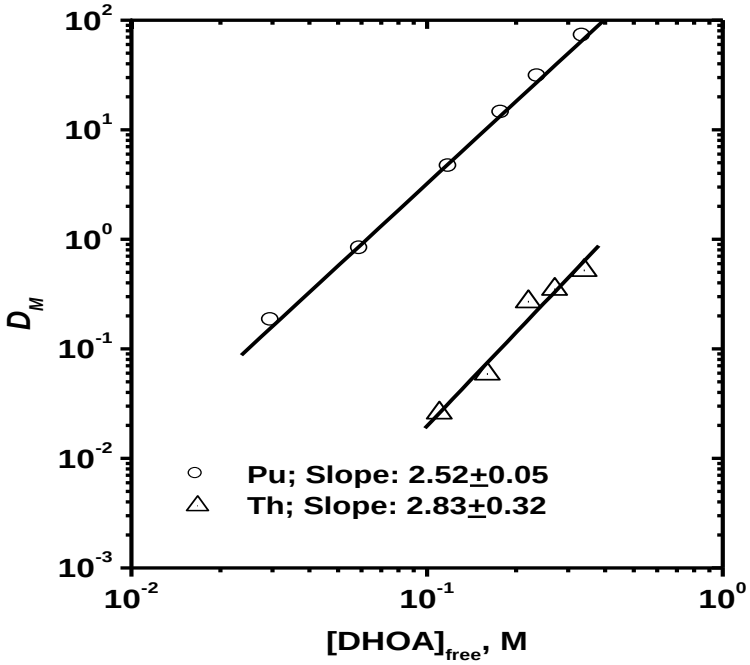

Fig. 5.4. D_{Pu} and D_{Th} as function of DHOA concentration; [Pu]: ~10^{-4} M; [Th]: ~10^{-4} M; [HNO_3]: 4 M; T: 298 K

5.2.1.5. Extraction behavior of minor actinides

The concentration of minor actinides produced in the discharged fuel of AHWR (viz. ^{231}Pa, ^{237}Np, ^{241}Am, ^{243}Am, ^{242}Cm, ^{243}Cm, and ^{244}Cm) for different fuel cycles (PWR, PHWR, AHWR) were compared using computer code ORIGEN-2 [**33**]. This study suggested that the production of minor actinides per unit energy was less in AHWR fuel cycle than those of PWR fuel (~ 29 %), but it was comparable to that of PHWR fuel. The minor actinides in the Th-U fuel per unit energy (TWh or GWy) are significantly less compared to uranium fuel. This is because, except for ^{231}Pa, most of the minor actinides are having mass numbers much higher than ^{232}Th, so at least 5 to 6 capture and decay reactions are required to generate those minor actinides. By contrast, the minor actinides per unit energy (TWh or GWy) for the plutonium pins are relatively higher because of Am and Cm isotopes. The concentrations (g/Te) of different minor actinides in AHWR spent fuel with average burn-up of 24,000 MWD/Te (~21000 MWD/Te for Th-Pu & 27000 MWD/Te for Th-U), and 10 years of cooling are: ^{231}Pa (2.2), ^{237}Np (5.7), ^{241}Am (512), ^{243}Am (25.7), ^{242}Cm (4.2×10^{-3}), ^{243}Cm (0.21), and ^{244}Cm (1.87) [**33**].

The reprocessing of AHWR spent fuel gets further complicated due to the formation of minor actinides such as ^{231}Pa, Np, Am and Cm isotopes. The extraction behavior of ^{237}Np (no valency adjustment) and ^{241}Am, were investigated under proposed AHWR spent fuel feed conditions employing 0.18 M TBP and 0.36 M DHOA as extractants. Both extractants showed appreciable extraction of Np (D_{Np}: 0.96 (0.18 M TBP) and 2.0 (0.36 M DHOA)) while negligible extraction of Am was observed (D_{Am}: $<10^{-3}$). From this study, it can be concluded that a separate actinide partitioning step is required after the reprocessing of the three components AHWR spent fuel.

5.2.1.6. Fission/activation products extraction studies

Batch extraction experiments were also performed on simulated AHWR feed solution spiked with a diluted aliquot of High Level Waste (HLW) sample from the PUREX process stream (from PREFRE plant, Tarapur) as the aqueous phase and 0.18 M TBP and 0.36 M DHOA solutions in *n*-dodecane as extractants. Addition of HLW helped to get composite fission product activity in the simulated AHWR feed solution. The distribution ratio values of fission/activation products (viz. ^{137}Cs, ^{144}Ce, ^{106}Ru, ^{60}Co etc.) were of the order of ~10^{-4}-10^{-3} suggesting better decontamination of U and Pu for both the solvents (viz. 0.18 M TBP and 0.36 M DHOA solutions in *n*-dodecane).

5.2.2. Mixer settler studies

Detailed batch studies revealed that under co-current mode and maintaining O/A as 1, only 6 and 10 contacts were required for quantitative extraction of U and Pu from simulated AHWR feed solution (Typical composition: [Th] = 102 g/L, [U] = 2 g/L, [Pu] = ~0.65 mg/L (i.e. 22,000 cpm/25 µL), [HNO_3] = 3.6 M, [HF] = ~0.01 M and [$Al(NO_3)_3$] = ~0.1 M) employing 0.18 M TBP/*n*-dodecane as solvent. By contrast, only 5 contacts of were sufficient for achieving quantitative extraction of U and Pu employing 0.36 M DHOA/*n*-dodecane. Based on these observations, it was of interest to evaluate 0.36 M DHOA/*n*-dodecane vis-à-vis 0.18 M TBP/*n*-dodecane as solvents under counter-current mode of operation. It is important to mention that in view of relatively more number of stages required for quantitative extraction of U and Pu, O/A was proposed to be maintained as 2 employing 0.18 M TBP/*n*-dodecane as the solvent in the extraction cycle [**115, 116**]. Batch studies also suggested that 4 M HNO_3 and 0.5 M HAN in 2 M HNO_3 can be used for the scrubbing of co-extracted Th and for Pu partitioning, respectively.

Loaded U was proposed to be efficiently stripped from organic phase using 0.01 M HNO_3.

5.2.2.1. Extraction cycle

Twelve stage mixer settler runs were carried out employing both the solvents i.e. 0.36 M DHOA and 0.18 M TBP dissolved in *n*-dodecane, under simulated AHWR feed conditions. No pre-equilibration of the organic phases was carried out during these runs. Flow rate of the organic and aqueous phases was maintained as 4-5 mL/minute.

5.2.2.1.1. DHOA as extractant

Negligible change in the concentration of nitric acid, thorium and uranium of various EXIT samples collected at different intervals suggested that equilibrium condition was attained within one hour after passing one bed volume (~1L) and maintaining O/A as ~1.15. The aqueous EXIT samples contained ~2 mg/L U suggesting >99 % extraction of uranium from the feed solution. Thorium and nitric acid concentrations in the aqueous EXIT samples were 97.4(±0.2) g/L and 3.14(±0.1) M, respectively. There was no significant change in thorium and nitric acid concentration in both the phases. Final composition of the loaded organic phase was: [U] = 1.7(±0.1) g/L; [Pu] = 0.65(±0.05) mg/L; [Th] = 4.8(±0.1) g/L and [HNO_3] = 0.36(±0.1) M [Decontamination Factor (DF), (Pu/Th): 21.3; (U/Th): 19.1].

Figures 5.5 and 5.6 show the stage wise concentration profiles of U and Pu in the organic and aqueous phases. There were negligible changes in the organic phase concentrations of nitric acid (0.36(±0.1) M) as well as of Th (4.8(±0.1) g/L) essentially due to the fact that D_{Th} and $D_{Nitric\ Acid}$ values are low. On the other hand, U concentration in the organic phase was found to increase gradually from Stage 1 (3 mg/L) to Stage 12

(1.7 g/L). Similarly, there was a gradual decrease in Pu concentration in the feed solution from stages 12 to stage 8 and beyond which the remaining Pu activity was negligible in the aqueous phase. These runs demonstrated that ~5 stages are sufficient for quantitative extraction of uranium and plutonium under the simulated AHWR feed conditions employing 0.36 M DHOA/*n*-dodecane as the solvent.

<table>
<tr><td colspan="4">Org. IN →</td><td></td><td></td><td></td><td></td><td colspan="4">Org. OUT →</td></tr>
<tr><td>1</td><td>2</td><td>3</td><td>4</td><td>5</td><td>6</td><td>7</td><td>8</td><td>9</td><td>10</td><td>11</td><td>12</td></tr>
<tr><td colspan="4">← Aq. OUT</td><td></td><td></td><td></td><td></td><td colspan="4">← Aq. IN</td></tr>
</table>

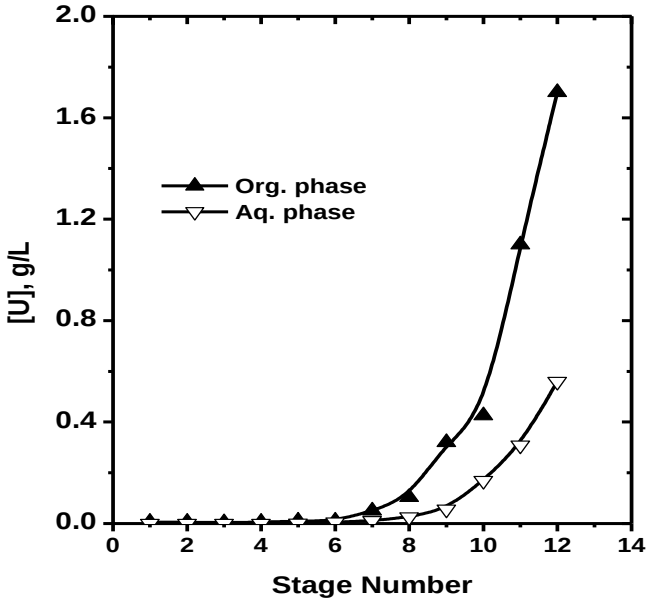

Fig. 5.5. U extraction profile under simulated AHWR feed condition; Solvent: 0.36 M DHOA/*n*-dodecane; O/A: 1.15

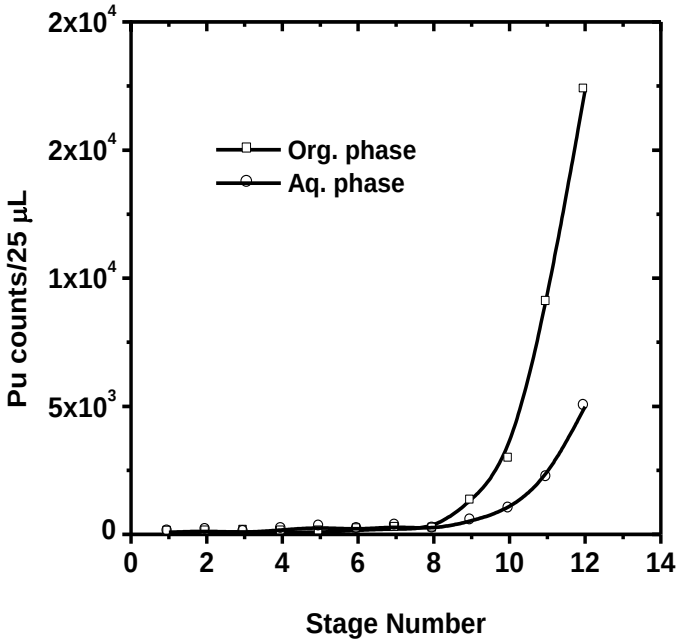

Fig. 5.6. Pu extraction profile under simulated AHWR feed condition; Solvent: 0.36 M DHOA/*n*-dodecane; O/A: 1.15

5.2.2.1.2. TBP as extractant

Under identical feed conditions, twelve stage mixer settler runs were carried out using 0.18 M TBP in *n*-dodecane as the solvent maintaining O/A ratio was as ~1. Equilibrium condition with respect to nitric acid as well as with respect to thorium was achieved within ~ 2 hours after passing one and half bed volume (~1.5 L). The aqueous raffinate contained ~0.7 mg/L U suggesting quantitative extraction (>99.9 %) of uranium. There was no significant change in thorium and nitric acid concentration in both the phases. Thorium and nitric acid concentrations in the aqueous EXIT samples were 95.4(±0.2) g/L and 3.30(±0.05) M, respectively. Final composition of the loaded organic phase was: [U] = 2.07(±0.04) g/L; [Pu] = 0.65(±0.03) mg/L; [Th] = 4.6(±0.2) g/L and [HNO_3] = 0.23(±0.02) M [DF, (Pu/Th): 20.3; (U/Th): 21.2].

Figures 5.7 and 5.8 present the stage wise concentration profile of U, and Pu in organic and aqueous phases. Uranium concentration in the organic phase was found to increase gradually at each stage [0.7 mg/L (stage 1) to 2.07 g/L (stage 12)]. Similarly, 12 stages were required for near quantitative extraction of Pu from simulated AHWR feed solution employing 0.18 M TBP/*n*-dodecane as the solvent. This behavior was attributed to lower distribution ratio values for Pu for TBP as compared to that of DHOA under identical experimental conditions. In view of these observations, O/A = 2 has been proposed for the reprocessing of three component AHWR spent fuel feed solution employing 0.18 M TBP/*n*-dodecane as the solvent [**116**]. However, extraction cycle data using these solvents suggest that DHOA offers advantages with respect to number of stages required for quantitative recovery of U and Pu (Table 5.5). These studies also indicate that even though the ligand inventory for both the extractants is same; the organic waste volume in the case of DHOA is generation is half of that of TBP.

Table 5.5: No. of stages required for 99.9 % U & Pu extraction from simulated AHWR feed solution in mixer settler runs; Extractants: TBP and DHOA; Diluent: *n*-dodecane; T: 25^{o}C

Extractants	**U**		**Pu**		**% Th extraction**
	O/A:1	O/A:2	O/A: 1	O/A: 2	
0.18 M TBP[#]	7	(5)	48	(9)	5
0.36 M DHOA	6	4	6	5	6

*Values in bracket are taken from ref. no. **[115]**.*

Org. IN →								Org. OUT →			
1	2	3	4	5	6	7	8	9	10	11	12
← Aq. OUT								← Aq. IN			

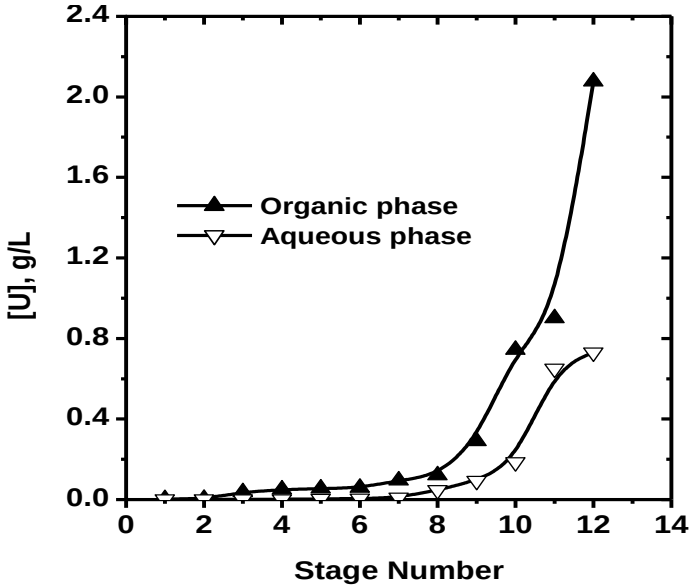

Fig. 5.7. U extraction profile under simulated AHWR feed condition; Solvent: 0.18 M TBP/*n*-dodecane; O/A: 1

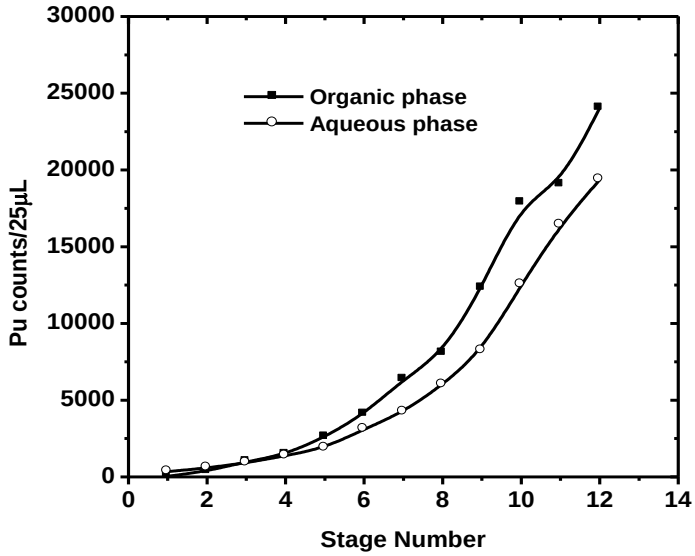

Fig. 5.8. Pu extraction profile under simulated AHWR feed condition; Solvent: 0.18 M TBP/*n*-dodecane; O/A: 1

5.2.2.2. Scrubbing cycle

Based on batch studies, 4 M HNO_3 was chosen for the scrubbing of Th from the loaded organic phases. These conditions were arrived at keeping in mind the minimization of the loss of U and Pu in the scrub solution. The mixer settler runs maintaining O/A~ 1 suggested that ~2 scrubbing stages were sufficient for complete removal of Th from the organic phases for both the solvents. However, 0.36 M DHOA appeared better with respect to U/Pu retention in the organic phase during the scrubbing cycle under the conditions of present studies. D_U and D_{Pu} values at 4 M HNO_3 were reported to be 2.8 and 1.2 (for 0.18 M TBP), and 2.3 and 2.4 (for 0.36 M DHOA).

The organic phase compositions obtained after scrubbing cycles were [U] = 1.3(±0.04) g/L; [Pu] = 0.42(±0.03) mg/L; [HNO_3] = 0.36(±0.1) M. for 0.36 M DHOA/*n*-dodecane and [U] = 1.3(±0.06) g/L; [Pu] = 0.33(±0.03) mg/L; [HNO_3] = 0.23(±0.02) M. for 0.18 M TBP/*n*-dodecane, respectively. The scrub solution containing lost U and Pu is proposed to be mixed with the feed solution. Based on these studies, it is proposed to maintain O/A = 0.33 for the scrubbing of thorium from the loaded organic phases. This will lead to small dilution of the feed solution with respect to U, Pu and Th concentrations. However, these solutions were effective for the removal of Th from the organic phases in 3-4 scrubbing stages. The extracted Th is completely removed in scrub cycle.

5.2.2.3. Stripping cycle

5.2.2.3.1. Pu partitioning

The scrubbed organic phases were used as the feed solutions for Pu partitioning experiments employing 0.5 M NH_2OH at 2 M HNO_3. These runs were performed

maintaining O/A ~1 and the organic and aqueous phase flow rates were maintained ~4-5 mL/minute. 3 stages are sufficient for quantitative stripping of Pu from 0.36 M DHOA/*n*-dodecane, whereas 4-5 stages are required in the case of 0.18 M TBP/*n*-dodecane as the organic phase (Figures 5.9 & 5.10). Studies suggested that Pu in the product stream can be concentrated by suitably increasing the O/A ratio without affecting significantly the stripping performance. This led us to Pu stripping studies maintaining O/A = 2 and similar results were obtained.

Org. IN →								**Org. OUT →**			
1	2	3	4	5	6	7	8	9	10	11	12
← Aq. OUT								**← Aq. IN**			

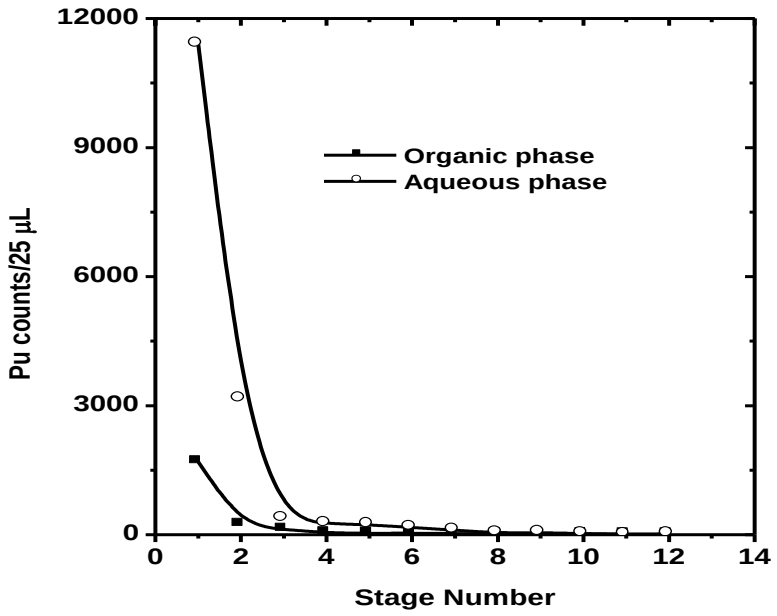

Fig. 5.9. Stage wise stripping profile from scrubbed organic phase; Solvent: 0.36 M DHOA /*n*-dodecane; strippant; 0.5 M NH_2OH at 2 M HNO_3; O/A: ~1

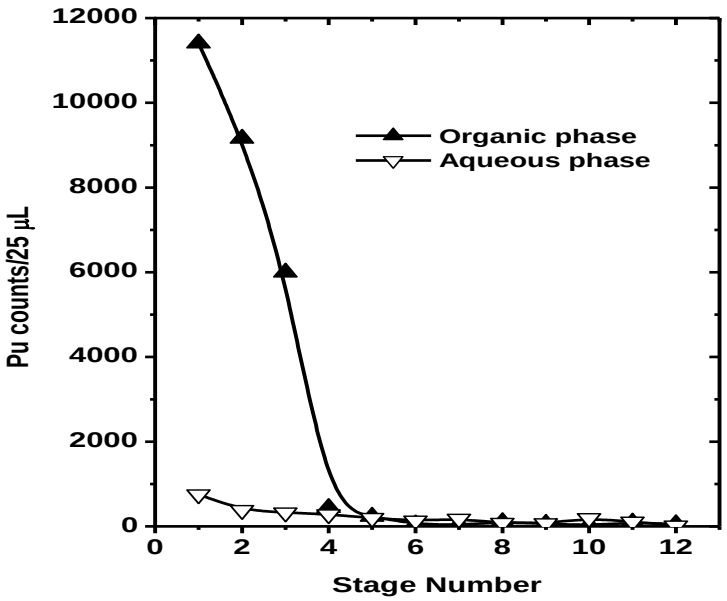

Fig. 5.10. Stage wise stripping profile from scrubbed organic phase; Solvent: 0.18 M DHOA /*n*-dodecane; strippant; 0.5 M NH_2OH at 2 M HNO_3; O/A: ~1

Based on these studies, it is proposed that Pu stripping can be performed employing 0.5 M NH_2OH at 2 M HNO_3 as strippant and maintaining O/A as 2. U loss (~55 % for 0.36 M DHOA/*n*-dodecane, $[U]_{org}$: 0.55 g/L and ~52 % for 0.18 M TBP/*n*-dodecane, $[U]_{org}$: 0.67 g/L) was also observed during 12 stages of Pu partitioning cycle. Therefore, it was essential to re-extract uranium after suitable aqueous phase acidity adjustment up to 3.5 M HNO_3 using ~7-8 M HNO_3. Under these conditions, 3-4 contacts were sufficient for the recovery of U from Pu product stream for both the solvents.

5.2.2.3.2. U stripping

The organic phases obtained after Pu stripping and after washing of Pu strip solution (containing U) were mixed together and were subjected for uranium stripping using 12 stage mixer settlers and 0.01 M HNO_3 as the aqueous phase and O/A ~ 1. Spectrophotometric analysis of the organic/aqueous phases showed that whereas 3-4 stages were sufficient for quantitative stripping of U from loaded 0.36 M DHOA/*n*-

dodecane while 5-6 stages were required in the case of 0.18 M TBP/*n*-dodecane as the solvent. Further experiments showed that uranium can be quantitatively stripped in 3-4 stages from loaded 0.36 M DHOA/*n*-dodecane even maintaining O/A = 2. These studies indicate that uranium stripping behavior is better in the case of 0.36 M DHOA/*n*-dodecane as the solvent. Interestingly, 4 stages have been proposed for quantitative stripping of U from 0.18 M TBP/*n*-dodecane as the solvent maintaining O/A =3 [**115**]. This behavior may be attributed to the use of 3 M HNO_3 as the scrub solution suggesting thereby less acid reflux from the organic phase during stripping cycle.

5.2.2.4. Proposed flow sheet

Based on batch and mixer settler studies, the following flow sheet (Figure 5.11) has been proposed for the reprocessing of three component AHWR spent fuel employing 0.36 M DHOA/*n*-dodecane as the solvent. Scrubbing and stripping solutions were 4 M HNO_3 and 0.5 M HAN at 2 M HNO_3, respectively. Even though Th is major composition, it is extracted in the extraction cycle and then selectively removed from the loaded organic phases in the scrubbing cycle. After Pu partitioning step, the stripped aqueous phase can be given a wash with fresh 0.36 M DHOA solution to recover uranium, which can be finally be stripped with 0.01 M HNO_3 solution. It is evident that 0.36 M DHOA/*n*-dodecane appears attractive with respect to (i) no. of stages required for quantitative extraction of ^{233}U and Pu, (ii) solvent requirement, (iii) no. of stages required for Th scrubbing from the loaded organic phase, (iv) ease of Pu partitioning from the loaded organic phase, (v) ease of U stripping from the loaded organic phase, and (vi) organic waste generation.

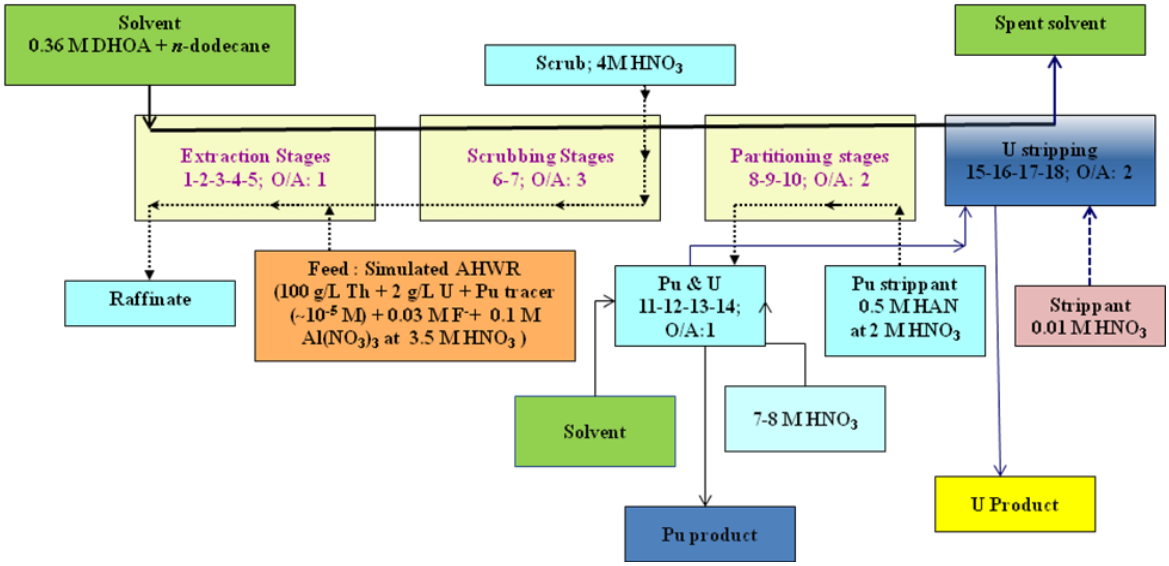

Fig. 5.11. Proposed flow sheet for AHWR spent fuel reprocessing using 0.36 M DHOA/*n*-dodecane as the solvent

5.2.3. Centrifugal contactor studies

Centrifugal contactor runs were performed using simulated AHWR feed [2 g/L U + 100 g/L Th + 0.03 M HF + 0.1 M $Al(NO_3)_3$ at 3.5 M HNO_3] using 0.18 M TBP and 0.36 M DHOA solutions in *n*-dodecane as solvents. Both the solvents displayed comparable extraction of U (~81%). However, Th extraction was higher in the case of 0.18 M TBP (6 %) as compared to 0.36 M DHOA (2 %). On the other hand, HNO_3 extraction was lower in the case of 0.18 M TBP (0.14 M) as compared to 0.36 M DHOA (0.28 M). Figures 5.12 (a) & 5.12 (b) show the stage wise concentration profiles of U, Th and HNO_3 for the 0.18 M TBP and 0.36 M DHOA solutions in *n*-dodecane during the extraction runs from simulated AHWR feed solution.

During scrubbing cycle, 86 % and 93 % of extracted Th were removed from the loaded 0.18 M TBP and 0.36 M DHOA solutions, respectively. The corresponding losses of U were 28 % and 33 % during scrubbing cycle. Uranium stripping runs from the

scrubbed organic phases showed only 86 % recovery in the case of 0.18 M TBP while quantitative stripping was achieved in the case of 0.36 M DHOA as the extractant. Table 5.6 shows extraction, scrubbing and stripping behavior of U, Th and HNO_3 under simulated AHWR feed conditions for both extractants. It is evident that DHOA appears superior as compared to TBP in the Th scrubbing and U stripping behavior.

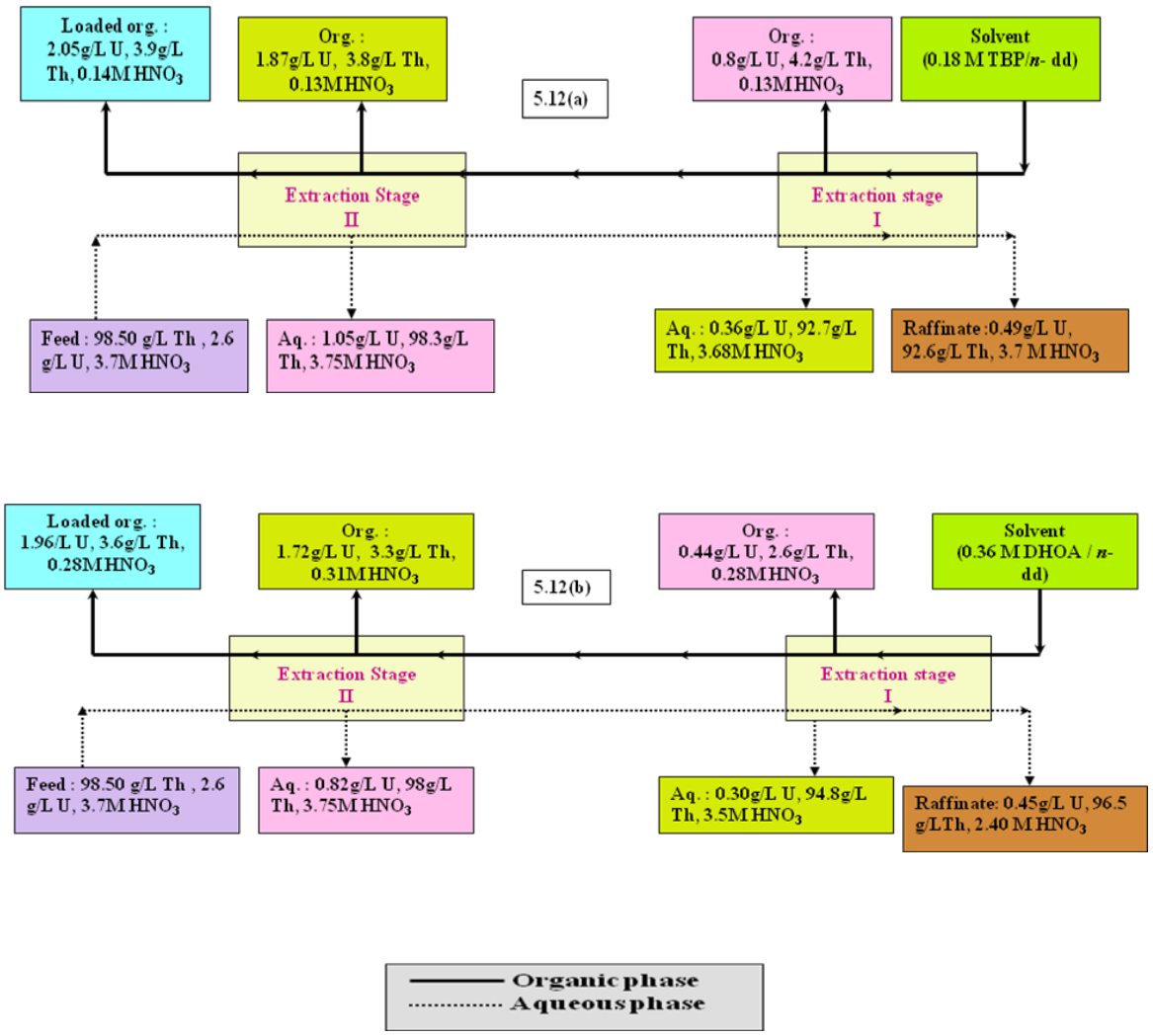

Figs. 5.12 (a) & 5.12 (b). Stage wise concentration profile during centrifugal contactor runs in extraction cycle with simulated AHWR feed using (a) 0.18 M TBP and (b) 0.36 M DHOA solutions in *n*-dodecane as solvents

Table 5.6: Extraction, scrubbing and stripping behavior of U, Th and HNO_3 under simulated AHWR feed[#] conditions [2 g/L U + 100 g/L Th + 0.03 M HF + 0.1 M $Al(NO_3)_3$ at 3.5 M HNO_3; O/A: 1; T: 298 K

Cycles	0.18 M TBP			0.36 M DHOA		
	U	Th	$[HNO_3]$, M	U	Th	$[HNO_3]$, M
Extraction (%)	81.3 %	5.9 %	0.14 M	80.6 %	2.2 %	0.28 M
Scrubbing (%)	27.8 %	86.1 %	3.94 M	32.7 %	96.7 %	4.05 M
Stripping (%)	85.9 %	76.0 %	0.16 M	99.8 %	96.6 %	0.47 M
Organic phase after stripping	0.22 g/L U, 0.13 g/L Th, 0.021M HNO_3			0.003 g/L U, 0.0 g/L Th, 0.013M HNO_3		
Aqueous phase after stripping	1.34 g/L U, 0.68 g/L Th, 0.16 M HNO_3			1.46 g/L U, 0.11 g/L Th, 0.27 M HNO_3		

5.2.4. Measurement of hydrodynamic parameters

Generally, the organic solvent is discarded after a certain number of hydrometallurgical (extraction/scrubbing/stripping) cycles because of the presence of the interfacially active solvent-degradation products, which may adversely affect the extraction performance and lead to a reduced the interfacial tension (IFT), leading to a slow phase-disengagement rate. In this context, these parameters were evaluated such as density (ρ, gcm^{-3}), viscosity (η, mPa·s) and IFT ($mN \cdot m^{-1}$) values with respect to the aqueous phase.

The viscosity is mainly associated with the self-association of the molecule due to inter-molecular bonding properties because of dipole-dipole interaction. On the other hand, IFT values are vital for the design, fabrication and operation of liquid-liquid

contactors. Too high IFT value may not allow proper mixing of one phase in the other affecting size of the organic phase droplets and, hence, mass transfer rates of the metal ions from the aqueous phases. The IFT between two immiscible phases, therefore, should be optimum for rapid phase disengagement. Typically, the IFT values for 1.1 M TBP in *n*-dodecane are in the range 12 to15 $mN \cdot m^{-1}$ under the *PUREX* process conditions [**192**]. The corresponding values for *N*,*N*-dialkyl amides are in the range 20 to 25 $mN \cdot m^{-1}$ [**142, 193**].

An attempt has been made to calculate the activation energy for viscous flow of the solvents from the viscosity data recorded at various temperatures. Measurements of IFT values have been carried out to arrive at the optimum composition of organic phase for smooth hydrometallurgical operations.

5.2.4.1. Density and viscosity measurements

The densities and viscosities of 0.18 M TBP and 0.36 M DHOA dissolved in *n*-dodecane were measured without or after equilibration with 3.5 M HNO_3/AHWR simulated feed solutions in the temperature range of 288 - 318 K. Both density and viscosity values were marginally higher in the case of 0.36 M DHOA/*n*-dodecane as compared to those of 0.18 M TBP/*n*-dodecane at a given temperature (Table 5.7). This behavior can be attributed to the higher concentration of DHOA in the proposed solvent. However, these values decreased with increased temperature for both the solvents. However both the solvents possess suitable density and viscosity values for counter-current operations even after equilibration with simulated AHWR feed solution in the temperature range 298 - 318 K.

Table 5.7: Density and viscosity data of the proposed solvents under different experimental conditions; Diluent: *n*-dodecane

Solvent	***T* (K)**	**ρ (gcm^{-3})**	**η (mPa·s)**
0.18 M TBP	288	0.7629(±0.0000)	1.6725(±0.0010)
	298	0.7555(±0.0000)	1.3924(±0.0002)
	308	0.7483(±0.0002)	1.1792(±0.0001)
	318	0.7408(±0.0001)	1.0143(±0.0010)
0.36 M DHOA	288	0.7669(±0.0000)	2.0529(±0.0016)
	298	0.7597(±0.0001)	1.6776(±0.0001)
	308	0.7526(±0.0001)	1.3997(±0.0003)
	318	0.7452(±0.0001)	1.1864(±0.0003)
0.18 M TBP equilibrated	288	0.7668(±0.0000)	1.6857(±0.0001)
with 3.5 M HNO_3	298	0.7594(±0.0001)	1.4041(±0.0028)
	308	0.7522(±0.0001)	1.1872(±0.0008)
	318	0.7448(±0.0001)	1.0148(±0.0003)
0.36 M DHOA equilibrated	288	0.7744(±0.0000)	2.1694(±0.0007)
with 3.5 M HNO_3	298	0.7671(±0.0001)	1.7578(±0.0002)
	308	0.7597(±0.0001)	1.4589(±0.0002)
	318	0.7525(±0.0001)	1.2157(±0.0004)
0.18 M TBP equilibrated	288	0.7750(±0.0000)	1.7506(±0.0019)
with simulated AHWR	298	0.7675(±0.0001)	1.4512(±0.0001)
feed solution	308	0.7612(±0.0001)	1.2513(±0.0000)
	318	0.7602(±0.0001)	1.0701(±0.0001)
0.36 M DHOA equilibrated	288	0.7836(±0.0000)	2.3606(±0.0015)
with simulated AHWR	298	0.7763(±0.0001)	1.8944(±0.0003)
feed solution	308	0.7689(±0.0001)	1.5525(±0.0004)
	318	0.7615(±0.0001)	1.2993(±0.0002)

An attempt was made to correlate the variation of viscosity with temperature using Andrade equation as given below **[194]**:

$$\eta = A \bullet \exp (E/RT) \quad (5.2)$$

where η is the viscosity (mPa·s), A, a system specific constant, E, the activation energy ($kJ \cdot mol^{-1}$) for viscous flow, R, the gas constant ($J \cdot mol^{-1} \cdot K^{-1}$), and T, the absolute temperature (K). On simplification, equation (5.2) may be written as:

$$\ln \eta = \ln A + E / RT \quad (5.3)$$

The values of E for the solvents under different conditions were determined from the slope analysis using Equation 5.3 after plotting ln η vs 1/T. There were marginal changes in the activation energy of the solvents as shown in Table 5.8 suggesting that, the extraction of acid or the metal ions from the simulated AHWR feed solution does not alter significantly the intermolecular interactions of the solvent molecules.

Table 5.8: Activation energy data of solvents from viscosity measurements at different temperature; Diluent: *n*-dodecane

Solvent	**E($kJ \cdot mol^{-1}$)**
0.18 M TBP	12.88(±0.01)
0.36 M DHOA	13.70(±0.01)
0.18 M TBP equilibrated with 3.5M HNO_3	12.88(±0.01)
0.36 M DHOA equilibrated with 3.5M HNO_3	14.47(±0.01)
0.18 M TBP equilibrated with simulated AHWR feed solution	11.70(±0.01)
0.36 M DHOA equilibrated with simulated AHWR feed solution	15.18(±0.01)

5.2.4.2. Interfacial tension measurements

Table 5.9 lists the IFT values of the solvents proposed for AHWR spent fuel reprocessing against different aqueous phases. It is observed that IFT values are between (15 - 20 $mN.m^{-1}$) suggesting the increased adsorption of surface-active extractant molecules at the interface with increase in their mole fractions in the organic phase [**195**]. From the present IFT data, it appears that both the solvents possess favorable interfacial tension to enable proper mixing and separation of the two phases.

Table 5.9: IFT data of the solvents proposed for AHWR spent fuel reprocessing; Diluent: *n*-dodecane

Solvent	**IFT ($mN \cdot m^{-1}$)**
0.18 M TBP versus 3.5M HNO_3	15.59(±0.02)
0.36 M DHOA versus 3.5M HNO_3	19.47(±0.02)
0.18 M TBP versus simulated AHWR feed solution	16.42(±0.07)
0.36 M DHOA versus simulated AHWR feed solution	18.88(±0.04)

5.2.5. Radiolytic degradation studies

To evaluate the applicability of DHOA as a process solvent for the reprocessing of AHWR spent fuel, it was essential to investigate its radiolytic degradation behavior under process conditions. Degradation studies were, therefore, carried out employing 0.18 M TBP and 0.36 M DHOA solutions in *n*-dodecane and in contact with simulated AHWR feed solution. Figures 5.13 & 5.14 show D_U values decreased continuously from 3.2 (without dose) to 2.3 (649 kGy dose) for 0.36 M DHOA/*n*-dodecane; the corresponding values for 0.18 M TBP/*n*-dodecane were 3.0 and 2.1, respectively. Similarly, the D_{Pu}

values decreased continuously from 3.3 (without dose) to 2.0 (530 kGy dose) for 0.36 M DHOA/*n*-dodecane; there was marginal decrease from 1.3 (without dose) to 1.0 (530 kGy dose) for 0.18 M TBP/*n*-dodecane.

Under identical experimental conditions, D_{Th} values decreased from 0.06 (no dose) to 0.025 (530 kGy) for 0.36 M DHOA/*n*-dodecane and the corresponding values for 0.18 M TBP/*n*-dodecane were 0.05 to 0.029. These studies suggested that there was a decrease in the distribution ratio values for U, Pu and Th in both the extractants due to radiolytic degradation. However, 0.36 M DHOA appears superior with respect to selective extraction of U, Pu (higher D values) over Th vis-à-vis 0.18 M TBP from AHWR feed solutions.

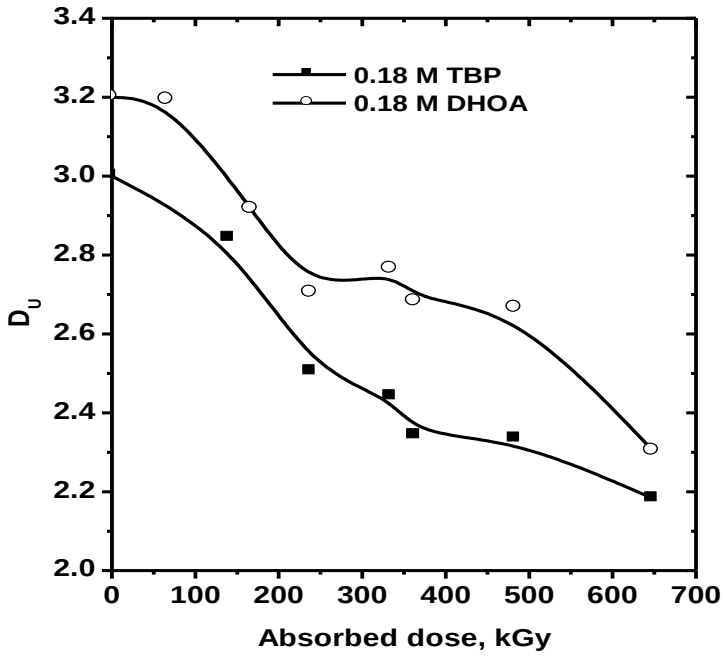

Fig. 5.13. Variation of D_U as a function of absorbed dose; Aqueous phase: Simulated AHWR feed solution; Diluent: *n*-dodecane

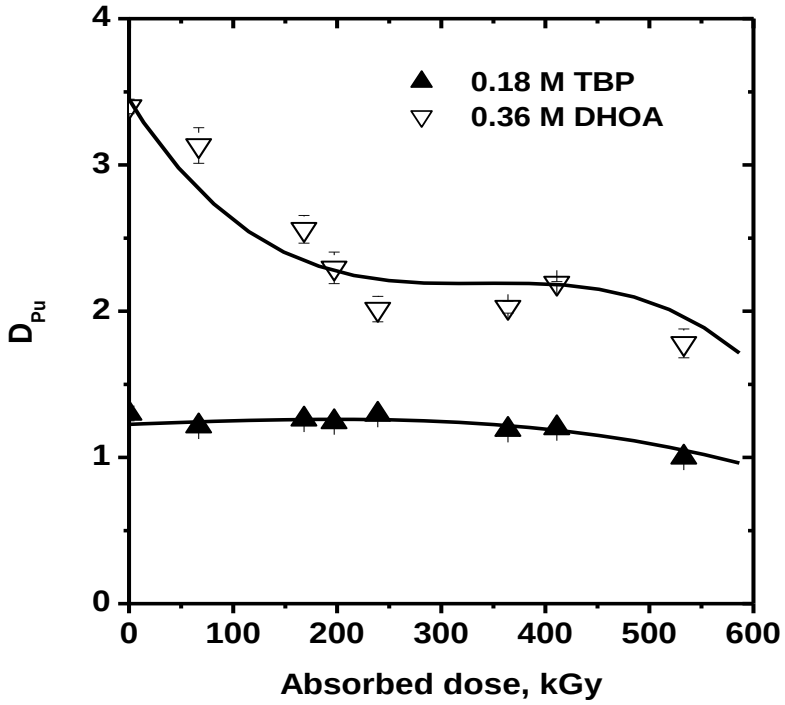

Fig. 5.14. Variation of D_{Pu} as a function of absorbed dose; Aqueous phase: Simulated AHWR feed solution; Diluent: *n*-dodecane

5.3. Third-phase formation Studies

The reprocessing is mainly focused on the recovery of ^{233}U and Pu from the spent fuels leaving bulk of Th (~100 g/L) in the High Level Waste (HLW) solutions. No systematic attempts have been made so far to identify suitable solvents for the recovery of thorium from AHWR-HLW solutions. It is a difficult problem in view of the third-phase formation tendency of different extractants during the extraction of large concentrations of Th(IV) from nitric acid solutions. Third phase formation appears to be a continuous phenomenon. The process of phase splitting is attributed to the formation of exceedingly large aggregates leading to a different and thermodynamically more stable phase devoid of the diluent molecules. Evaluation of two straight chain dialkyl amides such as DHOA,

and DHDA vis-à-vis TBP for the recovery of the thorium from AHWR-HLW solutions has been discussed in this chapter. These dialkyl amides were choosen based on their third-phase formation behavior during the extraction of Th(IV) from nitric acid medium [**90, 196**]. Limiting organic concentraction (LOC (g/L)) values of Th(IV) for 1.1 M solutions of DHOA, DHDA, and TBP in *n*-dodecane as the solvents were 33, 50, and ~35, respectively at 4 M HNO_3. To understand the third-phase formation / aggregation behavior during the Th(IV) extraction DLS studies were done. Measurements of aggregate sizes formed under different experimental conditions were done to explain the third-phase formation behavior of these extractants.

In addition, extraction behavior of $1x10^{-2}$-0.1 M U(VI) from aqueous phases containing 0.86 M (200 g/L) Th(IV) at 4 M HNO_3 in 1.1 M TBP and 1.1 M DHOA solutions in different diluents: *n*-dodecane, 10% 1-octanol + *n*-dodecane, and decahydronaphthalene (decalin) was studied. An empirical correlation was developed for the prediction of metal ion concentrations in the heavy organic phases (HOPs). Spectrophotometric investigations have been carried out to understand the spectral changes during third-phase formation using loaded organic phases under the conditions of work.

5.3.1. Aggregation studies using 1.1 M TBP/*n*-dodecane as solvent

Variation in the size of aggregates with increased Th(IV) loading as a function of nitric acid concentration in the aqueous phase are shown in Figures 5.15 and 5.16. Gradual increase in thorium extraction with increased aqueous phase acidities was observed.

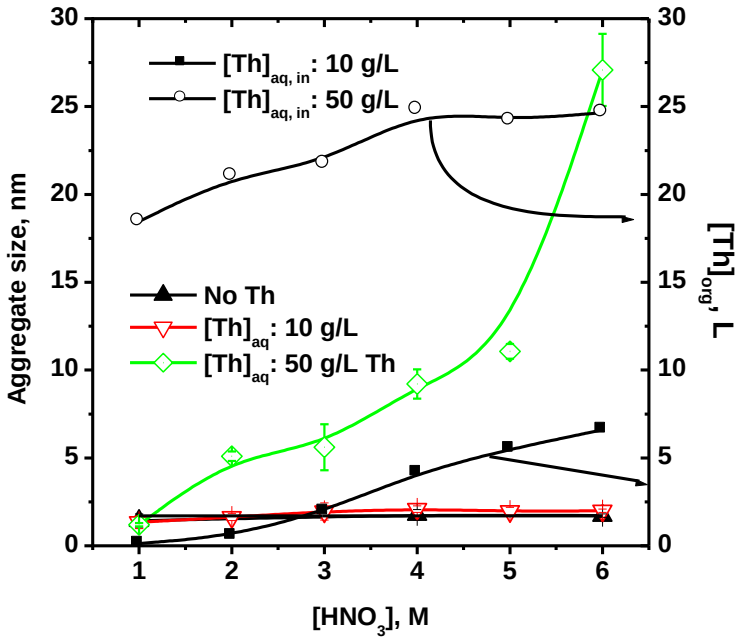

Fig. 5.15. Aggregation behavior of 1.1 M TBP/*n*-dodecane equilibrated with nitric acid solutions without/with Th; T: 298 K

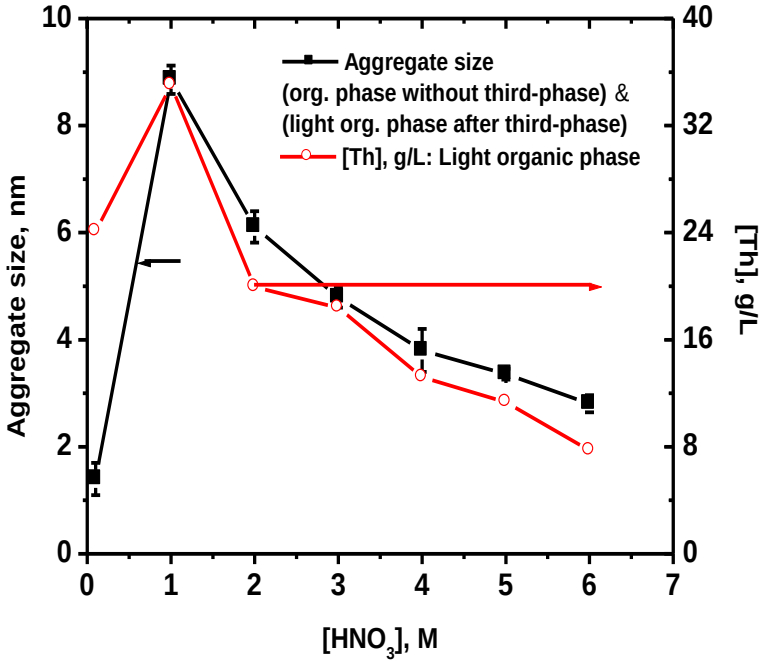

Fig. 5.16. Aggregation behavior of 1.1 M TBP/*n*-dodecane equilibrated with nitric acid solutions containing 100 g/L Th; T: 298 K

Only marginal variation in the aggregate size (1.64(±0.19) nm) was observed in the case of 1.1 M TBP/*n*-dodecane system in the absence of Th in the entire range of acidity (1-6 M HNO_3). By contrast, a significant enhancement in the aggregate sizes was observed with increasing concentration of thorium in the organic phase. The third-phase appeared in 1.1 M TBP/*n*-dodecane system for 100 g/L Th at ≥ 2 M HNO_3. The size of Light Organic Phase (LOP) decreased with increased acidity from 6.11(±0.29) nm (2 M HNO_3) to 2.81(±0.16) nm (6 M HNO_3); correspondingly a decrease in thorium concentration from 20 g/L to 7.7 g/L was observed. The average aggregate size and thorium concentration in the Heavy Organic Phase (HOP) were 12.83(±1.84) nm, and 105.9(±6.7) g/L, respectively.

These observations can be explained in terms of the swelling of the aggregates due to inter-particle attraction with increased loading of the organic phase with thorium prior to the appearance of the third-phase. Increase in the short range attractive forces between the polar cores of the reverse micelles due to dipole - dipole interactions probably expels the diluent molecules from the vicinity of the extracted species under third-phase conditions [82-88]. The diluent rich organic phase (LOP) showed no such strong interactions due to the presence of lower concentrations of thorium and the extractant.

The addition of 5 % (v/v) 1-octanol as modifier in 1.1 M TBP/*n*-dodecane system a remarkable difference in the aggregation behavior as compared to that of the pure solvent showed. There was no third-phase formation during the extraction of Th(IV) even from the aqueous phases containing 100 g/L Th(IV) at 1-5 M HNO_3. Figure 5.17 clearly shows the influence of 5% 1-octanol on the aggregation behavior of extracted species of

Th(IV) in the organic phase. It is worth mentioning that thorium uptake without/with phase modifier varied marginally (±4%) in the entire range of acidity studied.

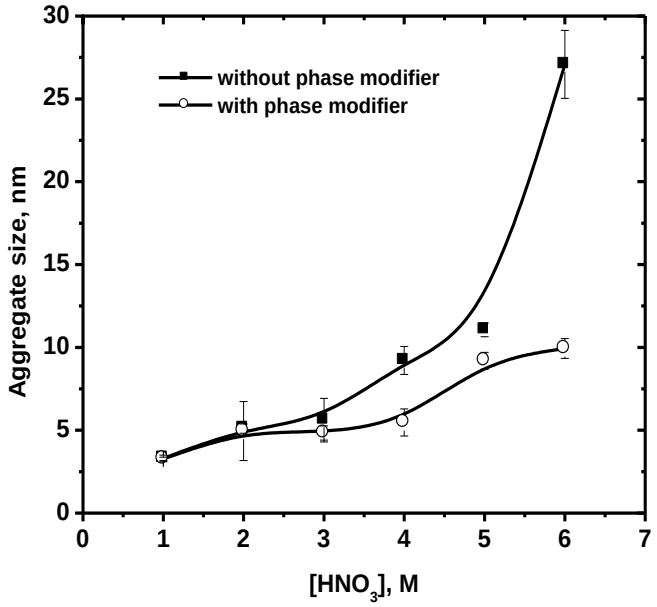

Fig. 5.17. Effect of 1-octanol (5 % v/v) as phase modifier on the aggregation behavior of 1.1 M TBP/*n*-dodecane during the extraction of Th from nitric acid medium; $[Th]_{aq,initial}$: 50 g/L; T: 298 K

The polar nature of 1-octanol weakens the intermicellar interaction and thereby reduces the size of aggregates formed in the organic phase. The absence of third-phase in the presence of 5% 1-octanol suggests effective solubilization of the extracted species. Two opposing physical forces viz. the thermal energy (k_BT) and the intermicellar attraction energy are responsible for solubilization of the extracted species (micelles) in the diluents phase [**92**]. The thermal energy helps in dispersing the micelles in the medium while the attractive forces are responsible for sticking them together. It appears that the addition of 5% 1-octanol in the organic phase prevents the swollen reverse micelles from reaching the level of intermicellar attraction energy required for third-phase

formation. The loaded organic phase will be stable when the two opposing forces are equal otherwise third-phase formation will take place when the attractive forces become stronger.

5.3.2. Aggregation studies using 1.1 M DHOA/*n*-dodecane as solvent

Thorium extraction studies were also performed using 1.1 M DHOA/*n*-dodecane system under identical experimental conditions. The aggregate size increases gradually with aqueous phase acidity and thorium loading in the organic phase. In this case, third-phase formation was appeared for $[Th]_{aq,initial}$: ≥ 100 g/L and at ≥ 5 M HNO_3 (Figure 5.18).

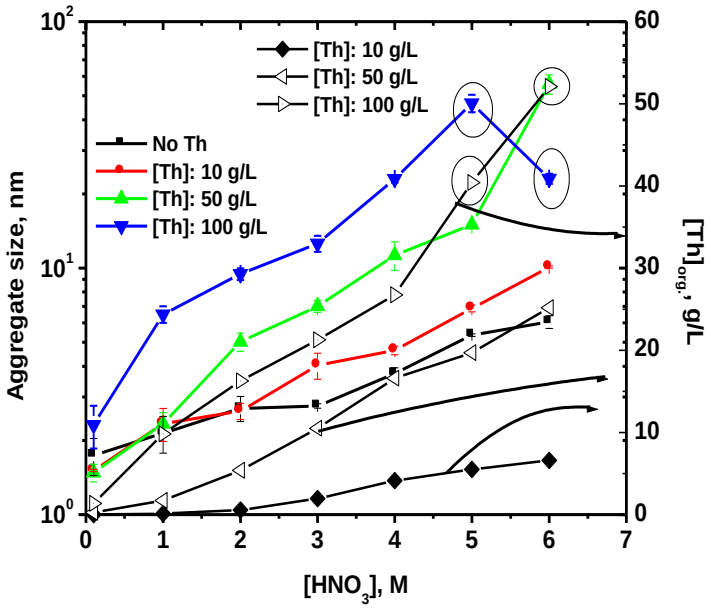

Fig. 5.18. Aggregation behavior of 1.1 M DHOA/*n*-dodecane equilibrated with nitric acid solutions without/with Th; T: 298 K; Points in circle refer to HOP

The diluent molecules dispersed in different portions of the aggregates are expelled from HOP after phase splitting resulting in a decrease in the aggregate size. The volume of the third-phase formed in the case of 1.1 M DHOA/*n*-dodecane was relatively

~2.2 times higher than that of 1.1 M TBP/*n*-dodecane system. This indicates that the swelling tendency is relatively higher in the case of DHOA as compared to that of TBP which may be attributed to its long chain alkyl substituent. These may be hindering the close approach of the micelles and lead to bulky aggregates.

5.3.3. Aggregation studies using 1.1 M DHDA/n-dodecane as solvent

Thorium extraction studies were also performed using 1.1 M DHDA/*n*-dodecane system under identical experimental conditions. It was of interest to compare its aggregation behavior with those of TBP and DHOA as extractants. Figure 5.19 shows the variation of aggregate sizes with thorium loading at different acidities. The aggregate size increased gradually with aqueous phase nitric acid concentration and increased thorium loading in the organic phase (Figure 5.20).

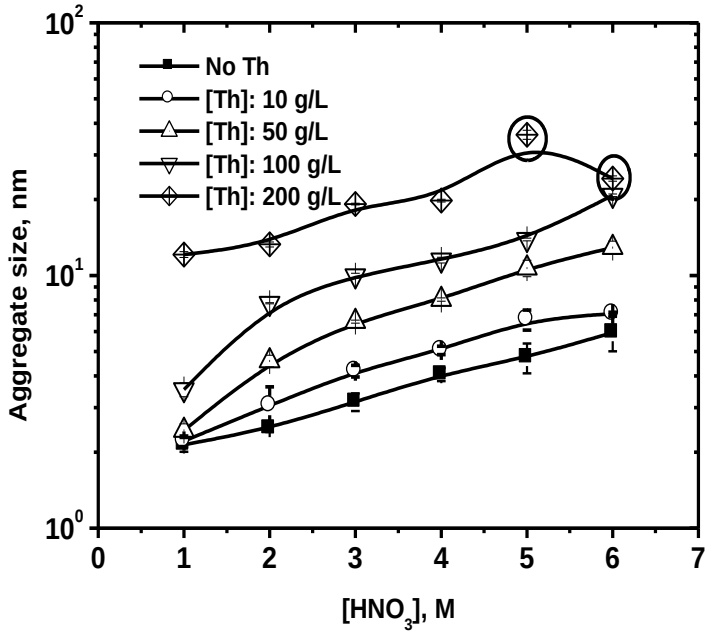

Fig. 5.19. Aggregation behavior of 1.1 M DHDA/*n*-dodecane equilibrated with nitric acid solutions without/with Th; T: 298 K; Points in circle refer to HOP

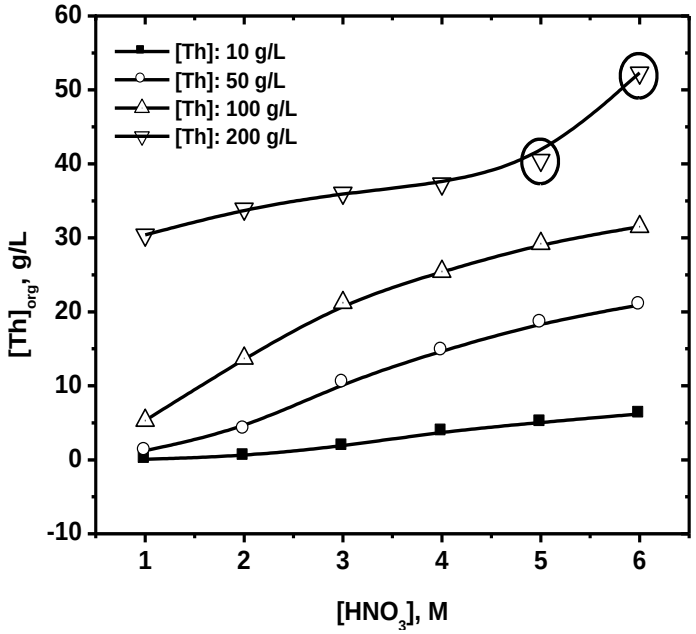

Fig. 5.20. Variation of Th(IV) concentration in the organic phase as a function of nitric acid concentration; Organic phase: 1.1 M DHDA/*n*-dodecane; T: 298 K; Points in circle refer to HOP

No third-phase formation was observed up to 100 g/L Th concentration in the aqueous phase in the entire range of acidity under this study. Third-phase appeared for 200 g/L Th concentration beyond 5 M HNO_3 resulting in a decrease in the aggregate size. These studies, show that long-chain alkyl substituent of DHDA help in solublizing the extracted species as compared to those of DHOA and TBP. Interestingly, both DHOA and TBP have comparable LOC values [**90**]. The presence of longer chain in DHDA alters the aggregation trend between the two extractants viz. DHOA and DHDA.

It was worth comparing the aggregation behavior of these extractants under identical experimental conditions. Therefore, the aggregate sizes were followed as a function of nitric acid concentration (1-6 M HNO_3) and maintaining $[Th]_{aq.,\ initial}$ as 50 g/L. It is clear from Figure 5.21 that the three solvents used in this study display almost

identical aggregation behavior up to 3 M HNO_3 beyond which a marked increase in their sizes is observed for both TBP and DHOA extractants.

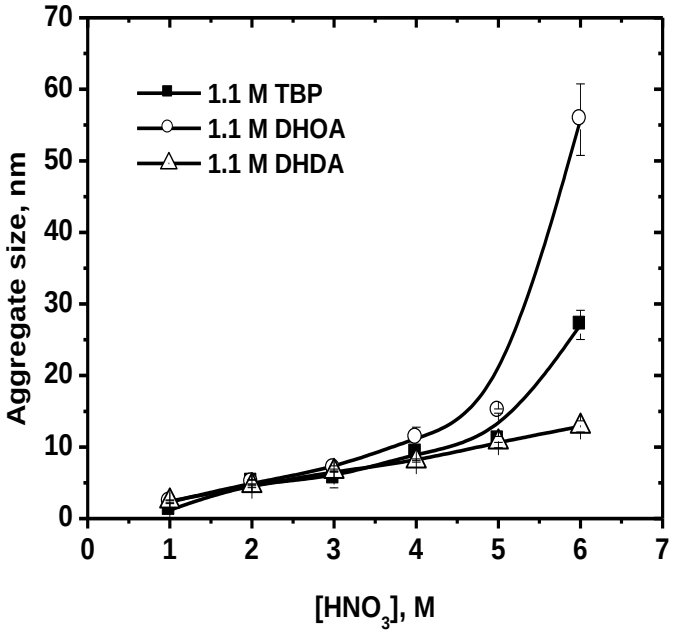

Fig. 5.21. Comparison of aggregation sizes for different extractants equilibrated with nitric acid solutions containing 50 g/L Th; Diluent: *n*-dodecane; T: 298 K

DHDA shows relatively smaller increase in the size of the aggregate with increased loading in the organic phase. These studies also confirm to the previous observations that increased chain length of alkyl substituents suppresses the third-phase formation tendency by forming relatively smaller size aggregates [**197**]. Similar observations are also reported during SANS studies on Th(IV)/TBP/HNO_3 system [**83**]. However, a significant increase in the size of the aggregates with increased Th(IV) loading in the organic phase up to LOC values beyond which third-phase formation takes place. The aggregate sizes in the LOP resulting from phase splitting, were smaller than those observed in the HOP samples.

5.3.4. U and Th extraction studies using *n*-dodecane as diluent

Table 5.10 shows that the organic phase uranium concentration increases with its initial aqueous phase concentration for both the extractants. However, uranium extraction was marginally lower in the case of DHOA as compared to that of TBP.

Table 5.10: Uranium extraction behavior using 1.1 M TBP and 1.1 M DHOA solutions in *n*-dodecane as extractants; Aqueous phase: 0.01-0.1 M U(VI) at 4 M HNO_3; T: 298 K

$[U(VI)]_{aq,in}$, M	1.1 M TBP/ *n*-dodecane		1.1 M DHOA/ *n*-dodecane	
	$[U(VI)]_{org}$, M	$[U(VI)]_{aq}$, M	$[U(VI)]_{org}$, M	$[U(VI)]_{aq}$, M
1×10^{-2}	9.5×10^{-3}	7.8×10^{-4}	8.7×10^{-3}	1.1×10^{-3}
2×10^{-2}	1.9×10^{-2}	1.5×10^{-3}	1.7×10^{-2}	1.8×10^{-3}
4×10^{-2}	3.9×10^{-2}	2.7×10^{-3}	3.0×10^{-2}	4.3×10^{-3}
6×10^{-2}	5.4×10^{-2}	3.1×10^{-3}	5.0×10^{-2}	8.8×10^{-3}
8×10^{-2}	7.6×10^{-2}	6.2×10^{-3}	6.9×10^{-2}	9.4×10^{-3}
10×10^{-2}	9.1×10^{-2}	7.8×10^{-3}	9.0×10^{-2}	1.1×10^{-3}

Table 5.11 shows a gradual decrease in Th(IV) concentration in the third-phase (Heavy Organic Phase, HOP) with increased aqueous U concentration [0.71 M (no U(VI)) to 0.61 M (0.1 M U(VI)) for TBP; 0.28 M (no U(VI)) to 0.22 M (0.1 M U(VI)) for DHOA]. The decrease in thorium concentration in HOP with increased uranium concentration suggested that Th(IV) was being replaced by U(VI). This behavior was attributed to the preference for uranium by forming disolvated species, while thorium is relatively poorly extracted due to the formation of sterically hindered trisolvated species [**114**]. Figure 5.22 clearly shows a decrease in Th(IV) concentration in the third-phase with increased uranium concentration.

Table 5.11: Comparison of thorium concentration during third-phase formation using 1.1 M TBP and 1.1 M DHOA solutions in *n*-dodecane as extractants; aqueous phase(s): (0-0.1 M) U(VI) + 0.86 M Th(IV) + at 4 M HNO_3; T: 298 K

1.1 M TBP/ *n*-dodecane				
Sample No.	$[U(VI)]_{aq,in}$, M	$[Th(IV)]_{aq,eq}$, M	[Th(IV)], M: DRP[#]	[Th(IV)], M: HOP[##]
1	0.00	0.50	$2.7x10^{-2}$	0.71
2	$1x10^{-2}$	0.52	$2.9x10^{-2}$	0.70
3	$2x10^{-2}$	0.53	$2.9x10^{-2}$	0.69
4	$4x10^{-2}$	0.54	$2.8x10^{-2}$	0.68
5	$6x10^{-2}$	0.54	$2.8x10^{-2}$	0.65
6	$8x10^{-2}$	0.55	$2.9x10^{-2}$	0.63
7	$10x10^{-2}$	0.56	$2.9x10^{-2}$	0.61
1.1 M DHOA/ *n*-dodecane				
1	0.00	0.61	$9.0x10^{-3}$	0.28
2	$1x10^{-2}$	0.62	$9.0x10^{-3}$	0.27
3	$2x10^{-2}$	0.62	$1.3x10^{-2}$	0.26
4	$4x10^{-2}$	0.63	$1.1x10^{-2}$	0.25
5	$6x10^{-2}$	0.64	$1.1x10^{-2}$	0.24
6	$8x10^{-2}$	0.64	$1.3x10^{-2}$	0.23
7	$10x10^{-2}$	0.64	$1.1x10^{-2}$	0.22

DRP[#]: Diluent rich – upper phase; HOP[##] : Heavy organic phase

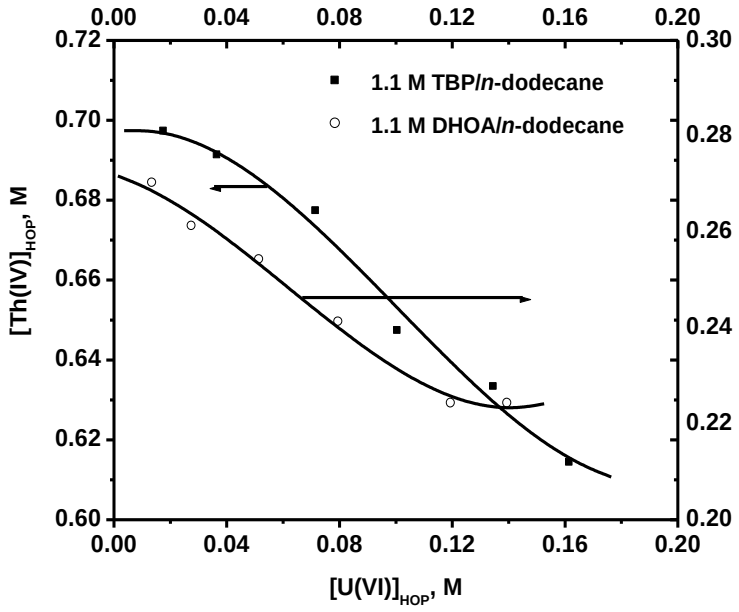

Fig. 5.22. Variation of uranium and thorium concentration in heavy organic phase; aqueous phase: 1×10^{-2} – 0.1 M U(VI) + 200 g/L Th(IV) at 4 M HNO_3; O/A: 1

U concentration in HOP also increased with its initial concentration in the aqueous phase (Table 5.12) [from $1.8x10^{-2}$ M ($1x10^{-2}$ M U(VI)) to 0.162 M (0.1 M U(VI)) for TBP and from $1.4x10^{-2}$ M ($1x10^{-2}$ M U(VI)) to 0.14 M (0.1 M U(VI)) for DHOA]. Nave et al. studied the structural aspects of third-phase formation behavior by the supramolecular organization of TBP/*n*-dodecane using different techniques [**82**]. It was observed that organic phases of TBP in equilibrium with acid solutions were organized as interacting aggregates, which were responsible for the formation of the third-phase.

An empirical correlation (Equation 5.4) was developed using the concentrations of uranium and thorium in the third-phase (HOP) for both the extractants using $1x10^{-2}$-0.1 M U(VI) + 0.86 M Th(IV) in 4 M HNO_3 as the aqueous phase. The empirical correlation was as follows:

$$y = a + b_1x + b_2x^2 + b_3x^3 \quad (5.4)$$

where x and y refer to uranium and thorium concentrations in the third-phase (HOP).

Table 5.12: Comparison of U concentrations during third-phase formation process using 1.1 M TBP and 1.1 M DHOA solutions in *n*-dodecane as extractants; Aqueous phase(s): (0-0.1 M) U(VI) + 0.86 M Th(IV) at 4 M HNO_3; T: 298 K

1.1 M TBP/ *n*-dodecane				
Sample No.	$[U(VI)]_{aq,in}$, M	$[U(VI)]_{aq,eq}$, M	[U(VI)], M: DRP[#]	[U(VI)], M: HOP[##]
1	$1x10^{-2}$	$1.8x10^{-3}$	$4.8x10^{-3}$	$1.8x10^{-2}$
2	$2x10^{-2}$	$4.1x10^{-3}$	$9.3x10^{-3}$	$3.7x10^{-2}$
3	$4x10^{-2}$	$6.4x10^{-3}$	$1.7x10^{-2}$	$7.2x10^{-2}$
4	$6x10^{-2}$	$8.2x10^{-3}$	$2.5x10^{-2}$	0.10
5	$8x10^{-2}$	$1.5x10^{-2}$	$3.4x10^{-2}$	0.14
6	$10x10^{-2}$	$1.7x10^{-2}$	$5.0x10^{-2}$	0.16
1.1 M DHOA/ *n*-dodecane				
1	$1x10^{-2}$	$1.4x10^{-3}$	$1.0x10^{-3}$	$1.4x10^{-2}$
2	$2x10^{-2}$	$3.8x10^{-3}$	$3.0x10^{-3}$	$2.8x10^{-2}$
3	$4x10^{-2}$	$4.6x10^{-3}$	$6.4x10^{-3}$	$5.2x10^{-2}$
4	$6x10^{-2}$	$6.5x10^{-3}$	$1.0x10^{-2}$	$8.0x10^{-2}$
5	$8x10^{-2}$	$1.1x10^{-2}$	$1.1x10^{-2}$	0.12
6	$10x10^{-2}$	$1.8x10^{-2}$	$5.0x10^{-2}$	0.14

DRP[#]: Diluent rich – upper phase; HOP[##]: Heavy organic phase

Table 5.13 lists the correlation coefficients for 1.1 M TBP and 1.1 M DHOA solutions in *n*-dodecane. Equation (5.4) can be used for predicting concentrations of one of the metal ions (Th(IV) or U(VI) in HOP).

Table 5.13: Correlation coefficients obtained by polynomial fit of the experimental data for two extractants

Extractant	**a**	**b_1**	**b_2**	**b_3**	**R^2**
1.1 M TBP/ *n*-dodecane	0.6970	0.1445	-0.8965	28.9264	0.988
1.1 M DHOA/ *n*-dodecane	0.2719	-0.1831	-4.8036	25.8925	0.992

5.3.5. U and Th extraction studies using 10% 1-octanol + n-dodecane and decalin as diluents

Table 5.14 and Table 5.15 show U and Th extraction using 1.1 M TBP and 1.1 M DHOA solutions dissolved in 10% 1-octanol (v/v) + *n*-dodecan and decalin, respectively. No third-phase formation was observed during the extraction of U and Th from the aqueous phases employing these diluents and the values refer to maximum achievable thorium/uranium loading under the conditions of present study.

Table 5.14: Comparison of thorium and uranium extraction behavior using 1.1 M TBP and 1.1 M DHOA solutions in 10% Octanol + *n*-dodecane as extractants; Aqueous phase(s): ($1x10^{-2}$-0.1 M) U(VI) + 0.86 M Th(IV) at 4 M HNO_3; T: 298 K

1.1 M TBP/ 10% Octanol + *n*-dodecane					
Sample No.	$[U(VI)]_{aq,in}$, M	$[U(VI)]_{org,eq}$, M	$[U(VI)]_{aq,eq}$, M	$[Th(IV)]^{**}_{org,eq}$, M	$[Th(IV)]_{aq,eq}$, M
1	$1x10^{-2}$	$8.9x10^{-3}$	$1.5x10^{-3}$	0.22	0.61
2	$2x10^{-2}$	$1.7x10^{-2}$	$3.7x10^{-3}$	0.22	0.62
3	$4x10^{-2}$	$3.7x10^{-2}$	$5.5x10^{-3}$	0.20	0.62
4	$6x10^{-2}$	$5.0x10^{-2}$	$8.1x10^{-3}$	0.20	0.64
5	$8x10^{-2}$	$6.8x10^{-2}$	$1.2x10^{-2}$	0.19	0.64
6	$10x10^{-2}$	$8.4x10^{-2}$	$1.4x10^{-2}$	0.18	0.64
1.1 M DHOA/ 10% Octanol + *n*-dodecane					
1	$1x10^{-2}$	$8.4x10^{-3}$	$1.1x10^{-3}$	0.13	0.67
2	$2x10^{-2}$	$1.7x10^{-2}$	$2.4x10^{-3}$	0.12	0.67
3	$4x10^{-2}$	$3.5x10^{-2}$	$4.8x10^{-3}$	0.10	0.67
4	$6x10^{-2}$	$4.9x10^{-2}$	$7.4x10^{-3}$	0.13	0.68
5	$8x10^{-2}$	$6.5x10^{-2}$	$1.1x10^{-3}$	0.12	0.71
6	$10x10^{-2}$	$8.1x10^{-2}$	$1.2x10^{-2}$	0.11	0.71

***: Maximum achievable concentration in the organic phase*

Table 5.15: Comparison of thorium and uranium extraction behavior using 1.1 M TBP and 1.1 M DHOA solutions in decalin as extractants; Aqueous phase(s): ($1x10^{-2}$-0.1 M) U(VI) + 0.86 M Th(IV) at 4 M HNO_3; T: 298 K

1.1 M TBP/ decalin					
Sample No.	$[U(VI)]_{aq,in}$, M	$[U(VI)]_{org,eq}$, M	$[U(VI)]_{aq,eq}$, M	$[Th(IV)]^{**}_{org,eq}$, M	$[Th(IV)]_{aq,eq}$, M
1	$1x10^{-2}$	$9.5x10^{-3}$	$7.8x10^{-4}$	0.26	0.59
2	$2x10^{-2}$	$1.9x10^{-2}$	$1.5x10^{-3}$	0.25	0.60
3	$4x10^{-2}$	$3.9x10^{-2}$	$2.7x10^{-3}$	0.24	0.61
4	$6x10^{-2}$	$5.4x10^{-2}$	$3.1x10^{-3}$	0.22	0.61
5	$8x10^{-2}$	$7.6x10^{-2}$	$6.2x10^{-3}$	0.21	0.63
6	$10x10^{-2}$	$9.1x10^{-2}$	$7.8x10^{-3}$	0.21	0.64
1.1 M DHOA/decalin					
1	$1x10^{-2}$	$8.7x10^{-3}$	$1.1x10^{-3}$	0.17	0.64
2	$2x10^{-2}$	$1.8x10^{-2}$	$1.8x10^{-3}$	0.16	0.66
3	$4x10^{-2}$	$3.4x10^{-2}$	$4.3x10^{-3}$	0.15	0.70
4	$6x10^{-2}$	$5.1x10^{-2}$	$8.7x10^{-3}$	0.15	0.65
5	$8x10^{-2}$	$6.9x10^{-2}$	$9.4x10^{-3}$	0.14	0.70
6	$10x10^{-2}$	$9.0x10^{-2}$	$1.1x10^{-2}$	0.14	0.70

From the data it can be inferred that higher Th(IV) concentration in the organic phase can be attributed to the relatively polar nature of these diluents. The dielectric constant values (ε) for 10% 1-octanol + *n*-dodecane and decalin were, 2.83 and 2.77,

respectively. U(VI) extraction was better for both the extractants using decalin as diluent as compared to that of 10% 1-octanol + *n*-dodecane. These studies suggested that either 10% 1-octanol + *n*-dodecane, or decalin were better choices as diluents for alleviating the third-phase formation during the reprocessing of spent thorium based fuels and can be particularly useful for the recovery of thorium from high-level waste (HLW) solutions.

5.3.6. Spectrophotometric studies

Spectral changes during third phase formation studies for both TBP and DHOA as extractants dissolved in different diluents were also investigated. Figure 5.23 compares the absorption spectra of uranium loaded in 1.1 M solutions of TBP/DHOA in *n*-dodecane from an aqueous phase containing 0.1 M U(VI) at 4 M HNO_3.

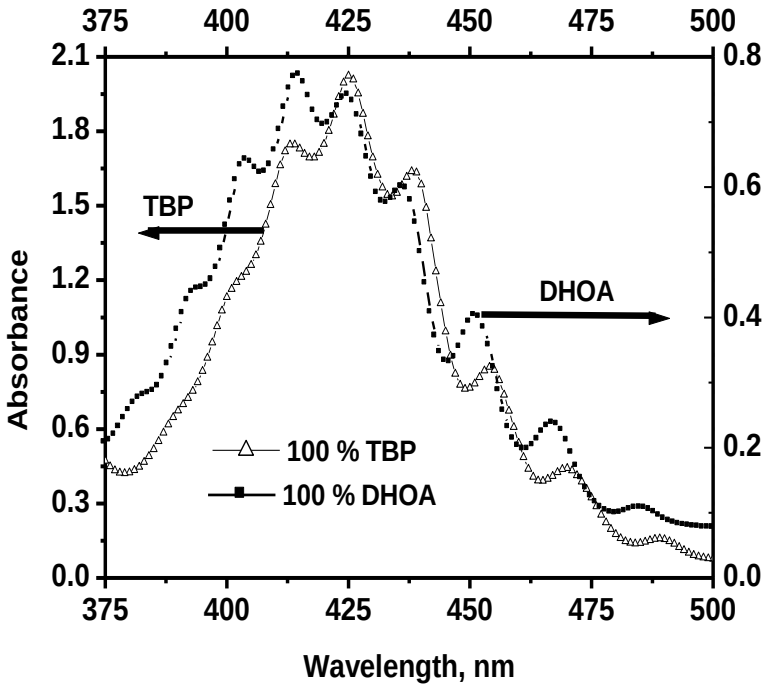

Fig. 5.23. Absorption spectra of uranium loaded in different organic phases; Aqueous phase: 0.1 M U(VI) at 4 M HNO_3

It can be seen from Figure 5.23, that absorption spectra of extracted disolvated uranyl nitrate species for the two extractants are fairly similar except one shoulder observed in the case of DHOA at ~400 nm [**90, 157**]. Both the extractants show bathochromic shifts (~10 nm) in the absorption spectra of extracted U(VI) complex (from ~415 nm (aq) to ~425 nm (extracted). It was observed that absorption spectra of U(VI) ion in the third-phase formed at ~3 M HNO_3 also had close resemblance to that of U(VI)-TBP extract [**89**]. It was observed that from Figures 5.24 and 5.25 the presence of Th(IV) in the third-phase (HOP) does not influence significantly the U(VI) absorption spectra for both the extractants. High and low absorbance values in heavy organic phases (HOPs) and diluent rich phases (DRPs) were attributed to U(VI) concentration in the respective phases (Tables 5.8-5.10).

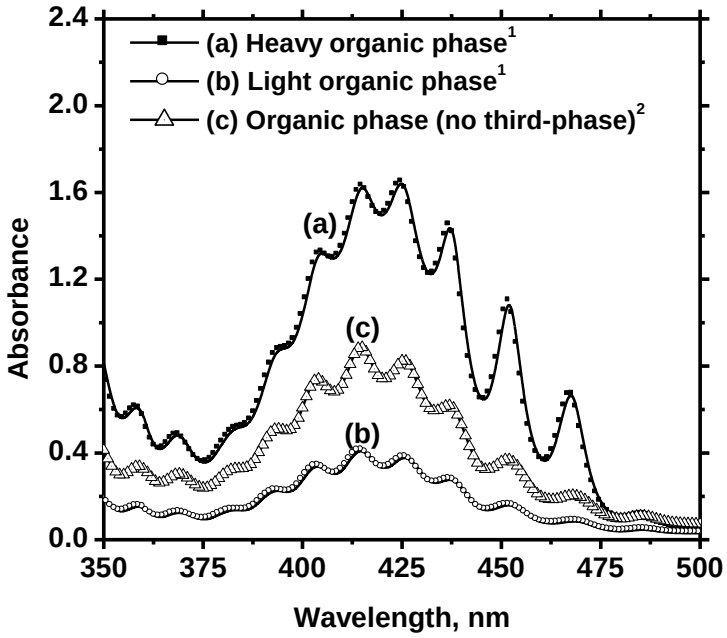

Fig. 5.24. Absorption spectra of uranium loaded in different organic phases; [extractant]: 1.1 M TBP/*n*-dodecane; [1]Aqueous phase: 0.1 M U(VI) + 0.86 M Th (IV) at 4 M HNO_3; [2]Aqueous phase: 0.1 M U(VI) at 4 M HNO_3

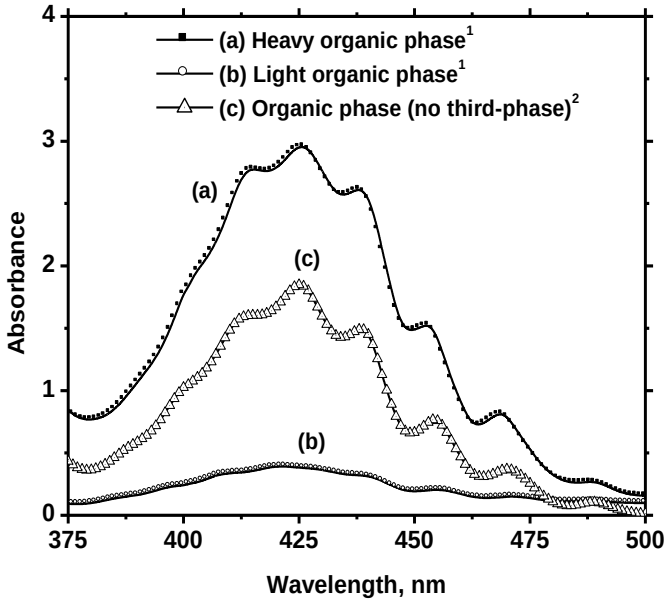

Fig. 5.25. Absorption spectra of uranium loaded in different organic phases; [extractant]: 1.1 M DHOA/*n*-dodecane; [1]Aqueous phase: 0.1 M U(VI) + 0.86 M Th (IV) at 4 M HNO_3; [2]Aqueous phase: 0.1 M U(VI) at 4 M HNO_3

Third-phase formation phenomenon in different extractants has been attributed to interaction of hard-sphere particles (reverse micelles) formed during the extraction of metal ions. It appears that the presence of diluents like 10% octanol + *n*-dodecane and decalin do not allow the interaction of the reverse micelles of the extracted metal ions avoiding the third-phase formation. Figures 5.26 and 5.27 show that the absorption spectra of U(VI) extracted in organic phases using 10 % 1-octanol + *n*-dodecane for both the extractants were similar to those obtained in *n*-dodecane as diluent.

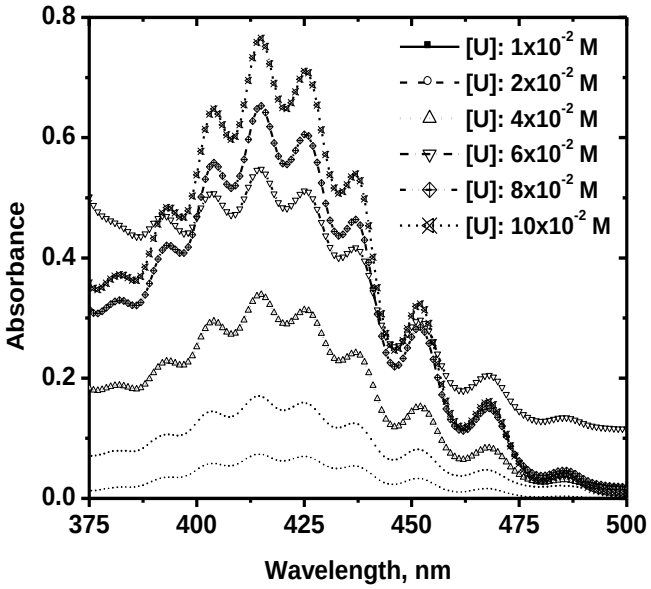

Fig. 5.26. Absorption spectra of uranium loaded in 1.1 M TBP solution in 10% octanol + *n*-dodecane; aqueous phase: 1×10^{-2} – 0.1 M U(VI) + 0.86 M Th (IV) at 4 M HNO_3

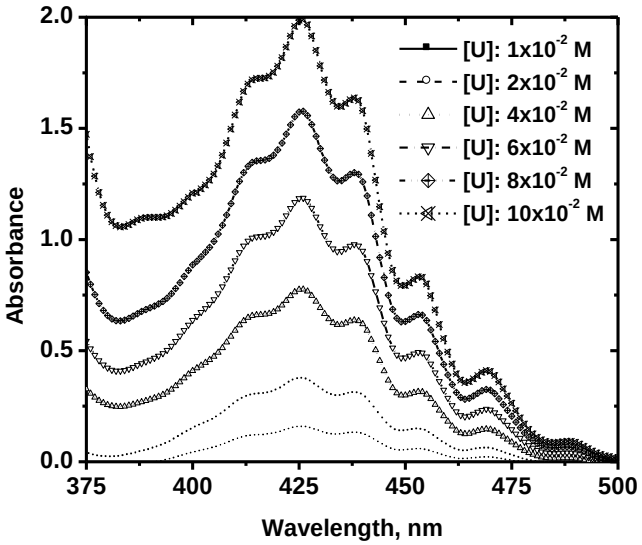

Fig. 5.27. Absorption spectra of uranium loaded in 1.1 M DHOA solution in 10% octanol + *n*-dodecane; aqueous phase: 1×10^{-2} – 0.1 M U(VI) + 0.86 M Th (IV) at 4 M HNO_3

U(VI) absorption spectra for extracted species of U(VI) cations for both the extractants in decalin medium were completely different from those obtained in *n*-

dodecane or in 10% octanol + *n*-dodecane, and only shoulders at 425 nm for different concentrations of U(VI) in the aqueous phase could be used to demonstrate its extraction (Figures 5.28 & 5.29).

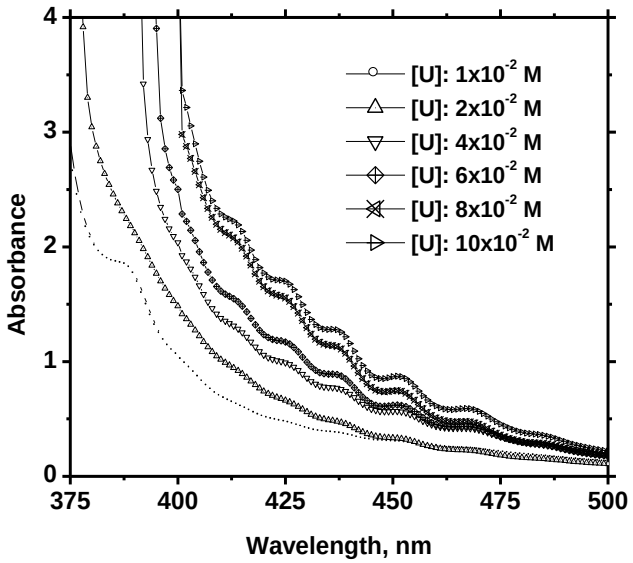

Fig. 5.28. Absorption spectra of uranium loaded in 1.1 M TBP solution in decalin; aqueous phase: 1×10^{-2} – 0.1 M U(VI) + 0.86 M Th (IV) at 4 M HNO_3

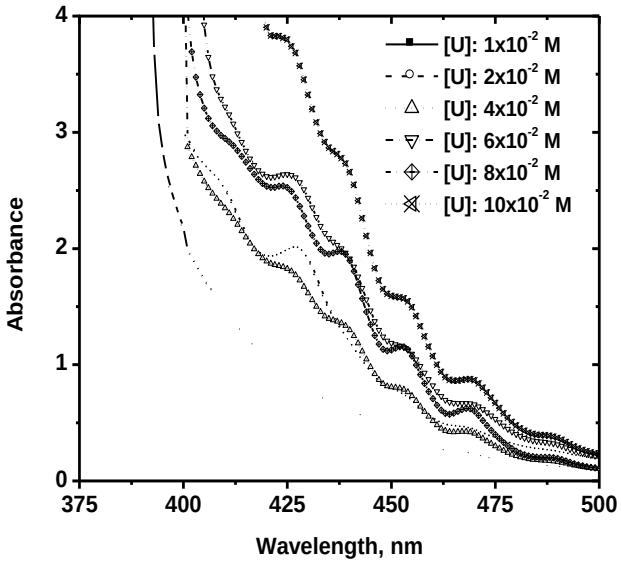

Fig. 5.29. Absorption spectra of uranium loaded in 1.1 M DHOA solution in decalin; aqueous phase: 1×10^{-2} – 0.1 M U(VI) + 0.86 M Th (IV) at 4 M HNO_3

CHAPTER 6: THERMAL DEGRADATION STUDIES OF *N,N*-DIHEXYLOCTANAMIDE / *n*-DODECANE SOLVENT

6.1. Introduction

Solvent extraction operations in nuclear industry are carried out at ambient conditions without applying any heat treatment and TBP has performed safely for decades. However, 'runaway reactions' of nitric acid and industrial solvent mixtures (like TBP/*n*-dodecane) are potentially damaging in nature. TBP reacts with nitric acid at elevated temperatures and forms a complex mixture known as "Red Oil" [**198**]. Thermal 'runaway' reaction occurs if reactants are heated to temperatures where the heat of reaction exceeds the heat loss from the system. There have been several instances of explosion with TBP/HNO_3 system in industrial processes [**199**]. One of the major occurrences was at TOMSK-7 facility in Russia at which runaway reaction of a solution of up to 500 liters of TBP saturated with strong nitric acid resulted in explosion and failure of the storage vessel and subsequently blowing out a wall of the reprocessing plant building. The damage to the building was possibility due to result of the deflagration of flammable gases like butene and CO released from the initiation reaction before the explosion [**200**].

6.2. Red oil formation: process equipments

Red oil formation takes place when nitric acid is heated in the presence of TBP. Source of heat can be external or it may be due to self heating as in TOMSK-7 event where heat was generated by reaction due to addition of highly concentrated nitric acid (14.2 M) to a solution of uranyl nitrate containing degraded organic products. Nitration of diluents and formation of butyl nitrate and several other exothermic reactions increased temperature of

the vessel. Inadequate venting of vessel contributed to pressure buildup and finally vessel exploded after a few hours of acid inlet [**201**].

Broadly, there are three types of process equipment in a reprocessing plant where conditions for red oil formation prevail. These are evaporators, acid concentrators, and denitrators [**202**].

6.2.1. Evaporators

These are used for concentration of high level aqueous product from solvent extraction processes and for the recovery of nitric acid.

6.2.2. Acid recovery units

Nitric acid evaporated from the evaporator is very dilute and contain radioactivity from uranium and plutonium purification steps followed in solvent extraction systems. Decontaminated nitric acid is separated in the acid concentrator which works according to the principles of distillation. The basic criteria for red oil production are met if inadvertent amounts of TBP are present in nitric acid.

6.2.3. Denitrators

Denitrators are devices that are used for heating concentrated solutions of uranium nitrate to the point of decomposition for the production of uranium oxide (UO_3). Since temperature of calcinations is greater than 300^{o}C, if traces of TBP are present in the solution, red oil may be formed. This event has been attributed to cause a red oil event at Savannah River Plant [**203**].

6.3. Conditions for red oil formation

The necessary conditions for the occurrences of runaway red oil reaction are:

1. Presence of TBP in organic phase.
2. Temperature of solution to be greater than 130 °C.
3. Insufficient venting area.
4. Presence of diluents.
5. Presence of metal ions in the aqueous phase.
6. Nitric acid concentration greater than 10 M.

6.4. Controls for the red oil phenomenon

Red oil formation, in general can be controlled by temperature, pressure, mass and concentration **[204]**. These controls should be used together for enhanced safety and prevention of a red oil explosion.

6.4.1. Control of temperature

Maintaining a temperature of less than 130^{o}C is generally accepted as a control for preventing red oil explosions. Red oil runaway reaction has not been reported at a temperature less than 130°C [**205**]. Good quality temperature sensors along with secondary cooling method should be adopted for temperature control. Sufficient venting provides a passive method for cooling by evaporative heat transfer and also prevents the red oil reaction from becoming autocatalytic.

6.4.2. Control of pressure

Sufficient venting also prevents pressure build-up and destruction of the process vessel. It also provides the means for evaporative cooling and red oil from reaching the initiation temperature. Pressure control only prevents explosion, it does not prevent the detonation of released gases. Other controls should also be employed along with pressure control to prevent the red oil reaction.

6.4.3. Control of mass

Mass control factors like diluents wash remove organic extractant capable of producing red oil. TBP is slightly soluble in water and nitric acid and its presence leads to red oil formation at elevated temperatures. Presence of TBP in aqueous phase by a certain amount is one of the reasons for red oil reaction. Degradation products of TBP also have greater aqueous phase solubility and their presence also can also lead to red oil formation [**206**]. So limiting the total amount of TBP and its degradation products in process vessels prevents red oil formation.

6.4.4. Control of concentration

Concentration control is utilized to keep the concentration of nitric acid below 10M. Keeping nitric acid concentration below 10 Mwill prevent a red oil runaway reaction. Table 6.1 lists some of the published information on red-oil events in industrial nuclear plants.

Table 6.1: Red-oil events in industrial nuclear plants

Date	Plant	Part of plant affected
12 Jan 1953	Defense Nuclear Facilities Complex, Hanford, USA	Evaporator destroyed.
12 Feb 1975	Savannah River Plant, USA	Denitrator was destroyed in red oil event and building damaged
11 March 1985	Savannah River Plant, USA	Fire in solvent incinerator, extensive damage to building.
06 April 1993	TOMSK-7 Reprocessing plant, Russia	Explosion without external heating in the tank
17 Nov 2002	NFC, Hyderabad, India	Evaporator

N,*N*-dialkyl amides have been evaluated extensively as alternative extractants to TBP in our laboratory and elsewhere [**207, 114**]. *N*,*N*-dihexyloctanamide (DHOA) has been particularly found to be a promising candidate among a number of extractants studied. To qualify DHOA as an extractant as better or comparable to TBP, pressurization studies were carried out in the presence of nitric acid under adiabatic conditions and closed vent conditions. In this chapter, experimental observations on these studies are presented and discussed.

6.5. Results and discussion

The experiments conducted with Advanced Reactive System Screening Tool (ARSST) mainly aimed at estimation of total pressure generated by decomposition of nitric acid containing DHOA solutions. To study of the role of concentration of nitric acid on

decomposition of DHOA, organic parts of equilibrated samples were tested for their pressurization effects.

Figures 6.1 (a) & (b) show that DHOA, generates ~200 psi/g pressure at 523 K within 110 minutes in 350 mL reaction vessel of ARSST. This is approximately double of TBP [**106**], which generates ~100 psi/g pressure under identical conditions. Temperature of the system was increased at 2 ^{o}C per minute. Fig. 6.1 (b) also shows the total time required by the system to attain maximum pressure from the start of experiment. Pressurization is on the higher side which suggests that DHOA being an amide based extractant, is more prone to thermal degradation as compared to TBP and generates volatile products.

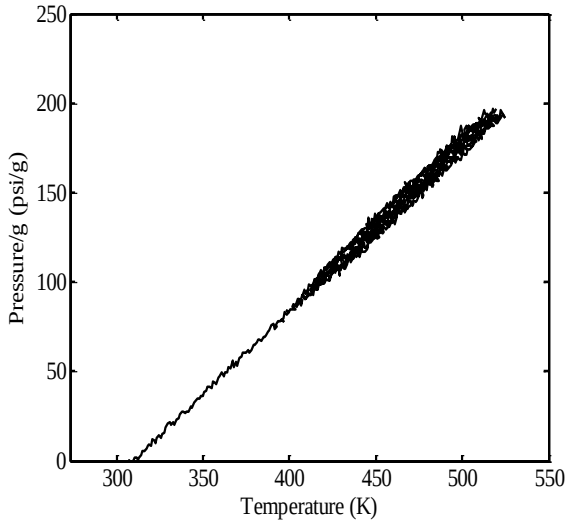

Fig. 6.1 (a)

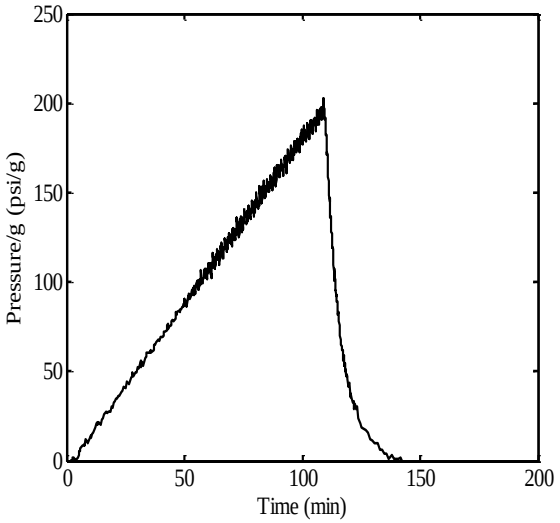

Fig. 6.1 (b)

Fig. 6.1 (a) & (b). Pressurization of DHOA with temperature and time; Reactor vessel capacity: 350 mL

Figures 6.2 (a) & (b), and 6.3 (a) & (b) show the pressurization profiles of 0.36 M DHOA and 1.1 M DHOA solutions in *n*-dodecane as function of temperature and time. Dodecane is a long chain hydrocarbon and its thermal degradation produces several alkanes & alkenes ranging from C_5 to C_{10} which are volatile in nature [**208-210**]. The degradation products may react with oxygen present in air to form volatile oxidation products. Therefore, 0.36 M and 1.1 M DHOA solutions in *n*-dodecane exhibit more pressurization in similar conditions with respect to pure DHOA as shown in Table 6.2. 0.36 M DHOA in *n*-dodecane generates ~230 psi/g and 1.1M DHOA in *n*-dodecane generated ~210 psi/g in 350 mL ARSST reactor. Higher pressurization for 0.36 M DHOA in *n*-dodecane may be due to higher dodecane fraction present in the solution.

Table 6.2: Pressurization/g for DHOA and DHOA/*n*-dodecane samples at 523 K in ARSST

Sample	**Pressure/g (psi/g)**
DHOA	195(±10)
1.1 M DHOA in *n*-dodecane	210(±10)
0.36 M DHOA in *n*-dodecane	230(±10)

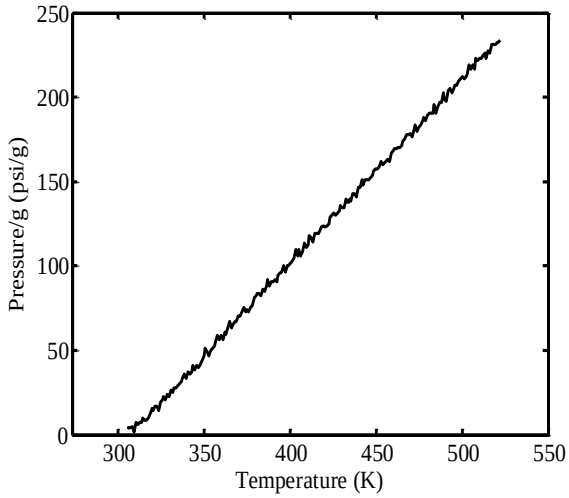

Fig. 6.2 (a)

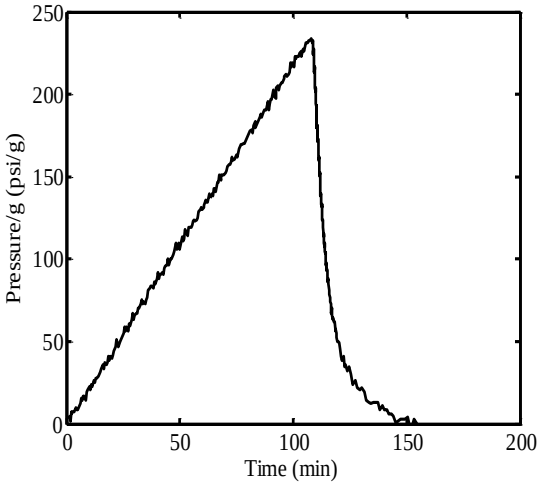

Fig. 6.2 (b)

Fig. 6.2 (a) & (b). Pressurization of 0.36 M DHOA/*n*-dodecane with temperature and time; Reactor vessel capacity: 350 mL

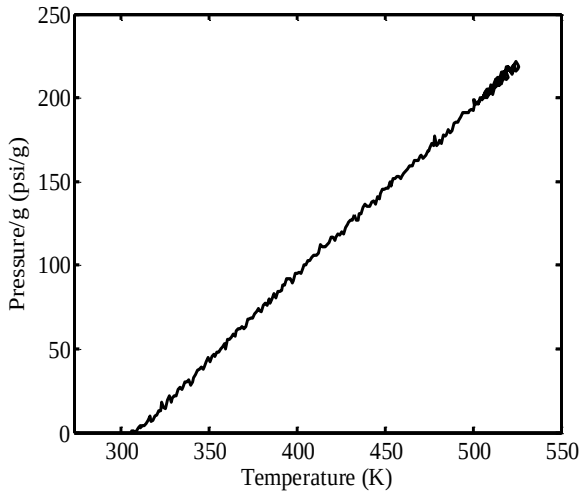

Fig. 6.3 (a)

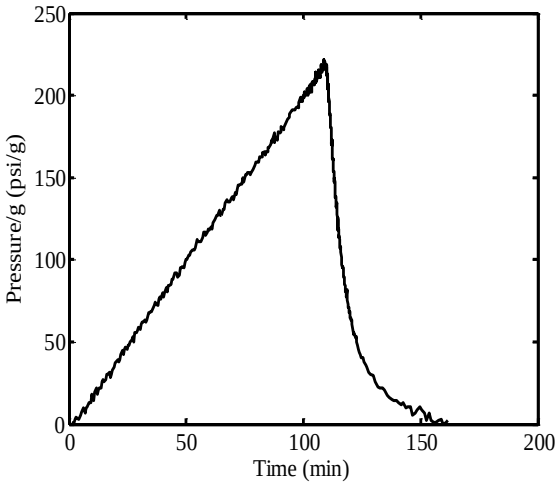

Fig. 6.3 (b)

Fig. 6.3 (a) & (b). Pressurization of 1.1 M DHOA/*n*-dodecane with temperature and time; Reactor vessel capacity: 350 mL

To understand the effect of nitric acid solution on thermal degradation (red oil formation behavior) 0.36 M and 1.1 M DHOA solutions in *n*- dodecane were equilibrated with nitric acid solutions (0.01-6 M HNO_3). The pressurization behavior was followed as a function of temperature and time for both organic and aqueous phases. Figures 6.4 (a) to 6.12 (b) show the pressure building profile for different samples at varying acidity. As dodecane is practically insoluble in nitric acid or water, it is expected that DHOA gets marginally transferred to aqueous phase. Generally, pressurization to a tune of ~200 psi/g was observed at 523 K in case of all the aqueous samples. This indicates that dissolved DHOA has practically very little influence on pressurization and observed pressurization is due to thermal decomposition of nitric acid solution only (Tables 6.3). As sample taken was in very less quantity (~50-100 mg), the nitric acid (NO_2) component was very less, it had very little effect on overall pressurization. The total pressurization observed for all samples were basically due to evaporation of water only.

Table 6.3: Pressurization of aqueous part of 0.36 M and 1.1 M DHOA solution in *n*-dodecane equilibrated with different concentrations of nitric acid at 523 K in ARSST

Acidity	**Pressure/g (psi/g)**	
	0.36 M DHOA	**1.1 M DHOA**
0.01M HNO_3	140(±10)	160(±10)
0.5M HNO_3	170(±10)	160(±10)
3M HNO_3	-	170(±10)
4M HNO_3	170(±10)	170(±10)
6M HNO_3	170(±10)	170(±10)

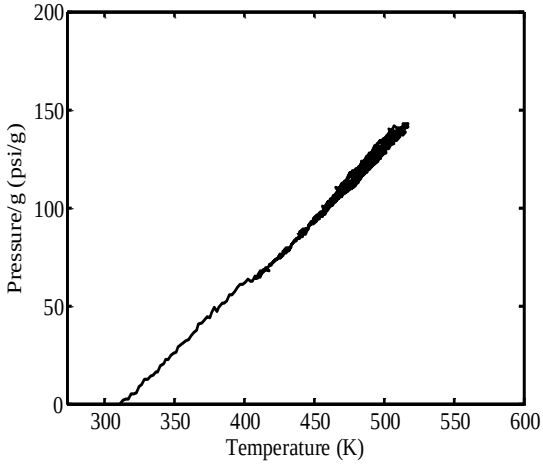

Fig. 6.4 (a)

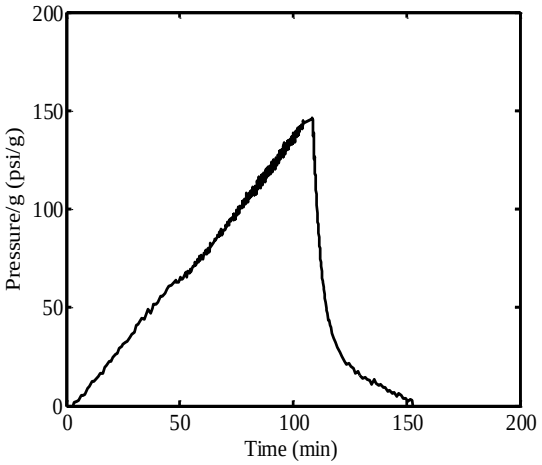

Fig. 6.4 (b)

Fig. 6.4 (a) & (b). Variation of pressurization with temperature and time for aqueous part of 0.36 M DHOA/*n*-dodecane equilibrated with 0.01 M HNO_3; Reactor vessel capacity: 350 mL

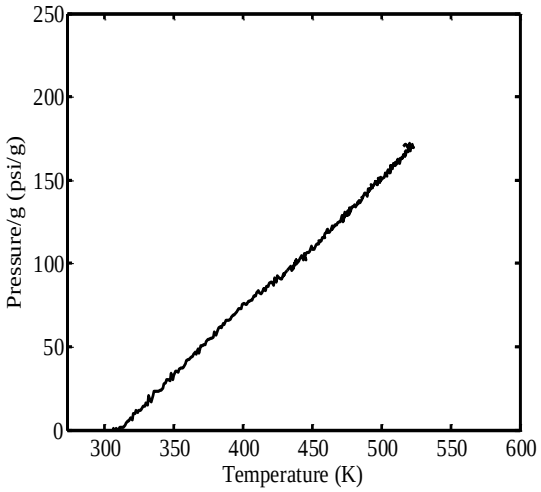

Fig. 6.5 (a)

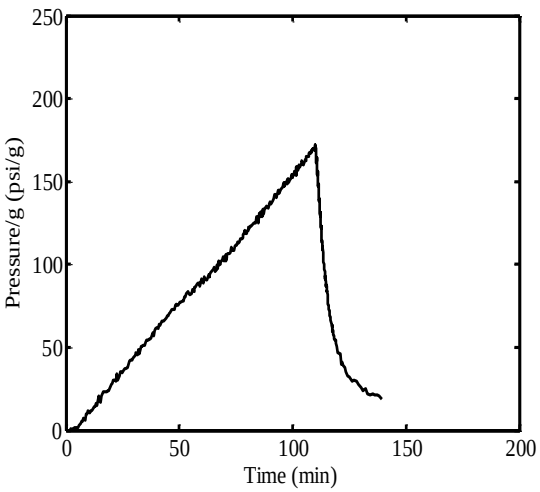

Fig. 6.5 (b)

Fig. 6.5 (a) & (b). Variation of pressurization with temperature and time for aqueous part of 0.36 M DHOA/*n*-dodecane equilibrated with 0.5 M HNO_3; Reactor vessel capacity: 350 mL

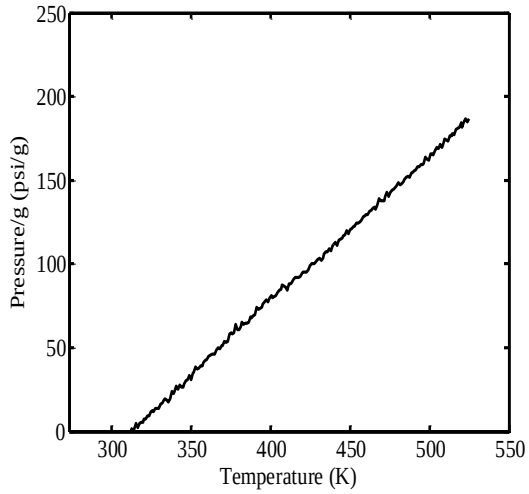

Fig. 6.6 (a)

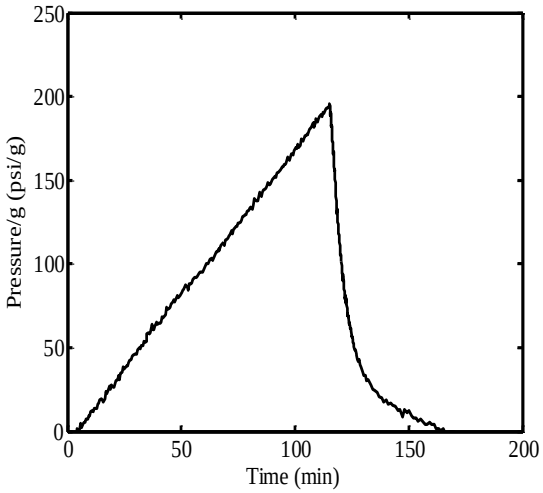

Fig. 6.6 (b)

Fig. 6.6 (a) & (b). Variation of pressurization with temperature and time for aqueous part of 0.36 M DHOA/*n*-dodecane equilibrated with 4 M HNO_3; Reactor vessel capacity: 350 mL

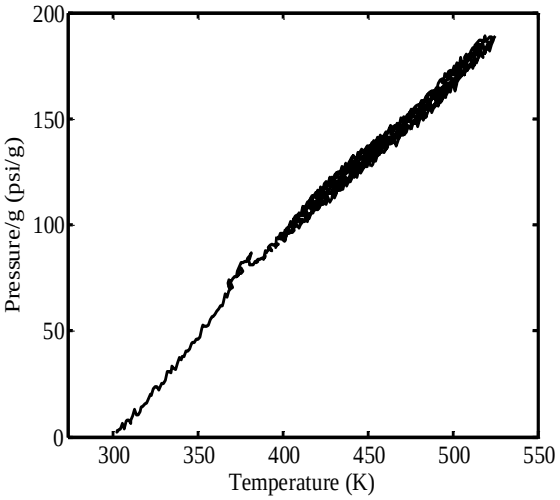

Fig. 6.7 (a)

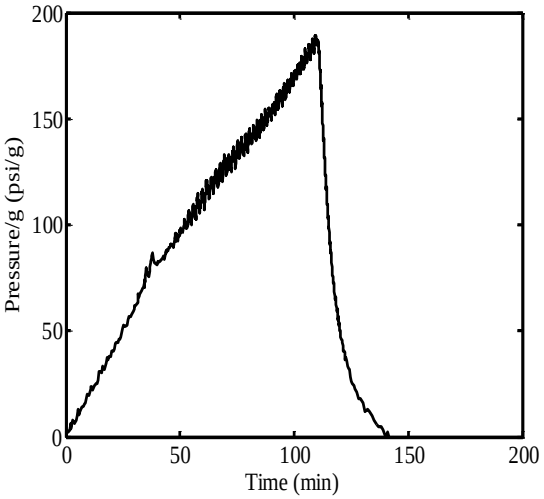

Fig. 6.7 (b)

Fig. 6.7 (a) & (b). Variation of pressurization with temperature and time for aqueous part of 0.36 M DHOA/*n*-dodecane equilibrated with 6 M HNO_3; Reactor vessel capacity: 350 mL

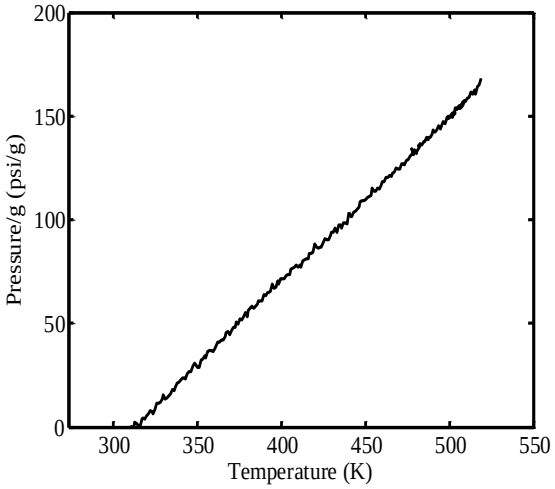

Fig. 6.8 (a)

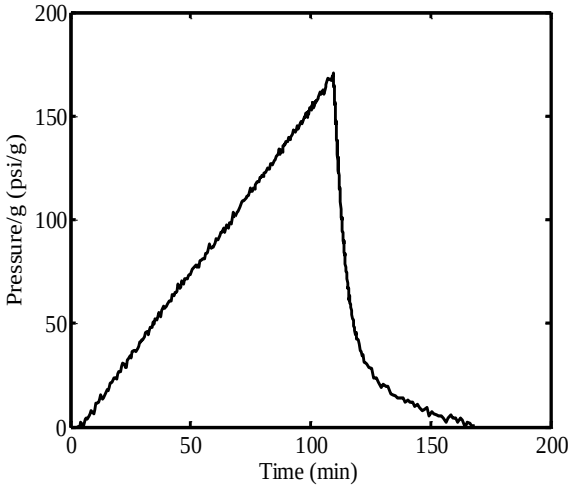

Fig. 6.8 (b)

Fig. 6.8 (a) & (b). Variation of pressurization with temperature and time for aqueous part of 1.1 M DHOA/*n*-dodecane equilibrated with 0.01 M HNO_3; Reactor vessel capacity: 350 mL

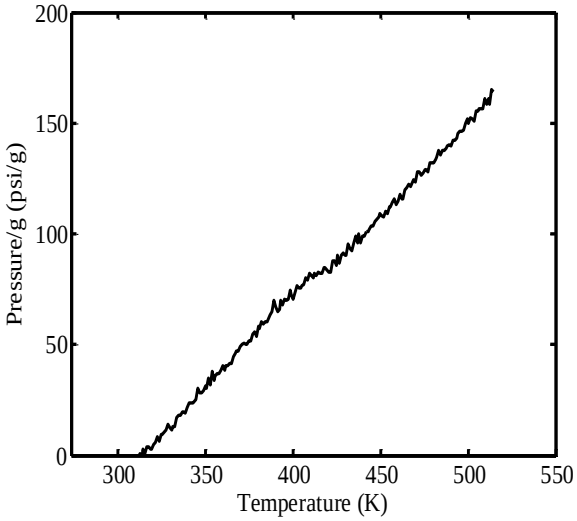

Fig. 6.9 (a)

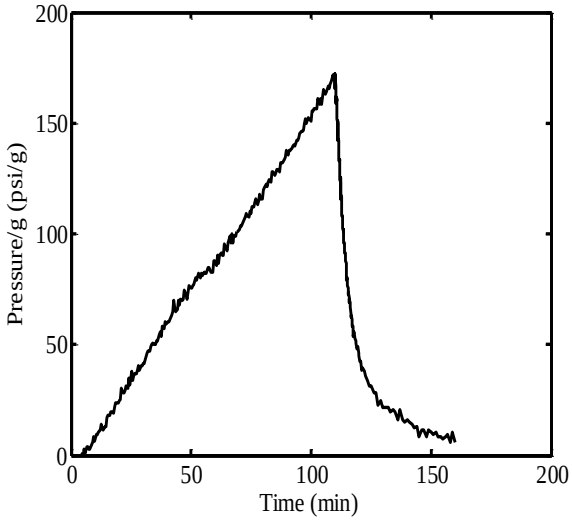

Fig. 6.9 (b)

Fig. 6.9 (a) & (b). Variation of pressurization with temperature and time for aqueous part of 1.1 M DHOA/*n*-dodecane equilibrated with 0.5 M HNO_3; Reactor vessel capacity: 350 mL

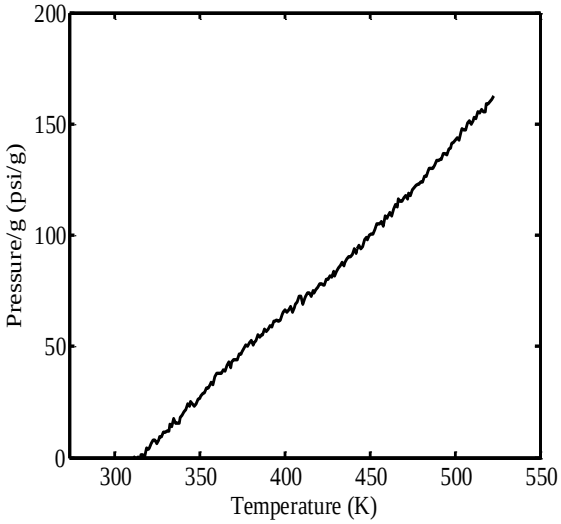

Fig. 6.10 (a)

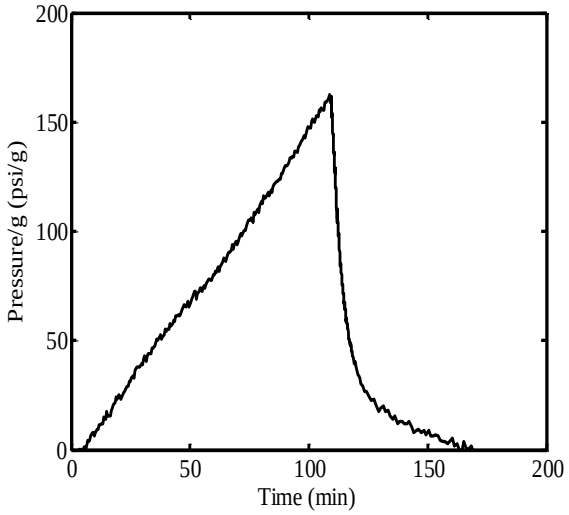

Fig. 6.10 (b)

Fig. 6.10 (a) & (b). Variation of pressurization with temperature and time for aqueous part of 1.1 M DHOA/*n*-dodecane equilibrated with 3 M HNO_3; Reactor vessel capacity: 350 mL

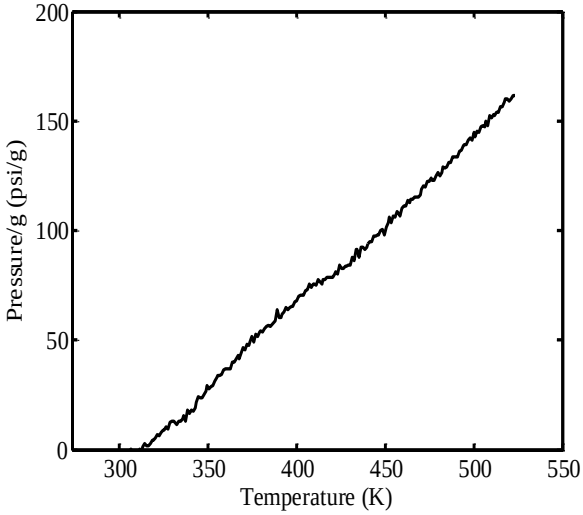

Fig. 6.11 (a)

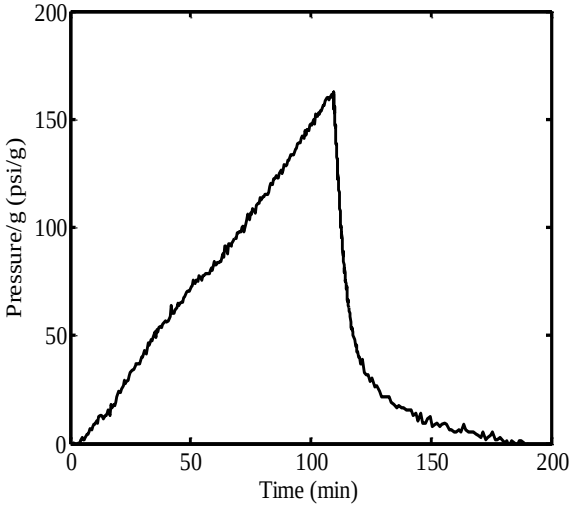

Fig. 6.11 (b)

Fig. 6.11 (a) & (b). Variation of pressurization with temperature and time for aqueous part of 1.1 M DHOA/*n*-dodecane equilibrated with 4 M HNO_3; Reactor vessel capacity: 350 mL

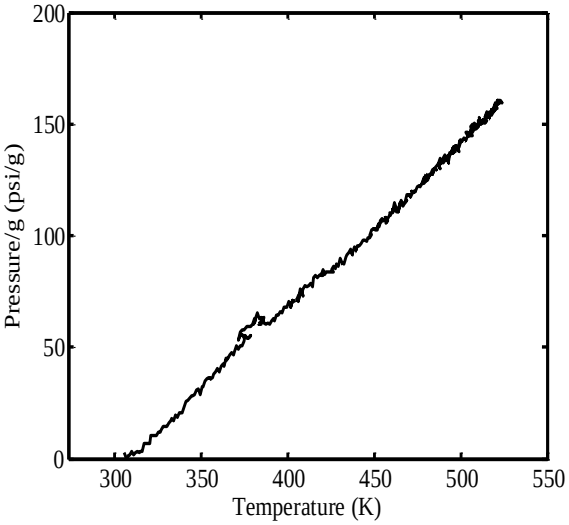

Fig. 6.12 (a)

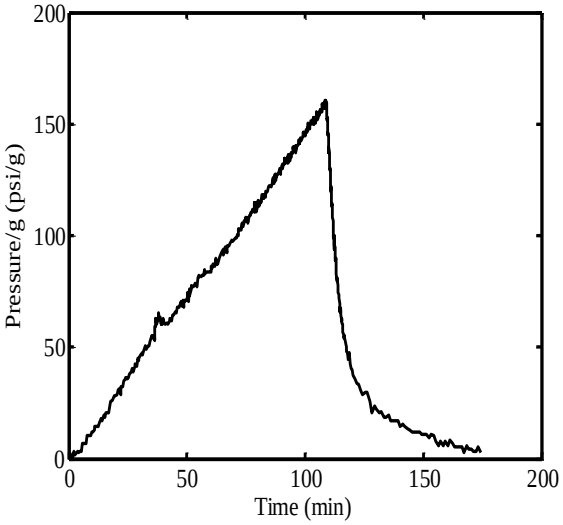

Fig. 6.12 (b)

Fig. 6.12 (a) & (b). Variation of pressurization with temperature and time for aqueous part of 1.1 M DHOA/*n*-dodecane equilibrated with 6 M HNO_3; Reactor vessel capacity: 350 mL

Similarly, Figures 6.13 (a) to 6.22 (b) show pressure curve for solutions containing dissolved nitric acid in 0.36 M and 1.1 M DHOA with respect to temperature and time. At 523 K, the pressure valves were observed to be 202(±18) psi/g for 0.36 M DHOA and 212(±20) for 1.1 M DHOA solution in *n*-dodecane (Table 6.4) which were close to the corresponding values of the fresh solvents. This observation suggests that chemical reaction, if any, taking place between aqueous and organic components at higher temperature results insignificant change in pressure.

Table 6.4: Pressurization behavior of organic phases obtained after contacting with nitric acid solution at 523 K in ARSST

Acidity	**Pressure/g (psi/g)**	
	0.36 M DHOA	**1.1 M DHOA**
0.01 M HNO_3	200(±10)	190(±10)
0.5 M HNO_3	200(±10)	200(±10)
3 M HNO_3	220(±10)	210(±10)
4M HNO_3	190(±10)	220(±10)
6 M HNO_3	180(±10)	220(±10)

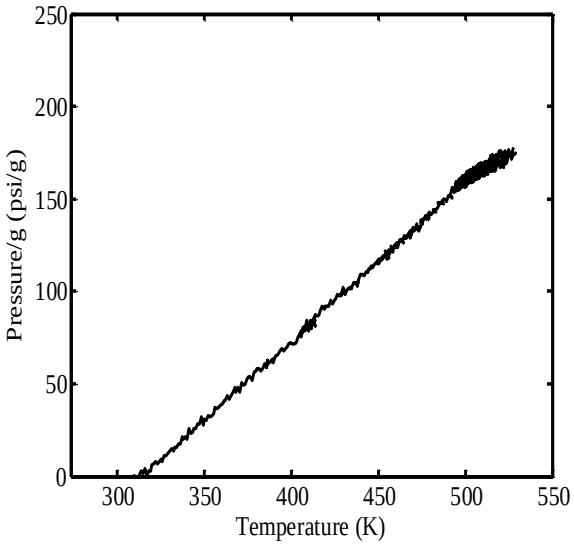

Fig. 6.13 (a)

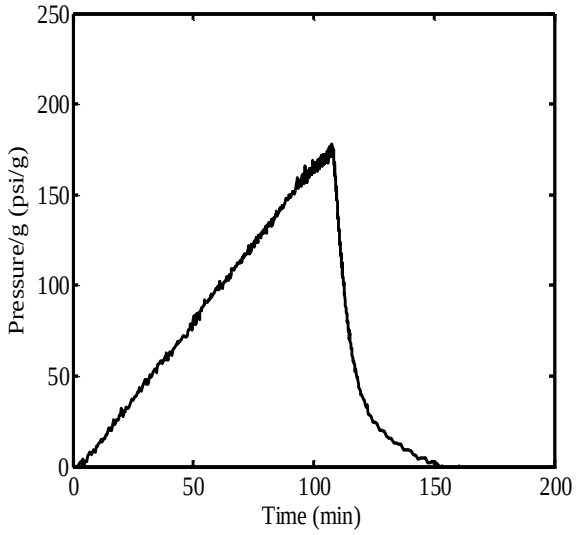

Fig. 6.13 (b)

Fig. 6.13 (a) & (b). Variation of pressurization with temperature and time for organic part of 0.36 M DHOA/*n*-dodecane equilibrated with 0.01 M HNO_3; Reactor vessel capacity: 350 mL

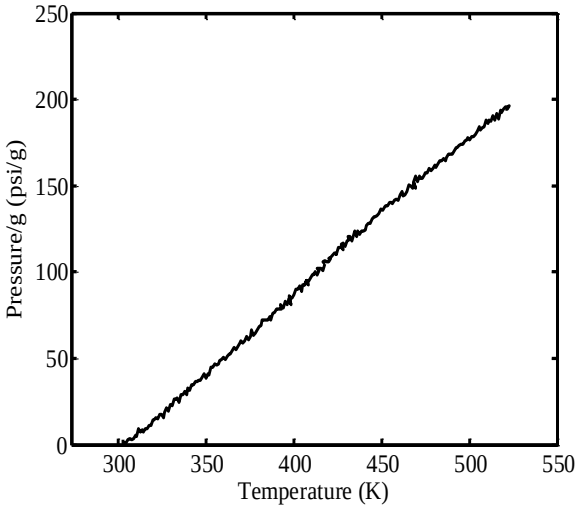

Fig. 6.14 (a)

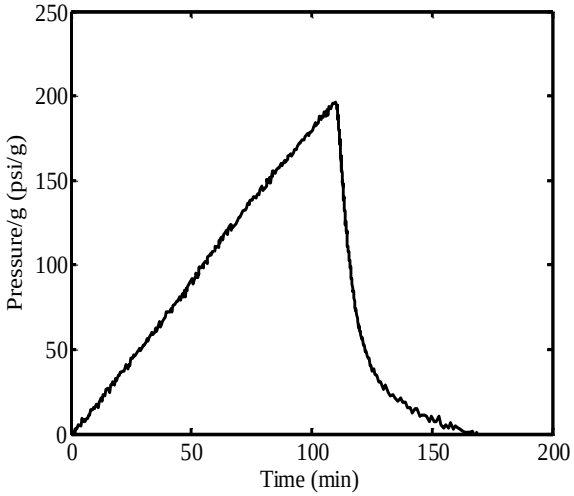

Fig. 6.14 (b)

Fig. 6.14 (a) & (b). Variation of pressurization with temperature and time for organic part of 0.36 M DHOA/*n*-dodecane equilibrated with 0.5 M HNO_3; Reactor vessel capacity: 350 mL

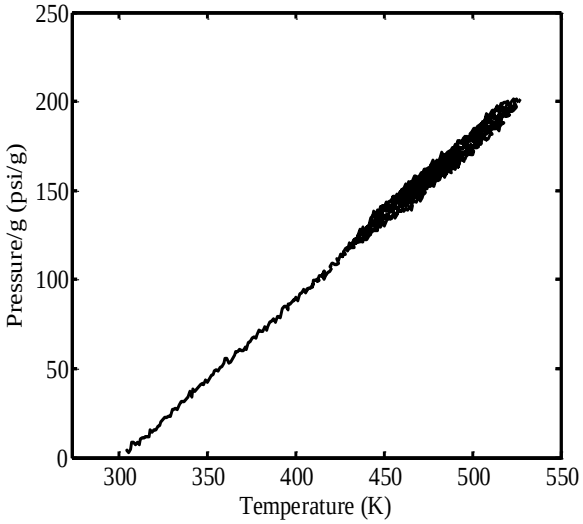

Fig. 6.15 (a)

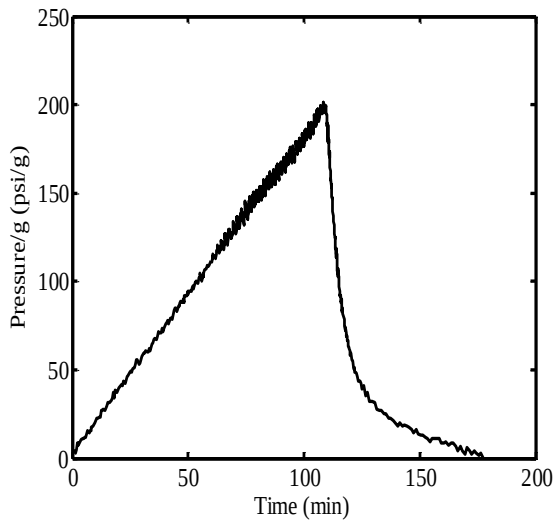

Fig. 6.15 (b)

Fig. 6.15 (a) & (b). Variation of pressurization with temperature and time for organic part of 0.36 M DHOA/*n*-dodecane equilibrated with 3 M HNO_3; Reactor vessel capacity: 350 mL

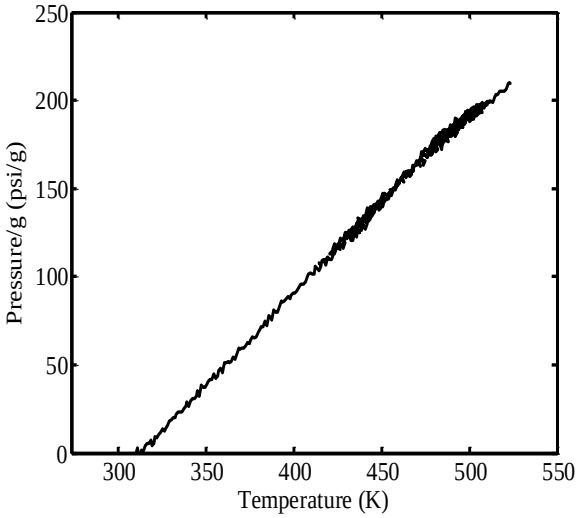

Fig. 6.16 (a)

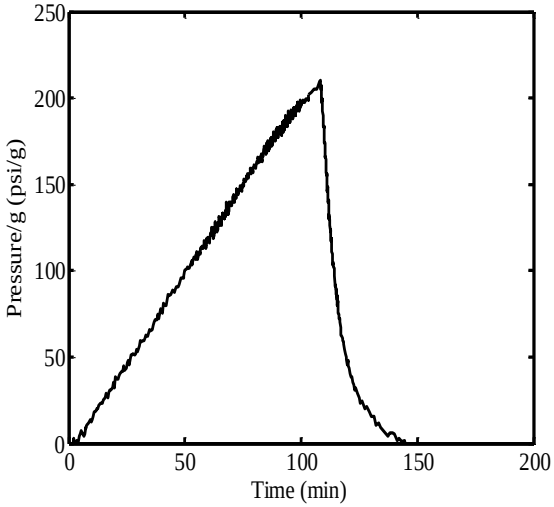

Fig. 6.16 (b)

Fig. 6.16 (a) & (b). Variation of pressurization with temperature and time for organic part of 0.36 M DHOA/*n*-dodecane equilibrated with 4 M HNO_3; Reactor vessel capacity: 350 mL

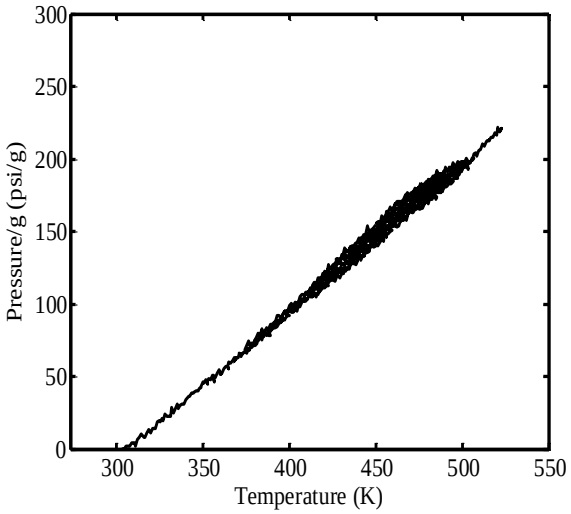

Fig. 6.17 (a)

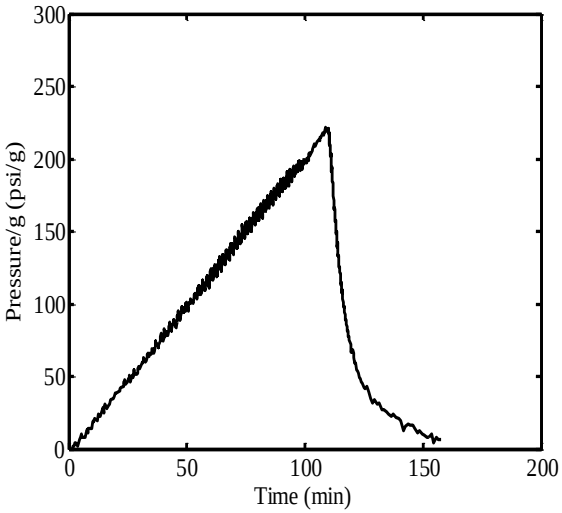

Fig. 6.17 (b)

Fig. 6.17 (a) & (b). Variation of pressurization with temperature and time for organic part of 0.36 M DHOA/*n*-dodecane equilibrated with 6 M HNO_3; Reactor vessel capacity: 350 mL

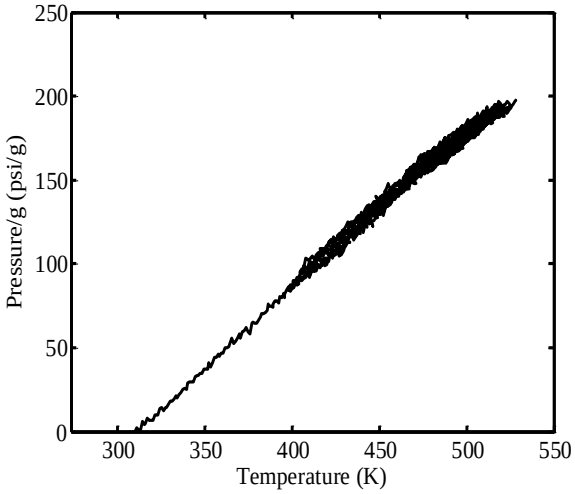

Fig. 6.18 (a)

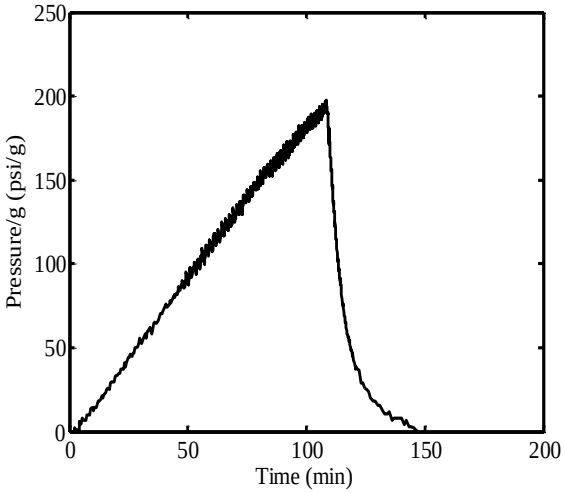

Fig. 6.18 (b)

Fig. 6.18 (a) & (b). Variation of pressurization with temperature and time for organic part of 1.1 M DHOA/*n*-dodecane equilibrated with 0.01 M HNO_3; Reactor vessel capacity: 350 mL

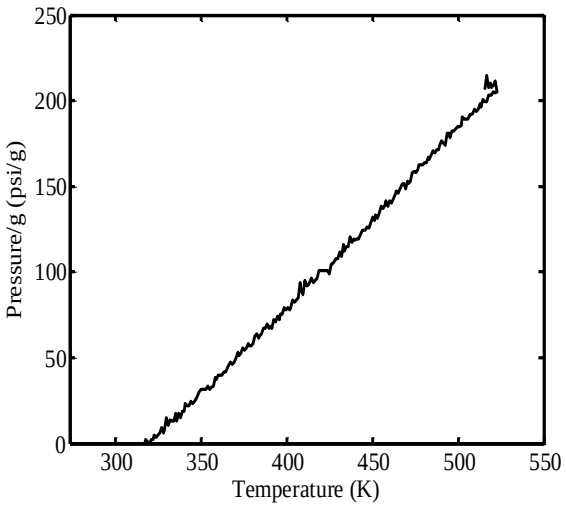

Fig. 6.19 (a)

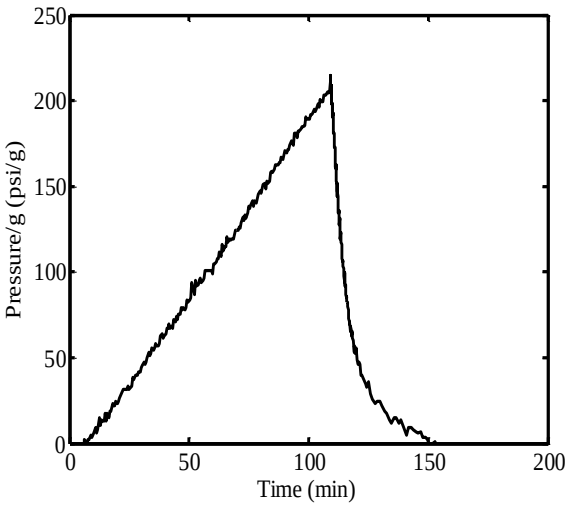

Fig. 6.19 (b)

Fig. 6.19 (a) & (b). Variation of pressurization with temperature and time for organic part of 1.1 M DHOA/*n*-dodecane equilibrated with 0.5 M HNO_3; Reactor vessel capacity: 350 mL

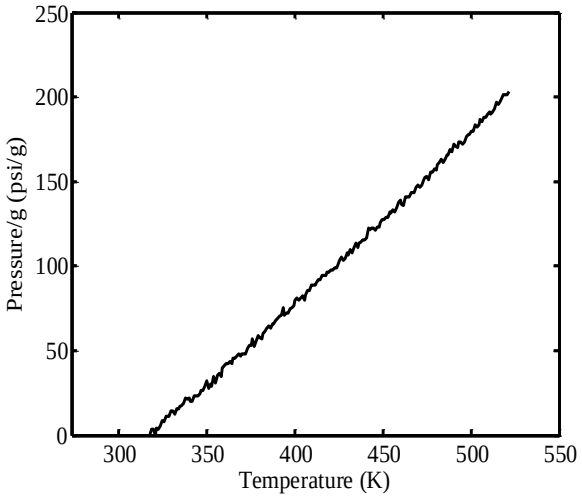

Fig. 6.20 (a)

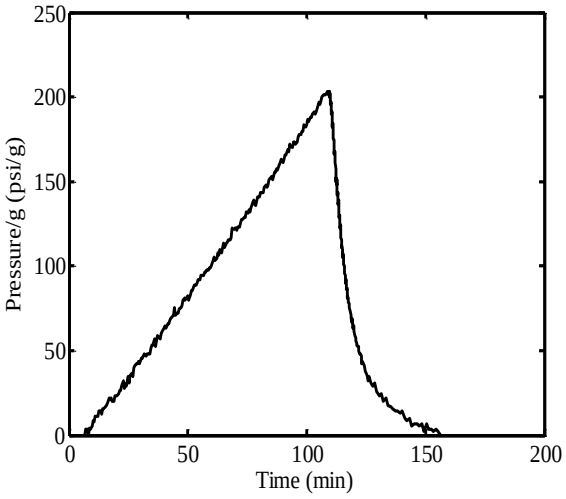

Fig. 6.20 (b)

Fig. 6.20 (a) & (b). Variation of pressurization with temperature and time for organic part of 1.1 M DHOA/*n*-dodecane equilibrated with 3 M HNO_3; Reactor vessel capacity: 350 mL

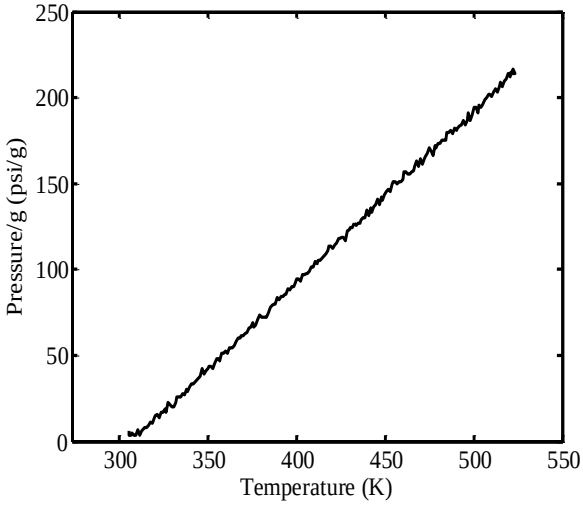

Fig. 6.21 (a)

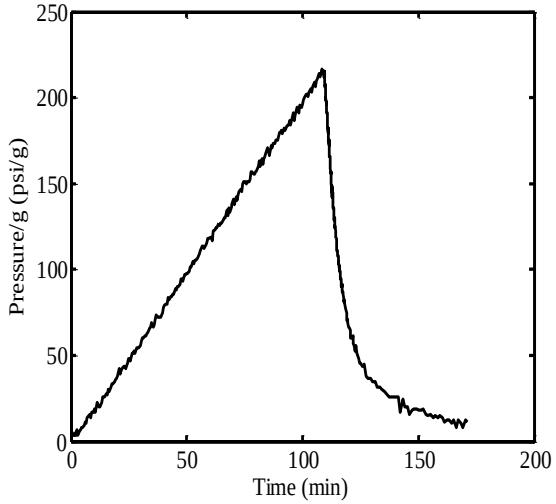

Fig. 6.21 (b)

Fig. 6.21 (a) & (b). Variation of pressurization with temperature and time for organic part of 1.1 M DHOA/*n*-dodecane equilibrated with 4 M HNO_3; Reactor vessel capacity: 350 mL

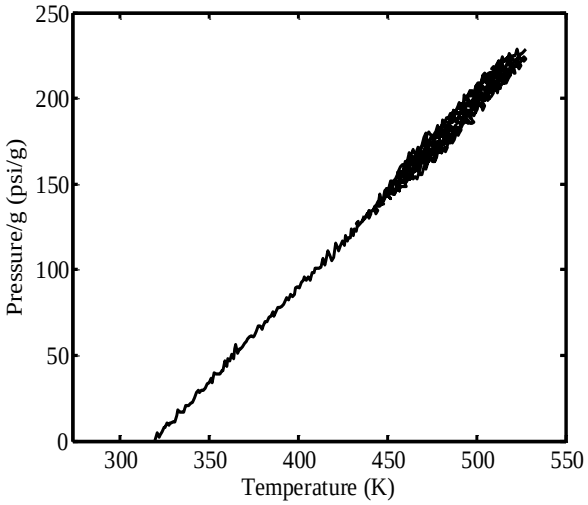

Fig. 6.22 (a)

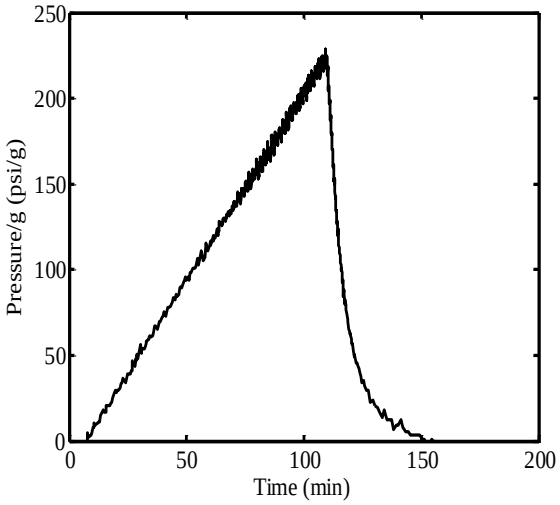

Fig. 6.22 (b)

Fig. 6.22 (a) & (b). Variation of pressurization with temperature and time for organic part of 1.1 M DHOA/*n*-dodecane equilibrated with 6 M HNO_3; Reactor vessel capacity: 350 mL

It was of interest to compare the pressurization trend of DHOA/*n*-dodecane and its nitric acid equilibrated solutions with the reported reverse TALSPEAK (RT) [0.3 M di-(2-ethyl hexyl) phosphoric acid or D2EPHA in 0.2 M TBP in normal paraffinic diluents solvent [**106**]. Pressurization of RT solvent increases with increase in acidity, while it remains more or less constant with the change in acidity for DHOA system. However, pressurization in the case of fresh RT solvent is almost half of pure DHOA and fresh DHOA/n-dodecane solutions. This indicates that the decomposition products of DHOA are of fairly lower molecular weight because of which it has more vapor pressure which in turns leads to higher pressurization. RT solvent which consists of D2EPHA and TBP yields products having lower vapor pressure.

Chapter 7

Summary and conclusions

Evaluation of *N*,*N*-dialkyl amides as alternative extractants of tributyl phosphate (TBP) for spent nuclear fuel reprocessing has been the main objective of the present work. These compounds are completely incinerable resulting in a restricted volume of secondary waste generated. Their physico-chemical properties can be modified by the judicious choice of the alkyl groups. This class of extractants offers better fission product decontamination as compared to that of TBP. In this context *N*,*N*-dihexyloctanamide (DHOA) has been identified as a promising alternative extractant for spent nuclear fuel reprocessing of Pressurized Heavy Water Reactor (PHWR). In the present work, DHOA has been evaluated for the reprocessing of Fast Reactor and Advanced Heavy Water Reactor (AHWR) spent fuels and the performance of DHOA was compared with TBP. The results are summarized as:

i. Dispersion number of DHOA was calculated and found to be 1.21×10^{-3}, which is in the range of Dispersion number for solvents such as TBP, hence showing good phase disengagement tendency.

ii. Various conditions such as flow rates and rotation per minute (rpm) has been optimize of uranium extraction using centrifugal contactor runs. Based on these studies, the optimum flow rates and rpm were chosen as 20mL/min, 1500 rpm, respectively.

iii. Batch extraction data of uranium and plutonium were used to make an estimate the number of extraction stages required during the mixer settler operations for Pu rich spent fuels reprocessing.

iv. The mixer settler and centrifugal contactor runs suggested that uranium extraction ability of DHOA is comparable to that of TBP. However, plutonium extraction appears to be better in DHOA as compared to TBP. DHOA extractes Pu more efficiently and have better stripping behavior of U and Pu as compared to TBP. Quantitative Pu stripping could be achieved employing 0.5 M NH_2OH in 0.5 M HNO_3 in the case DHOA in single contact. By contrast, 3-4 contacts were required for complete removal of plutonium from loaded TBP phase.

v. DHOA was also evaluated vis-à-vis TBP for selective extraction of U and Tc over Pu, and Np. It displayed better extraction of Tc over TBP under the experimental conditions of the present work. The proposed conditions for U and Tc extraction were: 1.1 M DHOA, 1 M HNO_3 and 0.5 M AHA as the as extractant, aqueous phase acidity, and the complexing/reducing agent, respectively. 1.1 M DHOA offered better decontamination of U and Tc as compared to that of 1.1 M TBP. Tc extraction studies as a function of DHOA concentration showed a gradual decrease in the slope values with increased aqueous phase acidity (3.93±0.04 (0.5 M HNO_3), 3.58±0.04 (1.0 M HNO_3), and 2.48±0.01 (4.0 M HNO_3)) suggesting the formation of higher solvates as compared to that of TBP as extractant. Extraction data of Tc, Pu, at 0.5 M AHA in 1 M HNO_3, as a function of time revealed marginal effect AHA hydrolysis/degradation on the extraction profiles of Tc, Pu under process conditions.

vi. Spectrophotometric studies clearly demonstrated that Pu(IV) speciation was affected by the concentration of AHA, nitric acid and time. AHA undergoes hydrolysis forming hydroxyl amine which was responsible for Pu reduction. AHA is quite stable and forms deep brown colored complex with Pu(IV) ion at 1 M

HNO_3. Unlike TBP, DHOA displayed negligible extraction of Pu-AHA-NO_3 complex which was responsible for better separation factor of Tc over Pu.

vii. Extraction behavior of neptunium has been compared employing TBP and DHOA as extractants as a function of nitric acid concentration (0.5-6 M HNO_3), uranium loading (50 and 300 g/L), and in the presence of oxidizing and reducing agents. It was found that TBP is a better extractant for U(VI) and Np(VI) ions than DHOA and $D_{U(VI)} > D_{Np(VI)}$ for both the extractants. Np(IV) extraction is comparable to TBP at higher acidities (3M HNO_3). DHOA shows better stripping behavior for Np(IV) at lower acidities even without the use of any reducing agent. In DHOA system stoichiometry of the extracted species of Np(IV) and Np(VI) in the organic phase were $Np(NO_3)_4 \cdot 3A$ and $NpO_2(NO_3)_2 \cdot 2A$. Neptunium extraction decreases in the presence of 50 g/L U (relevant to Pu rich reactor) and 300 g/L U PHWR) in the aqueous phase, in the entire range of acidity.

viii. The conditions for selective removal of U from PHWR-HLW solutions were optimized. In this context, the extraction and stripping behavior of uranium, plutonium, and neptunium was investigated employing 1.1 M solutions of TBP and DHOA dissolved in *n*-dodecane as extractants in the presence of 6 g/L U relevant to typical PHWR - HLW conditions. These studies suggested that (a) TBP displayed better extraction for U over Np and Pu, (b) DHOA showed a preference for Pu(IV) and Np(IV) over TBP. Stripping experiments suggested that two stages were sufficient for quantitative stripping of Np and Pu from loaded DHOA employing 0.5 M AHA at 1.5-2.0 M HNO_3 as the strippant. On the other hand, more than three stages were required for Np and Pu stripping from loaded TBP as extractant. Uranium loss to the aqueous phase is more in the case of

DHOA as compared to that of TBP. 0.5 M AHA at 2 M HNO_3 appears reducing agent for selective Np, Pu stripping for both the extractants in view of lower U loss to the aqueous phase.

ix. Batch extraction, mixer settler and centrifugal contactor studies were carried out to compare the extraction behavior of 0.18 M TBP and 0.36 M DHOA in *n*-dodecane and a reprocessing scheme has been propose for the three-component system (U, Pu, Th) under simulated AHWR feed solution arising from irradiated (Th,Pu)O_2 fuel. These studies showed that DHOA appears particularly promising for the preferential extraction of U and Pu from dissolver solution of AHWR spent fuel arising out of (Th,Pu)O_2 pins. 4 M HNO_3 was used for scrubbing of co-extracted thorium. Various reductants like 0.5 M HAN/AHA/HU/AOX at 2 M HNO_3, respectively were evaluated for the partitioning of plutonium from uranium. Appreciable extraction of Np was observed for both extractants (~50 % (0.18 M TBP); ~ 66 % (0.36 M DHOA) at O/A; 1) under simulated AHWR feed conditions. There was negligible extraction of Am and fission/activation products suggesting better decontamination of U and Pu. In addition, the organic waste volume generation in the case of 0.36 M DHOA/*n*-dodecane was approximate half of that generated using the flow sheet based on 0.18 M TBP/*n*-dodecane.

x. Dynamic Light Scattering (DLS) studies of two dialkyl amides viz. DHOA, DHDA vis-à-vis TBP were done to understand the third-phase formation behavior during the extraction of Th(IV) from nitric acid medium. There was an increase in the aggregate size with increased acidity and Th(IV) loading in the organic phases. The third-phase appeared in 1.1 M TBP/*n*-dodecane system for 100 g/L Th at $\geq$ 2 M HNO_3. The size of Light Organic Phase (LOP) decreased with

increased acidity from 6.11(±0.29) nm (2 M HNO_3) to 2.81(±0.16) nm (6 M HNO_3); correspondingly a decrease in thorium concentration from 20 g/L to 7.7 g/L was observed. The average aggregate size and thorium concentration in the heavy organic phase (HOP) were 12.83(±1.84) nm, and 105.9(±6.7) g/L, respectively. The addition of 5% (v/v) 1-octanol as phase modifier in 1.1 M TBP/*n*-dodecane suppressed the aggregation tendency without affecting the Th(IV) extraction as compared to that of *n*-dodecane system.

xi. 1.1 M DHOA/*n*-dodecane system also displayed similar behavior under identical experimental conditions. The aggregate size decreased beyond 5 M HNO_3 for $[Th]_{aq}$: 100 g/L which was attributed to third-phase formation.

xii. For 1.1 M DHDA at 100 g/L Th, the aggregate size increased from 3.17 nm (0.1 M HNO_3) to 20.78 nm (6 M HNO_3). However, at 200 g/L Th, the aggregate size increased from 6.19 nm (0.1 M HNO_3) to 19.78 nm (4 M HNO_3) beyond which the organic phase split into two phases. The average aggregate size and thorium concentration in the HOP were 36.62(±0.5) nm, and 41.35(±2) g/L at 5 M HNO_3 and 24.20(±0.58) nm, and 52.34(±1.5) g/L, at 6 M HNO_3, respectively. Th concentration also decreased in the LOP from 6.68 g/L (5 M HNO_3) to 3.08 g/L (6 M HNO_3). These studies demonstrate that alkyl substituents and phase modifiers influence the aggregation tendency of metal solvates in the organic phase.

xiii. Uranium extraction studies were done using $1x10^{-2}$-0.1 M U(VI) + 0.86 M Th(IV) at 4 M HNO_3 as the aqueous phase for 1.1M TBP and 1.1 M DHOA dissolved in different diluents viz. *n*-dodecane, 10% 1-octanol + *n*-dodecane, and decalin. Third-phase formation was observed for both extractants systems dissolved in *n*-dodecane. There was a gradual decrease in Th(IV) concentration in the third-phase

with increased aqueous U(VI) concentration, which suggested the replacement of Th(IV) by extracted U(VI). Uranium concentration in third-phase increased continuously with its initial concentration in the aqueous phase for both the extractants. An empirical correlation was developed for predicting the concentrations of uranium and thorium in the third-phase for both the extractants usi*ng n*-dodecane as diluent.

xiv. There was no significant change in the absorption spectra of U(VI) in the third-phase (in the presence of Th(IV)) as compared to that without third-phase. No third-phase formation was observed in the case of either 10% 1-octanol + *n*-dodecane or decalin as diluents under the conditions of present studies. These studies suggested that these diluents were promising alternatives of *n*-dodecane for alleviating the third-phase formation during the reprocessing of spent thorium based fuels.

xv. Thermal degradation studies were also performed for DHOA vis-à-vis TBP under identified experimental condition such as extractant concentration, aqueous phase acidity, pressure, temperature, and time using ARSST system. These studies indicated the formation of volatile / gaseous degradation products of DHOA were responsible for high pressurization as compared to that of TBP. However, the identification of products needs to be investigated.

FUTURE PERSPECTIVE

- These studies have shown that DHOA appears as a promising alternative of TBP for spent fuel reprocessing particularly for Pu rich and AHWR spent fuels.
- These studies need to be performed at relatively larger scale in suitable facility using the simulated / actual feed solution.
- Several interesting observation have been made with regard to preferential extraction of tetravalent metal ions such as Pu(IV) and Np(IV) over U(VI). This observation is in sharp contrast to the behavior of TBP where U(VI) is extracted better than Pu(IV) and Np(IV). This need to be understood by suitable techniques such as SANS and by theoretical calculation.
- The identification of the species formed during thermal degradation also needs to be identified.

REFERENCES

1. H.J. Arnikar, *Essentials of Nuclear Chemistry*, 2nd Edition, Wiley Eastern Limited, New Delhi, **1988**, p.200.
2. Department of Atomic Energy, India, *Annual Report*, **2011**, p.4.
3. International Atomic Energy Agency, *Thorium fuel cycle-Potential benefits and challenges*, IAEA-TECDOC-1450, **2005,** p.45.
4. World Nuclear Association, http://www.world-nuclear.org/info/Country-Profiles/Countries-G-N/India .
5. J.D. Thorn, C.T. John and R.F. Burstall, *Nuclear Power Technology: Fuel Cycle*, Ed. by W. Marshall, Oxford University Press, v.2, **1983**, p.380.
6. M. Benedict, T.H. Pigford and H.W. Levi, *Nuclear Chemical Engineering*, McGraw Hill Book Company, 2nd Edition, **198**1, p.86.
7. S. Sivasubramanian, S. M. Lee and S. A. Bhardwaj, *Proceedings of Annual Conference of Indian Nuclear Society*, INSAC - 2000/IT-1, Mumbai, India, v.2, **2000**, p.2.
8. K. Balakrishnan, in *XII ISAS National Symposium on Analytical Techniques for safety and sufficiency of natural resources / products (INSAT-97)*, IL-2, Kottayam, India, Feb. 20-22, **1997**, p.I-3.
9. Nuclear Power plant Standardization: Light Water Reactors, NTIS order # PB81-213589, April **1981**.
10. H.B. Stewart and S. Jaye, Tech. Rep., *GA-7642*, **1967.**
11. E.S. Bettis and R.C. Robertson, *Nucl. Appl. Tech.*, 8, **1970**, p.190.
12. A.S. Kitzes and R.N. Lyon, in *Proceedings of the International Conference on the Peaceful uses of Atomic Energy*, Geneva, v.9, **1956**, p.414.

13. M.R. Balakrishnan, in *Proceedings of the Indo-Japan Seminar on Thorium Utilisation*, Mumbai, Dec. 10, **1990**, p.62.

14. K. Balakrishnan and S.K. Mehta in *Proceedings of Thorium Fuel Cycle Development Activities in India (A Decade of Progress)*, Ed. by T. K. Basu and M. Srinivasan , Tech. Rep., BARC - 1532, Mumbai, **1990**, p.9.

15. International Atomic Energy Agency, *Status Report for Advanced Nuclear Reactor Designs: Advanced Heavy Water Reactor (AHWR) - Report 67*, Vienna, Austria, **2011**.

16. R.K. Sinha and A. Kakodkar, *Nucl. Engg. Design*, 236, **2006**, p.683.

17. E.R. Irish and W.H. Reas, *The PUREX process - a solvent extraction reprocessing method for irradiated uranium*, U. S. Tech. Rep., HW-49483 A , **1957**.

18. R.K. Sinha, H.S. Kushwaha, R.G. Agarwal, D. Saha, M.L. Dhawan, H.P. Vyas and B.B. Rupani, in *Proceedings of Annual Conference of Indian Nuclear Society*, INSAC - 2000/IT-4, Mumbai, India, v.2, June 1-2, **2000**, p.81.

19. V. Jagannathan, U. Pal, R. Karthikeyan, S. Ganesan, R.P. Jain and S.U. Kamat, *Nucl. Tech.*, 133, **2001**, p.1.

20. R.L. Stevenson and P.E. Smith, in *Reactor Hand Book: Fuel reprocessing*, Ed. by S.M. Stoller and R.B. Richards, Interscience Publishers & Inc., New York, v.2, **1961**, p.208.

21. H.C. Rathvon, A.G. Blasewitz, R. Maher, J.C. Eargle, Jr. and A.E. Wible in *Proceedings of International Thorium Fuel Cycle Symposium*, Gatlinburg, Tenn., May 3 - 6, **1966**, p.765.

22. K. Vijayan, S.S. Shinde, U. Jambunathan and A. Ramanujam, in *Proceedings of Annual Conference of Indian Nuclear Society*, INSAC - 2000/50, Mumbai, June 1-2, **2000**, p.148.

23. N.M. Sinalkar, C. Janardanan, K. Vijayan, S.S. Shinde, U. Jambunathan and A. Ramanujam, in *Proceedings of Nuclear and Radiochemistry Symposium*, *NUCAR-2001*, CARM-37, Pune, Feb. 7-10, **2001**, p.210.

24. R.H. Rainey and J.H. Moore, *USAEC Tech. Report*, ORNL - 3155, May **1952**.

25. P.R. Vasudeva Rao and T.G. Srinivasan, in *Proceedings of Nuclear and Radiochemistry Symposium*, *NUCAR-2001*, IT-11, Pune, Feb. 7-10, **2001**, p.59.

26. N. Srinivasan, M.N. Nadkarni, G.R. Balasubramanian, R.T. Chitnis and H. R. Siddiqui, Report, *Tech. Rep. BARC - 643*, Mumbai, India, **1972**.

27. A. Mukherjee, R.T. Kulkarni, S.G. Rege and P.V. Achuthan, in *Proceedings of DAE Symposium on Radiochemistry and Radiation Chemistry*, SC-12, Pune, 7-11 Dec., **1982,**.

28. R.T. Chitnis, K.G. Rajappan, S.V. Kumar and M.N. Nadkarni, *Tech. Rep., BARC - 1003*, Mumbai, India, **1979**.

29. A. Ramanujam, P.S. Dhami, V. Gopalkrishnan, A. Mukherjee and R.K. Dhumwad, *Tech. Rep., BARC - 1486*, Mumbai, India, **1989**.

30. P. Govindan, A. Palamalai, K.S. Vijayan, M. Raja, S. Parthasarathy, S.V. Mohan and R.V. Subba Rao, *J. Radioanal. and Nucl. Chem.*, 246(2), **2000**, p.441.

31. H. H. Anderson, and L. B. Asprey, *Solvent extraction process for plutonium*, US patent No. 2924506, **1947**.

32. E.R. Irish, *Description of PUREX plant process*, U. S. Tech. Rep., HW-60116, **1959.**

33. Sadhana Mukherji, P.D. Krishnani and R. Shrivenkatesan, *Radiotoxicities of the minor actinides of the discharged PWR, PHWR, and AHWR fuel in Nuclear Fuel Cycle Technologies, Closing the Fuel Cycle*, in *Proceedings of 14th Annual Conf. of Indian Nucl. Society (INSAC-2003)*, Ed. by B. Raj, P.R. V. Rao, IGCAR, Kalpakkam, Dec. 17-19, **2003**, p.395.

34. R. Natarajan and B. Raj, *Energy Procedia*, 7, **2011**, p.414.

35. R. Natarajan, *J. Nucl. Sci and Technol.*, 44, **2007**, p.393.

36. R. Natarajan, *Challenges in Fast Reactor Fuel Reprocessing, Indian Association of Nuclear Chemists and Allied Scientists Bulletin*, 14(2), **1998**, p.27.

37. J.J. Katz, G.T. Seaborg and L.R. Morss, *The Chemistry of the Actinide Elements*, 2nd Edition, Chapman and Hall, London, v.2, **1986,** p.1135.

38. A.F. Wells, *Structural Inorganic Chemistry*, 3rd Edition, Clarendon Press, Oxford, **1962,** p.953.

39. B.B. Cunningham, *Proc. of XVII international congress of pure and applied chemistry*, Butterworths, London, v.1, Aug. 30 - Sept. 6, **1959**, p.64.

40. S. Ahrland, J.O. Liljenzin and J. Rydberg, in *Comprehensive Inorganic Chemistry*, Ed. by J.C. Bailar Jr., H.J. Emeleus, R. Nyhlom and A.F.T. Dickenson, Pergamon Press, Oxford, v.5, **1973**, p.465.

41. V.I. Spitsyn, A.D. Gelman, N.N. Krot, M.P. Mefodiyeva, F.A. Zacharova, Y.A. Komokov, V.P. Shilov and I.V. Smirnovam, *J. Inorg. Nucl. Chem.*, 31, **1969**, p.2733.

42. K.A. Kraus, *Proc. First U.N. Conference on Peaceful Uses of Atomic Energy*, v.7

1956, p.245.

43. O.J. Wick, *Plutonium Hand Book: A Guide to the Technology*, Ed. by Gordon & Breach, New York, v.1, **1967,** p.438.

44. S. Ahrland, J.O. Liljenzin and J. Rydberg in *Comprehensive Inorganic Chemistry*, Ed. by J.C. Bailar Jr., H.J. Emeleus, R. Nhylom and A.F. Trotman-Dickenson, Pergamon Press, Oxford, v.5, **1973**, p.502.

45. R.G. Pearson, *J. Am. Chem. Soc.*, 85, **1963**, p.3533.

46. B.A. Moyer, *Ion exchange and solvent extraction: A Series of Advance*, Taylor and Francis, v.19, **2010,** p.68.

47. H.A.C. McKay and J.L. Woodhead, *J. Chem. Soc.*, **1964**, p.717.

48. J.M. Lehn and J.P. Sauvage, *J. Am. Chem. Soc.*, 97, **1975**, p.6700.

49. J. Dale, *Isr. J. Chem.*, 20, **1980**, p.3.

50. D.J. Cram, *Science*, 219, **1983**, p.1177.

51. P.K. Mohapatra and V.K. Manchanda, *Radiochim. Acta*, 55, **1991**, p.193.

52. W.H. Zachariasen, in *The Actinide Elements*, Ed. by G. T. Seaborg and J. J. Katz, National Nuclear Energy Series, NNES - IV, 14A, McGraw Hill, **1954**, p.769.

53. T. Sekine and Y. Hasegawa, *Solvent Extraction Chemistry: Fundamentals and Applications*, Marcel Dekker, New York, **1977**, p.60.

54. L. Alders, *Liquid-liquid Extraction*, 2nd Edition, Elsevier Publishing Company, **1959,** p.93.

55. M. Benedict, T.H. Pigford and H.W. Levi, *Nuclear Chemical Engineering*, 2nd Edition, McGraw Hill Book Company, **1981,** p.165.

56. S.V. Bagawade, P.R. Vasudeva Rao, V.V. Ramakrishna and S.K. Patil, *J. Inorg. Nucl. Chem.*, 40, **1978**, p.1913.

57. A. Ramanujam, M.N. Nadkarni, V.V. Ramakrishna and S.K. Patil, *J. Radioanal. Chem.*, 42, **1978**, p.349.

58. S.K. Patil, V.V. Ramakrishna, P.K.S. Kartha and N.M. Gudi, *Sep. Sci. Technol.*, 15, **1980**, p.1459.

59. M. Benedict, T.H. Pigford and H.W. Levi, *Nuclear Chemical Engineering*, 2nd Edition, McGraw Hill Book Company, **1981**, p.172.

60. H.A.C. McKay, J. H. Miles and J. L. Swanson, in *The PUREX Process, Science and Technology of Tributyl Phosphate, in: Applications of Tributyl Phosphate in Nuclear Fuel Reprocessing*, Ed. by W. W. Schulz, L. L. Burger, J. D. Navratil and K. P. Bender, CRC Press Inc., Boca Raton, Florida, v.3, **1990**.

61. D.D. Sood and S.K. Patil, *J. Radioanal. Nucl. Chem.*, 203, **1996**, p.547.

62. R.L. Stevenson and P.E. Smith, in *Reactor Hand Book: Fuel Reprocessing*, Ed. by S. M. Stoller, R. B. Richards, Interscience Publishers & Inc., New York, v.2, **1961**.

63. T.H. Siddall and R.M. Wallace, *Effect of solvent degradation on the PUREX process*, USDOE Tech. Rep. DP-286, **1960**.

64. D.S. Deshingkar, M. Ramaswamy, P.K.S. Kartha, P.V.E. Kutty and A. Ramanujam, *Treatment of tributyl phosphate wastes by extraction 350 cum pyrolysis process*, Tech. Rep. BARC-1480, Mumbai, India, **1989**.

65. T.H. Siddall III, *J. Phys. Chem.*, 64, **1960**, p.1863.

66. T.H. Siddall III, *USAEC Tech. Rep. DP - 541*, E. I. Du Pont de Nemours and Co. Alken, SC, **1961**.

67. T.H. Siddall III, *Solvent Extraction Chemistry*, Ed. by D. Dyrssen, J. Lijenjin and J. Rydberg, John Wiley and Sons Inc., **1967**, p.501.

68. K.B. Brown, C.A. Blake and J.M. Schmitt, *USAEC Tech. Rep., ORNL - 3452,* Chemical Technology Division, Oak Ridge National Laboratory, Oak Ridge, TN, **1963**, p.178.

69. K.B. Brown, *USAEC Tech. Rep., ORNL - 3496,* Chemical Technology Division, Chemical Development Section, Progress Report, Separation Chemistry and Separation Process Res., Oak Ridge National Laboratory, Oak Ridge, TN, Jan. - June, **1963**.

70. C. Musikas, *Sep. Sci. Technol.*, 23(12&13), **1988**, p.1211.

71. G. Thiollet and C. Musikas, *Sol. Ext. Ion Exch.*, 7(5), **1989**, p.813.

72. C. Musikas, N. Condamines and C. Cuillerdier, *Analytical Sciences,* v.7 (supp.), 1991 p.11.

73. C. Musikas, *Min. Pro. Ext. Met. Review*, 17, **1997**, p.109.

74. S.K. Patil, V. V. Ramakrishna, P.K.S. Kartha and N.M. Gudi, *Sep. Sci. and Tech.*, 15, **1980**, p.1459.

75. C. Yu, Z. Zhenwei, J. Runtian and S.G. Xin, *J. Radioanal. Nucl. Chem.*, 258(1), **2003,** p.171.

76. P.N. Pathak, D.R. Prabhu, A.S. Kanekar and V.K. Manchanda, *IOP Conf. Series: Materials Science and Engineering*, 9, **2010,** 012082.

77. P.N. Pathak, D.R. Prabhu, A.S. Kanekar, V.K. Manchanda, *Sep. Sci. and Tech.*, 44, **2009**, p.3650.

78. P.N. Pathak, D.R. Prabhu, A.S. Kanekar and V.K. Manchanda, *Radiochim. Acta*, 94, **2006**, p.193.

79. P.N. Pathak, D.R. Prabhu, G.H. Rizvi, P.B. Ruikar, L.B. Kumbhare, P. K. Mohapatra and V.K. Manchanda, *Radiochim. Acta*, 91, **2003**, p.379.

80. P.N. Pathak , D.R. Prabhu, P.B. Ruikar and V.K. Manchanda, *Sol. Ext. Ion Exch.*, 20, **2002**, p.293.

81. P.N. Pathak, D.R. Prabhu, A.S. Kanekar, P B. Ruikar, A. Bhattacharyya, P.K. Mohapatra and V.K. Manchanda, *Ind. Eng. Chem. Res.*, 43, **2004**, p.4369.

82. S. Nave, C. Mandin, L. Martinet, L. Berthon, F. Testard, C. Madic and Th. Zemb, *Phys. Chem. Chem. Phys.*, 6, **2004,** p.799.

83. M. Borkowski, R. Chiarizia, M.P. Jensen, J.R. Ferraro, P. Thiyagarajan and K.C. Littrell, *Sep. Sci. Technol.*, 38, **2003**, p.3333.

84. R. Chiarizia, K.L. Nash, M.P. Jensen, P. Thiyagarajan and K.C. Littrell, *Langmuir*, 19, **2003**, p.9592.

85. R. Motokawa, S. Suzuki, H. Ogawa, M. Antonio and T. J. Yaita, *Phys. Chem. B.*, 116, **2012**, p.1319.

86. R. Chiarizia, M.P. Jensen, P.G. Rickert, Z. Kolarik, M. Borkowski and P. Thiyagarajan, *Langmuir*, 20, **2004**, p.10798.

87. J. Plaue, A. Gelis, K. Czerwinski, P. Thiyagarajan and R. Chiarizia, *Solv. Extr. Ion Exch.*, 24, **2006**, p.283.

88. J. Plaue, A. Gelis, and K. Czerwinski, *Sep. Sci. Technol.*, 41, **2006**, p.2065.

89. K.K. Gupta, V.K. Manchanda, S. Sriram, G. Thomas, P.G. Kulkarni and R.K. Singh, *Solv. Ext. Ion Exch*., 18, **2000**, p.421.

90. R.K. Jha, K.K. Gupta, P.G. Kulkarni, P.B. Gurba, P. Janardan, R.D. Changarani, P.K. Deya, P.N. Pathak and V.K. Manchanda, *Desalination*, 232, **2008**, p.225.

91. R. Chiarizia and A. Briand, *Solv. Extr. Ion Exch.*, 25, **2007**, p.351.

92. K.V. Lohithakshan, V.K. Aswal and S.K. Aggarwal, *Radiochim. Acta*, 99, **2011**, p.179.

93. W. Davis Jr., *Tributyl phosphate-hydrocarbon diluent repurification in radiochemical processing at ORNL: status summary*, US Tech. Rep. ORNL-2848, **1960**.

94. R.G. Geier, *Purex process solvent literature review, Rockwell International Technical Report*, US Tech. Rep., RHO-LD-74, **1979**.

95. G.C. Young and D.W. Holladay, *Recovery of acid-degraded tributyl phosphate by solvent extraction*, ORNL Technical Report, conf-811108-1-0, **1981.**

96. B.J. Mincher, G. Modolo and S.P. Mezyk, *Solv. Extr. Ion Exch.*, 27, **2009**, p.1.

97. D. Lesage, H. Virelizier and C. K. Jankowski, *Spectroscopy*, 13, **1997**, p.275.

98. J.N. Sharma, R. Ruhela, K.K. Singh, M. Kumar, C. Janardhanan, P.V.S. Achutan, S. Manohar, P.K. Wattal and A.K. Suri, *Radiochim. Acta*, 98, **2010**, p.485.

99. R.B. Gujar, S.A. Ansari, A. Bhattacharyya, P.K. Mohapatra, A.S. Kanekar, P.N. Pathak and V.K. Manchanda, *J. Radioanal. Nucl. Chem.*, 288, **2011**, p.621.

100. R.B. Gujar, S.A. Ansari, A. Bhattacharyya, A.S. Kanekar , P.N. Pathak, P.K. Mohapatra and V.K. Manchanda, *Solv. Extr. Ion Exch*., 30, **2012**, p.278.

101. K.J. Parikh, P.N. Pathak, S.K. Misra, S.C. Tripathi, A. Dakshinamoorthy and V.K. Manchanda, *Solv. Extr. Ion Exch*., 27, **2009**, p.244.

102. R.M. Wagner, *Investigation of explosive characteristics of PUREX solvent decomposition products (Red Oil)*, U S Tech. Rep. HW-27492, Hanford works, Richland, **1953**.

103. T.S. Rudisill and W.J. Crooks III, *Sep. Sci. Technol*, 38(12&13), **2003**, p.2725.

104. L.K. Patil, V.G. Gaikar, S. Kumar, U.K. Mudali and R. Natarajan, *Thermal Decomposition of Nitrated Tri-n-Butyl Phosphate in a Flow Reactor*, International Scholarly Research Network ISRN Chemical Engineering, 193862, **2012**.

105. B. Das, S. Kumar, P. Mondal, U.K. Mudali and R. Natarajan, *J. Radioanal. Nucl. Chem*, 292, **2012,** p.1161.

106. P.K. Sinha, S. Kumar, U.K. Mudali and R. Natarajan, *J. Radioanal. Nucl. Chem*, 290, **2011**, p.667.

107. T. Dagnac, J.M. Guillot and P.L. Cloirec, *J. Anal. Applied Pyrolysis*, 37, **1996**, p.33.

108. G. Thompson, *Hazard Potential of the La Hague site: An Initial Review*, May **2000**, p. 41.

109. K.K. Gupta, V.K. Manchanda, M.S. Subramanian and R.K. Singh, *Solv. Extr. Ion Exch.*, 18, **2000**, p.273.

110. V.K. Manchanda, P.B. Ruikar, S. Sriram, M.S. Nagar, P.N. Pathak, K.K. Gupta, R.K. Singh, R.R. Chitnis, P.S. Dhami, and A. Ramanujam, *Nuclear Technology*, 134, **2001**, p.231.

111. S.S. Rattan, A.V.R. Reddy, V.S. Mallapurkar, R.J. Singh and Satya Prakash, *J. Radioanal. Nucl. Chem.*, 67, **1981,** p.85.

112. C.J. Hardy, D. Scargill and J.M. Fletcher**,** *J. Inorg. Nucl. Chem.*, 7, **1958**, p. 257.

113. D.E. Ryan and A.W. Wheelright, *Ind. Eng. Chem.*, 51, **1959**, p.60.

114. V. K. Manchanda and P. N. Pathak, *Sep. Purif. Technol.*, 35(2), **2004**, p.85.

115. P.S. Dhami, P. Jagasia, S. Panja, P.V. Achuthan, S.C. Tripathi, S.K. Munshi and P.K. Dey, *Sep. Sci. Technol*., 45, **2010**, p.1147.

116. P.S. Dhami, P. Jagasia, S. Panja, P.W. Naik, P.V. Achuthan, S.C. Tripathi, S.K. Munshi and P.K. Dey, *Desalination & Water Treatment*, 38, **2012**, p.184.

117. A. Suresh, , *Evaluation of trialkyl phosphates for the identification of a viable extractant for fast reactor fuel reprocessing*, *IT-5* in *Proceedings of SESTEC*-2012,

Ed. by P. N. Pathak, R. M. Sawant, P. K. Mohapatra, A. Goswami, Mumbai, INDIA, **2012**, p.12.

118. S.A. Ansari, D.R. Prabhu, R.B. Gujar, A.S. Kanekar, B. Rajeswari, M.J. Kulkarni, M.S. Murali, Y. Babu, V. Natarajan, S. Rajeswari, A. Suresh, R. Manivannan, M.P. Antony, T.G. Srinivasan**,** V.K. Manchanda, *Sep. & Purif. Technol.,* 66, **2009**, p.118.
119. M.S. Caceci and G.R. Choppin, *Radiochim. Acta*, 33, **1983**, p.113.
120. R.A. Leonard, D.B. Chamberlain and C. Conner, *Sep. Sci. Technol.*, 32, 1-4, **1997**, p.193.
121. R.A. Leonard and A.A. Ziegler, *Variation of maximum throughput with time in staged solvent extraction equipment*, American Institute of Chemical Engineers, National Meeting., Seattle, WA, USA, **1985**, p.19.
122. M. Balamurugan, S. Kumar, U.M. Kamachi and R. Natarajan, *J. Radioanal. Nucl. Chem.*, 289 (2), **2011**, p.507.
123. R.A. Leonard, *Sep. Sci. Technol.*, 30(7–9), **1995**, p.1103.
124. R.A. Leonard, *Sep. Sci. Technol.*, 23(12-13), **1988**, p.1473.
125. D.S. Webster, C.L. Williamson and J.F. Ward, *Hydraulic performance of a 5-inch centrifugal contactor*, USAEC Tech. Rep. DP-370, **1962**.
126. M. Takeuchi, H. Ogino, H. Nakabayashi, Y. Arai, T. Washiya, T. Kase and Y. Nakajima, *J. Nuc. Sci. Tech.*, 46(3), **2009**, p. 217.
127. D. Meikrantz, T. Garn, N. Mann, J.D. Law and T.A. Todd, *Hydraulic performance and mass transfer efficiency of engineering scale centrifugal contactors*, in *Proceeding of Advanced Nuclear Fuel Cycles and Systems, Global-2007*, Boise, Idaho, Sept. 9-13, **2007**.
128. H.K. Fauske, *Chem. Eng. Progress*, 96**(**2), **2000,** p.17.

129. J.W.T. Spinks and R.J. Woods, *An Introduction to Radiation Chemistry*, Wiley Interscience, London, 3rd Edition, **1990**.

130. M.A.J. Rodgers, *Radiation chemistry: Principles and applications*, VCH Publishers, **1987**.

131. R.W. Mathews, *Int. J. Appl. Rad. Isot.*, 33, **1982**, p.1159.

132. W.J. McDowell, in *Organic scintillators and liquid scintillation counting*, Ed. by D.L. Horrocks and L.T. Peng, Academic Press Inc., New York, **1971**, p. 937.

133. D.D. Sood, A.V.R. Reddy and N. Ramamoorthy, *Fundamentals of Radiochemistry*, 2nd Edition, IANCAS publication, BARC, Mumbai, **2004**, p.114.

134. G.F. Knoll, *J. Radioanal. Nucl. Chem.*, 243, **2000**, p.125.

135. G.F. Knoll, *Radiation detection and measurement*, 3rd Edition, John Willy and sons, New York **2000**, p.406.

136. W.J. Maeck, *Anal. Chem.*, 31, **1955**, p.1130.

137. W. Davies and W. Gray, *Talanta*, 11, **1964**, p.1203.

138. F.P. Roberts, R.J. Brouns, K.R. Byers, J.E. Fager, B.W. Smith, K.L. Swinth , *NUREG/CR-3584*, Method 3.0, **1984**.

139. G.H. Jeffery, J. Bassett, J. Mendham and R.C. Denney, *Vogel's Textbook of Quantitative Analysis*, 5th Edition, ELBS Longman Publishers, UK, **1996**, p.329.

140. Z. Marczenko and M.B. Zak, *Separation Preconcentration and spetrophotometry in Inorganic Analysis*, Elsevier Science, **2000,** p.425.

141. P.N. Pathak, D.R. Prabhu, M. Bindu, S.C. Tripathi and V.K. Manchanda, *J. Radioanal. Nucl. Chem.*, 288, **2010,** p.137.

142. P.N. Pathak, A.S. Kanekar, D.R. Prabhu and V.K. Manchanda, *Sol. Ext. Ion Exch.*, 27, **2009,** p.683.

143. N.N. Popova, I.G. Tananaev, S.I. Rovnyi and B.F. Myasoedov, *Technetium: behaviour during reprocessing of spent nuclear fuel and in environmental objects*. *Russian Chemical Reviews, 72,* **2003,** p.101.

144. S.A. Ansari, P.N. Pathak, P.K. Mohapatra, V.K. Manchanda, *Chem. Rev.*, 112(3), **2012**, p.1751.

145. C.V.S. Brahmmananda Rao, T.G. Srinivasan, P.R. Vasudeva Rao, *Solv. Extr. Ion Exch.*, 30 3, **2012**, p.262.

146. Global Nuclear Energy Partnership Strategic Plan, *GNEP-167312*, Rev 0, Jan., **2007**.

147. G.F. Vandegrift, M.C. Regalbuto, S. Aase, A. Bakel, T.J. Battisti, D. Bowers, J.P. Byrnes, M.A. Clark, J.W. Emery, J.R. Falkenberg, A.V. Gelis, C. Pereira, L. Hafenrichter, Y. Tsai, K.J. Quigley, M.H. Vander Pol, *Designing and Demonstration of the UREX^{+} Process Using Spent Nuclear Fuel,* in *Proceedings ATATLANTE, Advances for Future Nuclear Fuel Cycles,* International Conference, France, Jun. 21-24, **2004**.

148. B. Chatterjee, *Coord. Chem. Rev.*, **26, 1978**, p.281.

149. R.J. Taylor, I. May, A.L. Wallwork, I.S. Denniss, N.J. Hill, B. Ya, B. Galkin, Y. Zilberman, S. Yu and S. Fedorov, *J. Alloys Compounds*, 271-273, **1998**, p.534.

150. R.J. Taylor and I. May, *Czech. J. Phys.*, 49, **1999**, p 617.

151. L. Nuñez and G.F. Vandegrift, *Evaluation of hydroxamic acid in uranium extraction process: Literature review*, Tech. Rep. ANL-00/35**,** Chemical Technology Division, Argonne National Laboratory, USA, **2001**.

152. M.J. Carrott, O.D. Fox, C.J. Maher, C. Mason, R.J. Taylor, S.I. Sinkov and G.R. Choppin, *Solv. Extr. Ion Exch.,* 25, **2007,** p.723.

153. R.J. Taylor, S.I. Sinkov, G.R. Choppin and I. May, *Solv. Extr. Ion Exch.*, 26, **2008,** p.41.

154. A.M. El-Kot, *J. Radioanal. Nucl. Chem.*, 163, **1992,** p.363.

155. T.N. Jassim, J.O. Liljenzin, R. Lundqvist and G. Person, *Solv. Extr. Ion Exch.*, 2, **1984**, p.405.

156. M. Takeuchi, S. Tanaka, M. Yamawaki and S. Tachimori, *Solv. Extr. Ion Exch.*, 13, **1995**, p.43.

157. D.J. Pruett, *Sep. Sci. Technol.*, 16, **1981**, p.1157.

158. C.S. Gong, W.W. Lukens, F. Poineau and K.R. Czerwinski, *Inorg. Chem.*, 47, **2008**, p.6674.

159. P. Tkac and A. Paulenova, *Sep. Sci. Technol.*, 43, **2008**, p.2670.

160. T.H. Siddall III and E.K. Dukes, *J. Am. Chem. Soc.*, 81(4), **1959**, p.790.

161. **N.** Srinivasan, M.V. Ramaniah, S.K. Patil, V.V. Ramakrishna, R. Swarup and A. Chadha, *Process chemistry of neptunium, Part – I*, Tech. Rep. BARC-428, **1969.**

162. O. Tochiyama, Y. Nakamura, M. Hirota and Y. Inoue, *J. Nucl. Sci. Technol.*, 32(2), **1995**, p.118.

163. K. Kim, K. Song, E. Lee, I. Choi and J. Yoo, *J. Radioanal. Nucl. Chem.*, 246(1), **2000**, p.215.

164. Z. Kolarik and R. Schuler, *Separation of neptunium from uranium and plutonium in the PUREX process*, Chem. E. Symposium Series No. 88, **1984**, p. 83.

165. J.F. Ahearne, *Radioactive Waste: The Size of the Problem*, Physics Today, 50, **1997,** p.24.

166. S.A. Ansari, P.N. Pathak, M. Husain, A.K. Prasad, V.S. Parmar and V.K. Manchanda, *Solv. Extr. Ion Exch.*, 23, **2005**, p.463.

167. S. Manohar, J.N. Sharma, B.V. Shah and P.K. Wattal, *Nucl. Sci. Engg.*, 156, **2007,** p.96.

168. I. May, R.J. Taylor, G.C., Brown and N.J. Hill, *Radiochim. Acta.*, 83, **1998,** p.135.

169. R.J. Taylor, I.S. Denniss and A.L. Wallwork, *Nucl. Energy.*, 36, **1997,** p.39.

170. R.J. Taylor, V.S. Koltunov, O.A. Savilova, G.I. Zhuravleva, I.S. Denniss and A.L. Wallwork, *J. Alloys Compd.*, 271–273, **1998**, p.817.

171. A. Rineiski and G. Kessler, *Nucl. Engg. Design.*, 240, **2010**, p.500.

172. M.J. Sarsfield, H.E. Sims and R.J. Taylor, *Solv. Extr. Ion Exch.*, 27, **2009**, p.638.

173. M. Nakahara and Y. Sano, *Radiochim. Acta*, 97, **2009**, p.727.

174. M. Nakahara and Y. Koma, *J. Chem. Engg. Japan.*, 44, **2011**, p.313.

175. Y. Tsubata, T. Asakura and Y. Morita, *Trans. Atomic Energy Soc. Japan.*, 8, **2009**, p.211.

176. A. Zhang, J. Hu, Z. Xianye and W. Fangding, *Solv. Extr. Ion Exch.*, 19(6), **2001**, p.965.

177. M. Gazith, *Activity coefficients of various electrolytes: Molal and molar concentrations* Israel Atomic Energy Commission, Tech. Rep. IA-1004, **1964**.

178. S.K. Patil, V.V. Ramakrishna, G.V.N. Avadhany and M.V. Ramaniah, *J. Inorg. Nucl. Chem.*, 35(7), **1973**, p.2537.

179. D.G. Kalina, G.W. Mason and E.P. Horwitz, *J. Inorg. Nucl. Chem.*, 43(1), **1981**, p.159.

180. J.N. Mathur, P.B. Ruikar, M.V. Balarama Krishna, M.S. Murali, M.S. Nagar and R.H. Iyer, *Radiochim. Acta*, 73(4), **1996**, p.199.

181. A. Morgenstern, C. Apostolidis, H. Ottmar and K. Mayer, *Radiochim. Acta*, 90, **2002**, p.389.

182. Y. Morita and M. Kubota, *Solv. Ext. Ion Exch.*, 6, **1988**, p.233.

183. S.F. Marsh and T.D. Gallegos, *Chemical treatment of plutonium with hydrogen peroxide before nitrate anion exchange processing*, Tech. Rep. LA-10907, Los Alamos National Laboratory, U.S. **1987**.

184. Z. Zhaowu, H. Jianyu, Z. Zefu, Z. Yu, Z. Jianmin and Z. Weifang, *J. Radioanal. Nucl. Chem.*, 262, **2004a**, p.707.

185. Z. Zhaowu, H. Jianyu, Z. Zefu, Z. Yu and Z. Weifang, *J. Radioanal. Nucl. Chem.*, 260, **2004b**, p.601.

186. R. Chiarizia, M.P. Jensen, M. Borkowski, J.R. Ferraro, P. Thiyagarajan and KC. Littrell, *Solv. Extr. Ion Exch.*, 21, **2003**, p.1.

187. R. Chiarizia, M.P. Jensen, M. Borkowski, J.R. Ferraro, P. Thiyagarajan and K.C. Littrell, *Sep. Sci. Technol.*, 38, **2003**, p.3313.

188. R. Chiarizia, M.P. Jensen, M. Borkowski, P. Thiyagarajan and KC. Littrell, *Solv. Extr. Ion Exch.*, 22, **2004**, p.325.

189. B. Bhattacharjee, *An Overview of R&D in Fuel Cycle Activities of AHWR,* in Nuclear Fuel Cycle Technologies: Closing the Fuel Cycle, Ed. by B. Raj, P.R. V. Rao, INSAC-2003, Kalpakkam, Dec.17-19, 2003, p.3-32.

190. P.N. Pathak, R. Veeraraghavan, P.B. Ruikar and V.K. Manchanda, *Radiochim. Acta*, 86, **1999**, p.129.

191. R. Chiarizia, M.P. Jensen, M. Borkowski and K.L. Nash, *A new interpretation of third-phase formation in the solvent extraction of actinides by TBP*, Separations of Nuclear Fuel Cycle in the 21st Century, ACS Symposium Series, 933(9), **2006**, p.135.

192. S. Rajeswari, M.P. Antony, T.G. Srinivasan and P.R. Vasudeva Rao, in *Proceedings of International Symposium on Solvent Extraction*, ISSE, Bhubaneswar, India, Sept. 26-27, **2002**, p.459.

193. V. Vidyalakshmi, M.S. Subramanian, S. Rajeswari, T.G. Srinivasan and P.R. Vasudeva Rao, *Sol. Extr. Ion Exch.*, 21(3), **2003**, p.399.

194. S. Fang, C. Zhao and C.H. He, *J. Chem. Eng. Data*, 53, **2008**, p.2244.

195. J. Szymanowski, *Solv. Extr. Ion Exch.*, 18, **2000**, p.729.

196. R.K. Jha, P.N. Pathak, K.K. Gupta, P.G. Kulkarni, P.B. Gurba, P. Janardan, R.D. Changarani, P.K. Dey and V.K. Manchanda, *Desal. Water Treat.*, 12, **2009**, p.68.

197. P.R.V. Rao and Z. Kolarik, *Solv. Ext. Ion Exch.*, 14, **1996**, p.955.

198. M.H. Kurtis, *TBP Processes Investiation-Formation of Red Oil in Extraction Column Studies*. U. S. Tech. Rep. HW-19997-RD, **1951**.

199. N. J. James and G. T. Sheppard, *Nuc. Engg. & Design*, 130, **1991**, p.59.

200. The Radiological Accident in the Reprocessing Plant at Tomsk, International Atomic Energy Agency, Vienna, **1998 .**

201. G.S. Barney and T.D. Cooper, *Reactivity of Tributyl Phosphate Degradation Products with Nitric Acid: Relevance to the Tomsk-7 Accident*, Third U.S. –Russian Workshop on Non-Reactor Nuclear Safety by U. S. DoE. Aug.14-19, **1995**.

202. V. Mubayi and R.A. Bari, *Red oil excursions in the mixed oxide fuel fabrication facility*, *Overview and Summary Report*, Brookhaven National Laboratory, **2009**.

203. W.S. Durant, *Red Oil explosions at the Savannah River Plant*, E. I. du Pont de Nemours & Co. Savannah River Laboratory, Tech. Rep. DP-MS-83-142, **1984**.

204. R.N. Robinson, D.M. Gutowski and W. Yeniscavich, *Control of Red Oil Explosions in Defense Nuclear Facilities*, Defense Nuclear Facilities Safety Board, Tech. Rep. DNFSB/TECH-33, **2003**.

205. T.S. Rudisill and W.J. Crooks III, *Initiation Temperature for Runaway Tri-n-Butyl Phosphate/Nitric Acid Reaction*, Westinghouse Savannah River Company, Tech. Rep. WSRC-MS-2001-00214, **2000**.

206. M.L. Hyder, *Safe Handling of TBP and Nitrates in the Nuclear Process Industry (U),* Tech. Rep. WSRC-TR-94-0372, **1994**.

207. M. Casarci, G.M. Gasparini and G. Grossi, *Inorg. Chim. Acta*, 94(1-3), **1984**, 37.

208. O. Herbinet, P.M. Marquaire, F.B. Leclerc and R. Fournet, *J. Anal. App. Pyrolysis,* 78, 2, **2007**, p.419.

209. K.T. Reddy, N.P. Cernansky and R.S. Cohen, *Energy & Fuels*, 2(2), **1988**, p.205.

210. L. Merlo-Sosa and G. Soucy, *Int. J. Chem. Reactor Eng.*, 3, **2005**, p.3.